Kinematically nonlinear finite element model of a horizontal axis wind turbine. Part 1: Mathematical model and results

Thirstrup Petersen, J.

Publication date:
1992

Document Version
Publisher's PDF, also known as Version of record

Kinematically Nonlinear Finite Element Model of a Horizontal Axis Wind Turbine.

Part 1 : Mathematical Model and Results.

Jørgen Thirstrup Petersen
Wind Engineering Section

Dept. of Meteorology and Wind Energy
Risø National Laboratory
DK-4000 Roskilde
Denmark

July 11, 1990

Kinematically Nonlinear Finite Element Model of a Horizontal Axis Wind Turbine.

Part 1 : Mathematical Model and Results.

Jørgen Thirstrup Petersen

Abstract.

A mathematical time domain model for simulation of the dynamic response of a horizontal axis wind turbine is presented. The model concentrates on the correct representation of the inertia loads in the equations of motion, and aims at a final model well suited for parametric studies, offering the user the possibility of chosing the appropriate level of representation of dynamical effects.

A general kinematic analysis, which includes the elastic rotations at the tower top and at the shaft end, is the basis for the derivation of the local inertia loads. Nonlinear kinematic terms are retained in the expressions for these loads. The wind turbine structure is subdivided into three substructures, comprising the tower, the nacelle-shaft, and the rotor blades. Each substructure is described with reference to a local coordinate system.

The model is discretized by use of the finite element modelling technique. A simple two node prismatic beam element is used. General element inertia matrices and vectors are derived through consistent transformation of the inertia loads to the nodes. The kinematic analysis provides for the geometric compatibility at the coupling nodes between the substructures. Final assembly of the substructure equations of motion is carried through by imposing force equilibrium at the coupling nodes. The resulting coefficient matrices are nonsymmetric. Substructuring permits easy updating of changes in geometry, corresponding to rigid body rotations of the substructures and extends the limitations on the allowable displacements.

The loading on the wind turbine structure includes both the gravity and aerodynamic loads on the blades. Aerodynamic loads are derived by use of a quasi-steady theory. The model is fully aeroelastic, in that the influence of the elastic deformations on the aerodynamic force is taken into account. The free wind vector is composed of a deterministic contribution including wind shear and tower interference, and a stochastic component, which is generated by the Sandia method for time simulation of turbulence.

Based on the mathematical model a computer program has been developed. The program runs on a personal computer. The equations of motion are solved in the time domain by use of an implicit Newmark integration scheme, in combination with Newton-Raphson iterations, performed to ensure equilibrium at each time step. Eigensolutions are obtained for the structure including only the dominating influence of the rotating substructures. The eigenvalues are found by use of the Sturm-sequence property for the symmetric equations of motion. These eigenvalues are then used as starting values in an inverse iteration performed on the nonsymmetric equations from the substructure formulation to give the mode shapes. Results from a simulation of the response on a typical Danish three bladed stall regulated wind turbine are presented and compared with measurements.

Thesis submitted to the Technical University of Denmark in partial fulfilment of the requirements for the degree of Ph.D. (lic. techn.).

The thesis consists of 2 parts

Part 1 : Mathematical Model and Results.

Part 2 : Supplement. Inertia Matrices and Aerodynamic Model.

References between the two parts are cited as references in general. The notation of the two parts is in agreement.

Contents

List of Figures

Preface.

The present work has been performed in the Wind Engineering Section of the Department of Meteorology and Wind Energy at Risø National Laboratory under the Ph.D. (lic.techn.) programme of the Technical University of Denmark.

The study was supervised by Professor Poul Scheel Larsen and Associate Professor Bjarne Maribo Pedersen of the Technical University of Denmark, whose kind support is greatly appreciated.

Peter Hauge Madsen of Risø has been the local supervisor and the author wishes to express his gratitude to Madsen for his valuable guidance and inspiration, especially in the important stages of the work, when the paths to follow might seem a little obscure. Per Lundsager, who kindly assisted while Madsen was abroad, is thanked for his support.

The inspiring environment at the Department of Meteorology and Wind Energy has been of great value, and my colleagues are thanked for their free exchange of ideas and information. Sten Frandsen, further for his establishment of a peaceful, almost protected place, with all the needed remedies available.

The specific discussions with Allan Kretz, regarding the algebraic programming and in the course of the program debugging have been valuable and time saving, and the author wishes to express his gratitude for the support.

Finally, Michael S. Courtney is thanked for his conscientious assistance in avoiding the worst traps associated with the use of a foreign language. The obscure formulations that may still remain are not his responsibility.

1 Introduction.

The dominating design concept used for commercially manufactured wind turbines in the world today is the horizontal axis type connected to the electrical supply grid. The rotor configuration is usually two- or three-bladed, and power regulation is carried out either by stall- or pitch-regulation. Two-bladed rotors are often equipped with a teeter hinge, but the majority of wind turbines have a rigid hub.

The majority of the Danish wind turbines are of the three-bladed stall regulated type. Only three bladed turbines of the rigid hub type are commercially available in Denmark today. Very little attempt has been made to develop a more flexible and probably more optimal design, as for example, the two bladed teetered type.

The 200 kW Gedser wind turbine [L3] is often considered the model for the development of the new generation of stall regulated wind turbines in Denmark, which took its beginning in the late 1970's. During the last decade this concept has gone through a continuous development. In the early 1980's the manufacturers concentrated on the optimization of the components for wind turbines of the 55 kW size, with particular emphasis on production. The typical design engineer was almost completely occupied with problems related to production. The basis for dimensioning was the experience with prototypes together with the general rules supplied by The Test Station for Wind Turbines at Risø. These rules, of course, had to be conservative, because they apply to a complex product experiencing a complex loading, and yet be simple at the same time. The rules reflected the experience gained with a number of different wind turbines.

A theoretical approach to design was almost solely used by researchers employed in connection with the national programmes in relation to the bigger wind turbines, e.g. the 630 kW Nibe turbines [P2]. Allthough the results from these programmes are in the public domain, the influence of this research upon the commercially manufactured wind turbines has been very limited, or at least very much delayed. Only when results of special interest for the industry have been extracted from the research results can a clear influence be traced. The interest has often been stimulated by sudden problems, for which the industry needed help to find solutions, usually in a hurry. But the industrial approach was still mainly based on experience. One explanation for this might be that the manufacturers in the early 1980's were primarily small companies with very little tradition for basing their production on research and theory.

During the last years the industrial approach has changed more in the direction of the theoretical, and mathematical models have become more common. One of the reasons is probably that the size of the wind turbines has increased (400-500 kW) and that prototype testing is now too expensive compared to the implementation of an appropriate theoretical tool. Or put in another way, the theory can compete with the prototype testing, and help minimize the economic risk. Another reason is that the manufacturers have realized that experience alone is not sufficient for a satisfactory lifetime prediction. A third reason is that prouction needs much less attention from the design engineer, due to the experience of the staff and establishment of systematic quality control.

Altogether, it seems as if the industry, to a certain degree, is prepared to accept the theoretical approach and that it will be considered an important ingredient in the optimization process. When the conditions change in that direction, it is much easier to establish a fertile interaction between the research communities and the industry. Of course, the research communities have a responsibility in that process, in that the results of the research must be put in a form which makes it practicable for the recipient to use them.

During the last couple of years, work has been going on at Risø National Laboratory which aims at the development of a computer program (Design Basis [L1]) which is efficient for parametric studies on a personal computer. The first edition of the program has been published and distributed. This is a simple one bladed model (see Sec. 1.1), which is based on earlier research [M4] covering the complete rotor.

The main purpose of the present work is to support the continued development of the Design Basis code, especially concerning the proper inclusion of the dynamical effects when a relatively flexible structure is considered. Therefore the present model focuses on the modelling of the inertia loads. The model is developed in a form that makes it possible to identify the origin of the inertia loads and eliminate the associated contributions if they are found to be negligible for a given application.

In order to furnish the reader with some insight in the subject, it is found valuable to go through a presentation of the capability of existing, comparable models to include the inertia loads and place the present model in this context. This is done in the following Sec. 1.1. The introduction concludes with an overview of the elements of the present model and the scope of the thesis.

1.1 Placing the model in relation to existing models.

The following survey is not intended to be a general evaluation of the quality of the models but merely an assessment of their ability to incorporate significant dynamical effects, i.e. the inertia loads. The present work focuses primarily on the influence of the inertia loads, while other models have been developed with quite different main aims.

In the present model a kinematic analysis results in nonlinear expressions for the inertia loads, which to a great extent are retained in the equations of motion. Anticipating the results from later sections, the inertia loads for the blade will be the basis for the following survey.

The present model makes use of the finite element model (FEM) for discretization and the inertia loads are represented as node loads, resulting from consistent transformation of the distributed inertia loads to the nodes. When the origin of the coefficient matrices and vectors are made clear, it is possible to compare the present model with others that make use of different techniques for discretization.

1.1.1 Simplified expression for the blade inertia load.

When dealing with rotating substructures, important inertia forces may arise. If the structural elements are relatively stiff, it may be sufficient to determine the inertia force by assuming that the substructures behave as rigid bodies. If, furthermore, the angular velocities can be considered uniform, the inertia force may be incorporated simply as a centrifugal force. In the case of a wind turbine, it is equivalent to incorporate the centrifugal force on the blades, and when the rotor is symmetric the centrifugal force influences only the loads on the rotor, while other structural parts are unaffected.

However, the work going on with optimization of the wind turbines results inevitably in more flexible structures, and additional inertia forces are likely to be important. An example is given below of the origin of such loads. At the same time the example covers the inertia loads which are very likely to be important on some existing designs, but often neglected because the existing design tools are often incapable of including them.

The basis for the example is the schematic drawing in Fig.1 and a reduced expression for the inertia loads which are part of the mathematical model. The kinematic analysis in the model

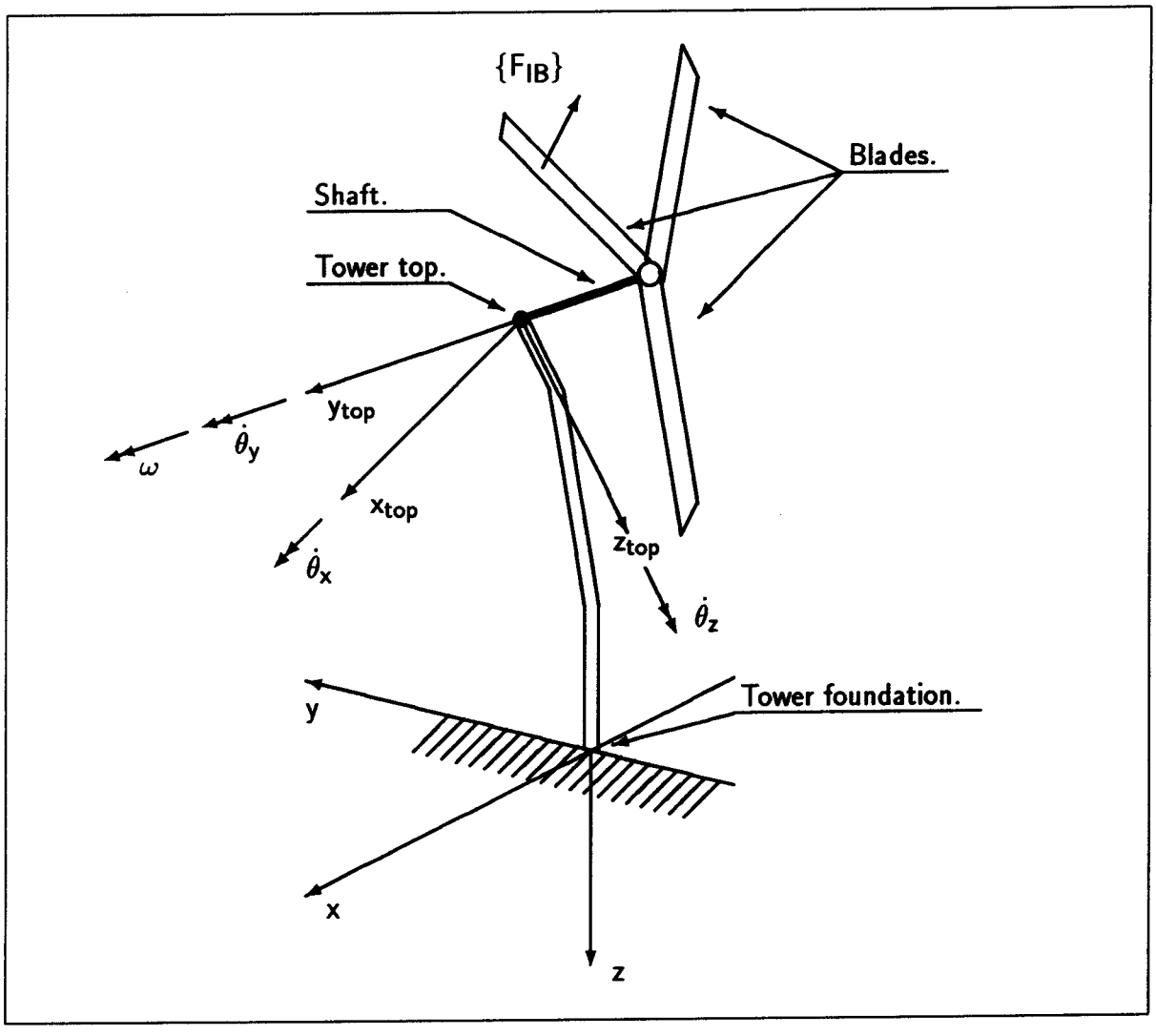

Figure 1: Tower top elastic rotations.

includes deformation at the shaft end, teeter and yaw but only the tower top deformation will be included in the following survey. The angular rotor velocity is assumed constant, in order to keep the expression for the blade inertia force as simple as possible.

Applying these simplifications the following formal expression for the inertia load at a blade point is obtained

$$
\begin{aligned}
-\{F_{IB}\} = & \\
& [M]\{\ddot{q}_B\} \quad \ldots\ldots\ldots\ldots\ldots\ldots \text{(mass)} \\
& + \left[C\left(\omega, \dot{\theta}_T\right)\right]\{\dot{q}_B\} \quad \ldots\ldots\ldots\ldots\ldots \text{(Coriolis)} \\
& + \left[K\left(\omega^2, \omega\dot{\theta}_T, \dot{\theta}_T\dot{\theta}_T, \ddot{\theta}_T\right)\right]\{q_B\} \quad \ldots \text{(softening)} \\
& + \left\{F\left(\omega^2, \omega\dot{\theta}_T, \dot{\theta}_T\dot{\theta}_T, r\right)\right\} \quad \ldots\ldots\ldots \text{(centrifugal + gyroscopic)} \\
& + \left[M_{\ddot{\theta}}\left(\ell_{shaft}, r\right)\right]\left\{\ddot{\theta}_T\right\} \quad \ldots\ldots\ldots\ldots \text{(rigid body rotation)} \\
& + \left[C_{\dot{\theta}}\left(\omega, \dot{\theta}_T, \ell_{shaft}, r\right)\right]\left\{\dot{\theta}_T\right\} \quad \ldots\ldots \text{(gyroscopic)} \\
& + [M_{\ddot{u}}]\{\ddot{u}_T\} \quad \ldots\ldots\ldots\ldots\ldots\ldots \text{(rigid body translation)}
\end{aligned} \tag{1.1.1}
$$

The expression has been derived in App. B, and it is possible through the description there to trace the origin of the terms in the model equations. Eq. 1.1.1 is a simplified version of Eq. B.0.11 in App. B. The relation between the two equations is kept unique by retaining the order of the terms.

Apart from the listed degrees of freedom and parameters, all the matrices and the centrifugal-gyroscopic vector depend on material parameters and geometry. Except for the mass matrix including azimuthal position and angular elastic deformations at the tower top.

The radial location of the blade point in question is given by r. The shaft is assumed stiff and its length is denoted by ℓ_{shaft}. The rotor is spinning with constant angular velocity (ω) relative to the tower top. The direction of the ω angular velocity vector is constrained by the shaft bearings. The tower is assumed flexible, so that the elastic rotations at the tower top are not negligible. These are assumed to be small so that they can be referenced to the coordinate axes and described as a vector. They are generally denoted θ, with indices x, y, and z in the figure corresponding to the respective axis. In the formal equation no distinction is made between the axes and the index T indicates that the rotation may be any of the three.

Our main interest in this context is to show how the flexible tower influences the inertia load. The elastic angular velocities that will occur must be added to the rotational speed (ω) in order to obtain the total speed of the rotor, and as the elastic rotations and their time derivatives (denoted by a dot) vary with time, both in direction and size, it becomes clear that all the accelerations, usually described by the well known four term acceleration expression for a rotating coordiante system, are present. This is reflected in the equation.

The influence of the inertia force on the terms related to local deformation ($\{q_B\}$) on the blade is reflected in line 2 and 3 of the equation, representing the Coriolis- and the softening-effects. The importance of these will depend very much on the actual properties of the blade.

In addition to the centrifugal forces gyroscopic forces are present in the equation, due to the resulting time varying rotation vector for the rotor. The gyroscopic terms are represented both in the vector of line 4 and the matrix of line 6. The gyroscopic forces appear in both terms due to the chosen discretization technique and to the level of reduction of the equations. For many designs it is probably very important to incorporate the gyroscopic forces.

The last terms to mention are the terms denoted rigid body terms in the equation. They are usually incorporated in the most models, which integrate the complete turbine. Their incorporation do not depend on a kinematic analysis.

1.1.2 Comparison of models.

Based on the expression for the inertia loads from Eq. 1.1.1 existing representative models for horizontal axis wind turbines will be described below, starting with the simplest models and carrying on with models of increasing complexity. Only models which have been specially developed for wind turbines will be considered, and only models in the public domain. This means that e.g. modified helicopter models and private manufacturer models are not considered, the former because they are usually very complex and it is difficult to extract information, which makes these models comparable with the specially designed wind turbine models, the latter category simply because details about these models are unknown. Within both categories important models exist.

The result of the model description will be a series of models, which provides a survey of the ability of the models to incorporate the inertia loads. At the same time the overview will serve to illustrate where the present model is placed in relation to existing models. Other important characteristics of the models, e.g. special degrees of freedom and aerodynamic model, will be mentioned briefly, in order to emphasize the aim of the model in question.

The models will be referred to three main categories. Within each category degrees of varying complexity exist. The first category covers models which only consider the dynamics of a single blade. Coupling to the other blades, the nacelle, and to the tower are not included, which means that the hub and the tower are assumed to be stiff. The second category covers models which consider dynamics of the whole rotor and perhaps a very simplified coupling to the tower. The models in this category assume that the tower is relatively stiff. The third category deals with the models which incorporate the complete structure, with a varying number of DOFs and with a varying degree of linearization.

1.1.2.1 Single blade models.

This category covers models which consider the dynamics of one single blade. They are usually very fast and effective, as appropriate when the main characteristics of the wind turbine are to be established. When the tower, nacelle, shaft and hub with good approximation can be considered stiff, the models will often give answers which are sufficient for the final design, perhaps modified according to results from prototype testing.

The ability of the models to incorporate the inertia loads can be roughly illustrated by use of Eq. 1.1.1, which after cancelling of the terms related to the tower DOFs is written

$$
\begin{aligned}
-\{F_{IB}\} = \\
&[M]\{\ddot{q}_B\} \quad \ldots\ldots\ldots \text{(mass)} \\
&+[C(\omega)]\{\dot{q}_B\} \quad \ldots\ldots \text{(Coriolis)} \\
&+\left[K\left(\omega^2\right)\right]\{q_B\} \quad \ldots \text{(softening)} \\
&+\left\{F\left(\omega^2, r\right)\right\} \quad \ldots\ldots \text{(centrifugal)}
\end{aligned} \tag{1.1.2}
$$

Here the deformation vector, $\{q_B\}$, covers only one single blade. The equation of motion is usually established in the rotating frame of reference following the blade. The equations are usually linearized and solved by a modal analysis technique, which reduces the number of degrees of freedom. The solution is often carried out in the frequency domain. It is mentioned below where the particular models deviate from the equation above.

One such model is described by Larsen [L1]. Blade displacement in flap- and chord-wise directions are considered, while torsion is excluded. The two directions are not structurally coupled, but coupled through the aerodynamics. Centrifugal stiffening is included. The equations of motion are solved both in the time and in the frequency domain by use of a modal technique, based on the mode shapes. This work focuses on the calculation of fatigue and extreme response.

A similar model is described by Øye in [Ø1] and [Ø2]. Here a more complete structural model is used. Structural coupling between the flap- and chord-wise directions and torsion are included. The influence of the centrifugal force is included in the stiffness, both in directions perpendicular to the blade axis, but also in the torsional direction. The latter may be important for blades designed with a considerable twist and low torsional stiffness. This effect is usually neglected, as in the present model. The model operates in the time domain and uses a modal technique based on the mode shapes for reduction of the degrees of freedom.

A third example in this category is the model described by Thresher [T1]. The model is restricted to consider only the flap-wise direction. The stiffening effect of the inertia loads is fully incorporated in this direction. The model allows for a prescribed yawing motion, which may be time varying. Its representation in the model is only restricted by the introduced linearization. This gives rise to additional gyroscopic forces through the product $\omega\dot{\theta}_T$ and further, when the yaw motion is time varying, additional inertia forces through the angular acceleration $\ddot{\theta}_T$. The solution is based on discretization and reduction of the DOFs by use of the Galerkin method. The equations of motion are integrated in the time domain.

1.1.2.2 Coupled rotor models.

Models in this category are characterized primarily by their ability to describe the dynamics of the coupled rotor, i.e. the rotor hub is no longer considered stiff. Apart from this, the basic approach may be very different. Also, the included dynamic effects are treated at different levels of refinement, primarily governed by the actual modelling employed and the solution technique. In spite of that, the inertia forces accounted for in the models can roughly be described by a common equation, which results from reduction of Eq. 1.1.1

$$
\begin{aligned}
-\{F_{IB}\} = & \\
& [M]\{\ddot{q}_B\} \quad \ldots\ldots\ldots\ldots\ldots \text{(mass)} \\
& + [C(\omega)]\{\dot{q}_B\} \quad \ldots\ldots\ldots\ldots \text{(Coriolis)} \\
& + \left[K\left(\omega^2\right)\right]\{q_B\} \quad \ldots\ldots\ldots \text{(softening)} \\
& + \left\{F\left(\omega^2, \omega\dot{\theta}_T, r\right)\right\} \quad \ldots\ldots \text{(centrifugal + gyroscopic)} \\
& + \left[M_{\ddot{\theta}}\left(\ell_{shaft}, r\right)\right]\left\{\ddot{\theta}_T\right\} \quad \ldots \text{(rigid body rotation)} \\
& + [M_{\ddot{u}}]\{\ddot{u}_T\} \quad \ldots\ldots\ldots\ldots \text{(rigid body translation)}
\end{aligned}
\tag{1.1.3}
$$

It is mentioned below, where the actual model deviates from this equation.

One model in this category is described by Madsen [M4]. The model is developed for solution in the frequency domain, and this is naturally reflected in the choice of representation of the dynamic terms. The modelling is carried through in the rotating frame of reference. A constant angular velocity of the rotor, ω, is asumed, but a periodic yaw motion , $\dot{\theta}_T$, is allowed

for, resulting in gyroscopic forces, represented in the vector $\{F\}$. The yaw acceleration is neglected, assuming slowly varying yaw velocity. The centrifugal stiffening is taken into account as geometric stiffness and softening in the plane of rotation is included through $[K]$. Coriolis forces are accounted for through $[C]$, yet, neglecting the influence of the yaw motion on the Coriolis force. The tower top DOFs are not included in the model, i.e. $[M_{\tilde{u}}]$ and $[M_{\tilde{\theta}}]$ are zero. As was the case with the model by Larsen [L1], the main purpose with this model is to calculate fatigue and extreme response.

A model using a finite element approach is described by Garrad [G1]. The model is almost identical to the one by Lobitz [L2]. Garrad integrates the tower, although without taking into account the additional gyroscopic and Coriolis forces on the rotor resulting from tower top angular motion. The tower is modelled in a fixed frame of reference and the rotor in a rotating frame of reference. The two sets of equations are coupled before solution by use of a time varying transformation matrix reflecting the hub configuration and taking care of the relative movement of the structures. The tower top deformations are treated as real DOFs, but because the rotor axis is assumed to be fixed in space in the kinematic analysis, the inertia terms depending on $\left\{\dot{\theta}_T\right\}$ are not taken into account. The solution of the equations is carried out in the time domain.

1.1.2.3 Integrated models.

The main characteristic of the models described in this category is their ability to incorporate the DOFs at the tower top in such a way that the influence of time varying angular rotations includes the angular velocities at the tower top. Still, the level of refinement is very broad, from those where the coefficient matrices do not depend on the DOFs to models that can be characterized as fully nonlinear. The discussion is carried through with basis in the original Eq. 1.1.1.

The first model to mention in this category is one specially developed for stability analysis of two bladed, teetered wind turbines by Janetzke [J1]. The model has only five DOFs including the teeter. The remaining DOFs are two generalized coordinates corresponding to the fundamental flapping mode for each blade, and two rotations at the tower top, corresponding to yaw and tilt directions, respectively. The equations of motion are linearized so that the coefficient matrices do not depend on the DOFs. The Coriolis term is neglected so that $[C] = [0]$. The softening is not included in the form of Eq. 1.1.1, but the stiffening due to the centrifugal force is taken into account, both on the blade and on the teeter DOF. The influence of the angular accelerations at the tower top on the blade inertia force as well as gyroscopic forces from the tower top angular velocities are taken into account, so that both $[M_{\tilde{\theta}}]$ and $[C_{\dot{\theta}}]$ are included. The solution is carried out in the time domain.

Allthough the model is rather simple, it demonstrates the important steps in the derivation of the equations of motion and how it is possible with models of this type to include only those DOFs that are important in an actual analysis .

Almost the same can be stated about the model by Madsen [M3]. It has been specially developed for investigation of the influence of rotationally sampled turbulence on the rotor loads. The model has only three DOFs which are the tower top displacement in the wind direction, the yaw and the tilt angle. The local blade dynamics is thus ignored and the rotor is modelled as a rigid body, and the structural mass and stiffness coupling has been disregarded. The tilt and yaw rotation couple through the gyroscopic forces. Considering the terms of Eq. 1.1.1 it is equivalent to exclude the three first lines of the equation. The model operates

in the frequency domain and allows for experimentally determined turbulence properties.

A model similar to the one by Janetzke [J1] has been developed by Garrad [G2]. As regards the representation of the inertia forces, it is basically almost identical to the model in the present work and differs in that respect only in the extent to which linearization has been introduced. The Garrad model has been linearized, so that the coefficient matrices are independent of the DOFs. However, by omitting the linearization, equations identical to Eq. 1.1.1 would be arrived at. The presentation of the model by Garrad in [G2] focuses on the application of the symbolic manipulation program Reduce and stability analysis.

The model presented by Schöttl [S1] is rather comprehensive, allowing for transient analysis in that the angular velocity of the rotor may be time varying. This means that Eq. 1.1.1 should be extended to include $\dot{\omega}$ as well, in order to describe the inertia forces in this model correctly, or more precisely, the azimuthal rotation should be treated as a real DOF. Further this model implements a vortex model in the aerodynamic analysis. The equations are solved in the time domain.

The last example to be mentioned in this survey is the nonlinear finite beam element model by Fabian [F1]. The equations of motion are established in the fixed frame of reference. The kinematic analysis is not carried through explicitly. Instead, the local accelerations are calculated numerically during solution in the time domain and treated as distributed forces. The basic tools in this calculation are position and orientation vectors for each finite element node. The time derivatives of these vectors are calculated during the solution process and used to generate the inertia forces. The model allows for arbitrarily large rotations of the elements and must be characterized as fully nonlinear. As regards the inertia loads, the model is capable of simulating all load situations for a wind turbine at the expense of computer storage and time.

1.1.3 The present model, its near relatives and why is it developed?

From the previous survey of representative existing models it can be seen that the present model is placed in the third category covering models of the complete integrated structure, somewhere in the vicinity of the Garrad [G2] and Schöttl [S1] models, at least when the ability to incorporate the influence of inertia loads is considered. So, in that sense these two models must be characterized as near relatives to the present model. But still the modelling approach differs at essential points, which will become clear when a comparison is made of other characteristics.

Both Garrad and Schöttl use modal expansion of the response as a discretization technique and for reducing the number of DOFs, while the present work makes use of the finite element discretization. The difference between the models can primarily be attributed to these choices.

This difference in approach is reflected in the choice of technique for derivation of the equations of motion (EOMs). Both Garrad and Schöttl make use of energy principles when deriving the EOMs, Lagrange's equations and Hamilton's principle, respectively. This is a natural choice to make, when the mode shapes are used as the basis for a series expansion, because the choice of mode shapes defines the generalized coordinates or equivalently the DOFs, which are used as the basic independent variables in the energy expressions. At the same time the mode shapes act as interpolation functions and enter the coefficient matrices as integrands in a straightforward manner. The method thus requires that the mode shapes, or good approximations (functions satisfying the geometric boundary contitions are admissible functions, [M6, pp. 242-252]) are known in advance, and further that integrals depending on the actual mode

shapes must be evaluated. Also, a means for truncation of the series expansion must be available.

As long as the structure is simple with respect to geometry and distribution of mass and stiffness and further relatively stiff, these requirements do not constitute a problem. Often a good understanding of the dynamic behaviour of the structure will be sufficient to make a good choice as regards the mode shapes and the number of terms in the expansion. Experience with similar structures may contribute valuable information. The evaluation of the integrals will in this case often be simple and is usually carried out numerically.

When the structural design gets more complicated or much more flexible, it will often be necessary to make use of a complementary model, which can be used to calculate the mode shapes. Further, this model can help in providing knowledge about the dynamic behaviour and thus provide a basis for truncation of the series expansion. A more complex structure may further give rise to more complicated integrals over the structural elements. However, the structure might be so complex that a satisfactory solution by use of the modal expansion is precluded [M6, pp. 328-329].

One of the main objectives with the present model is to develop a tool, which can be used to decide to what degree a model should be refined in order to include the important dynamic effects on an actual wind turbine structure, especially including the more complex and flexible structures, which are likely to emerge during the process of optimization. A model will be much more efficient for that study if the decision on model resolution is more integrated than is the case with the modal technique described above. Further, it has been found valuable to use a model which is better suited to deal with complex geometry and distribution of mass and stiffness than those based on modal expansion. An example of such a complex structure is the aerodynamic tip brake of a stall regulated horizontal axis wind turbine. These are the main reasons for chosing the finite element method in the present work.

When the equations of motion are derived for the FEM formulation, the use of the energy methods are less advantageous than they are in connection with the modal technique. Therefore, it has been chosen to use Newton's second law directly for derivation of the inertia loads. Through a general kinematic analysis (Sec. 3) the acceleration is derived for each material point on the structure, and the dynamic problem is converted to the equivalent static problem by use of d'Alembert's principle, which, according to Newton's second law, expresses that the inertia force on a mass particle is equal to the product of mass and acceleration and directed opposite to the acceleration.

The interpolation functions for the actual element are simple polynomials. The inertia force is treated as a distributed force and transformed to the nodes, consistent with the principle of virtual displacement. The integration over the element can be performed analytically resulting in closed form expressions for the terms of the coefficient matrices, thus eliminating errors that may result from numerical integration.

Use is made of the substructuring technique. The wind turbine structure is divided into substructures, which are coupled by imposing force equilibrium at the coupling nodes. The geometric compatibility at the coupling nodes is automatically satisfied by the chosen kinematic procedure. This is very much equivalent to what is done in the modal formulations, allthough very little attention has been payed to the subject by the authors of the texts, which describe the models mentioned above. Schöttl states that the FEM method prohibits the treatment of the angular rotation as time varying. This is certainly not the case. Basically the methods are identical, they only differ in the choice of discretization technique.

All three models discussed in this section make wide use of the algebraic programming system

Reduce [H2] for derivation of the EOMs. This reflects the common need for a convenient and safe method for handling very large and complicated algebraic expressions. Both Garrad and Schöttl accomplish the complete derivation of the energy expressions by use of Reduce, after having defined the position vectors. The present kinematic analysis is carried through by hand, resulting in expressions for the acceleration composed of matrix and vector products, and then only the final multiplication and reduction is done by Reduce.

This procedure is followed primarily because the matrix-vector form of the acceleration expression is found to be very informative, when the origin of the acceleration terms is considered. This may prove to be very useful, when a reduction is carried out during the process of optimization of the equations for special wind turbine configurations.

But further, the application of the more advanced and complex procedures in Reduce, requires, in the present authors opinion, a good deal of confidence in the system, which can only be achieved through experience with tasks of which the results can be checked.

1.2 Survey of the main elements of the model, and scope of the thesis.

In order to give a more coherent representation of the elements in the model than indirectly given through the previous comparison, the main elements of the model are described next. Further the scope of the thesis is described parallel with this exposition.

The wind turbine structure is subdivided into three substructures as described in Sec. 2

1. Tower.
2. Shaft-nacelle.
3. Blades (rotor).

This is primarily done in order to incorporate the elastic rotations at the tower top and at the shaft end in the derivation of the inertia loads. But at the same time the division has two other important consequences. One is that the substructure deformations now are described with reference to a local coordinate system, and this relaxes the limitations, which otherwise must be placed on the allowable deformation in order to be able to express rotations as a vector. The result is that the total deformations allowed on the blades relative to the tower support can be greater than would be the case if the substructures had been described within a common coordinate system. Another important consequence is that the equation structure, following from the division, makes it simple to update the equations at each time step with respect to the change in geometry due to elastic rotations at the tower top and the shaft end. The result is a more correct model, allowing for moderate geometric nonlinearities. Only moderate, because the local angular rotations still must be small in order to make the vector representation valid, including elastic rotations at the tower top and the shaft end. The bearing restrained rotations do not cause such problems, because the axis of rotation is uniquely defined, and the bearing rotations enter the equations as scalars.

Both yaw rotation and teeter rotation are also present in the model, and like the rotor azimuthal rotation they are treated as bearing rotations.

To summarize, the division into substructures has as a result that the rigid body motions of the substructures are fully taken into account, both as regards inertia loads and change in

geometry, and moderate geometric nonlinearities, as seen from a common coordinate system, are allowed for.

The finite element model is used for discretization of the structure. The reasons for that choice was given in Sec. 1.1.3.

The derivation of the element equation of motion (EOM) and the assembly to the substructure EOMs is described with reference to Fig. 2, which illustrates the procedure for the blade substructure.

Newton's direct method is used for derivation of the EOMs. The reason for this choice was given in the previous section in connection with the comparison with other models, Sec. 1.1.3.

Initially, the kinematic analysis is carried through, (Sec. 3). The aim is to derive velocity and acceleration for a material point on the element. The velocity is used in the aerodynamic calculation [Part 2, Sec. F].

Input to the kinematic analysis is basically the position vector to the point in question, $\{r_{SO}\}$. The velocity and the acceleration are derived as the first and the second time derivative to the position vector, respectively.

Information about geometry and DOFs is used in the kinematic analysis. Important variables are

1. Rotor azimuthal position: θ, $\dot{\theta} = \omega$, $\ddot{\theta}$, (bearing controlled).

3. Coupling DOFs between substructures:

   Tower top: $\left\{q_{T\ell}^T\right\}$, $\left\{\dot{q}_{T\ell}^T\right\}$, $\left\{\ddot{q}_{T\ell}^T\right\}$, (elastic deformation).

   Yaw: θ_{3N}^N, $\dot{\theta}_{3N}^N$, $\ddot{\theta}_{3N}^N$, (bearing controlled).

   Shaft end: $\left\{q_{Am}^A\right\}$, $\left\{\dot{q}_{Am}^A\right\}$, $\left\{\ddot{q}_{Am}^A\right\}$, (elastic deformation).

   Teeter: θ_{1H}^H, $\dot{\theta}_{1H}^H$, $\ddot{\theta}_{1H}^H$, (bearing controlled).

4. Shaft length: ℓ_{shaft}.

The transformation matrices needed in the description of the position vector $\{r_{SO}\}$, are derived from the elastic- and bearing-rotations, listed as number 3, and further the azimuthal position θ and the tilt angle θ_{1R}^R. Also the shaft length, ℓ_{shaft}, appears in the position vector.

The finite element used in the model is a simple two node prismatic beam element as described in Sec. 4, where also the complete element analysis is described. The interpolation functions are simple polynomials, which are derived as solutions to the static equilibrium equations for the element. The description includes shear rotation, which is usually unimportant for slender structures, but included for the sake of completeness, and keeping in mind the possibility of using the model for analyzing details of the structure. The coupling between bending and torsion, which arise when the shear center lies outside the elastic axis (neutral bending axis), is included.

The elastic stiffness matrix is derived by use of the constitutive relations and the principle of virtual displacements. A general expression for consistent transformation of the distributed loads to the nodes is derived. This expression is used for transformation of the inertia load to the nodes, resulting in element mass-, Coriolis-, and softening matrices as described in Sec. 4.11.

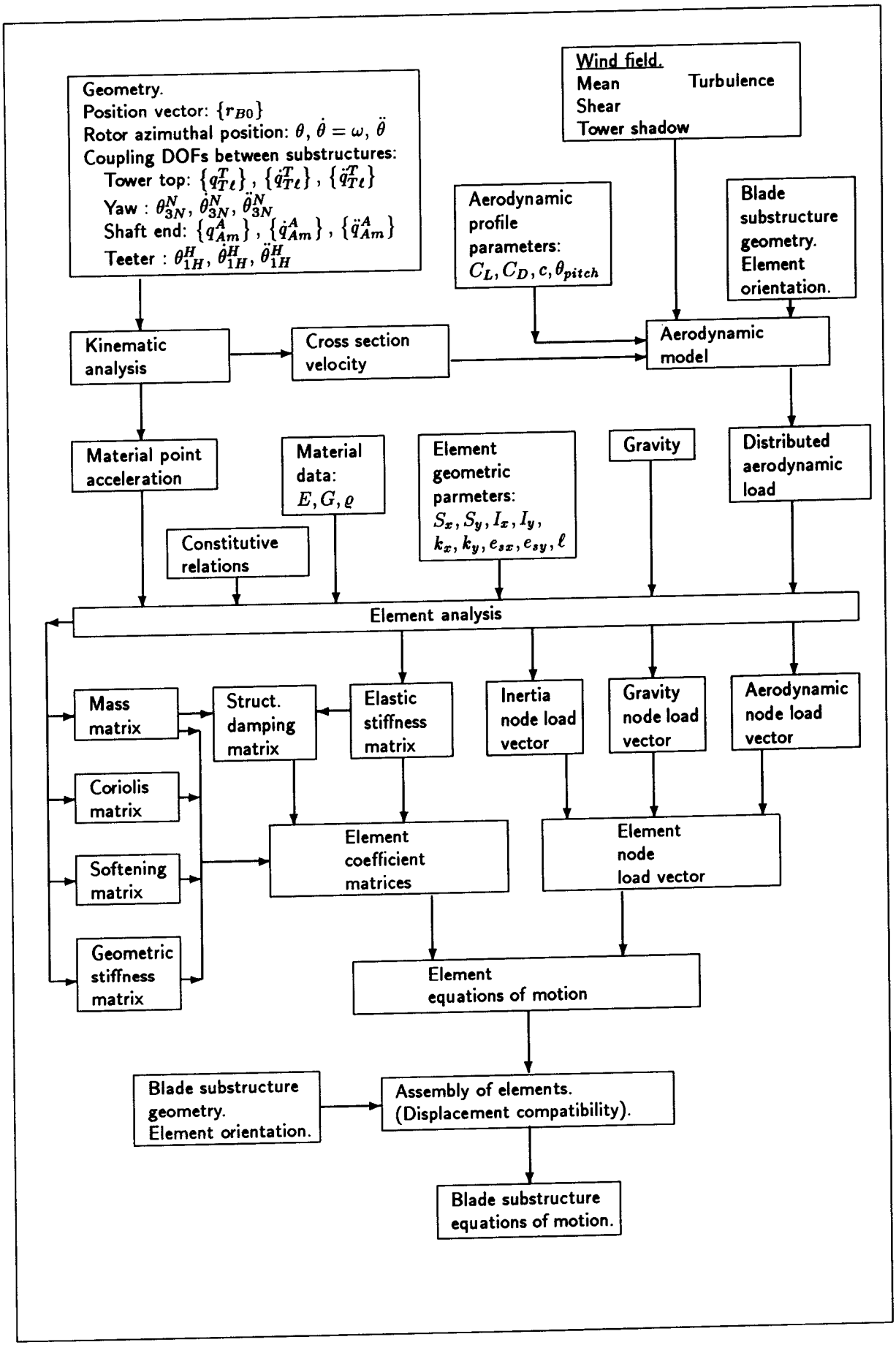

Figure 2: Derivation of blade substructure equations of motion.

Additional inertia loads, represented as vectors, result from this transformation. These vectors are composed of terms, which are functions of DOFs outside the blade substructure, and the angular velocity of the rotor, ω. The terms including DOFs can be extracted from the vectors, as shown for the example calculation in [Part 2, Sec. E], giving rise to additional mass- and Coriolis-matrices. The remaining terms in the inertia vectors are dominated by the centrifugal forces related to the square of the angular velocity of the rotor, ω^2.

The centrifugal force is used in the derivation of the geometric stiffness matrix, as described in Sec. 4.9.

Structural damping is taken into account in the form of Rayleigh damping, the element damping matrix being derived as a linear combination of the mass matrix and the elastic stiffness matrix, (Sec. 4.13).

The aerodynamic load is calculated by use of quasi-steady theory as described in [Part 2, Sec. F]. The wind field includes the mean wind influenced by shear and tower interference. Turbulence is simulated by use of the Sandia method, also described in [Part 2, Sec. F].

Influence of gravity is included in the model, but for the moment only on the blades. Extension to the complete structure is of course straightforward, but omitted because the influence on the dynamics is negligible.

Both aerodynamic load and gravity load are consistently transformed to the nodes.

By gathering the above mentioned terms in one equation, the EOMs for a blade element are obtained. Further, the substructure EOMs are derived by assembly of the element equations, the key for this being the condition on displacement compatibility at the nodes.

Similar procedures are followed for the tower and the shaft substructures.

As shown schematically in Fig. 3, the substructure equations are assembled (Sec. 6) by imposing force equilibrium at the coupling nodes. Further, the boundary conditions at the tower foundation are introduced, thus removing the rigid body motion of the total structure. These conditions are assumed to be purely geometric, equivalent to zero displacement. The displacement compatibility between substructures is ensured through the kinematic analysis.

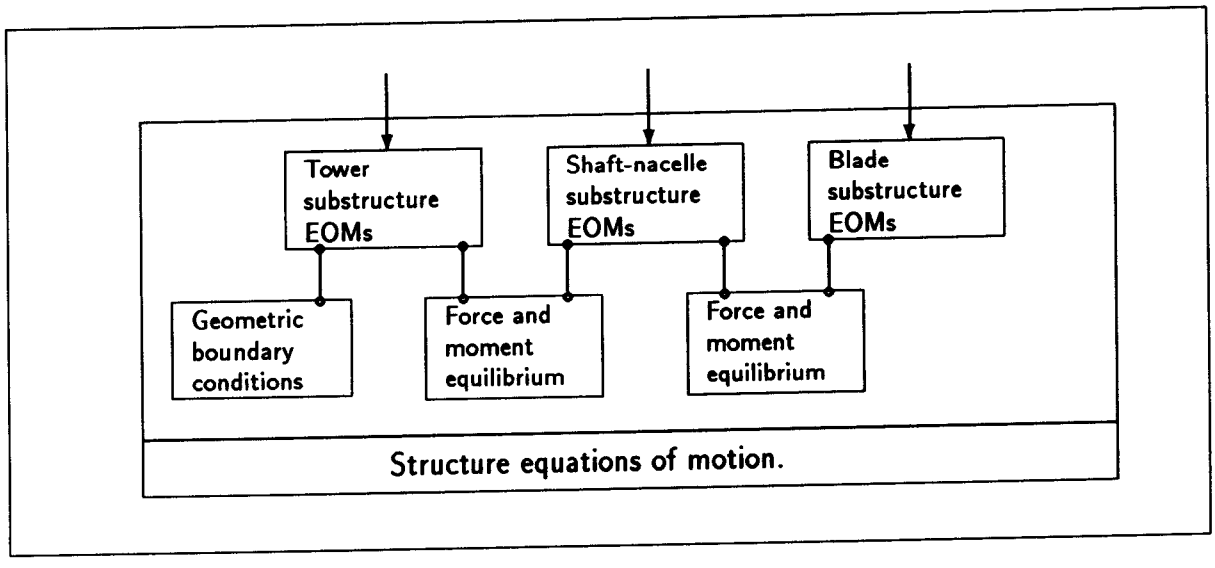

Figure 3: Assembly of substructure equations of motion.

As the resulting structure EOMs are rather complicated and strongly coupled and nonsymmetric, some attention has been payed to assess the validity of the assembly procedure. In

Sec. 5 the present form of the EOMs are compared with the usual symmetric form of the finite element equations, obtained when a common coordinate system is used. It is shown for a simple case, that it is possible to transform from one form to the other. It becomes evident that the real difference lies in the representation of the rigid body displacements in the two sets of equations.

Indirectly, the validity of the substructure formulation has further been partially investigated through an implementation of an eigensolution procedure (Sec. 7), allthough the purpose with this is different. When dealing with wind turbine dynamics, it is very instructive to be able to calculate the eigensolutions, both when models are established for simulation, but also when knowledge about the dynamic behaviour is required. For this reason an eigensolution procedure has been programmed. It is based on a calculation of the eigenvalues for the structure described in a common coordinate system and including only geometric stiffness and centrifugal stiffening, i.e. the EOMs are symmetric. The eigenvalues are found by use of the Sturm-sequence property for symmetric matrices. Next, these eigenvalues are used as the starting values in an inverse iteration performed on the substructure formulated EOMs to give the eigenfunctions (mode shapes). Identical eigenvalues are found within the numerical accuracy.

In Sec. 7 the procedures used for the solution of the equations are described. A schematic representation of the solution procedure is found in Fig. 19. The Newmark implicit integration scheme is applied. The method is unconditionally stable, when the coefficient matrices are not time dependent. However, the present implementation has not revealed any instability problems for the example calculations which have been carried through so far, even if the coefficient matrices are time dependent. Due to the kinematic nonlinearity of the equations it is in general necessary to combine the integration with iterations in order to achieve equilibrium at each time step. Omitting this will usually give erronous results, because an error is accumulated.

The mathematical model has resulted in a computer program written in Fortran 77. This closely follows the mathematical model and therefore a detailed description is unnecessary.

The thesis concludes with some calculation results. Example calculations have been carried through on a typical Danish three bladed wind turbine, which has been tested at the Test Station for Windmills at Risø, and the simulated results are compared with measurements. Reasonable agreement is demonstrated (Sec. 8).

In the example calculations the yaw DOF (θ_{3N}^{N}) and the tilt (θ_{1R}^{R}) have been omitted, and further the angular velocity (ω) has been assumed constant. This is done, simply, in order to reduce the expressions for velocity and acceleration. The tower top deformations and the shaft end deformations have been given the highest priority in the calculations. Omission of the tilt approximately halves the number of terms. The yaw DOF can still be represented in the calculations by assigning an appropriate torsional stiffness to the beam element at the tower top.

The thesis consists of two parts. Part 1 (the present part) covers the mathematical model and the results and constitutes the chief part of the thesis, while Part 2 is a supplement, where the most space consuming inertia matrices are listed, and some of the most important matrix manipulations are shown. Further, the complete aerodynamic model is described in Part 2. References between the two parts are given as references in general.

2 Model geometry.

The horizontal axis wind turbines commercially available today follow a similar structural design, regarding the main components, which are important when the overall dynamic response is considered. If the rotor shaft and its supporting connections to the tower is regarded as one main component, the wind turbine is naturally divided into 3 main components

1. The supporting tower
2. The rotor shaft
3. The rotor blades

At the same time the connections between these main components are usually characterized by important built in degrees of freedom (DOFs). Between the tower and the nacelle the yaw rotation takes place, usually controlled by a bearing with one rotational degree of freedom around a vertical axis. Further, if the simplification suggested above is taken literally, both the yaw rotation and the rotation of the rotor shaft can be considered as occuring at the connection between the tower and the shaft. Between the shaft and the rotor blades the teeter bearing is located.

If we can accept, that the model does not provide information about local response of details in the nacelle, the simplification relating to the nacelle and the shaft is reasonable, because it is possible to assign mass, stiffness and damping to the shaft elements, so that the overall coupling between the rotor shaft and the tower reflects the real construction in such a way that acceptable agreement is found for all lower order modes of practical interest. The results obtained with this simplified model will therefore provide the correct blade and rotor loads, which then can be used as input to a model with finer resolution, where the local details of special interest are analysed. Experience with existing response models and wind turbines confirms that the simplification is acceptable, e.g. Patel [P1] and Fabian [F1, pp. 25-34]. When we want to investigate relative changes in response, due to variation of structural parameters, the influence of the simplification is even less important.

2.1 Definition of substructures.

The present model is divided into 3 substructures corresponding to the 3 main components.

The term "substructure" is used by different researchers, but often in relation to different theoretical applications. Bathe [B1, p. 454] uses the term in connection with "substructure analysis", which makes use of static condensation for elimination of internal degrees of freedom. The total structure is considered to be an assemblage of substructures. Each substructure, in turn, is idealized as an assemblage of finite elements, and all internal DOFs are statically condensed out. Each substructure is used as a finite element, and the method is basically a tool for reduction of the number of DOFs. The method is particularly effective, when identical substructures are present.

Meirovitch [M6, pp.384-409] uses the term "substructure synthesis" to describe a wide range of basically identical techniques that analyse a structure by use of a linear combination of mode shapes, or more generally by use of the broader set of admissible functions satisfying the geometric boundary conditions [M6, pp. 242-252], for discretization of the substructures. The method is described as an alternative to the finite element method. The equations of motion

are obtained by use of an energy principle (Lagrange's equations). A very illustrative analysis in [M6, pp. 401-409] describes the theory applied on rotating substructures in general terms. This analysis has been very inspiring for the present work.

The present use of the "substructure" is not in total agreement with any of the two mentioned applications, but can merely be characterized as an appropriate subdivision of the structure, facilitating the actual analysis.

The purpose with the present division is primarily that we want to incorporate the influence on the inertia load of the elastic angular rotations at the tower top and at the shaft end. The chosen substructuring facilitates the introduction of these angular rotations in the kinematic analysis. The considered bearing controlled rotations are furthermore located at the same two points, or at least so close that they can be assumed coincident with good approximation, and no further substructuring is necessary. Other important positive implications follow from the substructuring which will be commented on later in Sec. 2.3, when the degrees of freedom have been defined.

Each substructure has a Cartesian coordinate system attached to it as shown in Fig. 4. The figure shows the undeformed structure. The final model is based on the finite element method using a simple two node prismatic beam element. A typical division of the structure in elements is shown in the figure. The local deformations are assumed small all over the structure, so that linear elastic material properties can be assumed, which means that the relation between the stress and strain is linear. This implies that the linear constitutive relations given in Eq. 4.2.1 are valid.

The elastic rotations of an element within a substructure are assumed infinitesimal, so that rotations still can be described as a vector ([M7, pp. 104-110], [G4, pp. 164-174]). This assumption is made in order to retain a simple relation between rotational degrees of freedom and transformation matrices, which transform vectors from one substructure coordinate system to another or from a finite element to a substructure coordinate system. If finite elastic rotations were allowed the rotations could no longer be described as a vector, which means that the order of the rotations encountered in a transformation would no longer be indifferent and more complicated expressions for the transformations would be necessary.

One possibility is to describe the transformation by use of the Euler angles ([M7, pp. 140-143], [G4, pp. 143-148]) , which refer to 3 rotation angles defined in relation to 3 specific axes. These axes are not perpendicular, but changes their relative position with the angles. Further, a specific sequence of the rotations is prescribed, which makes the transformation unique.

For these reasons the use of the Euler angles for description of finite rotations, partly composed of elastic deformations, will result in rather complicated expressions and additional degrees of freedom must be introduced in order to establish the equations of motion. The use of the simple two node beam element is excluded, and the method is not attractive in the present case.

In [R2] and [R3] the Euler angles have been used for a geometric nonlinear model of moving and rotating rods, resulting in rather complex equations of motion.

If finite rotations should be allowed within a substructure a reasonable description should at the same time allow for an updating of the equilibrium equations in accordance with the change in geometry. This possibility is inherent in many methods, especially those developed for the finite element models.

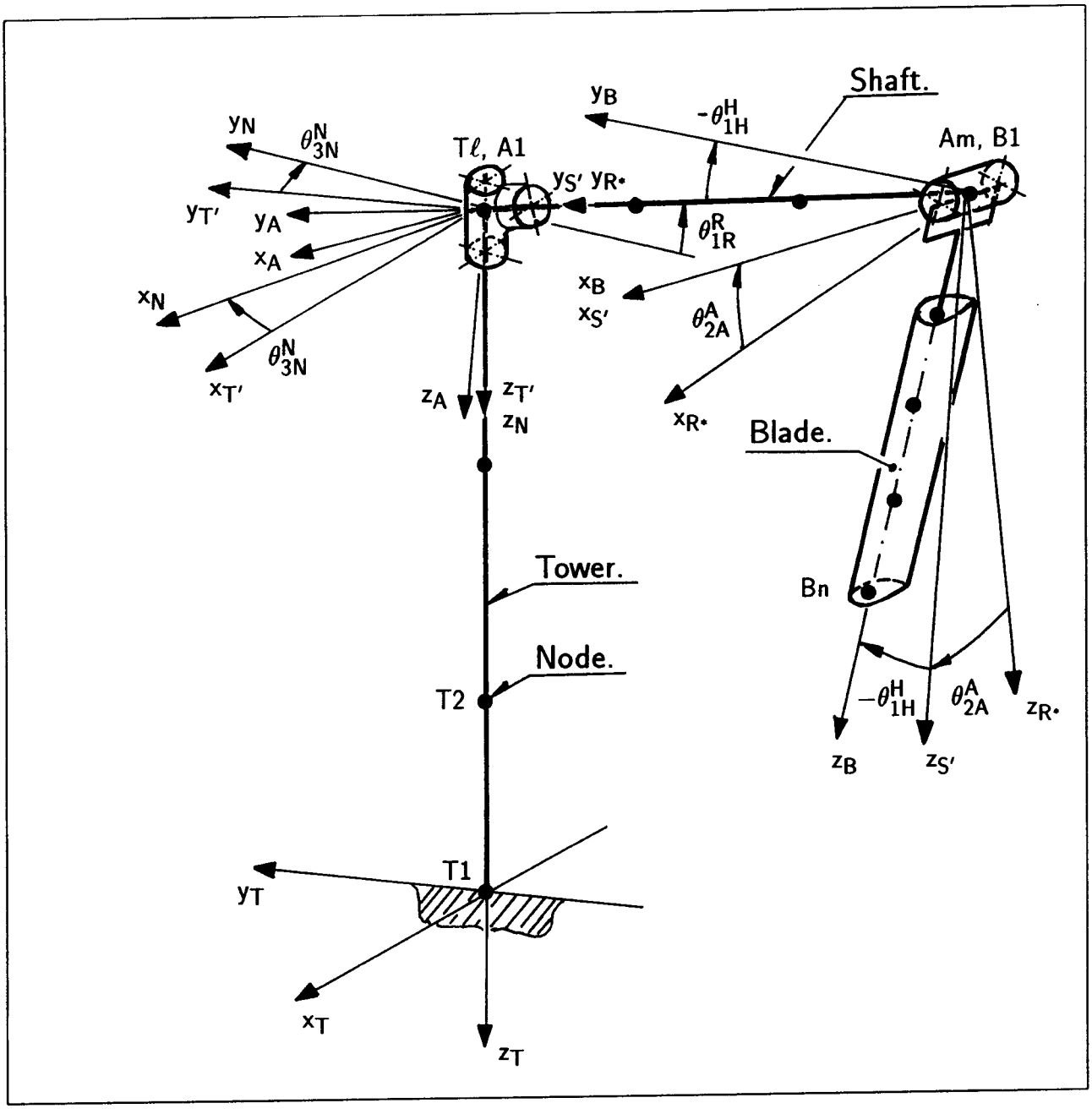

Figure 4: Substructures and coordinate systems. Undeformed state.

Another way of treating finite rotations, especially well suited for numerical solution on a computer, is described in the by now comprehensive litterature dealing with solution of nonlinear structural problems in the finite element method.

As an example, a detailed description is found in [B1, pp. 301-406], where the theory is developed in connection with special finite elements. The main principles in the method shall briefly be mentioned here. The orientation of the element undergoing finite rotations is described by a set of vectors connected to the element nodes. The solution of the structural response to a given load history is achieved by an incremental procedure, where the load is incremented in steps resulting in infinitesimal rotations. In each step the rotations can therefore be treated as vectors and the rotations related to the model DOFs in a straightforward way. Usually the geometry is updated following certain guidelines, but often less frequently than the load step.

The result is a time history of the DOFs comparable directly to what can be observed on the real structure, when the load is applied. Often it is necessary to combine the method with

iterations after each load increment, in order to achieve an acceptable state of equilibrium of the forces involved.

The method is equally well suited for static and dynamic problems, and for problems with all types of nonlinearities, and must be characterized as the most general for solution of structural problems, but constitutes a rather complex model which usually must be run on a main frame computer. The method used in [F1] is similar.

However, the experience with existing wind turbines shows that a model which is able to treat moderate geometric nonlinearities, will be adequate for modelling the next generation of turbines, which probably only will be slightly more flexible than the present generation, in that no big leaps in that direction can be expected, when the industry producing for the world market is considered. Therefore, the present model avoids the use of the more complex finite elements and accepts that only moderate rotations can be permitted.

In the following two subsections the coordinate systems and the transformation matrices involved in the model are described with reference to Fig. 4.

2.2 Definition of coordinate systems.

In Fig. 4 the wind turbine structure is shown in the undeformed state. The figure serves to define the substructures, the attached coordinate systems and the degrees of freedom.

Only one blade is shown, because the complete rotor is described in one common blade substructure coordinate system. The kinematic analysis for one blade point is therefore representative for the complete rotor. The rotor geometry is completely described within the finite element model, which means that for example coning angle, pitch angle and blade twist do not appear in the kinematic analysis.

Further, an example of division in finite elements and the sequence of the node numbering is shown. The node numbering for the blades is not shown in detail, only the numbers for the coupling node to the shaft $(B1)$ and the last node (Bn) are shown. The actual node numbering on the blades is important, when the element equations are assembled, and is shown in relation to the derivation of the substructure equations of motion in Sec. 6 Fig. 18.

The boundaries between substructures are assumed to be single point connections which can be represented by one node.

The node numbering is well suited for referencing the actual points on the structure. It has been chosen as follows

Tower: Nodes are numbered from 1 to ℓ.
Tower node $T1$ is at the tower support.
Tower node $T\ell$ is at the tower top, and common with shaft node $A1$.

Shaft: Nodes are numbered from 1 to m.
Shaft node $A1$ is at the joint to the tower, and common with tower node $T\ell$.
Shaft node Am is at the joint to the blade hub, and common with blade node $B1$.

Blade: Nodes are numbered from 1 to n.
Blade node $B1$ is at the joint to the shaft, and common with shaft node Am.

The reference systems are right handed, rectangular coordinate systems (Cartesian). The axis indices are designated by the symbols x, y, and z, or synonymously by 1, 2, and 3, respectively, throughout the thesis.

All the angles are defined relative to a coordinate axis, and are considered positive when a corresponding rotation of a right hand screw will move the screw in the positive direction of the axis. This definition is throughout the report referred to as e.g. the positive z_T-sense, or just the positive angle, when it is clear from the context which axis is the actual one.

Not all the coordinate systems used in the transformations are shown in Fig. 4 to avoid overcrowding the figure, and others have been displaced parallel relative to the original location, in order to show how other systems move relative to them. All applied coordinate systems will be defined uniquely, when the tranformations are described in Sec. 2.4.

Tower support.

The *tower substructure* coordinate system (index T) has its origin at the tower support at node $T1$. The x_T- and y_T-axis are in a horizontal plane and the z_T-axis is vertical downward. The tower is assumed to be rigidly supported, and the displacements to be zero at the support.

Connection between tower and shaft-nacelle.

At the tower top, at the common node between the tower (node No. $T\ell$) and the shaft (node No. $A1$), several coordinate systems have their origo. The node is the coupling node between the two substructures.

The *shaft substructure* coordinate system (index A) has its origin here. It is rigidly connected to the shaft and corotates with the shaft. The x_A- and z_A-axis are in a plane perpendicular to the shaft axis, and the y_A-axis is coinciding with the shaft axis in the undeformed state and oriented in direction of the mean wind. This set of axes also define the azimuthal position of the rotor, $\theta_{2A}^A = \theta$, which is zero when the z_A-axis is in the vertical plane. The angle is positive in the positive y_A-sense. Because the substructure coordinate system is rigidly attached to the shaft, the deformations of the shaft at this point are zero, measured relative to this reference system.

Further, at the tower top a coordinate system is rigidly attached (index T'). In the undeformed state its axes are parallel to the tower substructure coordinate axes (T). It follows the tower top during elastic deformation, and its angular rotations are identical to the angular deformation at the tower top node, $\left\{\theta_{T\ell}^T\right\}$.

An intermediate coordinate system (index N), serving to define the bearing controlled yaw rotation, is located at the same point. The coordinate system corotates with the nacelle. In the zero-yaw position and the undeformed state its axes are parallel to the tower substructure coordinate axes (T). The yaw angle θ_{3N}^N is the positive rotation about the tower z_T-axis.

The last coordinate system (index R) with origo at the tower top, is a system which is stationary in the nacelle, and has its y_R-axis coinciding with the shaft axis in the undeformed state, i.e. it coincides with the A-system, when the azimuthal position is zero. The coordinate system is rotated the positive angle θ_{1R}^R about the x_R-axis relative to the N-system. θ_{1R}^R is the tilt angle. This coordinate system is not shown in Fig. 4 in its original position, but in a parallel displaced version at the shaft end, identified by the index R^*.

Connection between shaft and blade.

The shaft end node (No. Am) and the center rotor blade node (No. $B1$) coincide, and the common node connects the two substructures.

In order to support the definition of the coordinate systems at this node, the stationary R-system has been parallel displaced to the node, indicated with an upper star on the axis index, R^*.

At the shaft end a coordinate system (index S') is rigidly attached to the node. In the undeformed state its axes are parallel with the axes of the A-coordinate system. The system follows the shaft end during elastic deformation, and its angular rotations are identical to the angular deformation at the shaft end $\left\{\theta^A_{Am}\right\}$, measured relative to the A-system.

The *blade substructure* coordinate system (index B) has its origo at this node. It is corotating with the rotor blades and is rigidly attached to the blades. Its neutral position is coinciding with the S'-system. The B-system can rotate about its x_B-axis. The rotation corresponds to the bearing controlled teeter rotation θ^H_{1H}, which is zero when the two coordinate systems are coincident, and positive in the positive x_B-sense. For a planar rotor, the z_B-axis can be chosen coincident with a blade axis. The actual choice is however not important for a symmetrical non-teetering rotor. Any rotor configuration can be modelled within the blade substructure coordinate system.

Because the substructure coordinate system is rigidly attached to the center blade node, the deformation of the blades at this point are zero, measured relative to this reference system.

2.3 Degrees of freedom.

According to the definitions above, a final summary of the degrees of freedom can be given.

The boundary conditions at the tower support, and the definitions of the substructure coordinate systems for the shaft and the blades, as rigidly attached to the respective substructures, imply that the degrees of freedom for the first node on all three substructures can be eliminated from the equations of motion. The kinematic analysis carried out according to these definitions will ensure that the displacement compatibility at the coupling nodes is fulfilled. The displacement vector at a node is defined by three translations and three rotations, for example for node No. i on the blade substructure (B) as

$$\left\{q^B_{Bi}(t)\right\} = \left\{ \begin{array}{c} \left\{u^B_{Bi}(t)\right\} \\ \left\{\theta^B_{Bi}(t)\right\} \end{array} \right\} = \left\{ \begin{array}{c} u^B_{xBi}(t) \\ u^B_{yBi}(t) \\ u^B_{zBi}(t) \\ \theta^B_{xBi}(t) \\ \theta^B_{yBi}(t) \\ \theta^B_{zBi}(t) \end{array} \right\} \tag{2.3.1}$$

where

u^B_{xBi}, u^B_{yBi}, u^B_{zBi} are translations at the node.

θ^B_{xBi}, θ^B_{yBi}, θ^B_{zBi} are rotations at the node.

Generally, the time dependency is not stated explicitly below, unless it is found that it helps in clarifying the context.

For the substructures, the internal node degrees of freedom are expressed by the vectors

$$\left\{q^B_{BB}\right\} = \begin{Bmatrix} \left\{q^B_{B2}\right\} \\ \left\{q^B_{B3}\right\} \\ \vdots \\ \left\{q^B_{Bn}\right\} \end{Bmatrix}, \quad \left\{q^A_{AA}\right\} = \begin{Bmatrix} \left\{q^A_{A2}\right\} \\ \left\{q^A_{A3}\right\} \\ \vdots \\ \left\{q^A_{A(m-1)}\right\} \end{Bmatrix}, \quad \text{and} \quad \left\{q^T_{TT}\right\} = \begin{Bmatrix} \left\{q^T_{T2}\right\} \\ \left\{q^T_{T3}\right\} \\ \vdots \\ \left\{q^T_{T(\ell-1)}\right\} \end{Bmatrix} \tag{2.3.2}$$

The coupling degrees of freedom are not included in these vectors, because they will appear separately in the equations of motion due to the kinematic coupling between the substructures. The coupling DOFs are

$$\left\{q^T_{T\ell}\right\} = \begin{Bmatrix} \left\{u^T_{T\ell}\right\} \\ \left\{\theta^T_{T\ell}\right\} \end{Bmatrix} = \begin{Bmatrix} u^T_{xT\ell} \\ u^T_{yT\ell} \\ u^T_{zT\ell} \\ \theta^T_{xT\ell} \\ \theta^T_{yT\ell} \\ \theta^T_{zT\ell} \end{Bmatrix} \tag{2.3.3}$$

and

$$\left\{q^A_{Am}\right\} = \begin{Bmatrix} \left\{u^A_{Am}\right\} \\ \left\{\theta^A_{Am}\right\} \end{Bmatrix} = \begin{Bmatrix} u^A_{xAm} \\ u^A_{yAm} \\ u^A_{zAm} \\ \theta^A_{xAm} \\ \theta^A_{yAm} \\ \theta^A_{zAm} \end{Bmatrix} \tag{2.3.4}$$

The remaining degrees of freedom, appearing as scalars in the equations of motion, are

$\theta^N_{3N}(t)$ the yaw angle

$\theta^H_{1H}(t)$ the teeter angle

$\theta^A_{2A}(t)$ the azimuthal position

The tilt angle θ^R_{1R} is constant.

Important implications of the substructuring.

In Sec. 2.1 it was mentioned that the substructuring had other important implications than the appropriate incorporation of the elastic rotations in the kinematic analysis. One implication is that the limitations on the allowable rotations at the nodes on the shaft and the blade substructures are extended, compared to the limitations that had to be imposed, if the structure was described within a common coordinate system, for example the tower system. The reason is

that the rigid body rotations, resulting from the rotations at the coupling nodes, are eliminated from the local substructure rotations, and relative to the common coordinates they can be larger than otherwise, and still be expressed as a vector.

Another implication is that the equations of motion can be easily updated during the solution, with respect to the change in geometry resulting from the coupling rotations, because the updating requires only a limited number of numerical operations. Thus, only the geometric nonlinearities within a substructure need to be considered when the structure is deformed.

2.4 Transformation matrices.

The purpose of this section is to derive the transformation matrices which change the vector components in accordance with change of reference system. Further, the angular velocities of the coordiante systems are introduced.

The components of the three dimensional vectors used to describe positions and deformations and their time derivatives can be referenced to any set of coordinate axes. Throughout the analysis it will be necessary frequently to change the basis for the vectors. The vector notation is explained at the beginning of the symbol list in App. A, and shall not be repeated here. Only, it is important to stress one feature of the notation. The upper right index of a vector indicates what coordinate system its components are referenced to. Only in cases when it is unimportant or when the context makes it clear, what coordinate system is actually used as reference, this identification shall be omitted. Allthough the notation, now and then, may seem to be a little inelegant, it has throughout the derivations proven to be a valuable help, in this way to make it clear, what coordinate system the actual vector is referenced to. Especially when vectors of different origin are combined in an expression. The notation can often serve as a means for control of a vector expression.

When the basis for a vector is changed, the appropriate transformations must be applied. Only when position vectors are dealt with, the actual spatial position of the vector must be taken into account. All other vectors are uniquely defined by their orientation and size, and they can be moved by a parallel displacement to an appropriate position before transformation. This is equivalent to consider the coordinate systems involved in a transformation as having common origin and the vector to start at this origin.

The transformation of such a three dimensional vector from, for example, the tower coordinate system (T) to the shaft coordinate system (A) is expressed by

$$\left\{u^A\right\} = [T_{TA}]\left\{u^T\right\} \tag{2.4.1}$$

where the matrix has dimension 3×3. The columns of the matrix are the components of the projections of the axis unit vectors of the T-system on the axes of the A-system. These components are often denoted the direction cosines of the unit vectors. The lower matrix index TA carries the information that the transformation is from the T- to the A-system. This meaning of the sequence of the indices is adhered to throughout the thesis.

When dealing with Cartesian coordinate systems, the linear transformation expressed by $[T_{TA}]$ is called an orthonormal transformation, because the column vectors of the matrix $\{e_i\}$ have the following properties

$$\{e_i\}^T \{e_j\} = \begin{cases} 1 & \text{for } i = j \\ 0 & \text{for } i \neq j \end{cases} \tag{2.4.2}$$

where i and j are the actual column numbers.

These properties further imply that

$$[T_{TA}]^T = [T_{TA}]^{-1} = [T_{AT}] \tag{2.4.3}$$

where the upper index T denotes the transpose, and the index -1 the inverse of the matrix. The involved transformation matrices and the corresponding angular velocities are derived next.

Tower – elastic tower, $[T_{TT'}]$.

In Fig. 5 the involved rotations are shown. The double arrows are not vectors. They only serve to show the actual rotation axis. The rotations are the elastic deformations at the tower top. The coordinate system with index T_0' corresponds to the undeformed state. The x'-, y'-, and z'-axes show intermediate positions, and the T'-axes correspond to the deformed state. During derivation of the transformation matrix the order of the rotations is assumed to be $\theta^T_{1T\ell}$, $\theta^T_{2T\ell}$, and $\theta^T_{3T\ell}$. In order to avoid the problem of managing the order of the rotations in the final expressions, they are assumed small ($\cos(\theta) \simeq 1$, $\sin(\theta) \simeq \theta$), and the relation to the vector representation of the deformations is kept unique.

The derivation of the transformation matrix and the angular velocity of the T'-system is addressed in App. C, where the linearization is introduced in the final expressions.

The resulting transformation matrix is

$$[T_{TT'}(t)] = \begin{bmatrix} 1 & \theta^T_{3T\ell} & -\theta^T_{2T\ell} \\ -\theta^T_{3T\ell} & 1 & \theta^T_{1T\ell} \\ \theta^T_{2T\ell} & -\theta^T_{1T\ell} & 1 \end{bmatrix} \tag{2.4.4}$$

and the angular velocity of the T'-system relative to the T-system in T-coordinates is

$$\left\{\omega^T_{T'T}(t)\right\} = \begin{Bmatrix} \dot{\theta}^T_{1T\ell} \\ \dot{\theta}^T_{2T\ell} \\ \dot{\theta}^T_{3T\ell} \end{Bmatrix} = \left\{\dot{\theta}^T_{T\ell}\right\} \tag{2.4.5}$$

Elastic tower – nacelle, $[T_{T'N}]$, yaw rotation.

The axes involved in the transformation are shown in Fig. 6

The resulting transformation matrix is

$$[T_{T'N}(t)] = \begin{bmatrix} \cos\left(\theta^N_{3N}\right) & \sin\left(\theta^N_{3N}\right) & 0 \\ -\sin\left(\theta^N_{3N}\right) & \cos\left(\theta^N_{3N}\right) & 0 \\ 0 & 0 & 1 \end{bmatrix} \tag{2.4.6}$$

and the angular velocity of the N-system relative to the T'-system in N-coordinates is

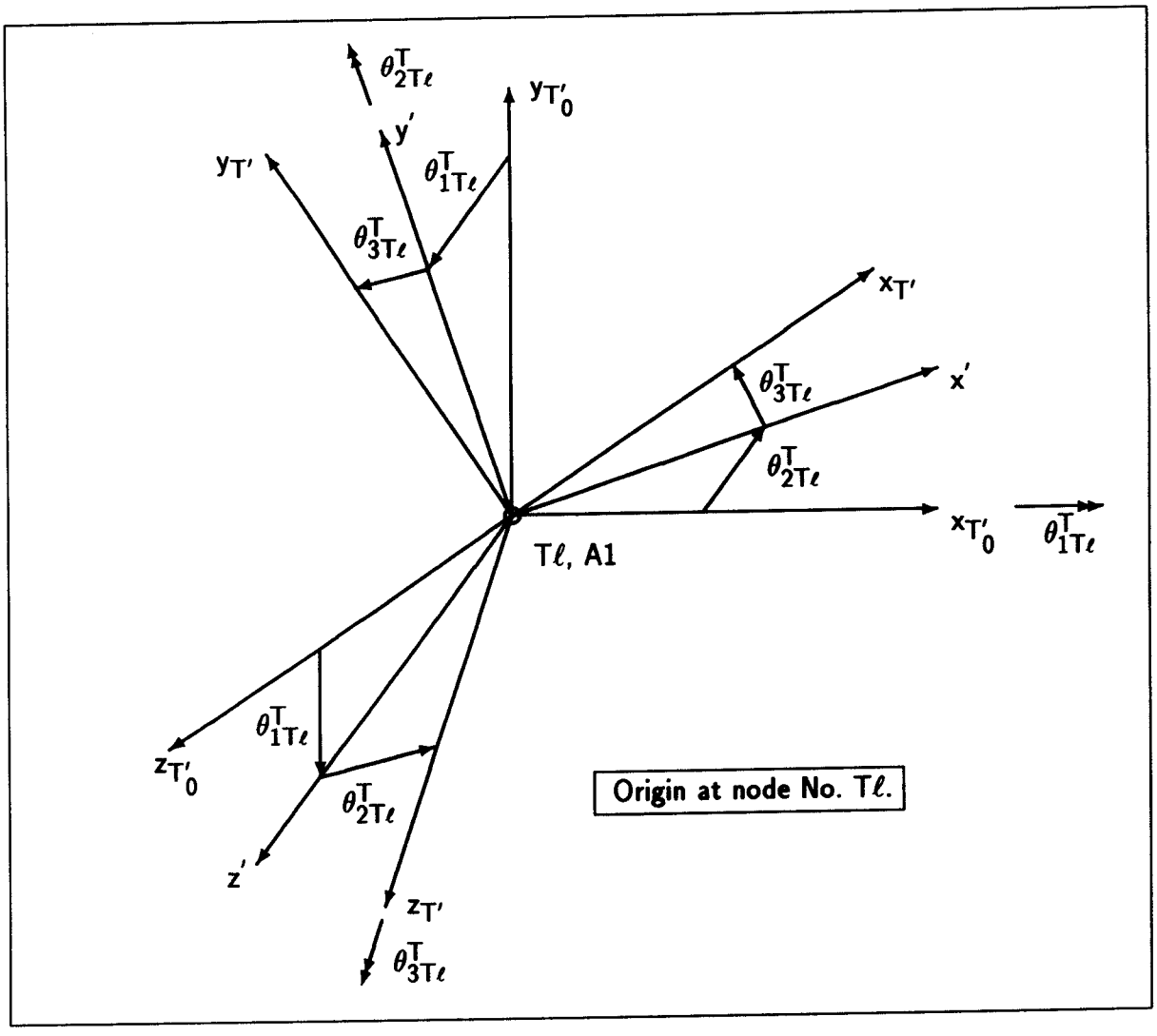

Figure 5: Elastic rotation at tower top, $\left\{\theta^T_{T\ell}\right\}$.

$$\left\{\omega^N_{NT'}(t)\right\} = \begin{Bmatrix} 0 \\ 0 \\ \dot{\theta}^N_{3N} \end{Bmatrix} \tag{2.4.7}$$

Nacelle – shaft tilted, $[T_{NR}]$, tilt angle.

The axes involved in the transformation are shown in Fig. 7

The resulting transformation matrix is

$$[T_{NR}] = \begin{bmatrix} 1 & 0 & 0 \\ 0 & \cos\left(\theta^R_{1R}\right) & \sin\left(\theta^R_{1R}\right) \\ 0 & -\sin\left(\theta^R_{1R}\right) & \cos\left(\theta^R_{1R}\right) \end{bmatrix} \tag{2.4.8}$$

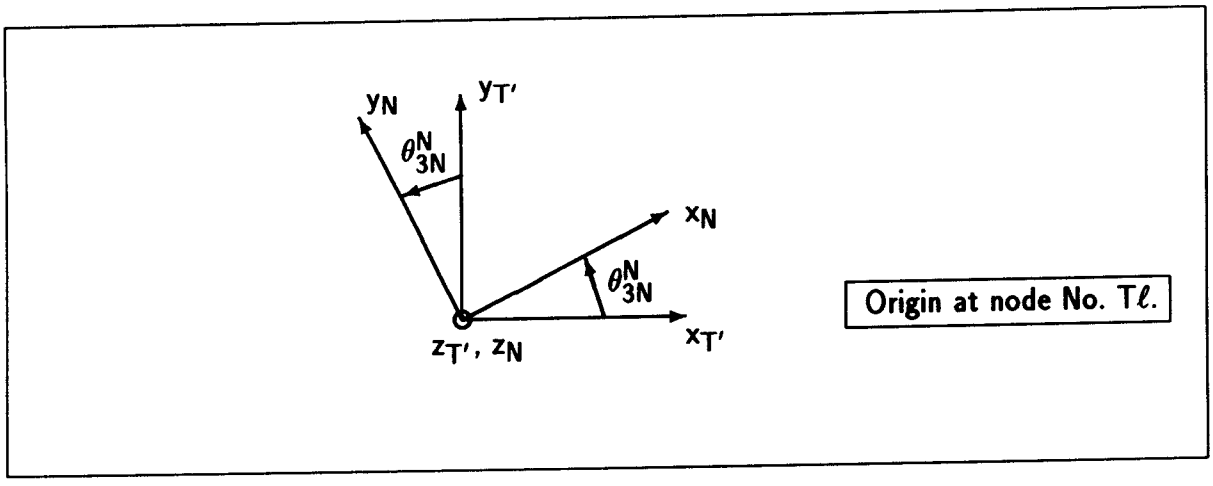

Figure 6: Yaw rotation, θ^N_{3N}.

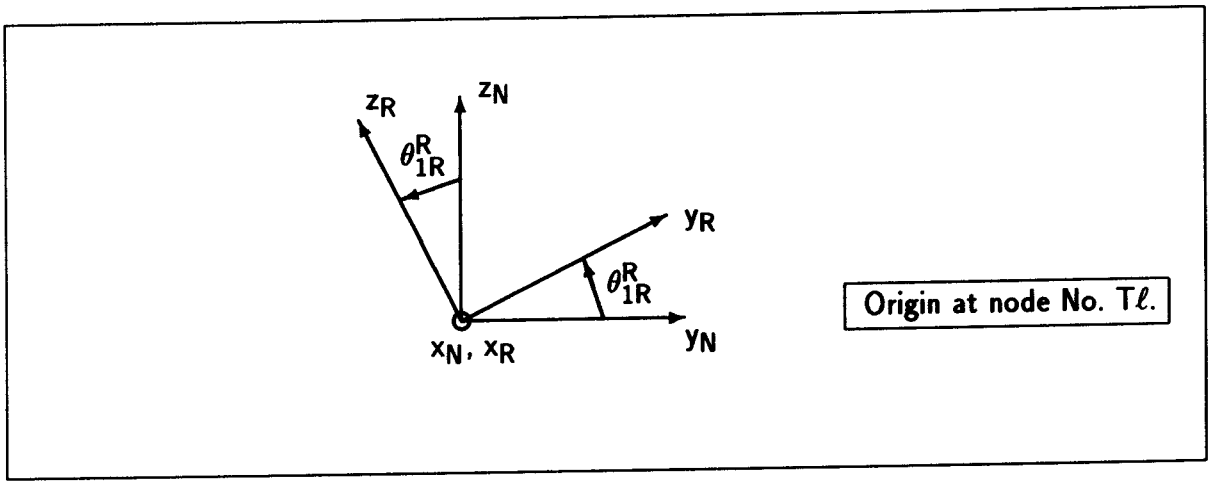

Figure 7: Tilt rotation, θ^R_{1R}.

The tilt angle θ^R_{1R} is constant and therefore the angular velocity of the R-system relative to the N-system is zero

$$\left\{\omega^R_{RN}\right\} = \{0\} \tag{2.4.9}$$

Shaft tilted – shaft substructure, $[T_{RA}]$, azimuthal rotation.

The axes involved in the transformation are shown in Fig. 8

The resulting transformation matrix is

$$[T_{RA}(t)] = \begin{bmatrix} \cos\left(\theta^A_{2A}\right) & 0 & -\sin\left(\theta^A_{2A}\right) \\ 0 & 1 & 0 \\ \sin\left(\theta^A_{2A}\right) & 0 & \cos\left(\theta^A_{2A}\right) \end{bmatrix} \tag{2.4.10}$$

and the angular velocity of the A-system relative to the R-system in A-coordinates is

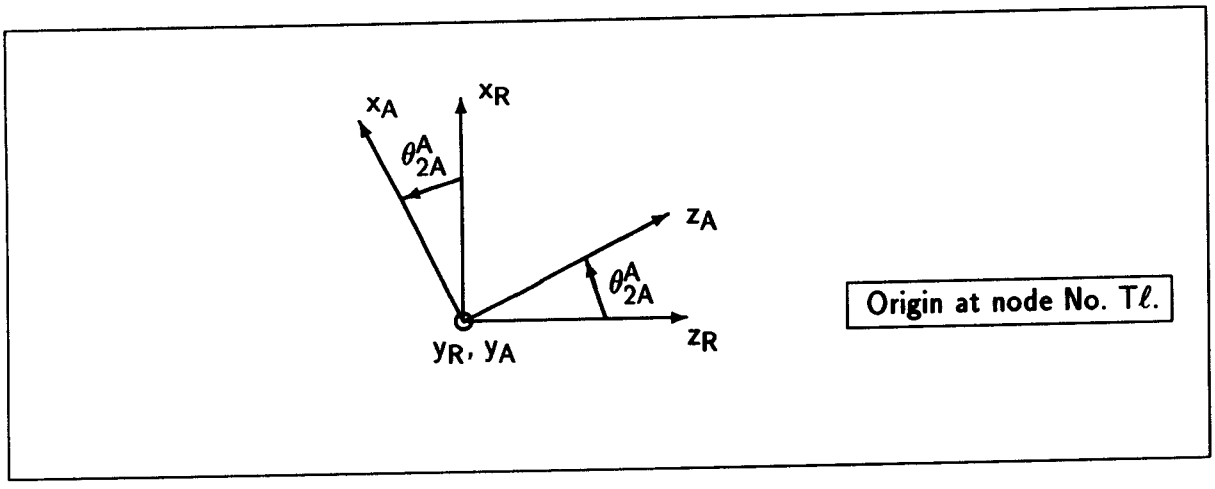

Figure 8: Azimuthal rotation, $\theta^A_{2A} = \theta$.

$$\left\{\omega^A_{AR}(t)\right\} = \left\{\begin{array}{c} 0 \\ \dot{\theta}^A_{2A} \\ 0 \end{array}\right\} = \left\{\begin{array}{c} 0 \\ \omega \\ 0 \end{array}\right\} \tag{2.4.11}$$

Shaft substructure – elastic shaft, $[T_{AS'}]$.

This transformation is equivalent to the transformation between the tower substructure T-system and the coordinate system following the tower top (T'), in that the rotations represent elastic deformations, here at the shaft end, $\left\{\theta^A_{Am}\right\}$.

The resulting transformation matrix is

$$[T_{AS'}(t)] = \left[\begin{array}{ccc} 1 & \theta^A_{3Am} & -\theta^A_{2Am} \\ -\theta^A_{3Am} & 1 & \theta^A_{1Am} \\ \theta^A_{2Am} & -\theta^A_{1Am} & 1 \end{array}\right] \tag{2.4.12}$$

and the angular velocity of the S'-system relative to the A-system in A-coordinates is

$$\left\{\omega^A_{S'A}(t)\right\} = \left\{\begin{array}{c} \dot{\theta}^A_{1Am} \\ \dot{\theta}^A_{2Am} \\ \dot{\theta}^A_{3Am} \end{array}\right\} = \left\{\dot{\theta}^A_{Am}\right\} \tag{2.4.13}$$

Elastic shaft – blade substructure, $[T_{S'B}]$, teeter angle.

The axes involved in the transformation are shown in Fig. 9

The resulting transformation matrix is

$$[T_{S'B}(t)] = \left[\begin{array}{ccc} 1 & 0 & 0 \\ 0 & \cos\left(\theta^H_{1H}\right) & \sin\left(\theta^H_{1H}\right) \\ 0 & -\sin\left(\theta^H_{1H}\right) & \cos\left(\theta^H_{1H}\right) \end{array}\right] \tag{2.4.14}$$

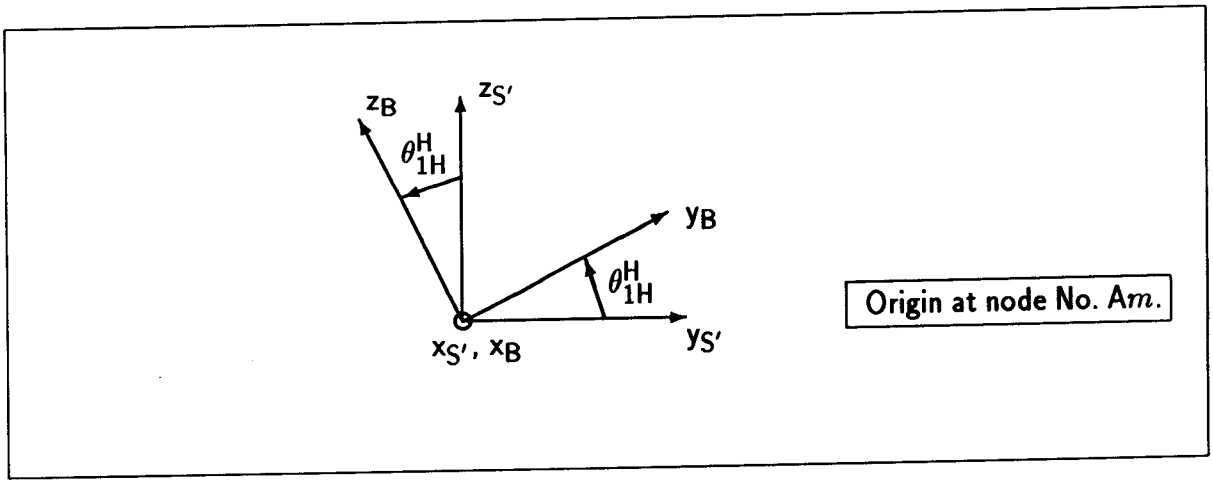

Figure 9: Teeter rotation, θ_{1H}^{H}.

and the angular velocity of the B-system relative to the S'-system in B-coordinates is

$$\left\{\omega_{BS'}^{B}(t)\right\} = \begin{Bmatrix} \dot{\theta}_{1H}^{H} \\ 0 \\ 0 \end{Bmatrix} \tag{2.4.15}$$

Transformation between finite element- and substructure-coordinate system.

The derivation of the matrix which transforms between the local element coordinate system and the substructure coordinate system is described in Sec. 4.8. This matrix is especially actual when the element equations are assembled to the substructure equations of motion, and when deriving the node inertia loads.

Contraction of matrix products.

In the kinematic analysis in Sec. 3, products of transformation matrices appear, representing a chain of successive transformations. In order to simplify the expressions, these products have been contracted, so that the resulting transformation matrix only refers to the first and the last coordinate system in the chain of transformations. But when differentiation with respect to time is carried out, the origin of these contracted matrix products must be remembered in order to differentiate the time dependent matrices correctly.

For example, the contraction of a matrix product representing transformation from the tower T- to the blade B-substructure coordinate system is expressed as

$$[T_{TB}] = [T_{S'B}]\,[T_{AS'}]\,[T_{RA}]\,[T_{NR}]\,[T_{T'N}]\,[T_{TT'}] \tag{2.4.16}$$

The inverse of this transformation matrix is denoted by

$$[T_{TB}]^{-1} = [T_{TB}]^{T} = [T_{BT}] \tag{2.4.17}$$

which expresses transformation from B- to T-coordinates.

3 Kinematic analysis.

In this section the general kinematic analysis for the shaft- and the blade-substructures is carried out. The purpose is to derive expressions for velocity and acceleration for material points on the blade substructure and acceleration for material points on the shaft substructure. The blade velocity enters the equations for aerodynamic force which are derived in [Part 2, Sec. F.3], and the accelerations are used when the distributed inertia loads are derived and transformed to the nodes as described in Sec. 4.11. Due to the chain like structure, the equations concerning the shaft will be a part of the equations concerning the blade. Therefore, the derivation is most conveniently carried out for the blade initially, and from the result of this derivation, the equations for the shaft can be identified.

3.1 Velocity of a point on the blade substructure.

Below, the velocity of a point on the blade substructure relative to the inertial coordinate system (T-system) is derived. The derivation is with reference to the substructures and the coordinate systems described in Sec. 2. The velocity is found as the first time derivative of the position vector from the origin of the tower coordinate system to the point in question. With reference to the tower coordinate system the position vector is written

$$\left\{r^T_{B0}\,(t)\right\} = \left\{r^T_{T\ell}\right\} + \left\{u^T_{T\ell}\,(t)\right\} + \left\{r^T_{Am}\right\} + \left\{u^T_{Am}\,(t)\right\} + \left\{r^T_B\right\} + \left\{u^T_B\,(t)\right\} \tag{3.1.1}$$

or in the shorter notation

$$\left\{r^T_{B0}\right\} = \left\{s^T_{T\ell}\right\} + \left\{s^T_{Am}\right\} + \left\{s^T_B\right\} \tag{3.1.2}$$

where

$\left\{r^T_{T\ell}\right\}$ is the substructure position vector to the tower top for the undeformed tower, i.e. the vector from node No. $T1$ to node No. $T\ell$, (constant)

$\left\{u^T_{T\ell}\right\}$ is the substructure elastic deformation at the tower top, measured relative to the tower substructure coordinates

$\left\{r^T_{Am}\right\}$ is the substructure position vector to the shaft end for the undeformed shaft, i.e. the vector from node No. $A1$ to node No. Am, (constant)

$\left\{u^T_{Am}\right\}$ is the substructure elastic deformation at the shaft end, measured relative to the shaft substructure coordinates

$\left\{r^T_B\right\}$ is the substructure position vector to the blade point for the undeformed blade, i.e. the vector from node No. $B1$ to the blade point, (constant)

$\left\{u^T_B\right\}$ is the substructure elastic deformation at the considered blade point, measured relative to the blade substructure coordinates

and

$\left\{s^T\,(t)\right\} = \left\{r^T\right\} + \left\{u^T\,(t)\right\}$ denotes the position vector in the deformed state.

The differentiation is facilitated when common matrix factors are placed outside a paranthesis, after the basic transformation matrices have been introduced

$$\left\{r^T_{B0}\right\} = \left\{s^T_{T\ell}\right\} + [T_{T'T}]\,[T_{NT'}]\,[T_{RN}]\,[T_{AR}]\left(\left\{s^A_{Am}\right\} + [T_{S'A}]\,[T_{BS'}]\left\{s^B_B\right\}\right) \tag{3.1.3}$$

Differentiating the matrix factors with respect to time, using the chain rule and the expression for differentiation of a time dependent transformation matrix, outlined in App. C, gives

$$\begin{aligned}\frac{d}{dt}\Big([T_{T'T}]\,[T_{NT'}]\,[T_{RN}]\,[T_{AR}]\Big) = \\ [T_{T'T}]\left[\omega^{T'}_{T'T}\right][T_{NT'}]\,[T_{RN}]\,[T_{AR}] + [T_{T'T}]\,[T_{NT'}]\left[\omega^{N}_{NT'}\right][T_{RN}]\,[T_{AR}] \\ + [T_{T'T}]\,[T_{NT'}]\,[T_{RN}]\,[T_{AR}]\left[\omega^{A}_{AR}\right]\end{aligned} \tag{3.1.4}$$

and

$$\frac{d}{dt}\Big([T_{S'A}]\,[T_{BS'}]\Big) = [T_{S'A}]\left[\omega^{S'}_{S'A}\right][T_{BS'}] + [T_{S'A}]\,[T_{BS'}]\left[\omega^{B}_{BS'}\right] \tag{3.1.5}$$

Eqs. 3.1.4 and 3.1.5 are used when differentiating in Eq. 3.1.3, and using the chain rule we get

$$\begin{aligned}\left\{\dot{r}^T_{B0}\right\} = \\ \left\{\dot{s}^T_{T\ell}\right\} \\ + \Big([T_{T'T}]\left[\omega^{T'}_{T'T}\right][T_{AT'}] + [T_{NT}]\left[\omega^{N}_{NT'}\right][T_{AN}] + [T_{AT}]\left[\omega^{A}_{AR}\right]\Big)\Big(\left\{s^A_{Am}\right\} + [T_{BA}]\left\{s^B_B\right\}\Big) \\ + [T_{AT}]\left[\left\{\dot{s}^A_{Am}\right\} + \Big([T_{S'A}]\left[\omega^{S'}_{S'A}\right][T_{BS'}] + [T_{BA}]\left[\omega^{B}_{BS'}\right]\Big)\left\{s^B_B\right\} + [T_{BA}]\left\{\dot{s}^B_B\right\}\right]\end{aligned} \tag{3.1.6}$$

where products of transformation matrices have been contracted, for example

$$[T_{AT'}] = [T_{NT'}]\,[T_{RN}]\,[T_{AR}] \tag{3.1.7}$$

The rotation matrix products are rewritten to vector cross products according to the rules arrived at in App. C, and we get for the velocity

$$
\begin{aligned}
\left\{\dot{r}^T_{B0}\right\} = & \\
& \left\{\dot{s}^T_{T\ell}\right\} \\
& + [T_{T'T}]\left[\left\{\omega^{T'}_{T'T}\right\} \times \left[[T_{AT'}]\left(\left\{s^A_{Am}\right\} + [T_{BA}]\left\{s^B_B\right\}\right)\right]\right] \\
& + [T_{NT}]\left[\left\{\omega^N_{NT'}\right\} \times \left[[T_{AN}]\left(\left\{s^A_{Am}\right\} + [T_{BA}]\left\{s^B_B\right\}\right)\right]\right] \\
& + [T_{AT}]\left[\left\{\omega^A_{AR}\right\} \times \left[\left\{s^A_{Am}\right\} + [T_{BA}]\left\{s^B_B\right\}\right]\right] \\
& + [T_{AT}]\left\{\dot{s}^A_{Am}\right\} \\
& + [T_{S'T}]\left[\left\{\omega^{S'}_{S'A}\right\} \times \left[[T_{BS'}]\left\{s^B_B\right\}\right]\right] \\
& + [T_{BT}]\left[\left\{\omega^B_{BS'}\right\} \times \left\{s^B_B\right\}\right] \\
& + [T_{BT}]\left\{\dot{s}^B_B\right\}
\end{aligned}
\tag{3.1.8}
$$

The velocity is needed in blade element coordinates for the aerodynamic calculation. The best we can do at this stage is to transform to the blade substructure coordinates, thus keeping the manipulations at the symbolic level as far as possible.

The transformation is carried out by premultiplication in Eq. 3.1.7 by $[T_{TB}]$, which gives

$$
\begin{aligned}
\left\{\dot{r}^B_{B0}\right\} = & \\
& [T_{TB}]\left\{\dot{u}^T_{T\ell}\right\} \\
& + \left([T_{TB}]\left\{\omega^T_{T'T}\right\}\right) \times \left[[T_{AB}]\left\{s^A_{Am}\right\} + \left\{s^B_B\right\}\right] \\
& + \left([T_{NB}]\left\{\omega^N_{NT'}\right\}\right) \times \left[[T_{AB}]\left\{s^A_{Am}\right\} + \left\{s^B_B\right\}\right] \\
& + \left([T_{AB}]\left\{\omega^A_{AR}\right\}\right) \times \left[[T_{AB}]\left\{s^A_{Am}\right\} + \left\{s^B_B\right\}\right] \\
& + [T_{AB}]\left\{\dot{u}^A_{Am}\right\} \\
& + \left([T_{AB}]\left\{\omega^A_{S'A}\right\}\right) \times \left\{s^B_B\right\} \\
& + \left\{\omega^B_{BS'}\right\} \times \left\{s^B_B\right\} \\
& + \left\{\dot{u}^B_B\right\}
\end{aligned}
\tag{3.1.9}
$$

where the coordinate reference for each of the rotation vectors $\left\{\omega^T_{T'T}\right\}$ and $\left\{\omega^A_{S'A}\right\}$ has been changed to the T- and A-coordinates, respectively. The two rotations represent elastic deformations, and these substructure coordinates are used in the finite element formulation. Further, the time derivatives of the position vectors have been replaced by the time derivatives of the deformations, which remain after differentiation.

This equation is the basis for calculation of the blade point velocity.

3.2 Acceleration of a point on the blade substructure.

The acceleration of a material point on the blade substructure is derived by taking the time derivative of the velocity from Eq. 3.1.6. Allthough the expressions get rather long, the derivation is straightforward, and steps are involved similar to those just shown for the derivation of the velocity. There is not much information for the reader to gain from this derivation, so the details will be omitted here.

The result in blade substructure coordinates is

$$
\begin{aligned}
\left\{\ddot{r}^B_{B0}\right\} = \\
&[T_{TB}]\left\{\ddot{u}^T_{T\ell}\right\} + [T_{AB}]\left\{\ddot{u}^A_{Am}\right\} + \left\{\ddot{u}^B_B\right\} \\
&+ \left([T_{TB}]\left\{\omega^T_{T'T}\right\}\right) \times \left[\left([T_{TB}]\left\{\omega^T_{T'T}\right\}\right) \times \left[[T_{AB}]\left\{s^A_{Am}\right\} + \left\{s^B_B\right\}\right]\right] \\
&+ \left[2\,[T_{TB}]\left\{\omega^T_{T'T}\right\} + [T_{NB}]\left\{\omega^N_{NT'}\right\}\right] \times \left[\left([T_{NB}]\left\{\omega^N_{NT'}\right\}\right) \times \left[[T_{AB}]\left\{s^A_{Am}\right\} + \left\{s^B_B\right\}\right]\right] \\
&+ \left[2\left([T_{TB}]\left\{\omega^T_{T'T}\right\} + [T_{NB}]\left\{\omega^N_{NT'}\right\}\right) + [T_{AB}]\left\{\omega^A_{AR}\right\}\right] \times \\
&\qquad \left[\left([T_{AB}]\left\{\omega^A_{AR}\right\}\right) \times \left[[T_{AB}]\left\{s^A_{Am}\right\} + \left\{s^B_B\right\}\right]\right] \\
&+ \left[2\left([T_{TB}]\left\{\omega^T_{T'T}\right\} + [T_{NB}]\left\{\omega^N_{NT'}\right\} + [T_{AB}]\left\{\omega^A_{AR}\right\}\right) + [T_{AB}]\left\{\omega^A_{S'A}\right\}\right] \times \\
&\qquad \left[\left([T_{AB}]\left\{\omega^A_{S'A}\right\}\right) \times \left\{s^B_B\right\}\right] \\
&+ \left[2\left([T_{TB}]\left\{\omega^T_{T'T}\right\} + [T_{NB}]\left\{\omega^N_{NT'}\right\} + [T_{AB}]\left\{\omega^A_{AR}\right\} + [T_{AB}]\left\{\omega^A_{S'A}\right\}\right) + \left\{\omega^B_{BS'}\right\}\right] \times \\
&\qquad \left\{\omega^B_{BS'}\right\} \times \left\{s^B_B\right\} \\
&+ 2\left[[T_{TB}]\left\{\omega^T_{T'T}\right\} + [T_{NB}]\left\{\omega^N_{NT'}\right\} + [T_{AB}]\left\{\omega^A_{AR}\right\}\right] \times \left[[T_{AB}]\left\{\dot{u}^A_{Am}\right\} + \left\{\dot{u}^B_B\right\}\right] \\
&+ 2\left[[T_{AB}]\left\{\omega^A_{S'A}\right\} + \left\{\omega^B_{BS'}\right\}\right] \times \left\{\dot{u}^B_B\right\} \\
&+ \left([T_{TB}]\left\{\dot{\omega}^T_{T'T}\right\} + [T_{NB}]\left\{\dot{\omega}^N_{NT'}\right\} + [T_{AB}]\left\{\dot{\omega}^A_{AR}\right\}\right) \times \left[[T_{AB}]\left\{s^A_{Am}\right\} + \left\{s^B_B\right\}\right] \\
&+ \left([T_{AB}]\left\{\dot{\omega}^A_{S'A}\right\} + \left\{\dot{\omega}^B_{BS'}\right\}\right) \times \left[\left\{s^B_B\right\}\right]
\end{aligned}
\tag{3.2.1}
$$

where only the local deformations remain in the position vectors, which have been differentiated with respect to time.

Allthough the expression is more complicated than the well known four term acceleration expression for a single rotating coordinate system, the terms representing the same types of acceleration can be identified in the present expression. The first line is translational acceleration. The following five terms, depending on position, represent centrifugal acceleration. The two terms, depending on the first time derivative of the deformation, represent the Coriolis acceleration. The two last terms in the present equation, depending on the time derivative of the angular velocity ($\{\dot{\omega}\} = \left\{\ddot{\theta}\right\}$), correspond to the fourth term in the simple acceleration expression, which represents nonuniform rotation.

3.3 Acceleration of a point on the shaft substructure.

The expression for the acceleration of a point on the shaft substructure is derived from Eq. 3.2.1, simply by cancelling terms, which are related to degrees of freedom outside the shaft point, where "outside" refers to the structure considered as a chain of elements from tower root to blade point. It is easily seen to be equivalent to carrying out the acceleration analysis for a shaft point, by taking the second time derivative to the position vector to the shaft point.

Cancelling terms in Eq. 3.2.1, and transforming to shaft coordinates at the same time, gives

$$\begin{aligned}
\left\{\ddot{r}^A_{A0}\right\} = & \\
& [T_{TA}]\left\{\ddot{u}^T_{T\ell}\right\} + \left\{\ddot{u}^A_A\right\} \\
& + \left([T_{TA}]\left\{\omega^T_{T'T}\right\}\right) \times \left[\left([T_{TA}]\left\{\omega^T_{T'T}\right\}\right) \times \left\{s^A_A\right\}\right] \\
& + \left[2\,[T_{TA}]\left\{\omega^T_{T'T}\right\} + [T_{NA}]\left\{\omega^N_{NT'}\right\}\right] \times \left[\left([T_{NA}]\left\{\omega^N_{NT'}\right\}\right) \times \left\{s^A_A\right\}\right] \\
& + \left[2\left([T_{TA}]\left\{\omega^T_{T'T}\right\} + [T_{NA}]\left\{\omega^N_{NT'}\right\}\right) + \left\{\omega^A_{AR}\right\}\right] \times \left[\left\{\omega^A_{AR}\right\} \times \left\{s^A_A\right\}\right] \\
& + 2\left[[T_{TA}]\left\{\omega^T_{T'T}\right\} + [T_{NA}]\left\{\omega^N_{NT'}\right\} + \left\{\omega^A_{AR}\right\}\right] \times \left\{\dot{u}^A_A\right\} \\
& + \left([T_{TA}]\left\{\dot{\omega}^T_{T'T}\right\} + [T_{NA}]\left\{\dot{\omega}^N_{NT'}\right\} + \left\{\dot{\omega}^A_{AR}\right\}\right) \times \left\{s^A_A\right\}
\end{aligned} \tag{3.3.1}$$

where now

$$\left\{s^A_A\right\} = \left\{r^A_A\right\} + \left\{u^A_A\right\} \tag{3.3.2}$$

is the position vector to the point in question, i.e. the vector from node No. $A1$ to the shaft point, in the deformed state. After differentiation of this vector with respect to time, only the local deformation remains.

3.4 Evaluation of expressions for velocity and acceleration.

Unfortunately, it is not possible to obtain the equations of motion directly from the relatively simple velocity and acceleration expressions above by manipulations with the expressions on the same level of detail.

In order to get rid of the cross products, the expressions must be evaluated by carrying out the multiplications involved, after introduction of the actual matrices and vectors, as defined in Sec. 2. The results are expressions of considerable length. Each vector component is a sum of products with the factors being transformation terms, components of position vectors, and degrees of freedom and their time derivatives. The majority of the product terms are nonlinear in the degrees of freedom, in the sense that more than one degree of freedom enter such a product.

The actual multiplication is carried out by use of the algebraic programming system Reduce [H2], where also any directions for cancelling of product terms are introduced. The

results from Reduce are sorted according to common factors of degrees of freedom and order of time derivatives, by use of a Fortran 77 filtering program, specially written for the purpose, primarily in order to exclude the introduction of errors during the manipulations, but also to make it easy to repeat the evaluation with a different choice of DOFs represented in the model. This filtering results in vectors and matrix products which are used directly in the final simulation program.

An example of the accelerations obtained in this way is presented in [Part 2, Sec. E]. Nonlinear kinematic terms are to a great extent retained in the acceleration expressions and in the resulting equations of motion. The evaluated velocity expressions are not presented.

4 General analysis of beam element.

In this section the details for the beam element used in the finite element model is outlined. The choice of an optimal element for a finite element model requires a thorough investigation of its own. It has been outside the scope of the present work to go into such detailed investigations. The simple prismatic beam element, equivalent to a Timoshenko beam, has been chosen, partly because it is known to provide a reasonable model of the bending modes which are dominant for the slender substructures of a wind turbine. Further, it has been chosen because it provides a simple model which facilitates the derivations of the element matrices. Especially the derivations of the inertia matrices are kept relatively simple. Still, it serves to illustrate the basic steps in this derivation, which has been found important.

The limitations of the element are primarily related to the blades. The blade is usually twisted and tapered. Due to the twist, the axial blade force will try to un-twist or straighten the blade giving rise to coupling between axial deformation and torsion. The effect may be important for flexible blades with considerable twist. This coupling is not taken care of by the beam element applied in this work. A simple modification to the stiffness matrix can incorporate the dominating part of this coupling [Ø1]. A tapered blade can be reasonably modelled by an appropriate choice of the number of elements.

Often the blades are made of inhomogeneous and anisotropic materials, and the cross section is usually thin-walled and multi-cellular. By calculating integrals of parameter functions over the cross section, reasonable approximations can be estimated for the beam element parameters. The beam element disregards the influence of warping due to shear stresses. In [K2] a method is described to incorporate the warping for cross sections of the present type, but the method is not directly applicable for the present work.

The chosen beam element is prismatic and has constant cross sectional parameters. A complete analysis of the element is carried through in this section. As regards the static equations the analysis follows basically Pedersen [P4, pp. 16-51]. General support has been found through the texts of Pedersen [P3] and Bathe [B1].

4.1 Coordinate system and degrees of freedom.

The element is described in a local element coordinate system with the x– and y–axis coincident with the principal bending axis of the cross section and the z–axis coincident with the elastic axis, which is also denoted the neutral bending axis. The coordinate system is shown in Figure 10.

The element is eventually described to allow for coupling between bending and torsion which may take place, when the shear center lies outside the elastic axis, as shown in Figure 11. The xy–coordinates for the shear center are $(x, y) = (e_{s1}, e_{s2})$. Further, the center of mass is allowed to be positioned outside the elastic axis, which may be the case for inhomogeneous material.

The element length is denoted by ℓ.

The following distributed forces may act on the beam element. They may arise from surface forces or body forces and are resolved after the coordinate axes

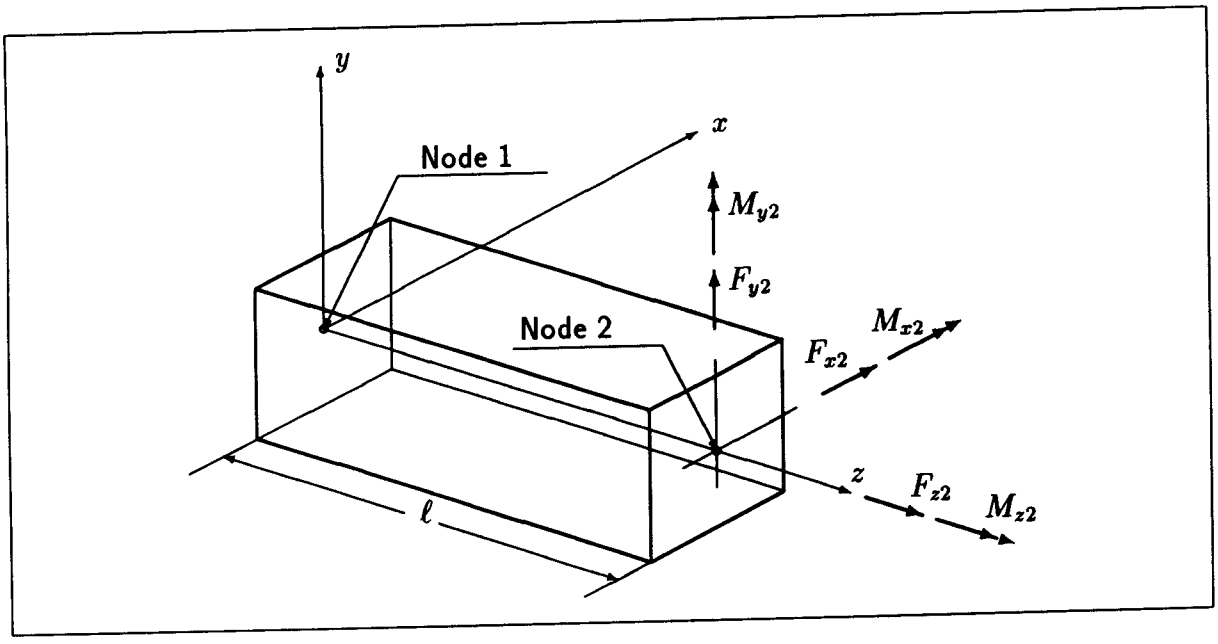

Figure 10: Element coordinate system.

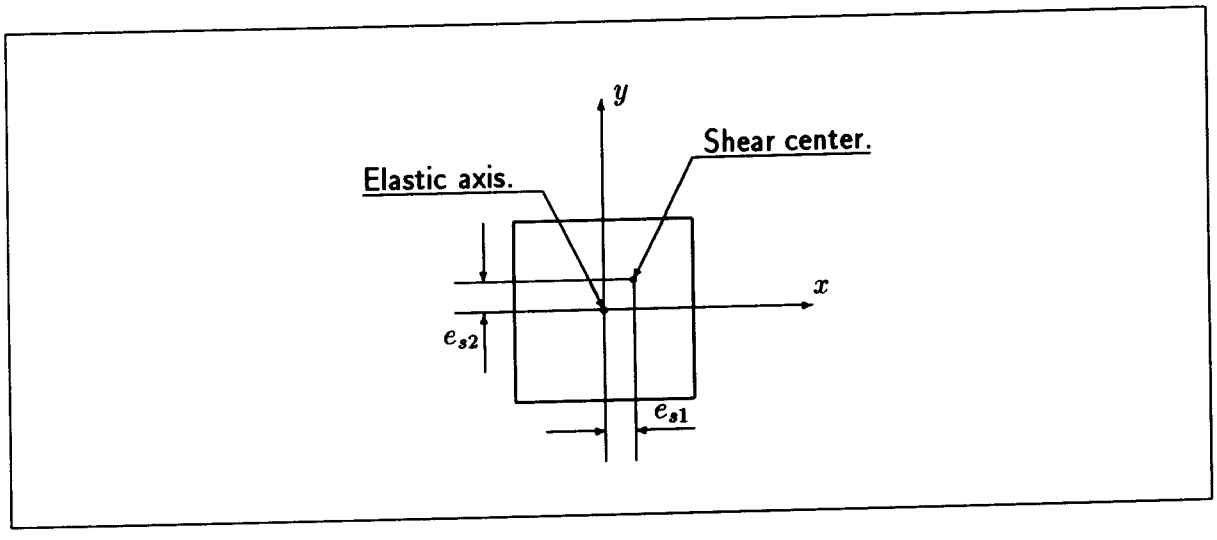

Figure 11: Cross section of beam element.

f_x, f_y, f_z	:	Components after coordinate axis of distributed force, (force per unit length)
m_x, m_y ,m_z	:	Components after coordinate axis of distributed moment, (moment per unit length)

The forces and moments at a cross section of the beam element are shown in Figure 10. Their components are measured in the element coordinate system.

F_x, F_y	:	Cross section shear forces.
F_z	:	Cross section normal force.
M_x, M_y	:	Cross section bending moments.
M_z	:	Cross section torsional moment.

The local deformations of the element are described by the following variables, which refer to the elastic center coordinate system, and still the torsion/bending coupling is not included

u_x : displacement in x–direction of elastic axis, resulting from bending moment about y–axis and shear force in x–direction
u_y : displacement in y–direction of elastic axis, resulting from bending moment about x–axis and shear force in y–direction
u_z : displacement in z–direction of elastic axis, resulting from normal force
θ_x : rotation of plane cross section about x–axis, resulting from bending moment
θ_y : rotation of plane cross section about y–axis, resulting from bending moment
θ_z : rotation about z–axis, resulting from torsional moment

The present theory assumes that the material is linear elastic, and that initially plane cross sections remain plane during the deformation. The warping of the cross section is neglected. The rotation of the elastic axis following from shear force deformation is included, which means that the total rotations of the elastic axis are

$$u_x' = \theta_y + \psi_y \tag{4.1.1}$$

and

$$u_y' = -\theta_x - \psi_x \tag{4.1.2}$$

where ψ_x and ψ_y are the shear rotations.

4.2 Constitutive relations.

With the previously mentioned assumptions the constitutive relations for the beam element can be written

$$\left.\begin{array}{rcl} M_x &=& EI_x\theta_x' \\ M_y &=& EI_y\theta_y' \\ M_{zs} &=& GI_{zs}\theta_z' \\ F_x &=& k_xGA\psi_y \\ F_y &=& -k_yGA\psi_x \\ F_z &=& EAu_z' \end{array}\right\} \tag{4.2.1}$$

where the symbols denote

E modulus of elasticity

G modulus of elasticity in shear

k_x, k_y form factor for shear related to forces in x– and y–direction respectively (calculation of these factors is addressed in [C2])

A cross sectional area

I_x, I_y principal moments of inertia of an area with respect to x– and y–principal bending axis

Further the following new inter–related symbols are introduced

M_{zs} moment about an axis, zs, through the shear center and parallel to the z–axis

I_{zs} torsion constant, (for a circular beam equal to the polar moment of inertia, but in general a more complex function of the geometry of the cross section)

The rotation about the zs–axis is equal to the rotation about the z–axis, $\theta_{zs} = \theta_z$.

By means of Eqs. 4.1.1 and 4.1.2 the shear rotations ψ_x and ψ_y can be eliminated. This reduces the number of deformation parameters to 6.

$$\left.\begin{array}{rcl} M_x &=& EI_x\theta_x' \\ M_y &=& EI_y\theta_y' \\ M_{zs} &=& GI_{zs}\theta_z' \\ F_x &=& k_xGA\left(u_x' - \theta_y\right) \\ F_y &=& k_yGA\left(u_y' + \theta_x\right) \\ F_z &=& EAu_z' \end{array}\right\} \tag{4.2.2}$$

4.3 Static equilibrium equations.

Next the static equilibrium equations are derived in the element coordinate system. Combination of these equations with the constitutive Eqs. 4.2.2 results in a set of differential equations for the deformations.

Moment about x–axis.

Considering an infinitesimal beam element we find

$$\frac{\partial M_x}{\partial z}dz - \frac{1}{2}f_y dz^2 - \frac{\partial F_y}{\partial z}dz^2 - F_y dz + m_x dz = 0 \tag{4.3.1}$$

In the limit this equation reduces to

$$\frac{\partial M_x}{\partial z} - F_y = -m_x \tag{4.3.2}$$

Moment about y–axis.

This is equivalent to Eq. 4.3.2 and omitting the detailled equilibrium eqations in the following we get

$$\frac{\partial M_y}{\partial z} - F_x = -m_y \tag{4.3.3}$$

Moment about zs–axis.

$$\frac{\partial M_{zs}}{\partial z} = -m_{zs} \tag{4.3.4}$$

Introduction of forces and moments measured in the elastic axis principal coordinate system yields

$$\frac{\partial M_z}{\partial z} + \frac{\partial F_x}{\partial z} e_{s2} - \frac{\partial F_y}{\partial z} e_{s1} = -m_z - f_x e_{s2} + f_y e_{s1} \tag{4.3.5}$$

Force in x–direction.

$$\frac{\partial F_x}{\partial z} = -f_x \tag{4.3.6}$$

Force in y–direction.

$$\frac{\partial F_y}{\partial z} = -f_y \tag{4.3.7}$$

Force in z–direction.

$$\frac{\partial F_z}{\partial z} = -f_z \tag{4.3.8}$$

By introduction of the constitutive relations from Eq. 4.2.2, and taking the appropriate derivatives, the forces and moments in Eqs. 4.3.1 – 4.3.8 can be eliminated. This results in the following differential equations

$$EI_x\theta_x'' - k_y GA\left(u_y' + \theta_x\right) = -m_x \tag{4.3.9}$$
$$EI_y\theta_y'' - k_x GA\left(u_x' - \theta_y\right) = -m_y \tag{4.3.10}$$
$$GI_{zs}\theta_z'' = -m_z - f_x e_{s2} + f_y e_{s1} \tag{4.3.11}$$
$$k_x GA\left(u_x'' - \theta_y'\right) = -f_x \tag{4.3.12}$$
$$k_y GA\left(u_y'' + \theta_x'\right) = -f_y \tag{4.3.13}$$
$$EAu_z'' = -f_z \tag{4.3.14}$$

These equations are 2^{nd} order ordinary differential equations with constant coefficients. In the present case the boundary conditions are all taken to be purely geometric, which means that the deformations at both ends of the element are assumed to be known

$$\left.\begin{array}{rcl} \{u\}^T_{x=0} &=& [u_{x1},\, u_{y1},\, u_{z1}] \\ \{u\}^T_{x=\ell} &=& [u_{x2},\, u_{y2},\, u_{z2}] \\ \{\theta\}^T_{x=0} &=& [\theta_{x1},\, \theta_{y1},\, \theta_{z1}] \\ \{\theta\}^T_{x=\ell} &=& [\theta_{x2},\, \theta_{y2},\, \theta_{z2}] \end{array}\right\} \tag{4.3.15}$$

The complete solution is now found as

$$\left\{ \begin{array}{l} \{u(z)\} \\ \{\theta(z)\} \end{array} \right\} = [N(z)]\{q\} + \{d(z)\} \tag{4.3.16}$$

where

$$\{q\}^T = [u_{x1},\, u_{y1},\, u_{z1},\, \theta_{x1},\, \theta_{y1},\, \theta_{z1},\, u_{x2},\, u_{y2},\, u_{z2},\, \theta_{x2},\, \theta_{y2},\, \theta_{z2}] \tag{4.3.17}$$

and

$[N(z)]$ is the interpolation matrix whose elements are the coefficients to the node deformations in the relation between local deformations $\{u(z)\}$ and node deformations $\{q\}$.
The matrix is found from the solution of the homogeneous Eqs. 4.3.9 – 4.3.14.

$\{d(z)\}$ is the solution to the inhomogenous set of differential equations with the homogeneous boundary conditions $\{q\} = \{0\}$.

4.4 Solution of homogeneous equilibrium equations.

In this section the solution to the homogeneous Eqs. 4.3.9–4.3.14 is determined.

First Eq. 4.3.9 is differentiated once and Eq. 4.3.13 is subtracted, giving

$$\theta'''_x = 0 \tag{4.4.1}$$

Integration gives

$$\theta_x = a_1 z^2 + b_1 z + c_1 \tag{4.4.2}$$

Introduction of the boundary conditions in this equation gives

$$\theta_{x1} = c_1 \tag{4.4.3}$$

$$\theta_{x2} = a_1 \ell^2 + b_1 \ell + c_1 \tag{4.4.4}$$

Eq. 4.3.9 is rearranged and the solution for θ_x is introduced

$$\begin{aligned} u'_y &= \frac{EI_x}{k_y GA}\theta''_x - \theta_x \\ &= \frac{EI_x}{k_y GA} 2a_1 - \left(a_1 z^2 + b_1 z + c_1\right) \end{aligned} \tag{4.4.5}$$

and after integration

$$u_y = -\frac{1}{3}a_1 z^3 - \frac{1}{2}b_1 z^2 + \left(\frac{EI_x}{k_y GA}2a_1 - c_1\right) z + d_1 \tag{4.4.6}$$

At the boundary we have

$$u_{y1} = d_1 \tag{4.4.7}$$

$$u_{y2} = -\frac{1}{3}a_1 \ell^3 - \frac{1}{2}b_1 \ell^2 + \left(\frac{EI_x}{k_y GA}2a_1 - c_1\right) \ell + d_1 \tag{4.4.8}$$

Combining Eqs. 4.4.4 and 4.4.8 the values of a_1 and b_1 can be found from

$$\left.\begin{array}{rcl} \ell^2 a_1 + \ell b_1 &=& \theta_{x2} - c_1 \\ \left(2\frac{EI_x}{k_y GA}\ell - \frac{1}{3}\ell^3\right) a_1 - \frac{1}{2}\ell^2 b_1 &=& u_{y2} + c_1\ell - d_1 \end{array}\right\} \tag{4.4.9}$$

The solution is

$$\left.\begin{array}{rcl} a_1 &=& \frac{1}{\ell^3}\left[6\left(u_{y2} - u_{y1}\right) + 3\left(\theta_{x1} + \theta_{x2}\right)\ell\right]\varrho_x \\ b_1 &=& \frac{1}{\ell^2}\left[-6\left(u_{y2} - u_{y1}\right) - 4\theta_{x1}\left(3\eta_x + 1\right)\ell + 2\theta_{x2}\left(6\eta_x - 1\right)\right]\varrho_x \end{array}\right\} \tag{4.4.10}$$

where

$$\eta_x = \frac{EI_x}{k_y GA\ell^2} \tag{4.4.11}$$

and

$$\varrho_x = \frac{1}{1 + 12\eta_x} \tag{4.4.12}$$

Substitution of the values for the constants a_1 and b_1 in Eqs. 4.4.2 and 4.4.6, and using $\varepsilon = \frac{z}{\ell}$ gives

$$\begin{aligned} \theta_x = {} & u_{y1}\left[6\tfrac{1}{\ell}\left(1 - \varepsilon\right)\right]\varepsilon\varrho_x + \\ & u_{y2}\left[-6\tfrac{1}{\ell}\left(1 - \varepsilon\right)\right]\varepsilon\varrho_x + \\ & \theta_{x1}\left[3\left(1 - \varepsilon\right) + 2\left(6\eta_x - 1\right)\right]\left(1 - \varepsilon\right)\varrho_x + \\ & \theta_{x2}\left[3\varepsilon + 2\left(6\eta_x - 1\right)\right]\varepsilon\varrho_x \end{aligned} \tag{4.4.13}$$

$$\begin{aligned} u_y = {} & u_{y1}\left[3\left(1 - \varepsilon\right) - 2\left(1 - \varepsilon\right)^2 + 12\eta_x\right]\left(1 - \varepsilon\right)\varrho_x + \\ & u_{y2}\left[3\varepsilon - 2\varepsilon^2 + 12\eta_x\right]\varepsilon\varrho_x + \\ & \theta_{x1}\left[\left(1 - \varepsilon\right)^2 - \left(1 - 6\eta_x\right)\left(1 - \varepsilon\right) - 6\eta_x\right]\left(1 - \varepsilon\right)\ell\varrho_x + \\ & \theta_{x2}\left[-\left(\varepsilon^2 - \left(1 - 6\eta_x\right)\varepsilon - 6\eta_x\right)\right]\varepsilon\ell\varrho_x \end{aligned} \tag{4.4.14}$$

The same procedure is repeated for Eqs. 4.3.10 and 4.3.12.

$$\theta_y''' = 0 \tag{4.4.15}$$

$$\theta_y = a_2 z^2 + b_2 z + c_2 \tag{4.4.16}$$

$$\theta_{y1} = c_2 \tag{4.4.17}$$

$$\theta_{y2} = a_2 \ell^2 + b_2 \ell + c_2 \tag{4.4.18}$$

$$\begin{aligned} u_x' &= -\frac{EI_y}{k_x GA}\theta_y'' + \theta_y \\ &= -\frac{EI_y}{k_x GA} 2a_2 + \left(a_2 z^2 + b_2 z + c_2\right) \end{aligned} \tag{4.4.19}$$

$$u_x = \frac{1}{3}a_2 z^3 + \frac{1}{2}b_2 z^2 - \left(\frac{EI_y}{k_x GA}2a_2 - c_2\right) z + d_2 \tag{4.4.20}$$

$$u_{x1} = d_2 \tag{4.4.21}$$

$$u_{x2} = \frac{1}{3}a_2 \ell^3 + \frac{1}{2}b_2 \ell^2 - \left(\frac{EI_y}{k_x GA}2a_2 - c_2\right) \ell + d_2 \tag{4.4.22}$$

$$\left.\begin{aligned} \ell^2 a_2 \;+\; \ell b_2 &= \theta_{y2} - c_2 \\ -\left(2\eta_y - \tfrac{1}{3}\right)\ell^3 a_2 \;+\; \tfrac{1}{2}\ell^2 b_2 &= u_{x2} - c_2\ell - d_2 \end{aligned}\right\} \tag{4.4.23}$$

$$\left.\begin{aligned} a_2 &= \tfrac{1}{\ell^3}\left[-6\left(u_{x2} - u_{x1}\right) + 3\left(\theta_{y1} + \theta_{y2}\right)\ell\right]\varrho_y \\ b_2 &= \tfrac{1}{\ell^2}\left[6\left(u_{x2} - u_{x1}\right) - 4\theta_{y1}\left(3\eta_y + 1\right)\ell + 2\theta_{y2}\left(6\eta_y - 1\right)\right]\varrho_y \end{aligned}\right\} \tag{4.4.24}$$

$$\eta_y = \frac{EI_y}{k_x GA\ell^2} \tag{4.4.25}$$

$$\varrho_y = \frac{1}{1 + 12\eta_y} \tag{4.4.26}$$

$$\begin{aligned} \theta_y = {} & u_{x1}\left[-6\tfrac{1}{\ell}\left(1-\varepsilon\right)\right]\varepsilon\varrho_y + \\ & u_{x2}\left[6\tfrac{1}{\ell}\left(1-\varepsilon\right)\right]\varepsilon\varrho_y + \\ & \theta_{y1}\left[3\left(1-\varepsilon\right) + 2\left(6\eta_y - 1\right)\right]\left(1-\varepsilon\right)\varrho_y + \\ & \theta_{y2}\left[3\varepsilon + 2\left(6\eta_y - 1\right)\right]\varepsilon\varrho_y \end{aligned} \tag{4.4.27}$$

$$\begin{aligned} u_x = {} & u_{x1}\left[3\left(1-\varepsilon\right) - 2\left(1-\varepsilon\right)^2 + 12\eta_y\right]\left(1-\varepsilon\right)\varrho_y + \\ & u_{x2}\left[3\varepsilon - 2\varepsilon^2 + 12\eta_y\right]\varepsilon\varrho_y + \\ & \theta_{y1}\left[-\left(\left(1-\varepsilon\right)^2 - \left(1-6\eta_y\right)\left(1-\varepsilon\right) - 6\eta_y\right)\right]\left(1-\varepsilon\right)\ell\varrho_y + \\ & \theta_{y2}\left[\varepsilon^2 - \left(1-6\eta_y\right)\varepsilon - 6\eta_y\right]\varepsilon\ell\varrho_y \end{aligned} \tag{4.4.28}$$

Eq. 4.3.11 is integrated to give θ_z

$$\theta_z = a_3 z + b_3 \tag{4.4.29}$$

while the boundary conditions determine the constants

$$a_3 = \tfrac{1}{\ell}(\theta_{z2} - \theta_{z1}) \tag{4.4.30}$$

$$b_3 = \theta_{z1} \tag{4.4.31}$$

$$\begin{aligned}\theta_z &= \theta_{z1}\left(1 - \frac{z}{\ell}\right) + \theta_{z2}\frac{z}{\ell} \\ &= \theta_{z1}(1-\varepsilon) + \theta_{z2}\varepsilon\end{aligned} \tag{4.4.32}$$

Eq. 4.3.14 is integrated to give u_z. The form of the solution is equivalent to Eq. 4.4.32

$$u_z = u_{z1}(1-\varepsilon) + u_{z2}\varepsilon \tag{4.4.33}$$

In order to simplify the appearance of the interpolation matrix $[N(z)]$, the following definitions are introduced

$$\left.\begin{aligned}
f_1 &= \varepsilon = \tfrac{z}{\ell} \\
f_2 &= (1-\varepsilon) \\
f_3^a &= f_1(3f_1 - 2f_1^2 + 12\eta_a)\varrho_a \\
f_4^a &= f_2(3f_2 - 2f_2^2 + 12\eta_a)\varrho_a \\
f_5^a &= \ell(f_1^2 - (1-6\eta_a)f_1 - 6\eta_a)f_1\varrho_a \\
f_6^a &= \ell(f_2^2 - (1-6\eta_a)f_2 - 6\eta_a)f_2\varrho_a \\
f_7^a &= \tfrac{6}{\ell}f_1 f_2 \varrho_a \\
f_8^a &= f_1(3f_1 - 2(1-6\eta_a))\varrho_a \\
f_9^a &= f_2(3f_2 - 2(1-6\eta_a))\varrho_a
\end{aligned}\right\} \tag{4.4.34}$$

where $a = x$ or $a = y$.

The shape of the functions in Eq. 4.4.34 are shown in Figure 12.

With these definitions the expressions for the deformations are written

$$\left.\begin{aligned}
u_x &= u_{x1}f_4^y + u_{x2}f_3^y + \theta_{y1}(-f_6^y) + \theta_{y2}f_5^y \\
u_y &= u_{y1}f_4^x + u_{y2}f_3^x + \theta_{x1}f_6^x + \theta_{x2}(-f_5^x) \\
u_z &= u_{z1}f_2 + u_{z2}f_1 \\
\theta_x &= u_{y1}f_7^x + u_{y2}(-f_7^x) + \theta_{x1}f_9^x + \theta_{x2}f_8^x \\
\theta_y &= u_{x1}(-f_7^y) + u_{x2}f_7^y + \theta_{y1}f_9^y + \theta_{y2}f_8^y \\
\theta_z &= \theta_{z1}f_2 + \theta_{z2}f_1
\end{aligned}\right\} \tag{4.4.35}$$

and from these equations the interpolation-matrix is directly derived

$$[N(z)] = \left[\begin{array}{ccc|ccc|ccc|ccc}
f_4^y & 0 & 0 & 0 & -f_6^y & 0 & f_3^y & 0 & 0 & 0 & f_5^y & 0 \\
0 & f_4^x & 0 & f_6^x & 0 & 0 & 0 & f_3^x & 0 & -f_5^x & 0 & 0 \\
0 & 0 & f_2 & 0 & 0 & 0 & 0 & 0 & f_1 & 0 & 0 & 0 \\
\hline
0 & f_7^x & 0 & f_9^x & 0 & 0 & 0 & -f_7^x & 0 & f_8^x & 0 & 0 \\
-f_7^y & 0 & 0 & 0 & f_9^y & 0 & f_7^y & 0 & 0 & 0 & f_8^y & 0 \\
0 & 0 & 0 & 0 & 0 & f_2 & 0 & 0 & 0 & 0 & 0 & f_1
\end{array}\right] \tag{4.4.36}$$

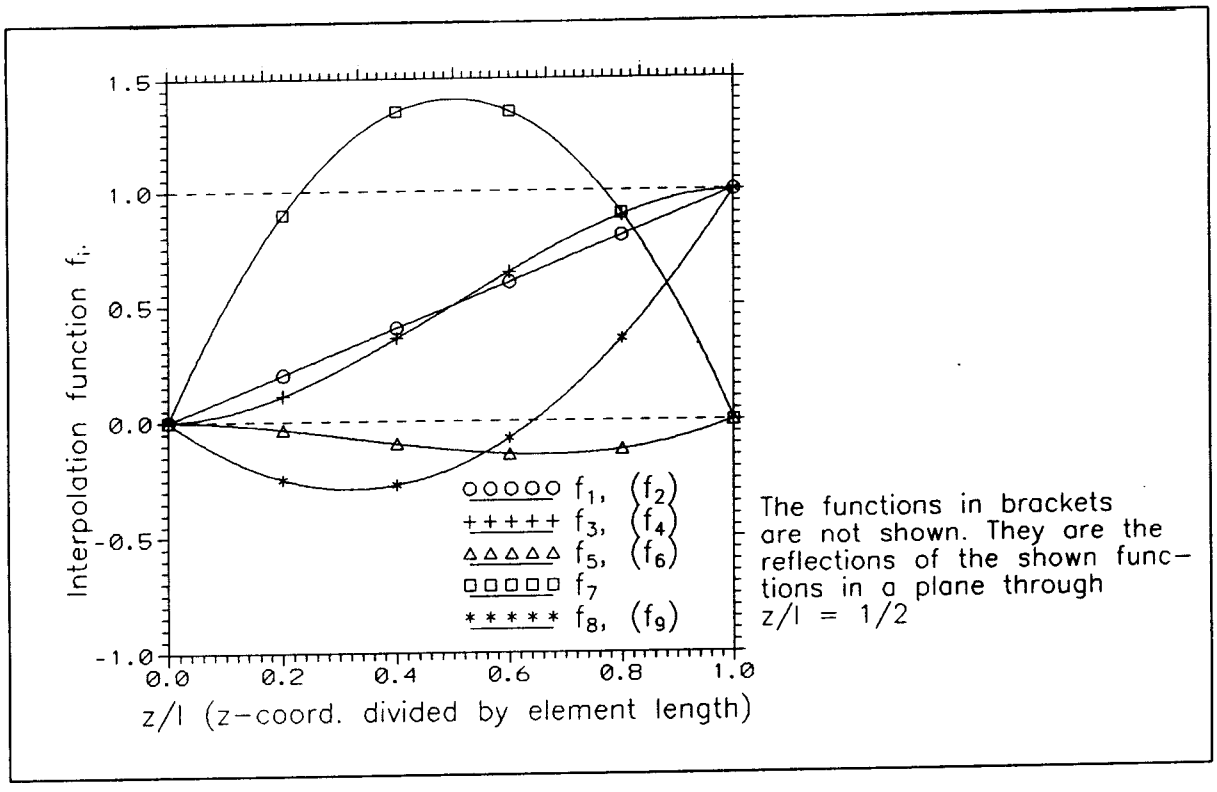

Figure 12: Interpolation functions.

Now the local deformations resulting from node deformations can be found as the first term on the right hand side of Eq. 4.3.16. The local deformations resulting from distributed forces and moments, as represented by the vector $\{d(z)\}$ in Eq. 4.3.16, may be derived from the inhomogeneous set of differential equations 4.3.9 – 4.3.14 with homogeneous boundary conditions, $\{q\} = \{0\}$. However, this solution is only of interest when the exact expression for the total deformations is needed, e.g. in a stress calculation. In the present context we are primarily concerned with the node deformations. They can be derived by a transformation of distributed forces and moments to the nodes, consistent with the principle of virtual displacements, and by solving the equilibrium equations, when the stiffness matrix is known.

The derived interpolation matrix $[N(z)]$, is the basis for the derivation of the stiffness matrix and the consistent node forces and moments. These derivations are outlined in the following subsections.

4.5 Derivation of the beam element stiffness matrix.

The principle of virtual displacements is used to derive the element stiffness matrix.

The work done by the generalized forces acting at the nodes during a virtual generalized displacement of the nodes in accordance with the geometric boundary conditions can be written

$$\delta W = \{\delta q\}^T \{F\} \tag{4.5.1}$$

The elastic energy in the element is given by the expression

$$E = \frac{1}{2}\int_0^\ell \left[\begin{Bmatrix} k_x GA\,(u_x' - \theta_y) \\ k_y GA\,(u_y' + \theta_x) \\ EAu_z' \end{Bmatrix}^T \begin{Bmatrix} u_x' - \theta_y \\ u_y' + \theta_x \\ u_z' \end{Bmatrix} + \begin{Bmatrix} EI_x\theta_x' \\ EI_y\theta_y' \\ GI_{zs}\theta_z' \end{Bmatrix}^T \begin{Bmatrix} \theta_x' \\ \theta_y' \\ \theta_z' \end{Bmatrix} \right] dz \tag{4.5.2}$$

The variation in elastic energy following from a virtual displacement of the nodes is derived from Eq. 4.5.2 and yields

$$\delta E = \int_0^\ell \left[\begin{Bmatrix} u_x' - \theta_y \\ u_y' + \theta_x \\ u_z' \end{Bmatrix}^T \begin{bmatrix} k_x GA & 0 & 0 \\ 0 & k_y GA & 0 \\ 0 & 0 & EA \end{bmatrix} \begin{Bmatrix} \delta u_x' - \delta\theta_y \\ \delta u_y' + \delta\theta_x \\ \delta u_z' \end{Bmatrix} + \begin{Bmatrix} \theta_x' \\ \theta_y' \\ \theta_z' \end{Bmatrix}^T \begin{bmatrix} EI_x & 0 & 0 \\ 0 & EI_y & 0 \\ 0 & 0 & GI_{zs} \end{bmatrix} \begin{Bmatrix} \delta\theta_x' \\ \delta\theta_y' \\ \delta\theta_z' \end{Bmatrix} \right] dz \tag{4.5.3}$$

Separation of the deformations and their derivatives gives

$$\begin{aligned} \delta E = \int_0^\ell \Bigg[& \begin{Bmatrix} u_x' \\ u_y' \\ u_z' \end{Bmatrix}^T \begin{bmatrix} k_x GA & 0 & 0 \\ 0 & k_y GA & 0 \\ 0 & 0 & EA \end{bmatrix} \begin{Bmatrix} \delta u_x' \\ \delta u_y' \\ \delta u_z' \end{Bmatrix} + \\ & \begin{Bmatrix} \theta_x' \\ \theta_y' \\ \theta_z' \end{Bmatrix}^T \begin{bmatrix} EI_x & 0 & 0 \\ 0 & EI_y & 0 \\ 0 & 0 & GI_{zs} \end{bmatrix} \begin{Bmatrix} \delta\theta_x' \\ \delta\theta_y' \\ \delta\theta_z' \end{Bmatrix} + \\ & \begin{Bmatrix} u_x' \\ u_y' \\ u_z' \end{Bmatrix}^T \begin{bmatrix} 0 & -k_x GA & 0 \\ k_y GA & & 0 \\ 0 & 0 & 0 \end{bmatrix} \begin{Bmatrix} \delta\theta_x \\ \delta\theta_y \\ \delta\theta_z \end{Bmatrix} + \\ & \begin{Bmatrix} \theta_x \\ \theta_y \\ \theta_z \end{Bmatrix}^T \begin{bmatrix} 0 & k_y GA & 0 \\ -k_x GA & & 0 \\ 0 & 0 & 0 \end{bmatrix} \begin{Bmatrix} \delta u_x' \\ \delta u_y' \\ \delta u_z' \end{Bmatrix} + \\ & \begin{Bmatrix} \theta_x \\ \theta_y \\ \theta_z \end{Bmatrix}^T \begin{bmatrix} k_y GA & & 0 \\ 0 & k_x GA & 0 \\ 0 & 0 & 0 \end{bmatrix} \begin{Bmatrix} \delta\theta_x \\ \delta\theta_y \\ \delta\theta_z \end{Bmatrix} \Bigg] dz \end{aligned} \tag{4.5.4}$$

The integral is simplified by introduction of the following symbols for vectors and matrices

$$\{u\} = \{u(z)\} = \begin{Bmatrix} u_x \\ u_y \\ u_z \\ \theta_x \\ \theta_y \\ \theta_z \end{Bmatrix} \tag{4.5.5}$$

$$[0_3] = \begin{bmatrix} 0 & 0 & 0 \\ 0 & 0 & 0 \\ 0 & 0 & 0 \end{bmatrix} \tag{4.5.6}$$

$$[S_{11}] = \begin{bmatrix} k_x GA & 0 & 0 \\ 0 & k_y GA & 0 \\ 0 & 0 & EA \end{bmatrix} \tag{4.5.7}$$

$$[S_{22}] = \begin{bmatrix} EI_x & 0 & 0 \\ 0 & EI_y & 0 \\ 0 & & GI_{zs} \end{bmatrix} \tag{4.5.8}$$

$$[S_{21}] = \begin{bmatrix} 0 & k_y GA & 0 \\ -k_x GA & 0 & 0 \\ 0 & 0 & 0 \end{bmatrix} \tag{4.5.9}$$

$$[S_{33}] = \begin{bmatrix} k_y GA & 0 & 0 \\ 0 & k_x GA & 0 \\ 0 & 0 & 0 \end{bmatrix} \tag{4.5.10}$$

$$[S_1] = \begin{bmatrix} [S_{11}] & [0_3] \\ [0_3] & [S_{22}] \end{bmatrix} \tag{4.5.11}$$

$$[S_2] = \begin{bmatrix} [0_3] & [0_3] \\ [S_{21}] & [0_3] \end{bmatrix} \tag{4.5.12}$$

$$[S_3] = \begin{bmatrix} [0_3] & [S_{21}]^T \\ [0_3] & [0_3] \end{bmatrix} = [S_2]^T \tag{4.5.13}$$

$$[S_4] = \begin{bmatrix} [0_3] & [0_3] \\ [0_3] & [S_{33}] \end{bmatrix} \tag{4.5.14}$$

With these definitions the integral in Eq. 4.5.4 reduces to

$$\delta E = \int_0^\ell \left[\{u'\}^T [S_1] \{\delta u'\} + \{u\}^T [S_2] \{\delta u'\} + \{u'\}^T [S_2]^T \{\delta u\} + \{u\}^T [S_4] \{\delta u\} \right] dz \tag{4.5.15}$$

Further the interpolation expression from Eq. 4.3.16 (without deformations resulting from distributed forces, $\{d(z)\}$) is substituted for the local deformation vector

$$\left.\begin{array}{rcl} \{u(z)\} & = & [N(z)]\{q\} \\ \{u'(z)\} & = & [N'(z)]\{q\} \\ \{u(z)\}^T & = & \{q\}^T[N(z)]^T \\ \{u'(z)\}^T & = & \{q\}^T[N'(z)]^T \\ \{\delta u(z)\} & = & [N(z)]\{\delta q\} \\ \{\delta u'(z)\} & = & [N'(z)]\{\delta q\} \end{array}\right\} \tag{4.5.16}$$

resulting in the energy variation

$$\delta E = \{\delta q\}^T \left(\int_0^\ell \left[[N']^T [S_1]^T [N'] + [N']^T [S_2]^T [N] + [N]^T [S_2] [N'] + [N]^T [S_4] [N] \right] dz \right) \{q\} \tag{4.5.17}$$

Equating the external virtual work from Eq. 4.5.1 with the internal virtual work stored as energy from Eq. 4.5.17, according to the principle of virtual displacements, we get the force-displacement relationship

$$\{F\} = [K]\{q\} \tag{4.5.18}$$

where the arbitrary chosen virtual displacement $\{\delta q\}$ has been cancelled by division on both sides of the equation.

From these expressions we get the stiffness matrix for the beam element, which still does not include coupling between bending and torsion

$$[K] = \int_0^\ell \left[[N']^T [S_1]^T [N'] + [N']^T [S_2]^T [N] + [N]^T [S_2] [N'] + [N]^T [S_4] [N] \right] dz \tag{4.5.19}$$

After integration the following symmetric 12×12 stiffness matrix is achieved

$[K] =$

u_{x1}	u_{y1}	u_{z1}	θ_{x1}	θ_{y1}	θ_{z1}	u_{x2}	u_{y2}	u_{z2}	θ_{x2}	θ_{y2}	θ_{z2}
$12\frac{EI_y}{l^3}\varrho_y$	0	0	0	$6\frac{EI_y}{l^2}\varrho_y$	0	$-12\frac{EI_y}{l^3}\varrho_y$	0	0	0	$6\frac{EI_y}{l^2}\varrho_y$	0
...	$12\frac{EI_x}{l^3}\varrho_x$	0	$-6\frac{EI_x}{l^2}\varrho_x$	0	0	0	$-12\frac{EI_x}{l^3}\varrho_x$	0	$-6\frac{EI_x}{l^2}\varrho_x$	0	0
...	...	$\frac{EA}{l}$	0	0	0	0	0	$-\frac{EA}{l}$	0	0	0
...	...	...	$4\frac{EI_x}{l}\alpha_x$	0	0	0	$6\frac{EI_x}{l^2}\varrho_x$	0	$2\frac{EI_x}{l}\beta_x$	0	0
...	...	...	...	$4\frac{EI_y}{l}\alpha_y$	0	$-6\frac{EI_y}{l^2}\varrho_y$	0	0	0	$2\frac{EI_y}{l}\beta_y$	0
...	...	sym−	...	...	$\frac{GI_{xx}}{l}$	0	0	0	0	0	$-\frac{GI_{xx}}{l}$
...	...	...	metric	...	...	$12\frac{EI_y}{l^3}\varrho_y$	0	0	0	$-6\frac{EI_y}{l^2}\varrho_y$	0
...	...	...	...	...	...	...	$12\frac{EI_x}{l^3}\varrho_x$	0	$6\frac{EI_x}{l^2}\varrho_x$	0	0
...	...	...	...	...	...	...	...	$\frac{EA}{l}$	0	0	0
...	...	...	...	...	...	...	...	...	$4\frac{EI_x}{l}\alpha_x$	0	0
...	...	...	...	...	...	...	...	...	...	$4\frac{EI_y}{l}\alpha_y$	0
...	...	...	...	...	...	...	...	...	...	...	$\frac{GI_{xx}}{l}$

(4.5.20)

In the matrix above the following new symbols have been introduced

$$\begin{aligned} \alpha_a &= (1+3\eta_a)\,\varrho_a \\ \beta_a &= (1-6\eta_a)\,\varrho_a \end{aligned}$$

where $a = x$ or $a = y$.

An element in the matrix, k_{ij}, expresses force/moment in degree of freedom No. i from a displacement/rotation in degree of freedom No. j.

4.6 Coordinate system and coupling between bending and torsion.

The displacements and rotations have so far been measured separately with reference to the axis with respect to which the single deformation takes place, as stated at the beginning of this section

u_x	:	displacement in x–direction of elastic axis, resulting from bending moment about y–axis and shear force in x–direction
u_y	:	displacement in y–direction of elastic axis, resulting from bending moment about x–axis and shear force in y–direction
u_z	:	displacement in z–direction of elastic axis, resulting from normal force
θ_x	:	rotation of plane cross section about x–axis, resulting from bending moment
θ_y	:	rotation of plane cross section about y–axis, resulting from bending moment
θ_z	:	rotation about z–axis, resulting from torsional moment

However, in the finite element formulation it is most convenient to measure the deformations in a common coordinate system. This coordinate system is here chosen to be the earlier described elastic axis, principal bending axis coordinate system.

When the neutral torsion axis (shear center) is lying outside the elastic axis, as shown in Fig. 13, where $(x, y) = (e_{s1}, e_{s2})$ are the coordinates of the shear center, torsion will contribute to the displacements u_x and u_y of the elastic axis measured in the chosen coordinate system.

During the derivation of the transformation of the separated deformations to the deformations measured in the common coordinate system, the former are represented unmarked, and the latter are marked with stars.

From Fig. 13 the following relationship can be derived

$$\left.\begin{aligned} u_x &= u_x^* - \theta_z^* e_{s2} \\ u_y &= u_y^* + \theta_z^* e_{s1} \\ u_z &= u_z^* \\ \theta_x &= \theta_x^* \\ \theta_y &= \theta_y^* \\ \theta_z &= \theta_z^* \end{aligned}\right\} \qquad (4.6.1)$$

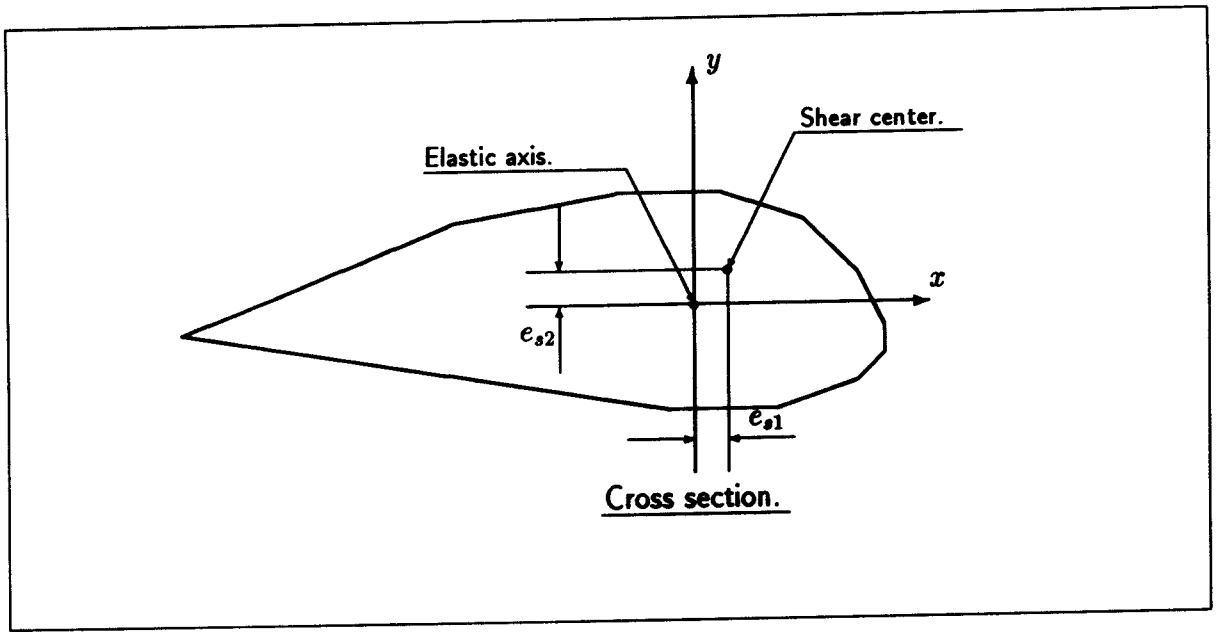

Figure 13: Position of shear center.

which in a matrix equation is expressed as

$$\begin{aligned}\{u\} &= \left[\begin{array}{ccc|ccc} 1 & 0 & 0 & 0 & 0 & -e_{s2} \\ 0 & 1 & 0 & 0 & 0 & e_{s1} \\ 0 & 0 & 1 & 0 & 0 & 0 \\ \hline 0 & 0 & 0 & 1 & 0 & 0 \\ 0 & 0 & 0 & 0 & 1 & 0 \\ 0 & 0 & 0 & 0 & 0 & 1 \end{array}\right] \{u^*\} \\ &= [T_{SB1}]\{u^*\}\end{aligned} \tag{4.6.2}$$

The transformation of the node–deformation vector $\{q\}$ with the double dimension (12×1) is analogously written

$$\{q\} = [T_{SB}]\{q^*\} \tag{4.6.3}$$

where

$$[T_{SB}] = \left[\begin{array}{cc} [T_{SB1}] & [0_3] \\ [0_3] & [T_{SB1}] \end{array}\right] \tag{4.6.4}$$

Equivalently, the relationship between force/moment vectors is derived

$$\left.\begin{array}{rcl} F_x &=& F_x^* \\ F_y &=& F_y^* \\ F_z &=& F_z^* \\ M_x &=& M_x^* \\ M_y &=& M_y^* \\ M_z &=& M_z^* - F_y^* e_{s1} + F_x^* e_{s2} \end{array}\right\} \tag{4.6.5}$$

or expressed as a matrix equation

$$\{F_1\} = [T_{SB1}]^{-T}\{F_1^*\} \tag{4.6.6}$$

where upper index $-T$ denotes inversion and transposition.

The connection between node displacements, $\{q^*\}$, and local displacements, $\{u^*\}$, referred to the elastic axis coordinate system, can now be derived, when coupling between bending and torsion takes place.

By substitution of the derived transformations from Eqs. 4.6.2 and 4.6.3 in the original interpolation relationship

$$\{u(z)\} = [N(z)]\{q\} \tag{4.6.7}$$

we get

$$[T_{SB1}]\{u(z)^*\} = [N(z)][T_{SB}]\{q^*\} \tag{4.6.8}$$

and multiplication on both sides of the equation with $[T_{SB1}]^{-1}$ gives

$$\begin{aligned}\{u(z)^*\} &= [T_{SB1}]^{-1}[N(z)][T_{SB}]\{q^*\} \\ &= [N_{SB}(z)]\{q^*\}\end{aligned} \tag{4.6.9}$$

from which the transformed interpolation matrix is identified as

$$[N_{SB}(z)] = [T_{SB1}]^{-1}[N(z)][T_{SB}] \tag{4.6.10}$$

Carrying out the matrix multiplication we find

$$[N_{SB}(z)] = \left[\begin{array}{ccc|ccc|ccc|ccc} f_4^y & 0 & 0 & 0 & -f_6^y & (f_2-f_4^y)e_{s2} & f_3^y & 0 & 0 & 0 & f_5^y & (f_1-f_3^y)e_{s2} \\ 0 & f_4^x & 0 & f_6^x & 0 & -(f_2-f_4^x)e_{s1} & 0 & f_3^x & 0 & -f_5^x & 0 & -(f_1-f_3^x)e_{s1} \\ 0 & 0 & f_2 & 0 & 0 & 0 & 0 & 0 & f_1 & 0 & 0 & 0 \\ \hline 0 & f_7^x & 0 & f_9^x & 0 & f_7^x e_{s1} & 0 & -f_7^x & 0 & f_8^x & 0 & -f_7^x e_{s1} \\ -f_7^y & 0 & 0 & 0 & f_9^y & f_7^y e_{s2} & f_7^y & 0 & 0 & 0 & f_8^y & -f_7^y e_{s2} \\ 0 & 0 & 0 & 0 & 0 & f_2 & 0 & 0 & 0 & 0 & 0 & f_1 \end{array}\right] \tag{4.6.11}$$

In the following the star index will be omitted, and unless otherwise stated, the deformations are referred to the elastic axis coordinate system.

4.7 Transformation of stiffness matrix to include coupling between bending and torsion.

The coupling between bending and torsion, described in section 4.6, requires a transformation of the stiffness matrix, when the elastic axis coordinate system is used as reference for the deformation.

Again, in what just follows, the separated deformations are unstarred and the deformations referred to the common elastic axis system are starred.

Recalling the force–displacement relationship from Eq. 4.5.18

$$\{F\} = [K]\{q\}$$

and introduction of the transformed vectors, after doupling the dimension of the vector in Eq. 4.6.6 to 12×1

$$\{F\} = [T_{SB}]^{-T}\{F^*\} \tag{4.7.1}$$

and

$$\{q\} = [T_{SB}]\{q^*\} \tag{4.7.2}$$

we get

$$\{F^*\} = [T_{SB}]^T[K][T_{SB}]\{q^*\} \tag{4.7.3}$$

which identifies the transformed stiffness matrix as

$$[K^*] = [T_{SB}]^T[K][T_{SB}] \tag{4.7.4}$$

The transformed matrix is still symmetric. This can be seen from a transposition of the matrix product, which results in the same matrix, characterizing a symmetric matrix.

Unless otherwise stated the transformed stiffness matrix will be referred to unstarred in the following.

Partitioning of the transformed stiffness matrix is introduced in order to simplify its representation

$$[K] = \begin{bmatrix} [K_{11}] & [K_{12}] \\ [K_{12}]^T & [K_{22}] \end{bmatrix} \tag{4.7.5}$$

where the 6×6 submatrices are achieved after multiplication in Eq. 4.7.4

$$[K_{11}] = \left[\begin{array}{ccc|ccc} 12\frac{EI_y}{\ell^3}\varrho_y & 0 & 0 & 0 & 6\frac{EI_y}{\ell^2}\varrho_y & -12\frac{EI_y e_{s2}}{\ell^3}\varrho_y \\ \dots & 12\frac{EI_x}{\ell^3}\varrho_x & 0 & -6\frac{EI_x}{\ell^2}\varrho_x & 0 & 12\frac{EI_x e_{s1}}{\ell^3}\varrho_x \\ \dots & \dots & \frac{AE}{\ell} & 0 & 0 & 0 \\ \hline sym- & \dots & \dots & 4\frac{EI_x}{\ell}\alpha_x & 0 & -6\frac{EI_x e_{s1}}{\ell^2}\varrho_x \\ \dots & metric & \dots & \dots & 4\frac{EI_y}{\ell}\alpha_y & -6\frac{EI_y e_{s2}}{\ell^2}\varrho_y \\ \dots & \dots & \dots & \dots & \dots & \left(\frac{GI_z}{\ell} + 12\frac{E\left(I_x e_{s1}^2 \varrho_x + I_y e_{s2}^2 \varrho_y\right)}{\ell^3}\right) \end{array}\right] \tag{4.7.6}$$

$$[K_{12}] = \left[\begin{array}{ccc|ccc} -12\frac{EI_y}{\ell^3}\varrho_y & 0 & 0 & 0 & 6\frac{EI_y}{\ell^2}\varrho_y & 12\frac{EI_y e_{s2}}{\ell^3}\varrho_y \\ 0 & -12\frac{EI_x}{\ell^3}\varrho_x & 0 & -6\frac{EI_x}{\ell^2}\varrho_x & 0 & -12\frac{EI_x e_{s1}}{\ell^3}\varrho_x \\ 0 & 0 & -\frac{AE}{\ell} & 0 & 0 & 0 \\ \hline 0 & 6\frac{EI_x}{\ell^2}\varrho_x & 0 & 2\frac{EI_x}{\ell}\beta_x & 0 & 6\frac{EI_x e_{s1}}{\ell^2}\varrho_x \\ -6\frac{EI_y}{\ell^2}\varrho_y & 0 & 0 & 0 & 2\frac{EI_y}{\ell}\beta_y & 6\frac{EI_y e_{s2}}{\ell^2}\varrho_y \\ 12\frac{EI_y e_{s2}}{\ell^3}\varrho_y & -12\frac{EI_x e_{s1}}{\ell^3}\varrho_x & 0 & -6\frac{EI_x e_{s1}}{\ell^2}\varrho_x & -6\frac{EI_y e_{s2}}{\ell^2}\varrho_y & \left(-\frac{GI_z}{\ell} - 12\frac{E\left(I_x e_{s1}^2 \varrho_x + I_y e_{s2}^2 \varrho_y\right)}{\ell^3}\right) \end{array}\right] \tag{4.7.7}$$

$$[K_{22}] = \left[\begin{array}{ccc|ccc} 12\frac{EI_y}{\ell^3}\varrho_y & 0 & 0 & 0 & -6\frac{EI_y}{\ell^2}\varrho_y & -12\frac{EI_y e_{s2}}{\ell^3}\varrho_y \\ \dots & 12\frac{EI_x}{\ell^3}\varrho_x & 0 & 6\frac{EI_x}{\ell^2}\varrho_x & 0 & 12\frac{EI_x e_{s1}}{\ell^3}\varrho_x \\ \dots & \dots & \frac{AE}{\ell} & 0 & 0 & 0 \\ \hline sym- & \dots & \dots & 4\frac{EI_x}{\ell}\alpha_x & 0 & 6\frac{EI_x e_{s1}}{\ell^2}\varrho_x \\ \dots & metric & \dots & \dots & 4\frac{EI_y}{\ell}\alpha_y & 6\frac{EI_y e_{s2}}{\ell^2}\varrho_y \\ \dots & \dots & \dots & \dots & \dots & \left(\frac{GI_z}{\ell} + 12\frac{E\left(I_x e_{s1}^2 \varrho_x + I_y e_{s2}^2 \varrho_y\right)}{\ell^3}\right) \end{array}\right] \tag{4.7.8}$$

4.8 Transformation between element- and substructure coordinates.

The transformation of vectors between the element coordinate system and the substructure coordinate system is described in the following.

When a finite beam element do not possess rotational symmetry as regards stiffness, the orientation of the principal bending axes must be taken into account. In the model this is taken care of by introduction of a direction node for each beam element. The node defines the orientation of the principal bending x-axis and thus the orientation of the coordinate system as a whole, in that the z-axis is directed from local node 1 to local node 2.

As the actual handling of these vectors in the model is primarily a matter of program implementation, the details about this are not described. So, below it is presumed that the local element coordinate system has been established. The unit vectors of the element coordinate sytem for element No. i are denoted

$$\left\{e^S_{xEi}\right\} = \begin{Bmatrix} e^S_{1xEi} \\ e^S_{2xEi} \\ e^S_{3xEi} \end{Bmatrix}, \left\{e^S_{yEi}\right\} = \begin{Bmatrix} e^S_{1yEi} \\ e^S_{2yEi} \\ e^S_{3yEi} \end{Bmatrix} \text{ and } \left\{e^S_{zEi}\right\} = \begin{Bmatrix} e^S_{1zEi} \\ e^S_{2zEi} \\ e^S_{3zEi} \end{Bmatrix} \tag{4.8.1}$$

where the components are referenced to the substructure coordinate system (S). They are the direction cosines of the vectors relative to the substructure axes.

The transformation matrix defining the transformation from element coordinates to substructure coordinates is thus expressed by

$$[T_{EiS}] = \begin{bmatrix} e^S_{1xEi} & e^S_{1yEi} & e^S_{1zEi} \\ e^S_{2xEi} & e^S_{2yEi} & e^S_{2zEi} \\ e^S_{3xEi} & e^S_{3yEi} & e^S_{3zEi} \end{bmatrix} \tag{4.8.2}$$

the columns being the components of the unit vectors.

4.9 Geometric stiffness.

When the equilibrium equations are set up in the undeformed state, even if the loads are calculated in the deformed state, the stiffening or softening of an element in the transverse direction, due to axial forces, is not taken into account in the equations, unless special steps have been taken to include this effect.

The stiffness associated with the axial force arranged as a matrix, is usually denoted the geometric stiffness matrix or the initial stress matrix ([P6, pp. 383-391], [C1, pp. 167-173], [Y1]). When the axial force is due mainly to tensile centrifugal forces, as on a wind turbine blade, the stiffening effect is often denoted the centrifugal stiffening. Even though we are dealing with wind turbines, the term geometric stiffness will be preferred in this context, partly because it is more general, but further because it gives associations to a non-negligible change in geometry as the source for the added stiffness terms.

One way to deal with important changes in geometry is to formulate the equilibrium equations for the deformed state and solve them by use of an incremental procedure, where the load is incremented. It is often necessary to iterate during each load increment in order to achieve acceptable equilibrium ([B1, pp. 489-491], [P3, pp. 51-54], [F1, pp. 9-13]). Strictly speaking, the conclusion that the change in geometry is important, is equivalent to conclude that the problem can no longer be considered linear, and nonlinear solution procedures are necessary, or alternatively, an improved linearization must be used. The incremental procedure in combination with iteration is one of the most general solution procedures for non-linear problems.

When the change in geometry is still moderate, a satisfactory linearization by use of a geometric stiffness can be carried through. The influence of the geometric stiffness is quite parallel to the elastic stiffness, and is directly added to the elastic stiffness matrix. Yet, when an element in the substructure formulation is exposed to rigid body rotations, it has an influence on the geometric stiffness, which must be explicitly accounted for in the coupled equations. As the deformations within the substructure coordinate systems are considered moderate, the linearization by use of the geometric stiffness will be applied in the present model.

It should be mentioned here that if the axial force is compressive, the formulation with geometrical stiffness is still adequate, and the equations including geometric stiffness are suitable for solution of column stability problems, e.g. for a slender tower. However, stability problems are not investigated in the present work, and the geometric stiffness is only introduced for the blade substructure.

The derivation of the geometric stiffness matrix is now carried out.

Consider an infinitesimal segment, dz, of a beam finite element with No. i, influenced by an axial force $\left\{F_a^{Ei}\right\}$ as shown in Fig. 14.

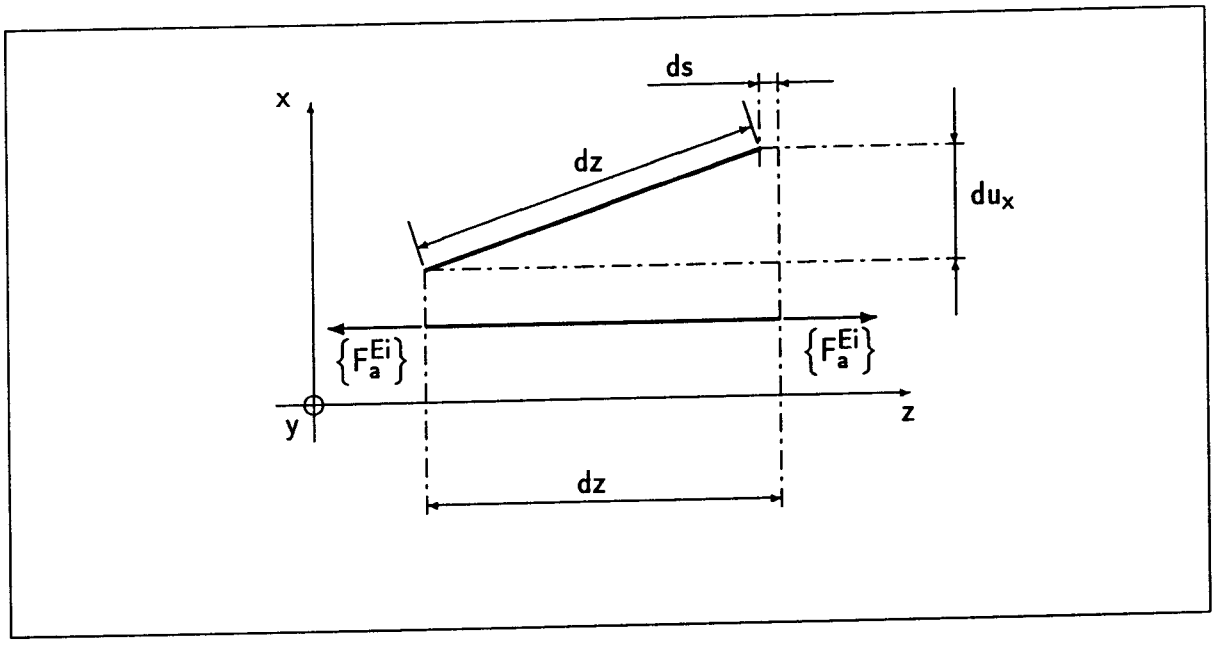

Figure 14: Derivation of geometric stiffness.

The element has been deformed in the tranverse direction resulting in a slope $\frac{du_x}{dz}$. For an element which can be assumed not to extend during the transverse deformation, the projection of the element upon the z-axis will be shortened by an amount of ds. The local work done by the axial force during the transverse deformation is expressed as

$$-dW_{ai}(z) = F_{ai}(z)\,ds \tag{4.9.1}$$

where

$F_{ai}(z) = \left|\left\{F_a^{Ei}(z)\right\}\right|$ is the numerical value of the projection of the axial force.

From a geometric consideration the shortening can be written

$$\begin{aligned} ds &= dz\left(1-\sqrt{1-\left(\frac{du_x}{dz}\right)^2}\right) \\ &\approx \frac{1}{2}\left(\frac{du_x}{dz}\right)^2 dz = \frac{1}{2}\left(u_x'\right)^2 dz \end{aligned} \tag{4.9.2}$$

where the approximation is in accordance with the small deflection assumption.

For beam element No. i of length ℓ_i we get the expression for the total work

$$-W_{ai} = \int_0^{\ell_i} F_{ai}(z)\frac{1}{2}\left[\left(u_x'(z)\right)^2+\left(u_y'(z)\right)^2\right]dz \tag{4.9.3}$$

Here the influence of the transverse displacement in the y-direction has been included analogously to what was done in the x-direction.

The axial force is generally varying with time, among other things caused by the changing influence of gravity. Usually, the contribution from the centrifugal force will be one order of magnitude greater than the contribution from the gravity force. For a typical blade of length 10 m the resulting centrifugal force will be about 20 times the maximum resulting gravity force at the span-wise midpoint of the blade.

Therefore, reasonable results can still be obtained by disregarding the gravity force. Further, when only operation with approximately constant rotor speed is considered, the time varying part of the inertia force can be disregarded, thus only including the dominating centrifugal force. This is done in the following.

The axial force for a finite beam element on the blade can be found approximately as the sum of the inertia forces, which have been consistently transformed to the nodes for all nodes in direction of the blade tip, relative to the element under consideration. As the two node beam finite element is used in the model, this results in a constant axial force along the element. If the beam elements on a blade are numbered from 1 to $(N-1)$, element index $i = 1,..,(N-1)$, and the nodes from 1 to N, node index $n = (i+1),...,N$, we get for element No. i

$$F_{ai} = \left|[T_{EiB}]^T \sum_{n=i+1}^{N}\left\{F_n^B\right\}\right|_{z_{Ei}} \tag{4.9.4}$$

where

$|\bullet|_{z_{Ei}}$ indicates that only the z_{Ei}-component of the force must be taken into account.

The axial force found in this way is only approximate, because it actually varies parabolically along the element. An accurate expression could be found by integrating the inertia force along the element under consideration and summing in Eq. 4.9.4 only the node contributions from the remaining elements in direction of the blade tip. The difference is thus only concerning the contribution from the actual element to node No. $i+1$. This complication is avoided here, keeping in mind that an appropriate resolution in finite elements can provide the wanted accuracy.

With the purpose of using the principle of virtual displacements, we first express the virtual work done by the axial force according to Eq. 4.9.3, when a virtual displacement $\left\{\delta q^{Ei}\right\}$ is imposed at the nodes. Variation of Eq. 4.9.3 gives

$$-\delta W_{ai} = F_{ai} \int_0^{\ell_i} \left[u'_x \delta u'_x + u'_y \delta u'_y \right] dz \tag{4.9.5}$$

Noting that

$$\left\{ \begin{array}{c} u_x \\ u_y \end{array} \right\} = [{}_iN_{SB2}(z)] \left\{ q^{Ei} \right\} \tag{4.9.6}$$

where

$[{}_iN_{SB2}(z)]$ is the submatrix composed of the two first rows of $[{}_iN_{SB}(z)]$, given in Eq. 4.6.11

the integral in Eq. 4.9.5 can be written

$$-\delta W_{ai} = F_{ai} \left\{ \delta q^{Ei} \right\}^T \left[\int_0^{\ell_i} [{}_iN'_{SB2}(z)]^T [{}_iN'_{SB2}(z)] \, dz \right] \left\{ q^{Ei} \right\} \tag{4.9.7}$$

The virtual work done by the node forces $\left\{ F_n^{Ei} \right\}$ is expressed as

$$\delta W_{ni} = \left\{ \delta q^{Ei} \right\}^T \left\{ F_n^{Ei} \right\} \tag{4.9.8}$$

Making use of the fact that the sum of the virtual work done by the external forces must be zero, we get the relation between node force and node deformation, by adding Eqs. 4.9.7 and 4.9.8

$$\left\{ F_g^{Ei} \right\} = \left[K_g^{Ei} \right] \left\{ q^{Ei} \right\} \tag{4.9.9}$$

where the arbitrary virtual displacement has been cancelled and

$$\left[K_g^{Ei} \right] = F_{ai} \left[\int_0^{\ell_i} [{}_iN'_{SB2}(z)]^T [{}_iN'_{SB2}(z)] \, dz \right] \tag{4.9.10}$$

is the geometric stiffness matrix for element No. i, which was sought. The matrix is symmetric and has dimension 12×12.

Transformation of Eq. 4.9.9 to blade substructure coordinates gives

$$\begin{aligned} \left\{ F_g^{Bi} \right\} &= [T_{EiB}] \left\{ F_g^{Ei} \right\} \\ &= [T_{EiB}] \left[K_g^{Ei} \right] [T_{EiB}]^T \left\{ q^{Bi} \right\} \\ &= \left[K_g^{Bi} \right] \left\{ q^{Bi} \right\} \end{aligned} \tag{4.9.11}$$

and this equation is ready for combination into the system equations of motion.

The geometric stiffness matrix for an element is in symbolic form given by

$[K_g^{Ei}] =$

F_{ai}

u_{x1}	u_{y1}	u_{z1}	θ_{x1}	θ_{y1}	θ_{z1}	u_{x2}	u_{y2}	u_{z2}	θ_{x2}	θ_{y2}	θ_{z2}
$K_{1,1}$	0	0	0	$K_{1,5}$	$K_{1,6}$	$-K_{1,1}$	0	0	0	$K_{1,5}$	$-K_{1,6}$
...	$K_{2,2}$	0	$K_{2,4}$	0	$K_{2,6}$	0	$-K_{2,2}$	0	$K_{2,4}$	0	$-K_{2,6}$
...	...	0	0	0	0	0	0	0	0	0	0
...	...	...	$K_{4,4}$	0	$K_{4,6}$	0	$-K_{2,4}$	0	$K_{4,10}$	0	$-K_{4,6}$
...	...	...	...	$K_{5,5}$	$K_{5,6}$	$-K_{1,5}$	0	0	0	$K_{5,11}$	$-K_{5,6}$
...	...	*sym–*	...	...	$K_{6,6}$	$-K_{1,6}$	$-K_{2,6}$	0	$K_{4,6}$	$K_{5,6}$	$-K_{6,6}$
...	...	...	*metric*	...	...	$K_{1,1}$	0	0	0	$-K_{1,5}$	$K_{1,6}$
...	...	...	...	...	...	...	$K_{2,2}$	0	$-K_{2,4}$	0	$K_{2,6}$
...	...	...	...	...	...	...	...	0	0	0	0
...	...	...	...	...	...	...	...	...	$K_{4,4}$	0	$-K_{4,6}$
...	...	...	...	...	...	...	...	...	...	$K_{5,5}$	$-K_{5,6}$
...	...	...	...	...	...	...	...	...	...	...	$K_{6,6}$

(4.9.12)

where only numerically different elements are listed according to the following recipe:

$K_{i,j}$ denotes the non–zero value of the element in row No. i and column No. j, where that particular value first appeared, when the matrix is traversed in a row–wise direction, starting with element $K_{1,1}$.

Next the values of the $K_{i,j}$–elements are listed following the guidelines outlined above, resulting in 13 numerically different elements:

$$
\left.\begin{aligned}
K_{1,1} &= \varrho_y^2(720\eta_y^2 + 120\eta_y + 6)/(5\ell) \\
K_{1,5} &= \varrho_y^2/10 \\
K_{1,6} &= -\left(\varrho_y^2 e_{s2}\left(720\eta_y^2 + 120\eta_y + 6\right)/5 - e_{s2}\right)/\ell \\
K_{2,2} &= \varrho_x^2\left(720\eta_x^2 + 120\eta_x + 6\right)/\left(5\ell\right) \\
K_{2,4} &= -\varrho_x^2/10 \\
K_{2,6} &= \left(\varrho_x^2 e_{s1}\left(720\eta_x^2 + 120\eta_x + 6\right)/5 - e_{s1}\right)/\ell \\
K_{4,4} &= \ell\varrho_x^2\left(180\eta_x^2 + 30\eta_x + 2\right)/15 \\
K_{4,6} &= -\left(\varrho_x^2 e_{s1}\right)/10 \\
K_{4,10} &= -\ell\varrho_x^2\left(360\eta_x^2 + 60\eta_x + 1\right)/30 \\
K_{5,5} &= \ell\varrho_y^2\left(180\eta_y^2 + 30\eta_y + 2\right)/15 \\
K_{5,6} &= -\left(\varrho_y^2 e_{s2}\right)/10 \\
K_{5,11} &= -\ell\varrho_y^2\left(360\eta_y^2 + 60\eta_y + 1\right)/30 \\
K_{6,6} &= \left(\varrho_x^2 e_{s1}^2\left(720\eta_x^2 + 120\eta_x + 6\right)/5\right. \\
&\quad \left. + \varrho_y^2 e_{s2}^2\left(720\eta_y^2 + 120\eta_y + 6\right)/5 - e_{s1}^2 - e_{s2}^2\right)/\ell
\end{aligned}\right\} \qquad (4.9.13)
$$

When the geometric stiffness is introduced in the substructure equilibrium equations, special attention must be payed to the rigid body rotations, which are eliminated in the equations, because these rotations influence the geometric stiffness as it appears in the coupled equations. This subject will be addressed in Sec. 5.

4.10 Consistent transformation of distributed forces and moments to the nodes.

In the finite element formulation the forces and moments, acting outside the nodes, must be transformed to the nodes. In the present context this is done by using the principle of virtual displacements. Formulated in words, the principle states that the work done by the distributed forces and moments must be equal to the work done by the forces and moments transformed to the nodes, when a small virtual node displacement is imposed on the element. The virtual displacements for distributed and node forces must be compatible and satisfy the geometric boundary conditions. Here the compatibility is ensured by the earlier derived interpolation functions represented by the interpolation matrix $[N(z)]$.

The total virtual work done by the distributed forces and moments is expressed in the equation

$$\begin{aligned} \delta W_d &= \int_V \{f_p(x,y,z)\}^T \{\delta u_p(x,y,z)\}\, dxdydz \\ &\quad + \int_0^\ell \{f_\ell(z)\}^T \{\delta u_\ell(z)\}\, dz \\ &= \delta W_p + \delta W_\ell \end{aligned} \tag{4.10.1}$$

where

$$\delta W_p = \int_V \{f_p(x,y,z)\}^T \{\delta u_p(x,y,z)\}\, dxdydz \tag{4.10.2}$$

is the work done by distributed body forces, force per unit volume

$$\{f_p(x,y,z)\}^T = [f_{px}(x,y,z), f_{py}(x,y,z), f_{pz}(x,y,z)] \tag{4.10.3}$$

acting upon an infinitesimal volume of the element, $dxdydz$, during the small virtual local displacement of the volume

$$\{\delta u_p(x,y,z)\}^T = \{\delta u_{px}(x,y,z), \delta u_{py}(x,y,z), \delta u_{pz}(x,y,z)] \tag{4.10.4}$$

and

$$\delta W_\ell = \int_0^\ell \{f_\ell(z)\}^T \{\delta u_\ell(z)\}\, dz \tag{4.10.5}$$

is the work done by the forces and moments distributed along the z–axis of the element, force per unit length

$$\{f_\ell(z)\}^T = [f_{\ell x}(z), f_{\ell y}(z), f_{\ell z}(z), m_{\ell x}(z), m_{\ell y}(z), m_{\ell z}(z)] \tag{4.10.6}$$

during the small virtual displacement (translations and rotations)

$$\{\delta u_\ell(z)\}^T = [\delta u_x(z), \delta u_y(z), \delta u_z(z), \delta\theta_x(z), \delta\theta_y(z), \delta\theta_z(z)] \tag{4.10.7}$$

These expressions are not quite general, because it is assumed that body moments are not present and that surface-forces and -moments have been transformed to the elastic axis. Further, concentrated forces and moments are neglected, because they are only present on a wind turbine in very special cases, and when they are, they can always be placed on the structure at the nodes.

The body forces arise from inertia forces and gravity forces, while the forces and moments, distributed along the elastic axis, will arise mainly from wind loading.

The displacements at a point of the element, with coordinates (x, y, z), are expressed by the relations (refer to Fig. 15)

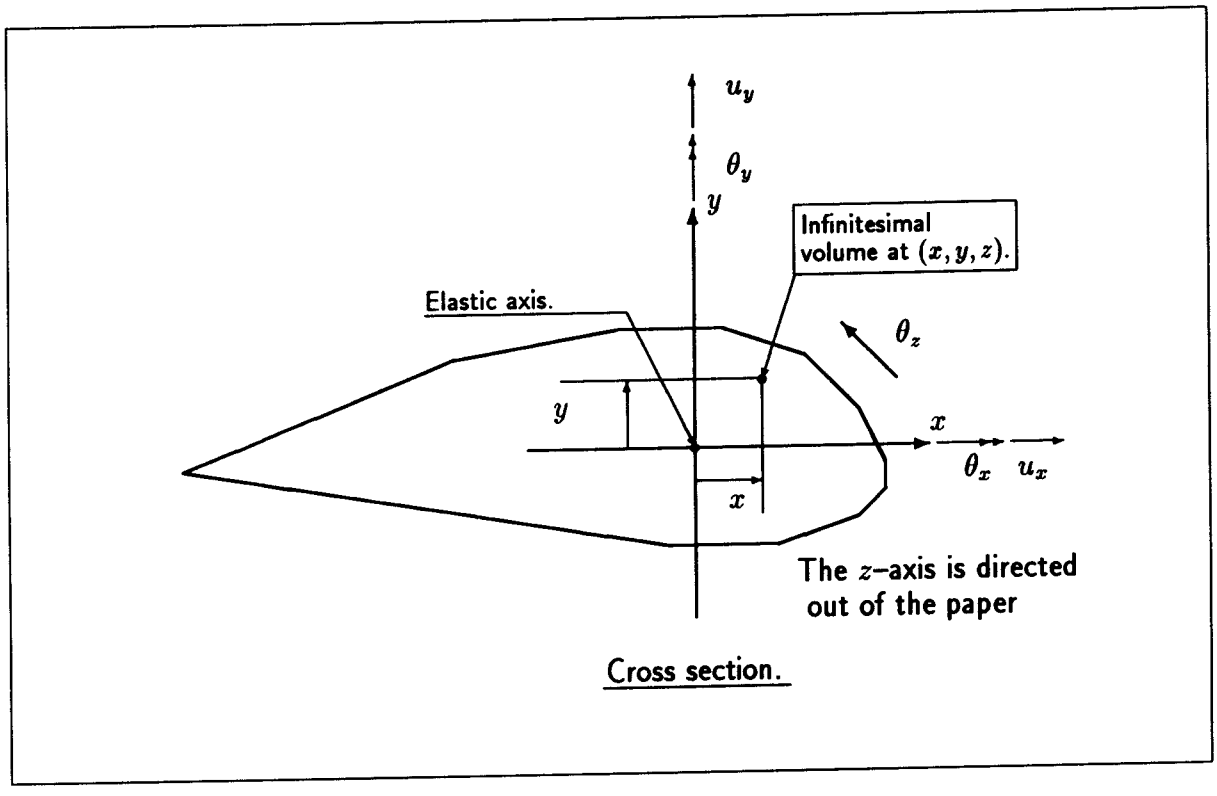

Figure 15: Position of infinitesimal volume.

$$\left.\begin{aligned} u_{px} &= u_x(z) - y\theta_z(z) \\ u_{py} &= u_y(z) + x\theta_z(z) \\ u_{px} &= u_z(z) + y\theta_x(z) - x\theta y(z) \end{aligned}\right\} \tag{4.10.8}$$

or written as a matrix equation

$$\{u_p(x, y, z)\} = [N_T(x, y)]\,\{u(z)\} \tag{4.10.9}$$

where

$$[N_T(x, y)] = \left[\begin{array}{ccc|ccc} 1 & 0 & 0 & 0 & 0 & -y \\ 0 & 1 & 0 & 0 & 0 & x \\ 0 & 0 & 1 & y & -x & 0 \end{array}\right] \tag{4.10.10}$$

and

$$\{u(z)\}^T = [u_x(z), u_y(z), u_z(z), \theta_x(z), \theta_y(z), \theta_z(z)] \tag{4.10.11}$$

is the displacement vector referred to the elastic axis coordinate system.

Now, $\{u(z)\}$ is replaced by the interpolation relationship from Eqs. 4.6.9 (unstarred here) in Eqs. 4.10.1 and 4.10.9 and the new expression for $\{u_p\}$ is introduced in Eq. 4.7.8

$$\begin{aligned} \delta W_d \;=\; \Bigg[& \int_V \{f_p(x,y,z)\}^T [N_T(x,y)]\,[N_{SB}(z)]\,dxdydz \\ & + \int_0^\ell \{f_\ell(z)\}^T [N_{SB}(z)]\,dz \Bigg] \{\delta q\} \end{aligned} \tag{4.10.12}$$

The work done by the forces and moments at the nodes, during the virtual node displacement $\{\delta q\}$, is expressed by

$$\delta W_n = \{F_n\}^T \{\delta q\} \tag{4.10.13}$$

Equating the two work expressions from Eqs. 4.10.12 and 4.10.13 and cancelling the arbitrary chosen virtual displacement $\{\delta q\}$ on both sides of the equation by division, we get the expression for the node forces equivalent to the distributed forces consistent with the principle of virtual displacements

$$\begin{aligned} \{F_n\} \;=\; & \int_V [N_{SB}(z)]^T [N_T(x,y)]^T \{f_p(x,y,z)\}\,dxdydz \\ & + \int_0^\ell [N_{SB}(z)]^T \{f_\ell(z)\}\,dz \end{aligned} \tag{4.10.14}$$

where both sides of the equation have been transposed.

The relevant terms in this equation are derived in following sections for each of the types of distributed force.

4.11 Consistent transformation of inertia loads to the nodes.

In general we consider a substructure of the wind turbine. The substructure is described in a local coordinate system, which may be moving both in translation and rotation. Further, the motion is general, so that both translational and rotational velocities are changing with time. Thus translational and rotational accelerations must be taken into account. The acceleration of a particle on a specific substructure, relative to the inertial coordinate system, is derived in Sec. 3, and it is there denoted by $\left\{\ddot{r}^S_{S0}(x,y,z,t)\right\}$. This acceleration includes both the acceleration of the substructure coordinate system and the local acceleration of the particle, and its components refer to the substructure coordinate system S, as indicated by the upper index S.

The acceleration results in an inertia force on the particle, which according to d'Alembert's principle is

$$\left\{{}_i f^S_{pI}(x,y,z,t)\right\} = -\varrho_i \left\{{}_i \ddot{r}^S_{S0}(x,y,z,t)\right\} \tag{4.11.1}$$

where the meaning of the indices are as follows

S	as upper index indicates that the components of the vector are measured in the substructure coordinate system, as lower index that the vector is to a point on substructure S.
p	refers to body force on a particle of infinitesimal volume.
I	refers to inertia force.
0	refers to inertial coordinate system.
i	refers to element number. In general the element index i is only retained in the equations, when new terms are introduced, and may later on be omitted in order to simplify the indexing, where the possibility for mistake is negligible.

The symbol

ϱ_i	denotes the density of the material for element No. i.

The following analysis of the inertia force considers a single beam element of the substructure. So the inertia force must be transformed to the element coordinate system

$$\left\{{}_i f_{pI}^{Ei}(x,y,z,t)\right\} = -\varrho_i \left[T_{EiS}\right]^T \left\{{}_i \ddot{r}_{S0}^{S}(x,y,z,t)\right\} \tag{4.11.2}$$

where

$[T_{EiS}]$	is the originally derived transformation matrix (refer to Sec. 4.8), which according to the general index rule, transforms a vector from the local element system for element No. i (index Ei) to the substructure system, (index S). Because the matrix is orthonormal, the transformation matrix needed here, the one transforming a vector from the S–system to the Ei–system, is simply the transpose of the originally derived matrix $[T_{SEi}] = [T_{EiS}]^{-1} = [T_{EiS}]^T$.

The upper index

Ei	means that the vector coordinates are with respect to the local element coordinate system.

The coordinate indexing for vectors is retained throughout the report, because the risk for mistake is always present here, and a mistake has serious consequences. The purpose of the following analysis is to transform the distributed inertia loads to consistent nodal loads in accordance with the theory outlined in Sec. 4.10.

To accomplish the analysis the acceleration must be expressed as a function of the substructure coordinates for the nodes and the node displacements.

The acceleration vector $\{\ddot{r}_{S0}^{S}\}$ is the second time derivative of the position vector in the inertial coordinate system to the particle in the substructure coordinate system, $\{r_{S0}^{S}\}$.

The general form of the acceleration $\{\ddot{r}_{S0}^{S}\}$, as derived through the kinematic analysis in Sec. 3, is

$$\{\ddot{r}^S_{S0}\} = [A_S]\{s^S_S\} + [B_S]\{\dot{u}^S_S\} + [C_S]\{\ddot{u}^S_S\} + \{a^S_{Sc}\} \tag{4.11.3}$$

Here, the elements in the coefficient matrices $[A_S]$, $[B_S]$ and $[C_S]$ and the vector $\{a^S_{Sc}\}$ are functions partly of the system parameters and partly of the degrees of freedom for the structure outside the substructure coordinate system, and their time derivatives.

The vector

$\{a^S_{Sc}\}$ is a function of the degrees of freedom, and it is therefore generally time dependent. The vector may be written as a matrix product.

Now the element node coordinates and the element node displacements are introduced in the expression for the acceleration vector in Eq. 4.11.3.

The position vector, in the substructure coordinate system to a particle on element no. i, is written

$$\begin{aligned}\{{}_is^S_S(x,y,z,t)\} &= \{{}_ir^S_1\} + \varepsilon_i\{{}_ir^S_{12}\} + [T_{EiS}]\left[\{{}_ir^{Ei}_p(x,y)\} + [N_T(x,y)][{}_iN_{SB}(z)]\{{}_iq^{Ei}(t)\}\right] \\ &= \{{}_ir^S_1\} + \varepsilon_i\left[\{{}_ir^S_2\} - \{{}_ir^S_1\}\right] \\ &\quad + [T_{EiS}]\left[\{{}_ir^{Ei}_p(x,y)\} + [N_T(x,y)][{}_iN_{SB}(z)]\{{}_iq^{Ei}(t)\}\right]\end{aligned} \tag{4.11.4}$$

where

$\{{}_ir^S_j\}$ is the position vector in the substructure coordinate system to node No. j, $j = 1,2$, for element No. i, (constant).

$\{{}_ir^S_{12}\}$ is the vector from node No. 1 to node No. 2, for element No. i, (constant).

$\{{}_ir^{Ei}_p(x,y)\}^T = [x,y,0]$ is the vector in the plane of the element cross section from the elastic axis to the position of the particle in question, with reference to the Ei–coordinates in the undeformed element.

$[N_T(x,y)][{}_iN_{SB}(z)]\{{}_iq^{Ei}\}$ is the displacement of the particle due to the deformation, which is expressed by the interpolation relation derived in Sec. 4.4. The lower matrix–index i indicates, that the matrix is related to element No. i. Again, the lower vector–index i indicates, that the node deformations are related to element No. i.

$\varepsilon_i = \frac{z}{\ell_i}$ is the normalized z–coordinate in the element coordinate system, $0 \le \varepsilon_i \le 1$.

ℓ_i is the element length.

The time derivatives of the position vector are

$$\{{}_i\dot{u}_S^S\} = [T_{EiS}][N_T][{}_iN_{SB}]\{{}_i\dot{q}^{Ei}\} \tag{4.11.5}$$

and

$$\{{}_i\ddot{u}_S^S\} = [T_{EiS}][N_T][{}_iN_{SB}]\{{}_i\ddot{q}^{Ei}\} \tag{4.11.6}$$

The Eqs. 4.11.4–4.11.6 are introduced into Eq. 4.11.3, which in turn is transformed to the element coordinate system, to give the node displacement dependency in Ei–coordinates for the acceleration (the S index is omitted on the $[A]$, $[B]$ and $[C]$ matrices below)

$$\begin{aligned}\{{}_i\ddot{r}_{S0}^{Ei}\} \;=\; [T_{EiS}]^T \Big[\;& [A]\Big[\{{}_ir_1^S\} + \varepsilon_i\left[\{{}_ir_2^S\} - \{{}_ir_1^S\}\right] \\ & \qquad +[T_{EiS}]\left[\{{}_ir_p^{Ei}\} + [N_T][{}_iN_{SB}]\{{}_iq^{Ei}\}\right]\Big] \\ & +[B][T_{EiS}][N_T][{}_iN_{SB}]\{{}_i\dot{q}^{Ei}\} \\ & +[C][T_{EiS}][N_T][{}_iN_{SB}]\{{}_i\ddot{q}^{Ei}\} + \{a_{Sc}^S\} \;\Big]\end{aligned} \tag{4.11.7}$$

and the inertia load

$$\{{}_if_{pI}^{Ei}\} = -\varrho_i\{{}_i\ddot{r}_{S0}^{Ei}\} \tag{4.11.8}$$

The distributed inertia forces are now transformed to the nodes consistent with the principle of virtual displacements, as outlined in Eq. 4.10.14

$$\{{}_iF_{nIS}^{Ei}\} = \int_V [{}_iN_{SB}]^T[N_T]^T\{{}_if_{pI}^{Ei}\}dxdydz \tag{4.11.9}$$

After substitution of Eqs. 4.11.7 and 4.11.8 into Eq. 4.11.9 and finally reordering the terms to facilitate integration we get

$$\begin{aligned}\{{}_iF_{nIS}^{Ei}\} \;=\; & \left(-\int_0^{\ell_i}[{}_iN_{SB}]^T\left(\int_{A_i}\varrho_i[N_T]^T[T_{EiS}]^T[C][T_{EiS}][N_T]dxdy\right)[{}_iN_{SB}]dz\right)\{{}_i\ddot{q}^{Ei}\} \\ & +\left(-\int_0^{\ell_i}[{}_iN_{SB}]^T\left(\int_{A_i}\varrho_i[N_T]^T[T_{EiS}]^T[B][T_{EiS}][N_T]dxdy\right)[{}_iN_{SB}]dz\right)\{{}_i\dot{q}^{Ei}\} \\ & +\left(-\int_0^{\ell_i}[{}_iN_{SB}]^T\left(\int_{A_i}\varrho_i[N_T]^T[T_{EiS}]^T[A][T_{EiS}][N_T]dxdy\right)[{}_iN_{SB}]dz\right)\{{}_iq^{Ei}\} \\ & +\left(-\int_0^{\ell_i}[{}_iN_{SB}]^T\left(\int_{A_i}\varrho_i[N_T]^T[T_{EiS}]^T[A][T_{EiS}]\{{}_ir_p^{Ei}\}dxdy\right)dz\right) \\ & +\left(-\int_0^{\ell_i}[{}_iN_{SB}]^T\left(\int_{A_i}\varrho_i[N_T]^Tdxdy\right)\varepsilon_idz\right)[T_{EiS}]^T[A]\left(\{{}_ir_2^S\} - \{{}_ir_1^S\}\right) \\ & +\left(-\int_0^{\ell_i}[{}_iN_{SB}]^T\left(\int_{A_i}\varrho_i[N_T]^Tdxdy\right)dz\right)[T_{EiS}]^T\left([A]\{{}_ir_1^S\} + \{a_{Sc}^S\}\right)\end{aligned} \tag{4.11.10}$$

where every single integral now has been divided into a double integral. The inner integral is taken over the cross section and the outer integral over the element length. The inner integrals are all independent of the z–coordinate, which means that the integration in principle can be carried out in two separate steps, the only complication being the fact that the integrals are composed of matrix products, and the order of the factors must be retained.

The integrals in Eq. 4.11.10 are now determined. The integrals covering the area consist in reality of only three different types, because the matrices $[A]$, $[B]$ and $[C]$ all are independent of the coordinates.

For reasons of simplification the following symbols are introduced

$$[T_{EiS}]^T[X][T_{EiS}] = [T^X] \tag{4.11.11}$$

where the elements in the matrix $[T^X]$ are denoted by

$$T^X_{ij} \qquad i,j = 1,2,3 \text{ and } X = A,B,C$$

where X also may be omitted when there is no possibility for mistake.

Further, the following integrals are defined. They appear as results from the integration over the cross section:

$m_i = \int_{A_i} \varrho_i dxdy$: mass per unit length, $[\frac{kg}{m}]$.

$S_{xi} = \int_{A_i} \varrho_i y dxdy$: 1^{st} mass moment with respect to x–axis per unit length $[kg]$.

$S_{yi} = \int_{A_i} \varrho_i x dxdy$: 1^{st} mass moment with respect to y–axis per unit length $[kg]$.

$I_{xi} = \int_{A_i} \varrho_i y^2 dxdy$: mass moment of inertia with respect to x–axis per unit length $[kgm]$.

$I_{yi} = \int_{A_i} \varrho_i x^2 dxdy$: mass moment of inertia with respect to y–axis per unit length $[kgm]$.

$I_{pi} = \int_{A_i} \varrho_i xy dxdy$: product of mass inertia with respect to z–axis per unit length $[kgm]$. $I_{pi} = 0$ here because the coordinate system has been chosen as the principal bending axis system, which is just characterized by the vanishing of I_{pi}.

(4.11.12)

By division of the integrals in Eq. 4.11.12, of order 1 and higher, by m_i, we get the following commonly used quantities:

$$\left.\begin{array}{ll}
\frac{S_{xi}}{m_i} = r_{xi} & : y\text{–coordinate for center of mass.} \\
\frac{S_y}{m_i} = r_{yi} & : x\text{–coordinate for center of mass.} \\
\frac{I_{xi}}{m_i} = r_{Ixi}^2 & : \text{squared radius of inertia, } y\text{–coordinate.} \\
\frac{I_{yi}}{m_i} = r_{Iyi}^2 & : \text{squared radius of inertia, } x\text{–coordinate.}
\end{array}\right\} \tag{4.11.13}$$

The integrations over the cross section area are now carried out. The element number index i and the X–index on the $[T^X]$–matrix are omitted during the derivation, except for the defining equations.

1^{st} integral type over the cross section.

We define the 6×6 matrix

$$[{}_iI_{1AX}] = \int_{A_i} \varrho_i [N_T]^T [T^X] [N_T] dxdy \tag{4.11.14}$$

The matrix product is partitioned in 3×3 matrices

$$[I_{1A}] = \int_A \varrho \begin{bmatrix} [N_{1T}]^T \\ [N_{2T}]^T \end{bmatrix} [T] \left[[N_{1T}] [N_{2T}] \right] dxdy \tag{4.11.15}$$

where

$$[N_{T1}] = \begin{bmatrix} 1 & 0 & 0 \\ 0 & 1 & 0 \\ 0 & 0 & 1 \end{bmatrix} \tag{4.11.16}$$

$$[N_{T2}] = \begin{bmatrix} 0 & 0 & -y \\ 0 & 0 & x \\ y & -x & 0 \end{bmatrix} \tag{4.11.17}$$

The following equation defines the partitioned result

$$[I_{1A}] = \begin{bmatrix} [I_{1A11}] & [I_{1A12}] \\ [I_{1A21}] & [I_{1A22}] \end{bmatrix} \tag{4.11.18}$$

The submatrices in Eq. (4.11.18) are now calculated

$$\begin{aligned}[I_{1A11}] &= \int_A \varrho [N_{T1}]^T [T][N_{T1}] dxdy \\ &= \int_A \varrho [T] dxdy \\ &= m[T] \end{aligned} \tag{4.11.19}$$

The second top–row submatrix is derived

$$\begin{aligned}[I_{1A12}] &= \int_A \varrho [N_{T1}]^T [T][N_{T2}] dxdy \\ &= \int_A \varrho [T][N_{T2}] dxdy \\ &= \int_A \varrho \left[\begin{array}{c|c|c} T_{13}y & -T_{13}x & (-T_{11}y + T_{12}x) \\ T_{23}y & -T_{23}x & (-T_{21}y + T_{22}x) \\ T_{33}y & -T_{33}x & (-T_{31}y + T_{32}x) \end{array}\right] dxdy \\ &= \left[\begin{array}{c|c|c} T_{13}S_x & -T_{13}S_y & (-T_{11}S_x + T_{12}S_y) \\ T_{23}S_x & -T_{23}S_y & (-T_{21}S_x + T_{22}S_y) \\ T_{33}S_x & -T_{33}S_y & (-T_{31}S_x + T_{32}S_y) \end{array}\right] \end{aligned} \tag{4.11.20}$$

Next we look at

$$[I_{1A12}] = \int_A [N_{T2}]^T [T][N_{T1}] dxdy \tag{4.11.21}$$

This matrix is similar to $[I_{1A12}]^T$, only the rows and the columns in $[T]$ have to be interchanged, $T_{ij} = T_{ji}$, in order to achieve agreement.

Finally we integrate

$$\begin{aligned}[I_{1A22}] &= \int_A \varrho [N_{T2}]^T [T][N_{T2}] dxdy \\ &= \int_A \varrho \begin{bmatrix} 0 & 0 & -y \\ 0 & 0 & x \\ y & -x & 0 \end{bmatrix} \left[\begin{array}{c|c|c} T_{13}y & -T_{13}x & (-T_{11}y + T_{12}x) \\ T_{23}y & -T_{23}x & (-T_{21}y + T_{22}x) \\ T_{33}y & -T_{33}x & (-T_{31}y + T_{32}x) \end{array}\right] dxdy \\ &= \int_A \varrho \left[\begin{array}{c|c|c} T_{33}y^2 & -T_{33}xy & (-T_{31}y^2 + T_{32}xy) \\ -T_{33}xy & T_{33}x^2 & (T_{31}xy - T_{32}x^2) \\ (-T_{13}y^2 + T_{23}xy) & (T_{13}xy - T_{23}x^2) & \begin{pmatrix} T_{11}y^2 - T_{12}xy \\ -T_{21}xy + T_{22}x^2 \end{pmatrix} \end{array}\right] dxdy \\ &= \left[\begin{array}{c|c|c} T_{33}I_x & -T_{33}I_p & (-T_{31}I_x + T_{32}I_p) \\ -T_{33}I_p & T_{33}I_y & (T_{31}I_p - T_{32}I_y) \\ (-T_{13}I_x + T_{23}I_p) & (T_{13}I_p - T_{23}I_y) & \begin{pmatrix} T_{11}I_x - T_{12}I_p \\ -T_{21}I_p + T_{22}I_y \end{pmatrix} \end{array}\right] \end{aligned} \tag{4.11.22}$$

The complete matrix in Eq. 4.11.18 can now be written. We make use of the fact, that $I_p = 0$ in the principal axis coordinate system. Further all elements are divided by m, which is placed

as a common factor in front of the matrix, making use of Eqs. 4.11.12 and 4.11.13, when the resulting matrix elements are derived

$$[I_{1A}] =$$

$$\mathrm{m}\left[\begin{array}{ccc|ccc} T_{11} & T_{12} & T_{13} & T_{13}r_x & -T_{13}r_y & (-T_{11}r_x + T_{12}r_y) \\ T_{21} & T_{22} & T_{23} & T_{23}r_x & -T_{23}r_y & (-T_{21}r_x + T_{22}r_y) \\ T_{31} & T_{32} & T_{33} & T_{33}r_x & -T_{33}r_y & (-T_{31}r_x + T_{32}r_y) \\ \hline T_{31}r_x & T_{32}r_x & T_{33}r_x & T_{33}r_{Ix}^2 & 0 & -T_{31}r_{Ix}^2 \\ -T_{31}r_y & -T_{32}r_y & -T_{33}r_y & 0 & T_{33}r_{Iy}^2 & -T_{32}r_{Iy}^2 \\ (-T_{11}r_x + T_{21}r_y) & (-T_{12}r_x + T_{22}r_y) & (-T_{13}r_x + T_{23}r_y) & -T_{13}r_{Ix}^2 & -T_{23}r_{Iy}^2 & (T_{11}r_{Ix}^2 + T_{22}r_{Iy}^2) \end{array}\right] \tag{4.11.23}$$

2^{nd} integral type over the cross section.

Here we define the 6×1 vector

$$\{{}_iI_{2A}\} = \int_{A_i} \varrho_i [N_T]^T [T^X] \{{}_ir_p^{Ei}\} dxdy \tag{4.11.24}$$

where multiplication gives

$$[T]\{r_p^{Ei}\} = \left\{\begin{array}{lcl} T_{11}x & + & T_{12}y \\ T_{21}x & + & T_{22}y \\ T_{31}x & + & T_{32}y \end{array}\right\} \tag{4.11.25}$$

and further

$$[N_T][T]\{r_p^{Ei}\} = \left\{\begin{array}{lcl} T_{11}x & + & T_{12}y \\ T_{21}x & + & T_{22}y \\ T_{31}x & + & T_{32}y \\ T_{31}xy & + & T_{32}y^2 \\ -\ T_{31}x^2 & - & T_{32}xy \\ -\ T_{11}xy & - & T_{12}y^2 \quad + \quad T_{21}x^2 \quad + \quad T_{22}xy \end{array}\right\} \tag{4.11.26}$$

which after integration and factorization with respect to m and further making use of $I_p = 0$ gives

$$\{I_{2A}\} = m\left\{\begin{array}{lcl} T_{11}r_y & + & T_{12}r_x \\ T_{21}r_y & + & T_{22}r_x \\ T_{31}r_y & + & T_{32}r_x \\ T_{32}r_{Ix}^2 & & \\ -\ T_{31}r_{Iy}^2 & & \\ -\ T_{12}r_{Ix}^2 & + & T_{21}r_{Iy}^2 \end{array}\right\} \tag{4.11.27}$$

3^{rd} integral type over the cross section.

Here we define the 6×3 matrix

$$[{}_iI_{3A}] = \int_{A_i} \varrho_i [N_T]^T dxdy \tag{4.11.28}$$

which is integrated to give

$$\begin{aligned} [I_{3A}] &= \int_A \varrho \begin{bmatrix} 1 & 0 & 0 \\ 0 & 1 & 0 \\ 0 & 0 & 1 \\ 0 & 0 & y \\ 0 & 0 & -x \\ -y & x & 0 \end{bmatrix} dxdy \\ &= m \begin{bmatrix} 1 & 0 & 0 \\ 0 & 1 & 0 \\ 0 & 0 & 1 \\ 0 & 0 & r_x \\ 0 & 0 & -r_y \\ -r_x & r_y & 0 \end{bmatrix} \end{aligned} \tag{4.11.29}$$

where again m has been placed as a factor and the appropriate division has taken place in the matrix elements. The integration in Eq. 4.11.10 is continued by derivation of the integrals over the element length. The integrals are referred to by the actual line number in the equation, lines 1–6.

Integration of the 3 first lines in Eq. 4.11.10 over element length.

The first 3 lines in Eq. 4.11.10 are almost identical. Inside the brackets only the central matrices are different in the three cases. They are, in the previous integration over the cross section, represented by the common symbol $[X]$ and the similarity transformed matrix $[T_{EiS}]^T[X][T_{EiS}]$ by the symbol $[T^X]$ or simply $[T]$. The order of the factors in the matrix product, which has to be integrated over the element length, must be retained. The integral, which results in a 12×12 matrix, is written as

$$[{}_iI_{1LX}] = -\int_0^{\ell_i} [{}_iN_{SB}(z)]^T [{}_iI_{1AX}][{}_iN_{SB}(z)]dz \tag{4.11.30}$$

where the sign has to be changed if the inertia forces are placed on the same side as the elastic stiffness term in the equations of motion, according to common practice.

The steps in this integration are not shown in detail here, because it is rather lengthy, when we are looking at a rotating substructure and several degrees of freedom for the surrounding structure are retained. Further, the derivation will not contribute with much useful information for the reader. The integration is straightforward and may either be carried out by partial integration or simply by initial multiplication of the three matrices and finally integration of the single elements in the resulting 12×12 matrix.

The latter procedure is applied here and only the results are given. The general matrix is listed in [Part 2, Sec. D].

4.11.1 The mass matrix.

The $[C]$–matrix in line 1 of Eq. 4.11.10 is a unity matrix, because no non–local degrees of freedom enter the coefficients for the second time derivatives in the substructure coordinate system, $\{\ddot{u}_S\}$, so the third term in Eq. 4.11.3 is simply the local acceleration vector. Because of the orthonormality of the transformation matrix, $[T_{EiS}]$, the $[T^C]$–matrix is also a unity matrix, and this integral is much simplified compared to the integrals in the lines 2 and 3.

The integral results in the mass matrix for the element. It is obvious from the symmetry of the matrix product in line 1, that the mass matrix is symmetric. First the mass matrix is shown in symbolic form

$[M] =$

u_{x1}	u_{y1}	u_{z1}	θ_{x1}	θ_{y1}	θ_{z1}	u_{x2}	u_{y2}	u_{z2}	θ_{x2}	θ_{y2}	θ_{z2}
$M_{1,1}$	0	$M_{1,3}$	0	$M_{1,5}$	$M_{1,6}$	$M_{1,7}$	0	$M_{1,3}$	0	$M_{1,11}$	$M_{1,12}$
...	$M_{2,2}$	$M_{2,3}$	$M_{2,4}$	0	$M_{2,6}$	0	$M_{2,8}$	$M_{2,3}$	$M_{2,10}$	0	$M_{2,12}$
...	...	$M_{3,3}$	$M_{3,4}$	$M_{3,5}$	$M_{3,6}$	$-M_{1,3}$	$-M_{2,3}$	$M_{3,9}$	$M_{3,10}$	$M_{3,11}$	$-M_{3,6}$
...	...	...	$M_{4,4}$	0	$M_{4,6}$	0	$-M_{2,10}$	$M_{3,10}$	$M_{4,10}$	0	$M_{4,12}$
...	...	...	...	$M_{5,5}$	$M_{5,6}$	$-M_{1,11}$	0	$M_{3,11}$	0	$M_{5,11}$	$M_{5,12}$
...	...	*sym–*	...	...	$M_{6,6}$	$M_{1,12}$	$M_{2,12}$	$M_{3,6}$	$-M_{4,12}$	$-M_{5,12}$	$M_{6,12}$
...	...	...	*metric*	...	...	$M_{1,1}$	0	$-M_{1,3}$	0	$-M_{1,5}$	$M_{1,6}$
...	...	...	...	...	...	...	$M_{2,2}$	$-M_{2,3}$	$-M_{2,4}$	0	$M_{2,6}$
...	...	...	...	...	...	...	...	$M_{3,3}$	$M_{3,4}$	$M_{3,5}$	$-M_{3,6}$
...	...	...	...	...	...	...	...	...	$M_{4,4}$	0	$-M_{4,6}$
...	...	...	...	...	...	...	...	...	...	$M_{5,5}$	$-M_{5,6}$
...	...	...	...	...	...	...	...	...	...	...	$M_{6,6}$

(4.11.31)

where

$M_{i,j}$ denotes the non–zero value of the element in row No. i and column No. j, where that particular value first appeared, when the matrix is traversed in a row–wise direction, starting with element $M_{1,1}$.

Next the values of the $M_{i,j}$–elements are listed following the guidelines outlined above, resulting in 31 numerically different elements ($M = m\ell$ is total mass of the element)

<u>1^{st} row :</u>

$$
\begin{aligned}
M_{1,1} &= M\varrho_y^2\left[\left(48\eta_y^2+\frac{42}{5}\eta_y+\frac{13}{35}\right)+\frac{6}{5}\left(\frac{r_{Iy}}{\ell}\right)^2\right]\\
M_{1,3} &= \frac{1}{2}M\varrho_y\frac{r_y}{\ell}\\
M_{1,5} &= M\ell\varrho_y^2\left[\left(6\eta_y^2+\frac{11}{10}\eta_y+\frac{11}{210}\right)-\left(6\eta_y-\frac{1}{10}\right)\left(\frac{r_{Iy}}{\ell}\right)^2\right]\\
M_{1,6} &= -Me_{s2}\varrho_y^2\left[\left(48\eta_y^2+\frac{42}{5}\eta_y+\frac{13}{35}\right)+\frac{6}{5}\left(\frac{r_{Iy}}{\ell}\right)^2\right]\\
&\quad -M\varrho_y\left(r_x-e_{s2}\right)\left[4\eta_y+\frac{7}{20}\right]
\end{aligned}
$$

$$
\begin{aligned}
M_{1,7} &= M\varrho_y^2\left[24\eta_y^2+\frac{18}{5}\eta_y+\frac{9}{70}-\frac{6}{5}\left(\frac{r_{Iy}}{\ell}\right)^2\right]\\
M_{1,11} &= -M\ell\varrho_y^2\left[6\eta_y^2+\frac{9}{10}\eta_y+\frac{13}{420}+\left(6\eta_y-\frac{1}{10}\right)\left(\frac{r_{Iy}}{\ell}\right)^2\right]\\
M_{1,12} &= -Me_{s2}\varrho_y^2\left[24\eta_y^2+\frac{18}{5}\eta_y+\frac{9}{70}-\frac{6}{5}\left(\frac{r_{Iy}}{\ell}\right)^2\right]\\
&\quad -M\varrho_y\left(r_x-e_{s2}\right)\left[2\eta_y+\frac{3}{20}\right]
\end{aligned}
$$

2nd row:

$$
\begin{aligned}
M_{2,2} &= M\varrho_x^2\left[\left(48\eta_x^2+\frac{42}{5}\eta_x+\frac{13}{35}\right)+\frac{6}{5}\left(\frac{r_{Ix}}{\ell}\right)^2\right]\\
M_{2,3} &= \frac{1}{2}M\varrho_x\frac{r_x}{\ell}\\
M_{2,4} &= -M\ell\varrho_x^2\left[\left(6\eta_x^2+\frac{11}{10}\eta_x+\frac{11}{210}\right)-\left(6\eta_x-\frac{1}{10}\right)\left(\frac{r_{Ix}}{\ell}\right)^2\right]\\
M_{2,6} &= Me_{s1}\varrho_x^2\left[\left(48\eta_x^2+\frac{42}{5}\eta_x+\frac{13}{35}\right)+\frac{6}{5}\left(\frac{r_{Ix}}{\ell}\right)^2\right]\\
&\quad +M\varrho_x\left(r_y-e_{s1}\right)\left[4\eta_x+\frac{7}{20}\right]\\
M_{2,8} &= M\varrho_x^2\left[24\eta_x^2+\frac{18}{5}\eta_x+\frac{9}{70}-\frac{6}{5}\left(\frac{r_{Ix}}{\ell}\right)^2\right]\\
M_{2,10} &= M\ell\varrho_x^2\left[6\eta_x^2+\frac{9}{10}\eta_x+\frac{13}{420}+\left(6\eta_x-\frac{1}{10}\right)\left(\frac{r_{Ix}}{\ell}\right)^2\right]\\
M_{2,12} &= Me_{s1}\varrho_x^2\left[24\eta_x^2+\frac{18}{5}\eta_x+\frac{9}{70}-\frac{6}{5}\left(\frac{r_{Ix}}{\ell}\right)^2\right]\\
&\quad +M\varrho_x\left(r_y-e_{s1}\right)\left[2\eta_x+\frac{3}{20}\right]
\end{aligned}
$$

3rd row:

$$
\begin{aligned}
M_{3,3} &= \frac{1}{3}M\\
M_{3,4} &= M\varrho_x r_x\left[4\eta_x+\frac{1}{12}\right]\\
M_{3,5} &= -M\varrho_y r_y\left[4\eta_y+\frac{1}{12}\right]\\
M_{3,6} &= \frac{1}{2}M\left[\frac{e_{s1}\varrho_x r_x-e_{s2}\varrho_y r_y}{\ell}\right]\\
M_{3,9} &= \frac{1}{6}M\\
M_{3,10} &= M\varrho_x r_x\left[2\eta_x-\frac{1}{12}\right]\\
M_{3,11} &= -M\varrho_y r_y\left[2\eta_y-\frac{1}{12}\right]
\end{aligned}
$$

4^{th} row:

$$
\begin{aligned}
M_{4,4} &= M\ell^2\varrho_x^2\left[\frac{6}{5}\eta_x^2+\frac{1}{5}\eta_x+\frac{1}{105}+\left(48\eta_x^2+2\eta_x+\frac{2}{15}\right)\left(\frac{r_{Ix}}{\ell}\right)^2\right]\\
M_{4,6} &= -M\ell e_{s1}\varrho_x^2\left[6\eta_x^2+\frac{11}{10}\eta_x+\frac{11}{210}-\left(6\eta_x-\frac{1}{10}\right)\left(\frac{r_{Ix}}{\ell}\right)^2\right]\\
&\quad -M\ell\varrho_x\left(r_y-e_{s1}\right)\left[\frac{1}{2}\eta_x+\frac{1}{20}\right]\\
M_{4,10} &= -M\ell^2\varrho_x^2\left[\frac{6}{5}\eta_x^2+\frac{1}{5}\eta_x+\frac{1}{140}+\left(-24\eta_x^2+2\eta_x+\frac{1}{30}\right)\left(\frac{r_{Ix}}{\ell}\right)^2\right]\\
M_{4,12} &= -M\ell e_{s1}\varrho_x^2\left[6\eta_x^2+\frac{9}{10}\eta_x+\frac{13}{420}+\left(6\eta_x-\frac{1}{10}\right)\left(\frac{r_{Ix}}{\ell}\right)^2\right]\\
&\quad -M\ell\varrho_x\left(r_y-e_{s1}\right)\left[\frac{1}{2}\eta_x+\frac{1}{30}\right]
\end{aligned}
$$

5^{th} row:

$$
\begin{aligned}
M_{5,5} &= M\ell^2\varrho_y^2\left[\frac{6}{5}\eta_y^2+\frac{1}{5}\eta_y+\frac{1}{105}+\left(48\eta_y^2+2\eta_y+\frac{2}{15}\right)\left(\frac{r_{Iy}}{\ell}\right)^2\right]\\
M_{5,6} &= -M\ell e_{s2}\varrho_y^2\left[6\eta_y^2+\frac{11}{10}\eta_y+\frac{11}{210}-\left(6\eta_y-\frac{1}{10}\right)\left(\frac{r_{Iy}}{\ell}\right)^2\right]\\
&\quad -M\ell\varrho_y\left(r_x-e_{s2}\right)\left[\frac{1}{2}\eta_y+\frac{1}{20}\right]\\
M_{5,11} &= -M\ell^2\varrho_y^2\left[\frac{6}{5}\eta_y^2+\frac{1}{5}\eta_y+\frac{1}{140}+\left(-24\eta_y^2+2\eta_y+\frac{1}{30}\right)\left(\frac{r_{Iy}}{\ell}\right)^2\right]\\
M_{5,12} &= -M\ell e_{s2}\varrho_y^2\left[6\eta_y^2+\frac{9}{10}\eta_y+\frac{13}{420}+\left(6\eta_y-\frac{1}{10}\right)\left(\frac{r_{Iy}}{\ell}\right)^2\right]\\
&\quad -M\ell\varrho_y\left(r_x-e_{s2}\right)\left[\frac{1}{2}\eta_y+\frac{1}{30}\right]
\end{aligned}
$$

6^{th} row:

$$
\begin{aligned}
M_{6,6} &= Me_{s1}^2\varrho_x^2\left[48\eta_x^2+\frac{42}{5}\eta_x+\frac{13}{35}+\frac{6}{5}\left(\frac{r_{Ix}}{\ell}\right)^2\right]\\
&\quad +Me_{s2}^2\varrho_y^2\left[48\eta_y^2+\frac{42}{5}\eta_y+\frac{13}{35}+\frac{6}{5}\left(\frac{r_{Iy}}{\ell}\right)^2\right]\\
&\quad +Me_{s1}\varrho_x\left(r_y-e_{s1}\right)\left[8\eta_x+\frac{7}{10}\right]\\
&\quad +Me_{s2}\varrho_y\left(r_y-e_{s2}\right)\left[8\eta_y+\frac{7}{10}\right]\\
&\quad +\frac{1}{3}M\left(e_{s1}^2+e_{s2}^2+r_{Ix}^2+r_{Iy}^2-2e_{s1}r_y-2e_{s2}r_x\right)\\
M_{6,12} &= Me_{s1}^2\varrho_x^2\left[24\eta_x^2+\frac{18}{5}\eta_x+\frac{9}{70}-\frac{6}{5}\left(\frac{r_{Ix}}{\ell}\right)^2\right]\\
&\quad +Me_{s2}^2\varrho_y^2\left[24\eta_y^2+\frac{18}{5}\eta_y+\frac{9}{70}-\frac{6}{5}\left(\frac{r_{Iy}}{\ell}\right)^2\right]
\end{aligned}
$$

$$+ Me_{s1}\varrho_x (r_y - e_{s1}) \left[4\eta_x + \frac{3}{10}\right]$$
$$+ Me_{s2}\varrho_y (r_y - e_{s2}) \left[4\eta_y + \frac{3}{10}\right]$$
$$+ \frac{1}{6}M \left(e_{s1}^2 + e_{s2}^2 + r_{Ix}^2 + r_{Iy}^2 - 2e_{s1}r_y - 2e_{s2}r_x\right)$$

The integrals in the lines 2 and 3 of Eq. 4.11.10 do not in general result in symmetric matrices. Depending on the number of retained degrees of freedom and the extent to which linearization has taken place, the matrices are more or less full. It has therefore been chosen to derive the matrix for the general case, where the elements of the $[T^X]$–matrix appear in the elements of the resulting matrix denoted by $[I_{1LX}]$ in [Part 2, Sec. D]. The actual matrix can only be calculated, when the $[T^X]$–matrix is known during the solution of the equations of motion.

4.11.2 The Coriolis matrix.

The matrix in line 2 of Eq. 4.11.10 has the status of a damping matrix and is referred to at times as the gyroscopic matrix and at other times as the Coriolis matrix. Here, we will use the name Coriolis matrix, $[C_C]$, because it results from the $[B]$–matrix, which has angular velocities as part of its terms, and the resulting loads are therefore of the same nature as the loads usually known as Coriolis loads. The matrix is calculated directly from the $[I_{1LX}]$–matrix in [Part 2, Sec. D] by introducing the appropriate T_{ij}^B–terms. The sign must be changed when the inertia load is placed on the same side as the elastic stiffness term in the equations of motion. The matrix is skew symmetric.

4.11.3 The inertia stiffness matrix.

The matrix in line 3 of Eq. 4.11.10 is comparable with a stiffness matrix. In the present context it is referred to as the inertia stiffness or the softening matrix, $[K_I]$, because its origin is the change in inertia force with position. The elements in the $[A]$–matrix are composed of angular accelerations, giving rise to forces proportional to the displacement, and equivalent to the elastic restoring forces as represented by the $[K]$–matrix, apart from the sign, that might be negative, so that the forces have a softening effect. The matrix is calculated directly from the $[I_{1LX}]$–matrix in [Part 2, Sec. D] by introducing the appropriate T_{ij}^A–terms. Also, here it must be remembered that the sign has to be changed, when the inertia load is placed on the same side as the elastic stiffness term in the equations of motion. In general, the matrix is not symmetric.

4.11.4 Inertia loads depending on DOFs outside the substructure.

Integration of the 4^{th} line in Eq. 4.11.10.

The integration symbol

$$[{}_iI_{2L}] = \int_0^{\ell_i} [{}_iN_{SB}(z)]^T \, dz \tag{4.11.32}$$

is defined for the 12×6 matrix, resulting from integration over the element length. Integration gives

$$[I_{2L}] = \left[\begin{array}{ccc|ccc} \frac{1}{2}\ell & 0 & 0 & 0 & -\varrho_y & 0 \\ 0 & \frac{1}{2}\ell & 0 & \varrho_x & 0 & 0 \\ 0 & 0 & \frac{1}{2}\ell & 0 & 0 & 0 \\ 0 & -\frac{1}{12}\ell^2 & 0 & 6\ell\varrho_x\eta_x & 0 & 0 \\ \frac{1}{12}\ell^2 & 0 & 0 & 0 & 6\ell\varrho_y\eta_y & 0 \\ 0 & 0 & 0 & \varrho_x e_{s1} & \varrho_y e_{s2} & \frac{1}{2}\ell \\ \hline \frac{1}{2}\ell & 0 & 0 & 0 & \varrho_y & 0 \\ 0 & \frac{1}{2}\ell & 0 & -\varrho_x & 0 & 0 \\ 0 & 0 & \frac{1}{2}\ell & 0 & 0 & 0 \\ 0 & \frac{1}{12}\ell^2 & 0 & 6\ell\varrho_x\eta_x & 0 & 0 \\ -\frac{1}{12}\ell^2 & 0 & 0 & 0 & 6\ell\varrho_y\eta_y & 0 \\ 0 & 0 & 0 & -\varrho_x e_{s1} & -\varrho_y e_{s2} & \frac{1}{2}\ell \end{array}\right] \tag{4.11.33}$$

The final result of the integrations in line 4 is obtained by multiplication of the matrices $[I_{2L}]$ from Eq. 4.11.33 and $[I_{2A}]$ from Eq. 4.11.27. We get the 12×1 vector

$$\begin{aligned} \left\{{}_iF^{Ei}_{n4S}\right\} &= [{}_iI_{2L}]\,\{{}_iI_{2A}\} \\ &= M \left\{\begin{array}{l} (T_{11}r_y + T_{12}r_x)\frac{1}{2} + T_{31}r^2_{Iy}\varrho_y\frac{1}{\ell} \\ (T_{21}r_y + T_{22}r_x)\frac{1}{2} + T_{32}r^2_{Ix}\varrho_x\frac{1}{\ell} \\ (T_{32}r_x + T_{31}r_y)\frac{1}{2} \\ -(T_{21}r_y + T_{22}r_x)\frac{\ell}{12} + 6T_{32}\varrho_x\eta_x r^2_{Ix} \\ (T_{11}r_y + T_{12}r_x)\frac{\ell}{12} - 6T_{31}\varrho_y\eta_y r^2_{Iy} \\ -\left(T_{12}r^2_{Ix} - T_{21}r^2_{Iy}\right)\frac{1}{2} + T_{32}\varrho_x r^2_{Ix}\frac{e_{s1}}{\ell} - T_{31}\varrho_y r^2_{Iy}\frac{e_{s2}}{\ell} \\ \hline (T_{11}r_y + T_{12}r_x)\frac{1}{2} - T_{31}r^2_{Iy}\varrho_y\frac{1}{\ell} \\ (T_{21}r_y + T_{22}r_x)\frac{1}{2} - T_{32}r^2_{Ix}\varrho_x\frac{1}{\ell} \\ (T_{32}r_x + T_{31}r_y)\frac{1}{2} \\ (T_{21}r_y + T_{22}r_x)\frac{\ell}{12} + 6T_{32}\varrho_x\eta_x r^2_{Ix} \\ -(T_{11}r_y + T_{12}r_x)\frac{\ell}{12} - 6T_{31}\varrho_y\eta_y r^2_{Iy} \\ -\left(T_{12}r^2_{Ix} - T_{21}r^2_{Iy}\right)\frac{1}{2} - T_{32}\varrho_x r^2_{Ix}\frac{e_{s1}}{\ell} + T_{31}\varrho_y r^2_{Iy}\frac{e_{s2}}{\ell} \end{array}\right\} \end{aligned} \tag{4.11.34}$$

where the T_{ij}–terms are equal to T^A_{ij}, with the units $[sec^{-2}]$. $M = m\ell$ is the total mass of the element.

Integration of the 5^{th} line in Eq. 4.11.10.

The integration symbol

$$[{}_iI_{3L}] = \int_0^{\ell_i} [{}_iN_{SB}(z)]^T\, \varepsilon_i dz \tag{4.11.35}$$

is defined for the 12×6 matrix resulting from integration along the element length. Integration gives

$[I_{3L}] =$

$$\ell \left[\begin{array}{ccc|ccc} \varrho_y\left(2\eta_y+\frac{3}{20}\right) & 0 & 0 & 0 & -\frac{\varrho_y}{2\ell} & 0 \\ 0 & \varrho_x\left(2\eta_x+\frac{3}{20}\right) & 0 & \frac{\varrho_x}{2\ell} & 0 & 0 \\ 0 & 0 & \frac{1}{6} & 0 & 0 & 0 \\ \hline 0 & -\ell\varrho_x\left(\frac{1}{2}\eta_x+\frac{1}{30}\right) & 0 & \varrho_x\left(2\eta_x-\frac{1}{12}\right) & 0 & 0 \\ \ell\varrho_y\left(\frac{1}{2}\eta_y+\frac{1}{30}\right) & 0 & 0 & 0 & \varrho_y\left(2\eta_y-\frac{1}{12}\right) & 0 \\ -e_{s2}\left[\varrho_y\left(2\eta_y+\frac{3}{20}\right)-\frac{1}{6}\right] & +e_{s1}\left[\varrho_x\left(2\eta_x+\frac{3}{20}\right)-\frac{1}{6}\right] & 0 & \frac{\varrho_x}{2\ell}e_{s1} & \frac{\varrho_y}{2\ell}e_{s2} & \frac{1}{6} \\ \hline \varrho_y\left(4\eta_y+\frac{7}{20}\right) & 0 & 0 & 0 & \frac{\varrho_y}{2\ell} & 0 \\ 0 & \varrho_x\left(4\eta_x+\frac{7}{20}\right) & 0 & -\frac{\varrho_x}{2\ell} & 0 & 0 \\ 0 & 0 & \frac{1}{3} & 0 & 0 & 0 \\ \hline 0 & \ell\varrho_x\left(\frac{1}{2}\eta_x+\frac{1}{20}\right) & 0 & \varrho_x\left(4\eta_x+\frac{1}{12}\right) & 0 & 0 \\ -\ell\varrho_y\left(\frac{1}{2}\eta_y+\frac{1}{20}\right) & 0 & 0 & 0 & \varrho_y\left(4\eta_y+\frac{1}{12}\right) & 0 \\ -e_{s2}\left[\varrho_y\left(4\eta_y+\frac{7}{20}\right)-\frac{1}{3}\right] & e_{s1}\left[\varrho_x\left(4\eta_x+\frac{7}{20}\right)-\frac{1}{3}\right] & 0 & -\frac{\varrho_x}{2\ell}e_{s1} & -\frac{\varrho_y}{2\ell}e_{s2} & \frac{1}{3} \end{array}\right] \tag{4.11.36}$$

The final result of the integrations in line 5 is achieved by multiplication of the matrices $[I_{3L}]$ from Eq. 4.11.36 and $[I_{3A}]$ from Eq. 4.11.29. We get the 12×3 matrix ($M = m\ell$)

$[{}_iF_5] = [{}_iI_{3L}]\,[{}_iI_{3A}] =$

$$M \left[\begin{array}{ccc} \varrho_y\left(2\eta_y+\frac{3}{20}\right) & 0 & \varrho_y\frac{r_y}{\ell}\frac{1}{2} \\ 0 & \varrho_x\left(2\eta_x+\frac{3}{20}\right) & \varrho_x\frac{r_x}{\ell}\frac{1}{2} \\ 0 & 0 & \frac{1}{6} \\ 0 & -\varrho_x\ell\left(\frac{1}{2}\eta_x+\frac{1}{30}\right) & \varrho_x r_x\left(2\eta_x-\frac{1}{12}\right) \\ \varrho_y\ell\left(\frac{1}{2}\eta_y+\frac{1}{30}\right) & 0 & -\varrho_y r_y\left(2\eta_y-\frac{1}{12}\right) \\ -\left(2\eta_y+\frac{3}{20}\right)\varrho_y e_{s2}+(e_{s2}-r_x)\frac{1}{6} & \left(2\eta_x+\frac{3}{20}\right)\varrho_x e_{s1}-(e_{s1}-r_y)\frac{1}{6} & \left(\varrho_x\frac{e_{s1}}{\ell}r_x-\varrho_y\frac{e_{s2}}{\ell}r_y\right)\frac{1}{2} \\ \hline \varrho_y\left(4\eta_y+\frac{7}{20}\right) & 0 & -\varrho_y\frac{r_y}{\ell}\frac{1}{2} \\ 0 & \varrho_x\left(4\eta_x+\frac{7}{20}\right) & -\varrho_x\frac{r_x}{\ell}\frac{1}{2} \\ 0 & 0 & \frac{1}{3} \\ 0 & \varrho_x\ell\left(\frac{1}{2}\eta_x+\frac{1}{20}\right) & \varrho_x r_x\left(4\eta_x+\frac{1}{12}\right) \\ -\varrho_y\ell\left(\frac{1}{2}\eta_y+\frac{1}{20}\right) & 0 & -\varrho_y r_y\left(4\eta_y+\frac{1}{12}\right) \\ -\left(4\eta_y+\frac{7}{20}\right)\varrho_y e_{s2}+(e_{s2}-r_x)\frac{1}{3} & \left(4\eta_x+\frac{7}{20}\right)\varrho_x e_{s1}-(e_{s1}-r_y)\frac{1}{3} & -\left(\varrho_x\frac{e_{s1}}{\ell}r_x-\varrho_y\frac{e_{s2}}{\ell}r_y\right)\frac{1}{2} \end{array}\right] \tag{4.11.37}$$

Integration of the 6^{th} line in Eq. 4.11.10.

Here the necessary integrations have already been carried out, and we define the resulting 12×3 matrix by ($M = m\ell$)

$$
\begin{aligned}
[{}_iF_6] &= [{}_iI_{2L}]\,[{}_iI_{3A}] \\
&= M \begin{bmatrix}
\frac{1}{2} & 0 & \varrho_y \frac{r_y}{\ell} \\
0 & \frac{1}{2} & \varrho_x \frac{r_x}{\ell} \\
0 & 0 & \frac{1}{2} \\
0 & -\frac{1}{12}\ell & 6\varrho_x \eta_x r_x \\
\frac{1}{12}\ell & 0 & -6\varrho_y \eta_y r_y \\
-\frac{1}{2}r_x & \frac{1}{2}r_y & \varrho_x \frac{e_{s1}}{\ell} r_x - \varrho_y \frac{e_{s2}}{\ell} r_y \\
\frac{1}{2} & 0 & -\varrho_y \frac{r_y}{\ell} \\
0 & \frac{1}{2} & -\varrho_x \frac{r_x}{\ell} \\
0 & 0 & \frac{1}{2} \\
0 & \frac{1}{12}\ell & 6\varrho_x \eta_x r_x \\
-\frac{1}{12}\ell & 0 & -6\varrho_y \eta_y r_y \\
-r_x \frac{1}{2} & r_y \frac{1}{2} & -\varrho_x \frac{e_{s1}}{\ell} r_x + \varrho_y \frac{e_{s2}}{\ell} r_y
\end{bmatrix}
\end{aligned}
\tag{4.11.38}
$$

Final result.

The final result after integration in Eq. 4.11.10 has now been achieved

$$
\begin{aligned}
\left\{{}_iF_{IS}^{Ei}\right\} &= -[{}_iM_S]\left\{{}_i\ddot{q}^{Ei}\right\} - [{}_iC_{SC}]\left\{{}_i\dot{q}^{Ei}\right\} - [{}_iK_{SI}]\left\{{}_iq^{Ei}\right\} \\
&\quad - \left\{{}_iF_{4S}^{Ei}\right\} \\
&\quad - [{}_iF_5]\,[T_{EiS}]^T\,[A_S]\left(\left\{{}_ir_2^S\right\} - \left\{{}_ir_1^S\right\}\right) \\
&\quad - [{}_iF_6]\,[T_{EiS}]^T\left([A_S]\left\{{}_ir_1^S\right\} + \left\{a_{Sc}^S\right\}\right)
\end{aligned}
\tag{4.11.39}
$$

where the lower vector index n – for node force – has been omitted. This will be done throughout the rest of the report, and the vectors will be representing quantities related to the nodes, unless otherwise stated.

4.12 Gravity node force.

The distributed gravity load is transformed to the nodes by use of Eq. 4.10.14

$$
\begin{aligned}
\left\{{}_iF_{ng}^{Ei}\right\} &= \varrho_i \int_V [{}_iN_{SB}(z)]^T\,[{}_iN_T(x,y)]^T \left\{g^{Ei}\right\} dxdydz \\
&= \varrho_i \Big(\int_V [{}_iN_{SB}(z)]^T\,[{}_iN_T(x,y)]^T\,dxdydz\Big)\left\{g^{Ei}\right\}
\end{aligned}
\tag{4.12.1}
$$

where

$\left\{g^{Ei}\right\}$ is the gravity acceleration in element coordinates.

The integral above is identical to the integral of the 6^{th} line in Eq. 4.11.10, which was derived in the previous section, and we get the result

$$\left\{{}_iF_{ng}^{Ei}\right\} = [{}_iF_6]\left\{g^{Ei}\right\} \tag{4.12.2}$$

4.13 Structural damping.

The structural damping accounts for the energy dissipation during the system response. In genral, it is not possible to derive the element damping matrix from element parameters in a way similar to the derivation of the stiffness- and mass-matrix. Experience shows that the representation of the damping is important in order to get reasonable response calculations. The most commonly applied damping model is the one which assumes that the damping matrix can be expressed as a linear combination of the mass- and the stiffness-matrices

$$[C_s] = \alpha[M] + \beta[K] \tag{4.13.1}$$

where α and β are constant scalars, the former having units $[sec^{-1}]$ and the latter having units $[sec]$. This way of representing damping is referred to as proportional damping or Rayleigh damping [B1, pp. 527-532].

The practical estimation of the proportionality constants is often carried out with recourse to the logarithmic decrement, corresponding to two unequal eigenfrequencies for the complete structure or alternatively for the substructures. The logarithmic decrement is the logarithm to the ratio between two successive vibration amplitudes of the free vibration and is assumed to represent the decay of the vibration due to dissipation of energy. The logarithmic decrement can be related to the damping ratios which are next used for the estimation of α and β. Experience and comparison of simulated and measured results are often important ingredients, when damping parameters are derived.

5 General about coupling of substructure equations.

The general procedure for coupling of the substructure equations is basically identical to what is usually done in the finite element analysis (FEM), when the coupled equations are set up with reference to a common global coordinate system, allthough the resulting equations are quite different. In the present work each substructure is described in its own coordinate system, which is rigidly attached to the substructure at the node, where the actual substructure is coupled to the neighbouring substructure. This has as a result that the rigid body displacements of the substructure relative to the inertial system, translations and rotations, are eliminated from the equations of motion.

One main purpose with the actual choice of division into substructures is to facilitate the kinematic analysis, as described in Sec. 3, by chosing the substructure coupling nodes at positions on the substructure, where important built in degrees of freedom (DOFs) are located. These DOFs will then enter the equations in a straightforward manner. Further it has as a consequence, that the influence of these DOFs will be easier to identify, when the model is developed with the purpose of being used in a parametric study. One could with some justification claim, that the physics of the structure is better reflected in the equations, at least compared to one of the more refined models, which uses a quite general numerical procedure for description of the state of each structural element, without distinguishing between actual structural main components.

The actual division into substructures has as an important positive implication that the equation structure is simplified, and the work with updating of the equations of motion, necessary on account of the change in geometry, mainly attributed to the rigid body motions of the substructures, is essentially reduced because it is related to the few DOFs identified in advance. This is done during the solution of the equations of motion as shown in Fig. 19 Sec. 7.

A disadvantage with the present substructuring technique is that the coefficient matrices of the equations of motion all become nonsymmetric and full in columns corresponding to the coupling DOFs on one triangle of the matrices. This does not really constitute a problem but increases the computational work.

As the coupling of the substructure equations is very central in the present formulation, it will deserve a more detailed description, the main purpose of which is to show that the present substructure formulation is equivalent to the well known finite element formulation within a common coordinate system, and thus it is indirectly shown that the accepted formulation is valid. As a quite general proof of this equivalence is rather comprehensive, when the complete set of dynamic equations are involved, the technique will be shown below only for the more simple static case. Further, the purpose is to show that the key for coupling of the substructure equations, is to impose force equilibrium at the coupling nodes.

An initially straight beam, divided into two beam elements, as shown in Fig. 16, is considered. The beam is clamped at one end. Each element is at the same time considered to be a substructure, numbered 1 and 2 enclosed in circles. The substructure coordinate system for element 1 is denoted the G-system. It is attached to the clamped end of element 1 and identical to the global system, which usually would be chosen in an ordinary FEM analysis. The substructure coordinate system for element 2 is denoted the L-system. It is rigidly attached to the node of element two, which corresponds to the global node 1, as shown in Fig. 16. The generalized forces and displacements at the two nodes are shown symbolically. The generalized force vectors $\{F_{10}\}$ and $\{F_{20}\}$ thus include both forces and moments, and the generalized

displacement vectors $\{q_{10}\}$ and $\{q_{20}\}$ include translations and rotations.

This simple example may be used without any loss of generality, because only the elements closest to the coupling node are involved in the more impenetrable change in equation structure. The coupling of the complete set of dynamic equations in Sec. 6 will help throwing light on the complete coupling schedule.

Only elastic stiffnesses and external node forces are taken into account.

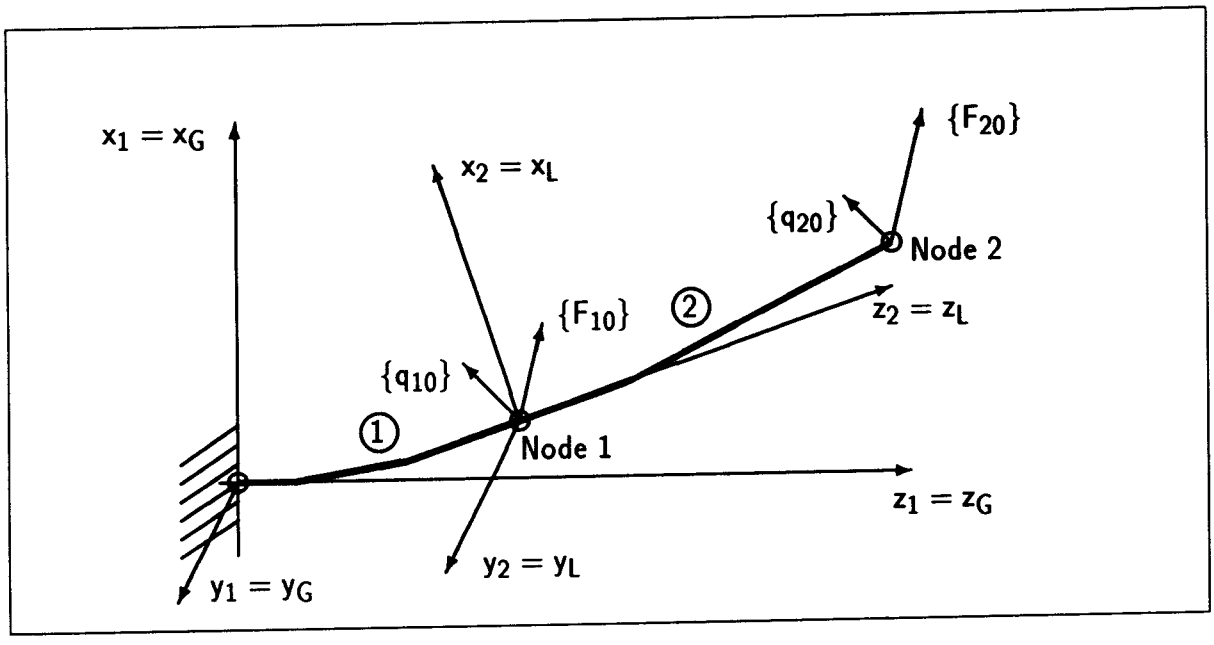

Figure 16: Coupling of substructures.

5.1 Coupling procedure in usual FEM formulation.

The equilibrium equations for element 1 is written as

$$\begin{bmatrix} [K^1_{11}] & [K^1_{12}] \\ [K^1_{21}] & [K^1_{22}] \end{bmatrix} \begin{Bmatrix} \{q^G_{11}\} \\ \{q^G_{12}\} \end{Bmatrix} = \begin{Bmatrix} \{F^G_{11}\} \\ \{F^G_{12}\} \end{Bmatrix} \tag{5.1.1}$$

The boundary conditions at the clamped end imply that

$$\{q^G_{11}\} = \{0\} \tag{5.1.2}$$

and the first matrix row of Eq. 5.1.1 only serves to find the reactions. The second matrix row of Eq. 5.1.1 gives

$$[K^1_{22}]\{q^G_{12}\} = [K^1_{22}]\{q^G_{10}\} = \{F^G_{12}\} = \{F^G_{12e}\} + \{F^G_{12r}\} \tag{5.1.3}$$

where

$\{F^G_{12e}\}$ is the external force on element 1, transformed to node 1 (node 2 of element 1)

and

$\left\{F^G_{12r}\right\}$ is the reaction on element 1 at node 1 from element 2

Equivalently, the equilibrium of element 2 is expressed by

$$\begin{bmatrix} [K^{2*}_{11}] & [K^{2*}_{12}] \\ [K^{2*}_{21}] & [K^{2*}_{22}] \end{bmatrix} \begin{Bmatrix} \{q^G_{21}\} \\ \{q^G_{22}\} \end{Bmatrix} = \begin{Bmatrix} \{F^G_{21}\} \\ \{F^G_{22}\} \end{Bmatrix} \tag{5.1.4}$$

or

$$\begin{bmatrix} [K^{2*}_{11}] & [K^{2*}_{12}] \\ [K^{2*}_{21}] & [K^{2*}_{22}] \end{bmatrix} \begin{Bmatrix} \{q^G_{10}\} \\ \{q^G_{20}\} \end{Bmatrix} = \begin{Bmatrix} \{F^G_{21e}\} + \{F^G_{21r}\} \\ \{F^G_{22e}\} \end{Bmatrix} \tag{5.1.5}$$

where

$\left[K^{2*}_{ij}\right]$ $= [T_{21}]\left[K^2_{ij}\right][T_{12}]$ is the similarity transformed stiffness submatrix arising from the transformation to global coordinates (G)

$\left\{F^G_{21e}\right\}$ is the external force on element 2 transformed to node 1 (node 1 of element 2)

$\left\{F^G_{21r}\right\}$ is the reaction on element 2 at node 1 from element 1

$\left\{F^G_{22e}\right\}$ is the external force on element 2 transformed to node 2 (node 2 of element 2)

The displacement compatibility at the coupling node is satisfied by the requirement that the displacements at the nodes, regarded as individual element nodes, must be equal. In the equations, this requirement is met by expressing the common displacement by the DOFs at the common node. The result is that the total number of DOFs are reduced by 6 each time an element is coupled at a global node, compared to the DOFs for the individual elements.

The final coupling of the equations is carried through by use of the equilibrium condition at global node 1, expressing that the reaction at the node on element 1 is equal to the reaction at the node on element 2 with opposite sign

$$\left\{F^G_{12r}\right\} = -\left\{F^G_{21r}\right\} \tag{5.1.6}$$

The equilibrium expression for the complete structure is obtained by substituting the expressions for the reactions from Eqs. 5.1.3 and 5.1.5 into Eq. 5.1.6. The result is

$$\begin{bmatrix} ([K^1_{22}] + [K^{2*}_{11}]) & [K^{2*}_{12}] \\ [K^{2*}_{21}] & [K^{2*}_{22}] \end{bmatrix} \begin{Bmatrix} \{q^G_{10}\} \\ \{q^G_{20}\} \end{Bmatrix} = \begin{Bmatrix} \{F^G_{10}\} \\ \{F^G_{20}\} \end{Bmatrix} \tag{5.1.7}$$

where now the external node forces are composed of

$$\left.\begin{aligned} \{F^G_{10}\} &= \{F^G_{12e}\} + \{F^G_{21e}\} \\ \{F^G_{20}\} &= \{F^G_{22e}\} \end{aligned}\right\} \quad \text{and} \tag{5.1.8}$$

Eq. 5.1.7 is the usual FEM equation, when the equilibrium is expressed in the common global coordinate system (G). The equation reflects the well known rule that the global stiffness matrix is obtained by adding stiffness contributions from the single elements at matrix positions, which correspond to the actual nodes. The stiffness matrix is symmetric.

5.2 Coupling procedure in the substructure FEM formulation.

In the present work the local or substructure DOFs are retained and the equilibrium equations appear in a different form. These equations are derived for the example structure below.

The equilibrium equation for element 1 is the same as Eq. 5.1.3.

Considering element 2 as a substructure described in the local substructure coordinate system (L) attached to node 1, an equilibrium equation of the same form, as that for the clamped element, is arrived at. The substructure coordinate ystem (L) is following the node during deformation, so that the deformation at node 1 of element 2, measured relative to the substructure coordinates, are $\{0\}$ or $\left\{q_{21}^L\right\} = \{0\}$. This is equivalent to elimination of the substructure DOFs at the coupling node, and the compatibility condition is automatically fulfilled at the node by this choice.

The equilibrium of element 2 with reference to substructure coordinates is expressed by

$$\left[K_{12}^2\right]\left\{q_{22}^L\right\} = \left\{F_{21}^L\right\} = \left\{F_{21e}^L\right\} + \left\{F_{21r}^L\right\} \tag{5.2.1}$$

and

$$\left[K_{22}^2\right]\left\{q_{22}^L\right\} = \left\{F_{22e}^L\right\} \tag{5.2.2}$$

As the displacement compatibility at the coupling node is implicitly accounted for through the consistent choice of nodal DOFs and substructure coordinate system at an actual coupling node, as mentioned above, the final coupling of the equations is carried through by imposing force equilibrium at the coupling node (node 1), which results in the coupling condition

$$[T_{21}]\left\{F_{21r}^L\right\} = -\left\{F_{12r}^G\right\} \tag{5.2.3}$$

By use of Eq. 5.2.2, Eqs. 5.1.3, 5.2.1 and 5.2.2 are combined to give the equilibrium equation for the total structure

$$\begin{bmatrix} [K_{22}^1] & [T_{21}][K_{12}^2] \\ [0] & [K_{22}^2] \end{bmatrix} \begin{Bmatrix} \{q_{10}^G\} \\ \{q_{22}^L\} \end{Bmatrix} = \begin{Bmatrix} \{F_{10}^G\} \\ \{F_{20}^L\} \end{Bmatrix} \tag{5.2.4}$$

where

$$\left\{F_{10}^G\right\} = \left\{F_{12e}^G\right\} + [T_{21}]\left\{F_{21e}^L\right\} \tag{5.2.5}$$

and

$$\left\{F_{20}^L\right\} = \left\{F_{22e}^L\right\} \tag{5.2.6}$$

It is important here to keep in mind that the first matrix row in Eq. 5.2.4 refers to global coordinates (G) and the second row to substructure coordinates (L). It is observed that the coefficient matrix (the stiffness matrix) in Eq. 5.2.4 is not symmetric.

5.3 Transformation of substructure FEM to usual FEM.

The two sets of equilibrium equations, Eq. 5.1.7 for the usual FEM formulation and Eq. 5.2.4 for the present substructure formulation, should give an identical solution for the displacements, if the expression in Eq. 5.2.4 is valid, presuming that we accept the validity of the usual FEM formulation. This is not immediately obvious, when we just look at the final equations. Eq. 5.2.4 is not symmetric as Eq. 5.1.7 and further the vectors are with reference to different coordinate systems in Eq. 5.2.4.

The difference in the two sets of equations is due to the fact that rigid body displacements of element 2 are eliminated in the substructure formulation of Eq. 5.2.4. This can be seen from the following derivation, where a transformation of Eq. 5.2.4 to Eq. 5.1.7 is carried out in order to show the legality of Eq. 5.2.4.

The means to carry through the derivation, is to transform $\{q_{22}^L\}$ in Eq. 5.2.4 to global coordinates, by including the rigid body displacements.

The rigid body displacements of a point on element 2 are first expressed by the deformations at node 1.

The rigid body translations can be expressed as

$$\{u_R^G\} = \{u_{10}^G\} + \{\theta_{10}^G\} \times \{r_L^G\} \tag{5.3.1}$$

$\{u_{10}^G\}$ is the translation at node 1 relative to the global coordinates.

$\{\theta_{10}^G\}$ is the rotation (infinitesimal) at node 1 relative to the global coordinates. It is obvious here that infinitesimal rotations must be assumed in order to express the rotations as a vector.

$\{r_L^G\}$ is the position vector to the point in question on the substructure.

The rigid body rotation at the point is expressed by

$$\{\theta_R^G\} = \{\theta_{10}^G\} \tag{5.3.2}$$

The vector cross product in Eq. 5.3.1 can be rewritten as a matrix product

$$\begin{aligned} \{\theta_{10}^G\} \times \{r_L^G\} &= -\begin{bmatrix} 0 & -r_z^G & r_y^G \\ r_z^G & 0 & -r_x^G \\ -r_y^G & r_x^G & 0 \end{bmatrix} \{\theta_{10}^G\} \\ &= [R^G]\{\theta_{10}^G\} \end{aligned} \tag{5.3.3}$$

where

$$[R^G] = [T_{21}] \begin{bmatrix} 0 & r_z^L & -r_y^L \\ -r_z^L & 0 & r_x^L \\ r_y^L & -r_x^L & 0 \end{bmatrix} [T_{12}] \tag{5.3.4}$$

If the general case with 6 DOFs at each node is considered, the displacement vector relative to the global axes for node 2 can be expressed in global coordinates as

$$\begin{aligned}\left\{q_{20}^G\right\} &= \begin{Bmatrix} \left(\left\{u_{10}^G\right\} + \left[R^G\right]\left\{\theta_{10}^G\right\} + \left\{u_{22}^G\right\}\right) \\ \left(\left\{\theta_{10}^G\right\} + \left\{\theta_{22}^G\right\}\right) \end{Bmatrix} \\ &= \left\{q_{10}^G\right\} + \left\{q_R^G\right\} + \left\{q_{22}^G\right\} \end{aligned} \tag{5.3.5}$$

where

$\left\{q_{10}^G\right\} = \begin{Bmatrix} \left\{u_{10}^G\right\} \\ \left\{\theta_{10}^G\right\} \end{Bmatrix}$ is the deformation at node 1 relative to global coordinates

$\left\{q_R^G\right\} = \begin{Bmatrix} \left[R^G\right]\left\{\theta_{10}^G\right\} \\ \{0\} \end{Bmatrix}$ is the rigid body displacement due to rotation at node 1

$\left\{q_{22}^G\right\} = \begin{Bmatrix} \left\{u_{22}^G\right\} \\ \left\{\theta_{22}^G\right\} \end{Bmatrix}$ is the local elastic deformation relative to the substructure coordinates.

Further, it is possible to rewrite Eq. 5.3.5 so that the node DOFs appear explicitly in the equation by noting that

$$\begin{aligned}\left\{q_{10}^G\right\} + \left\{q_R^G\right\} &= \begin{bmatrix} [I] & \left[R^G\right] \\ [0] & [I] \end{bmatrix}\left\{q_{10}^G\right\} \\ &= [R_0]\left\{q_{10}^G\right\} \end{aligned} \tag{5.3.6}$$

where $[I]$ is the 3×3 unity matrix.

Isolating $\left\{q_{22}^L\right\}$, which is wanted for substitution in Eq. 5.2.4 we get

$$\left\{q_{22}^L\right\} = [T_{12}]\left(\left\{q_{20}^G\right\} - [R_0]\left\{q_{10}^G\right\}\right) \tag{5.3.7}$$

Now, considering the second matrix column of Eq. 5.2.4 involving $\left\{q_{22}^L\right\}$ and transforming the second matrix row to global coordinates yields

$$\begin{bmatrix} [T_{21}][K_{12}^2] \\ [T_{21}][K_{22}^2] \end{bmatrix}[T_{12}]\left(\left\{q_{20}^G\right\} - [R_0]\left\{q_{10}^G\right\}\right) = \begin{bmatrix} -[T_{21}][K_{12}^2][T_{12}][R_0] & [T_{21}][K_{12}^2][T_{12}] \\ -[T_{21}][K_{22}^2][T_{12}][R_0] & [T_{21}][K_{22}^2][T_{12}] \end{bmatrix}\begin{Bmatrix} \left\{q_{10}^G\right\} \\ \left\{q_{20}^G\right\} \end{Bmatrix} \tag{5.3.8}$$

This expression is substituted in Eq. 5.2.4 and we get the result

$$\begin{bmatrix} ([K_{22}^1] - [T_{21}][K_{12}^2][T_{12}][R_0]) & [T_{21}][K_{12}^2][T_{12}] \\ -[T_{21}][K_{22}^2][T_{12}][R_0] & [T_{21}][K_{22}^2][T_{12}] \end{bmatrix}\begin{Bmatrix} \left\{q_{10}^G\right\} \\ \left\{q_{20}^G\right\} \end{Bmatrix} = \begin{Bmatrix} \left\{F_{10}^G\right\} \\ \left\{F_{20}^G\right\} \end{Bmatrix} \tag{5.3.9}$$

This equation should be identical to Eq. 5.1.7, if the substructure related Eq. 5.2.4 should be valid. This implies that it must be required that

$$\left[K_{11}^{2*}\right] = -\left[T_{21}\right]\left[K_{12}^{2}\right]\left[T_{12}\right]\left[R_0\right] \tag{5.3.10}$$

and

$$\left[K_{21}^{2*}\right] = -\left[T_{21}\right]\left[K_{22}^{2}\right]\left[T_{12}\right]\left[R_0\right] \tag{5.3.11}$$

This is in general true for an element stiffness matrix, and will be shown here only for the simple case when the two-element structure is a straight beam. We then have

$$[T_{12}] = [T_{21}] = [I] \tag{5.3.12}$$

$$\begin{bmatrix} [K_{11}] & [K_{12}] \\ [K_{21}] & [K_{22}] \end{bmatrix} = \left[\begin{array}{ccc|ccc} u_{x1} & u_{z1} & \theta_{y1} & u_{x2} & u_{z2} & \theta_{y2} \\ \hline \frac{12EI}{\ell^3} & 0 & \frac{6EI}{\ell^2} & -\frac{12EI}{\ell^3} & 0 & \frac{6EI}{\ell^2} \\ 0 & \frac{EA}{\ell} & 0 & 0 & -\frac{EA}{\ell} & 0 \\ \frac{6EI}{\ell^2} & 0 & \frac{4EI}{\ell} & -\frac{6EI}{\ell^2} & 0 & \frac{2EI}{\ell} \\ \hline -\frac{12EI}{\ell^3} & 0 & -\frac{6EI}{\ell^2} & \frac{12EI}{\ell^3} & 0 & -\frac{6EI}{\ell^2} \\ 0 & -\frac{EA}{\ell} & 0 & 0 & \frac{EA}{\ell} & 0 \\ \frac{6EI}{\ell^2} & 0 & \frac{2EI}{\ell} & -\frac{6EI}{\ell^2} & 0 & \frac{4EI}{\ell} \end{array}\right] \tag{5.3.13}$$

$$[R_0] = \begin{bmatrix} 1 & 0 & \ell \\ 0 & 1 & 0 \\ 0 & 0 & 1 \end{bmatrix} \tag{5.3.14}$$

And it is immediately observed that Eqs. 5.3.10 and 5.3.11 are fulfilled, simply by carrying out the multiplications on the submatrices in Eq. 5.3.13. The multiplications are straightforward and simple and will not be shown in detail here.

A quite parallel derivation may be carried through for the dynamic equations corresponding to the mass matrices. As long as only inertia forces corresponding to the second time derivative of the DOFs are included, and nonlinearities are neglected, the derivation is straightforward. This means that an unambiguous connection exists between the present substructure formulation and the commonly used FEM formulation, where the equations of motion are established within a common global coordinate system. The derivation for the mass matrices will not be reproduced here, because the steps are quite analogous to what was done to show the relationship between the stiffness matrices. Further, a detailed derivation of the equations of motion for the present formulation is given in Sec. 6.

When nonlinearities are present, it is considerably more difficult to establish the connection between different formulations, and the subject will not be pursued any further here. However, since the geometric stiffness has been introduced in the present formulation, it may serve as a good illustration of the traps that are present, when one formulation is transformed to another. In the litterature, the geometric stiffness is generally treated quite as the elastic stiffness, and in the usual FEM formulation the two types of matrices are simply added and combined into the equations in a complete analogous manner. However, this does not apply in the present formulation, because the rigid body displacements of the substructures have been eliminated from the equations. The rigid body translations do not influence the geometric stiffness, but the rigid body rotations do, because a rotation of an element will result in moments from the axial force, while a translation does not.

Again, using the simple example of Fig. 16, it is easy to show how this rigid body rotation must be accounted for in the substructure formulation.

The equilibrium equations 5.2.1 and 5.2.2 above for element 2, regarding elastic stiffness, must, when used for geometric stiffness, further include stiffness terms resulting from rigid body rotations of element 2, i.e. the rotations at node 1.

The modified equations are now written (excluding elastic stiffness)

$$\left[K^2_{g12}\right]\left\{q^L_{22}\right\} + [G]\left\{q^L_{10}\right\} = \left\{F^L_{21e}\right\} + \left\{F^L_{21r}\right\} \tag{5.3.15}$$

and

$$\left[K^2_{g22}\right]\left\{q^L_{22}\right\} - [G]\left\{q^L_{10}\right\} = \left\{F^L_{22e}\right\} \tag{5.3.16}$$

where the last terms on the left side of the equations account for the added stiffness resulting from the rigid body rotation. The lower index g indicates that the submatrix represents the conventional geometric stiffness derived in Sec. 4.9 and

$$[G] = \begin{bmatrix} & \begin{bmatrix} 0 & -F_a & 0 \\ F_a & 0 & 0 \\ 0 & 0 & 0 \end{bmatrix} & \\ [0] & & [0] \\ & & \end{bmatrix} \tag{5.3.17}$$

Again, imposing the force equilibrium at the coupling node (node 1) results in the equilibrium equation equivalent to the elastic stiffness equilibrium as expressed in Eq. 5.2.4

$$\begin{bmatrix} \left(\left[K^1_{g22}\right] + [T_{21}]\,[G]\,[T_{12}]\right) & [T_{21}]\left[K^2_{g12}\right] \\ -[G]\,[T_{12}] & \left[K^2_{g22}\right] \end{bmatrix} \begin{Bmatrix} \left\{q^G_{10}\right\} \\ \left\{q^L_{22}\right\} \end{Bmatrix} = \begin{Bmatrix} \left\{F^G_{10}\right\} \\ \left\{F^L_{20}\right\} \end{Bmatrix} = \tag{5.3.18}$$

Further, following the previously outlined steps, it is easy to show that equivalence exists between this formulation and the general FEM formulation, which accounts for the rigid body rotations implicitly.

It should be mentioned here that an indirect test of the stated equivalence has been carried through by solving the eigenvalue problem for both formulations. The eigenvalues are found to agree within the numerical accuracy, as will be shown in the test example in Sec. 8.

The steps outlined above, when coupling of the substructure equations is carried out, are followed in the derivation of the complete set of dynamic equations in Sec. 6, the key being the establishment of force equilibrium at the coupling nodes.

6 Derivation of equations of motion for the complete structure.

In the following sections the derivation of the equations of motion (EOMs) for the complete structure is outlined.

The essential part of this work is derivation of the terms in the inertia load equation 4.11.39. This is carried out with reference to a specific choice of degrees of freedom (DOFs) for the involved substructures, tower, shaft, and blades. Further, the boundary conditions between the substructures may introduce additional DOFs that have to be integrated in the complete model. This is the case here, because the teeter DOF is retained at the boundary or coupling node between the shaft and the blade. The tilt is omitted.

The considered model retains the following DOFs, generally 3 translations, $\left\{u_S^S\right\}$, and 3 rotations, $\left\{\theta_S^S\right\}$, at each node:

$$
\left.
\begin{aligned}
\text{Tower} \quad : \left\{q_T^T\right\}^T &= \left[\left\{u_T^T\right\}^T, \left\{\theta_T^T\right\}^T\right] \neq \{0\}^T \\
\left\{\dot{q}_T^T\right\}^T &= \left[\left\{\dot{u}_T^T\right\}^T, \left\{\dot{\theta}_T^T\right\}^T\right] \neq \{0\}^T \\
\left\{\ddot{q}_T^T\right\}^T &= \left[\left\{\ddot{u}_T^T\right\}^T, \left\{\ddot{\theta}_T^T\right\}^T\right] \neq \{0\}^T \\
\\
\text{Shaft} \quad : \left\{q_A^A\right\}^T &= \left[\left\{u_A^A\right\}^T, \left\{\theta_A^A\right\}^T\right] \neq \{0\}^T \\
\left\{\dot{q}_A^A\right\}^T &= \left[\left\{\dot{u}_A^A\right\}^T, \left\{\dot{\theta}_A^A\right\}^T\right] \neq \{0\}^T \\
\left\{\ddot{q}_A^A\right\}^T &= \left[\left\{\ddot{u}_A^A\right\}^T, \left\{\ddot{\theta}_A^A\right\}^T\right] \neq \{0\}^T \\
\\
\text{Teeter} \quad : \theta_{1H}^H,\ \dot{\theta}_{1H}^H,\ \ddot{\theta}_{1H}^H &\neq 0 \\
\\
\text{Blade} \quad : \left\{q_B^B\right\}^T &= \left[\left\{u_B^B\right\}^T, \left\{\theta_B^B\right\}^T\right] \neq \{0\}^T \\
\left\{\dot{q}_B^B\right\}^T &= \left[\left\{\dot{u}_B^B\right\}^T, \left\{\dot{\theta}_B^B\right\}^T\right] \neq \{0\}^T \\
\left\{\ddot{q}_B^B\right\}^T &= \left[\left\{\ddot{u}_B^B\right\}^T, \left\{\ddot{\theta}_B^B\right\}^T\right] \neq \{0\}^T
\end{aligned}
\right\} \qquad (6.0.1)
$$

The node numbering is as shown in fig. 17

Tower: Nodes are numbered from 1 to ℓ
Tower node $T1$ is at the tower support
Tower node $T\ell$ is at the tower top, and common with shaft node $A1$.

Shaft: Nodes are numbered from 1 to m
Shaft node $A1$ is at the joint to the tower, and common with tower node $T\ell$
Shaft node Am is at the joint to the blade hub, and common with blade node $B1$

Blade: Nodes are numbered from 1 to n
Blade node $B1$ is at the joint to the shaft, and common with shaft node Am
Further details concerning the node numbering for the blade substructure is given in sec. 6.3

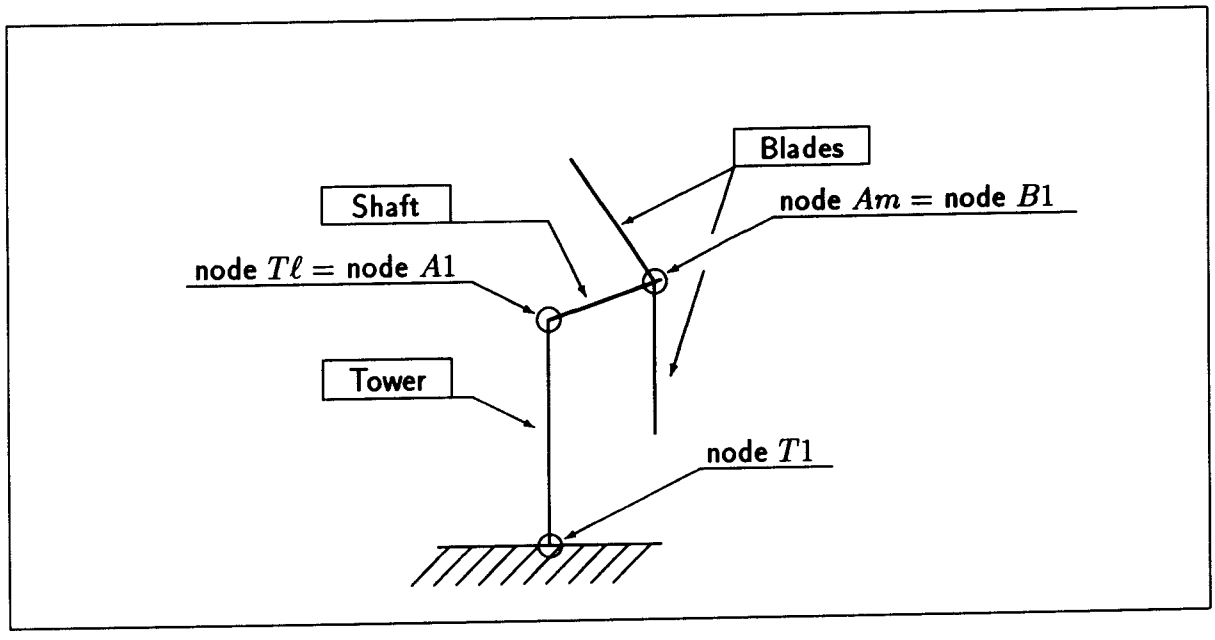

Figure 17: Node numbering for boundary nodes of the substructures.

The details of the derivation and evaluation of the respective substructure accelerations are given in Sec. 3. Below, inertia matrices and vectors are used, which result from rewriting the acceleration expressions. The rewriting has character of a decomposition, based on sorting of the acceleration expressions according to common factors of degrees of freedom and their order with respect to time derivation. A complete listing of these matrices and vectors can be found in [Part 2, Sec. E], where also the introduced linearizations are described. A description of their origin is found there as well.

6.1 Derivation of EOM for the tower substructure.

The inertia loads at the nodes can be read directly from Eq. 4.11.39, noticing that the $[A_T]$- and the $[B_T]$-matrix are identically zero, resulting in

$$\left.\begin{array}{l} [{}_iK_{TI}] = [{}_iC_{TC}] = [0] \quad \text{and} \\ \left\{{}_iF_{4T}^{Ei}\right\} = \left\{{}_iF_{5T}^{Ei}\right\} = \left\{{}_iF_{6T}^{Ei}\right\} = \{0\} \end{array}\right\} \tag{6.1.2}$$

where

$$\left.\begin{array}{l} \left\{{}_iF_{5T}^{Ei}\right\} = [{}_iF_5]\,[T_{EiT}]^T\,[A_T]\left\{{}_ir_{12}^T\right\} \quad \text{and} \\ \left\{{}_iF_{6T}^{Ei}\right\} = [{}_iF_6]\,[T_{EiT}]^T\left([A_T]\left\{{}_ir_1^T\right\} + \left\{a_{Tc}^T\right\}\right) \end{array}\right\} \tag{6.1.3}$$

Here it has been utilized that $\left\{a_{Tc}^T\right\} = \{0\}$ at the tower substructure.

The EOM for an element on the tower substructure is therefore written as

$$[{}_iM]\left\{{}_i\ddot{q}_T^{Ei}\right\} + [{}_iC_s]\left\{{}_i\dot{q}_T^{Ei}\right\} + [{}_iK_s]\left\{{}_iq_T^{Ei}\right\} = \left\{{}_iF_T^{Ei}\right\} \tag{6.1.4}$$

where

$[{}_iM]$ is the element mass matrix, Eq. 4.11.31
$[{}_iC_s]$ is the element structural damping matrix , Eq. 4.13.1, and
$[{}_iK_s]$ is the element stiffness matrix, resulting from material elasticity, Eq. 4.7.5

If concentrated node masses are present, they have to be added to the diagonal elements of the mass matrix.

$\left\{{}_iF_T^{Ei}\right\}$ is composed of the externally applied loads, including gravity and aerodynamic loads, consistently transformed to the nodes.This transformation is described in Sec. 4.10. At the boundary nodes the vector further includes the reactions.

The element EOM is transformed according to the general rule in order to have the equation expressed in tower coordinates and prepared for coupling of the elemental EOMs to the tower substructure EOM. The transformed Eq. 6.1.4 yields

$$\begin{aligned}[T_{EiT}]\,[{}_iM]\,[T_{EiT}]^T\left\{{}_i\ddot{q}_T^T\right\} + [T_{EiT}]\,[{}_iC_s]\,[T_{EiT}]^T\left\{{}_i\dot{q}_T^T\right\} \\ + [T_{EiT}]\,[{}_iK_s]\,[T_{EiT}]^T\left\{{}_iq_T^T\right\} \;=\; [T_{EiT}]\left\{{}_iF_T^{Ei}\right\}\end{aligned} \tag{6.1.5}$$

The tower substructure EOM obtained by coupling of the elemental EOMs of the form given in Eq. 6.1.5 is written

$$[M_T]\left\{\ddot{q}_T^T\right\} + [C_T]\left\{\dot{q}_T^T\right\} + [K_T]\left\{q_T^T\right\} = \left\{F_T^T\right\} \tag{6.1.6}$$

This equation is partitioned in order to allow for introduction of boundary conditions. The boundary conditions at the root of the tower are taken to be purely geometric, i.e., the deformations and their time derivatives at the root node are assumed to be zero

$$\left\{q_{T1}^T\right\} = \left\{\dot{q}_{T1}^T\right\} = \left\{\ddot{q}_{T1}^T\right\} = \{0\} \tag{6.1.7}$$

Further, the boundary conditions at the coupling node between the tower and the shaft are purely static, i.e., the reactions from the shaft (forces and moments) are imposed on the tower node by expressing the reactions by means of the shaft degrees of freedom and thus obtaining a static coupling condition, as shown below.

The partitioned EOM Eq. 6.1.6 is written

$$\begin{bmatrix} [M_{11}] & [M_{1T}] & [M_{1\ell}] \\ [M_{T1}] & [M_{TT}] & [M_{T\ell}] \\ [M_{\ell 1}] & [M_{\ell T}] & [M_{\ell\ell}] \end{bmatrix} \begin{Bmatrix} \{\ddot{q}^T_{T1}\} \\ \{\ddot{q}^T_{TT}\} \\ \{\ddot{q}^T_{T\ell}\} \end{Bmatrix} + \begin{bmatrix} [C_{11}] & [C_{1T}] & [C_{1\ell}] \\ [C_{T1}] & [C_{TT}] & [C_{T\ell}] \\ [C_{\ell 1}] & [C_{\ell T}] & [C_{\ell\ell}] \end{bmatrix} \begin{Bmatrix} \{\dot{q}^T_{T1}\} \\ \{\dot{q}^T_{TT}\} \\ \{\dot{q}^T_{T\ell}\} \end{Bmatrix} + \begin{bmatrix} [K_{11}] & [K_{1T}] & [K_{1\ell}] \\ [K_{T1}] & [K_{TT}] & [K_{T\ell}] \\ [K_{\ell 1}] & [K_{\ell T}] & [K_{\ell\ell}] \end{bmatrix} \begin{Bmatrix} \{q^T_{T1}\} \\ \{q^T_{TT}\} \\ \{q^T_{T\ell}\} \end{Bmatrix} = \begin{Bmatrix} \{F^T_{T1}\} \\ \{F^T_{TT}\} \\ \{F^T_{T\ell}\} \end{Bmatrix} \tag{6.1.8}$$

Now, the submatrices $[X_{1\ell}]$ and $[X_{\ell 1}]$, $(X = M, C, K)$, are zero, when node numbering is carried out in succession, e.g. from root to top of the tower, and the difference in node numbers for every single element is 1. The matrices will thus have a banded structure.

By carrying out the multiplications in Eq. 6.1.8, the relevant degrees of freedom and reactions may be isolated.

The result of the multiplication is

$$[M_{1T}]\{\ddot{q}^T_{TT}\} + [C_{1T}]\{\dot{q}^T_{TT}\} + [K_{1T}]\{q^T_{TT}\} = \{F^T_{T1E}\} + \{F^T_{T1R}\} \tag{6.1.9}$$

$$[M_{TT}]\{\ddot{q}^T_{TT}\} + [M_{T\ell}]\{\ddot{q}^T_{T\ell}\} + [C_{TT}]\{\dot{q}^T_{TT}\} + [C_{T\ell}]\{\dot{q}^T_{T\ell}\} + [K_{TT}]\{q^T_{TT}\} + [K_{T\ell}]\{q^T_{T\ell}\} = \{F^T_{TT}\} \tag{6.1.10}$$

$$[M_{\ell T}]\{\ddot{q}^T_{TT}\} + [M_{\ell\ell}]\{\ddot{q}^T_{T\ell}\} + [C_{\ell T}]\{\dot{q}^T_{TT}\} + [C_{\ell\ell}]\{\dot{q}^T_{T\ell}\} + [K_{\ell T}]\{q^T_{TT}\} + [K_{\ell\ell}]\{q^T_{T\ell}\} = \{F^T_{T\ell E}\} + \{F^T_{T\ell R}\} \tag{6.1.11}$$

Here the following notation is used

$\{F^T_{TkE}\}$ is external forces on the element, transformed to node k. Included are distributed external forces and gravity forces.

$\{F^T_{TiR}\}$ is reaction forces at node i.

$\{F^T_{T1R}\}$ expresses reactions from the support at node 1, the node at the root of the tower.

$\{F^T_{T\ell R}\}$ expresses reactions from the shaft substructure at the coupling node ℓ.

Eq. 6.1.9 is extracted from the system EOM and is merely used for derivation of the reaction $\{F^T_{T1R}\}$. Because of the banded structure of the coefficient matrices the equation can be reduced to include only the degrees of freedom for node 2

$$[M^1_{12}]\{\ddot{q}^T_{T2}\} + [C^1_{12}]\{\dot{q}^T_{T2}\} + [K^1_{12}]\{q^T_{T2}\} = \{F^T_{T1E}\} + \{F^T_{T1R}\} \tag{6.1.12}$$

where the dimension of the coefficient matrices now are 6×6.

$\left\{F^T_{T1R}\right\}$ can be found from Eq. 6.1.12.

Eq. 6.1.10 is part of the system EOM, and so is Eq. 6.1.11, where the reactions $\left\{F^T_{T\ell R}\right\}$ have to be expressed by means of the equations for the shaft substructure.

This relation will result from the following derivation of the EOM for the shaft substructure.

6.2 Derivation of EOM for the shaft substructure.

With the actual DOFs, the acceleration on the shaft substructure is written as (refer to Eq. 4.11.3)

$$\left\{\ddot{r}^A_{A0}\right\} = [A_A]\left\{s^A_A\right\} + [B_A]\left\{\dot{u}^A_A\right\} + [C_A]\left\{\ddot{u}^A_A\right\} + \left\{a^A_{Ac}\right\} \tag{6.2.1}$$

where

$$\left\{a^A_{Ac}\right\} = [D_A]\left\{\ddot{u}^T_{T\ell}\right\} \tag{6.2.2}$$

and $[C_A]$ is equal to the unity matrix.

From Eq. 4.11.39 all the terms will now contribute to the EOM for an element.

The three last lines of Eq. 4.11.39 shall first be rewritten, taking advantage of the possibility of extracting DOFs from the $[A_A]$–matrix. As shown in [Part 2, Sec. E.3], the inertia vector $\left\{{}_iF^A_{4A}\right\}$ for the shaft, according to [Part 2, Eq. E.3.1], can be written

$$\left\{{}_iF^A_{4A}\right\} = [{}_iFT2_{4A}]\left\{\ddot{\theta}^T_{T\ell}\right\} + \left\{{}_iFT^A_{4A}\right\} \tag{E.3.1}$$

where the matrix

$[{}_iFT2_{4A}]$ originates from the skew-symmetric part of the $[A_A]$-matrix.

The product

$[A_A]\left\{{}_ir^A_j\right\}, j = 1, 12$

is rewritten by initial multiplication and next writing the resulting vector as a product of matrices and DOFs. The result is [Part 2, Sec. E.1]

$$[A_A]\left\{{}_ir^A_j\right\} = [{}_iAT2_j]\left\{\ddot{\theta}^T_{T\ell}\right\} + [{}_iAT1_j]\left\{\dot{\theta}^T_{T\ell}\right\} + \left\{{}_iAC0^A_j\right\} \tag{6.2.3}$$

where now

$[{}_iAT2_j] = [{}_iAT2_j\,({}_ir_{1j},\ {}_ir_{2j},\ {}_ir_{3j})]$,

$[{}_iAT1_j] = [{}_iAT1_j\,({}_ir_{1j},\ {}_ir_{2j},\ {}_ir_{3j})]$, and

$\left\{{}_iAC0^A_j\right\} = \left\{{}_iAC0^A_j\,({}_ir_{1j},\ {}_ir_{2j},\ {}_ir_{3j})\right\}$

are functions of the vector coordinates for $\left\{{}_i r_j^A\right\}$.

By introducing Eq. 6.2.3 into line 3 of eq. 4.11.39 this line changes to

$$\begin{aligned} &-\left[{}_iF_5\right]\left[T_{EiA}\right]^T\left[A_A\right]\left\{{}_i r_{12}^A\right\} = \\ &\quad -\left[{}_iF_5\right]\left[T_{EiA}\right]^T\left[\left[{}_iAT2_{12}\right]\left\{\ddot{\theta}_{T\ell}^T\right\}+\left[{}_iAT1_{12}\right]\left\{\dot{\theta}_{T\ell}^T\right\}+\left\{{}_iAC0_{12}^A\right\}\right] \end{aligned} \tag{6.2.4}$$

For reasons of simplification of the written expressions, the following substitution is used for the matrix product

$$\left[T_{EiA}^*\right]\left[{}_iF_k\right]\left[T_{EiA}\right]^T = \left[{}_iF_{kA}^*\right] \tag{6.2.5}$$

where $k = 5, 6$ and

$$\left[T_{EiA}^*\right] = \begin{bmatrix} [T_{EiA}] & [0] & [0] & [0] \\ [0] & [T_{EiA}] & [0] & [0] \\ [0] & [0] & [T_{EiA}] & [0] \\ [0] & [0] & [0] & [T_{EiA}] \end{bmatrix} \tag{6.2.6}$$

resulting in a 12×12 matrix, which gives the correct transformation of the 12×1 vector.

Using the substitution from Eq. 6.2.5, the following matrices are now defined

$$\left.\begin{aligned} \left[{}_iF_{5A}^*\right]\left[{}_iAT2_{12}\right] &= \left[{}_iFT2_{5A}\right] \\ \left[{}_iF_{5A}^*\right]\left[{}_iAT1_{12}\right] &= \left[{}_iFT1_{5A}\right] \\ \left[{}_iF_{5A}^*\right]\left\{{}_iAC0_{12}^A\right\} &= \left\{{}_iFC0_{5A}^A\right\} \end{aligned}\right\} \tag{6.2.7}$$

The definitions from Eq. 6.2.7 are introduced into Eq. 6.2.4 and we get

$$\begin{aligned} &-\left[T_{EiA}^*\right]\left[{}_iF_5\right]\left[T_{EiA}\right]^T\left[A_A\right]\left\{{}_i r_{12}^A\right\} = \\ &\quad -\left[{}_iFT2_{5A}\right]\left\{\ddot{\theta}_{T\ell}^T\right\}-\left[{}_iFT1_{5A}\right]\left\{\dot{\theta}_{T\ell}^T\right\}-\left\{{}_iFC0_{5A}^A\right\} \end{aligned} \tag{6.2.8}$$

The resulting vector is with reference to the shaft coordinate system.

An analogous procedure is carried out for line 4 in Eq. 4.11.39, and the following matrices are defined

$$\left.\begin{aligned} \left[{}_iF_{6A}^*\right]\left[{}_iAT2_1\right] &= \left[{}_iFT2_{6A}\right] \\ \left[{}_iF_{6A}^*\right]\left[{}_iAT1_1\right] &= \left[{}_iFT1_{6A}\right] \\ \left[{}_iF_{6A}^*\right]\left\{{}_iAC0_1^A\right\} &= \left\{{}_iFC0_{6A}^A\right\} \\ \left[{}_iF_{6A}^*\right]\left[D_A\right] &= \left[{}_iFD_{6A}\right] \end{aligned}\right\} \tag{6.2.9}$$

With these definitions the last line in Eq. 4.11.39 is written

$$
\begin{aligned}
&-[T^{*}_{EiA}]\,[{}_iF_6]\,[T_{EiA}]^T\left([A_A]\left\{{}_ir^A_1\right\}+\left\{a^A_{Ac}\right\}\right)= \\
&\quad -[{}_iFT2_{6A}]\left\{\ddot{\theta}^T_{T\ell}\right\}-[{}_iFT1_{6A}]\left\{\dot{\theta}^T_{T\ell}\right\}-\left\{{}_iFC0^A_{6A}\right\}-[{}_iFD_{6A}]\left\{\ddot{u}^T_{T\ell}\right\}
\end{aligned}
\tag{6.2.10}
$$

Eq. 4.11.39 for a shaft element may now be rewritten, using Eqs. E.3.1, 6.2.8 and 6.2.10. Introducing structural damping and stiffness at the same time, the result is equivalent to the EOM for the element, excluding external forces and boundary conditions for convenience

$$
\begin{aligned}
&[{}_iM_A]\left\{{}_i\ddot{q}^A_A\right\}+[{}_iC_A]\left\{{}_i\dot{q}^A_A\right\}+[{}_iK_A]\left\{{}_iq^A_A\right\}= \\
&\quad -\left(\left\{{}_iFT^A_{4A}\right\}+\left\{{}_iFC0^A_{5A}\right\}+\left\{{}_iFC0^A_{6A}\right\}\right) \\
&\quad -\left([{}_iFT2_{4A}]+[{}_iFT2_{5A}]+[{}_iFT2_{6A}]\right)\left\{\ddot{\theta}^T_{T\ell}\right\} \\
&\quad -\left([{}_iFT1_{5A}]+[{}_iFT1_{6A}]\right)\left\{\dot{\theta}^T_{T\ell}\right\} \\
&\quad -[{}_iFD_{6A}]\left\{\ddot{u}^T_{T\ell}\right\}
\end{aligned}
\tag{6.2.11}
$$

where

$$
\left.
\begin{aligned}
[{}_iC_A]&=[{}_iC_{AC}]+[{}_iC_s]\ \text{and}\\
[{}_iK_A]&=[{}_iK_{AI}]+[{}_iK_s]
\end{aligned}
\right\}
\tag{6.2.12}
$$

The indices refer to the origin of the matrix, which is inertia or structural properties

$[C_{AC}]$ is the Coriolis matrix, which is related to the $[B_A]$–matrix

$[K_{AI}]$ is the inertia stiffness matrix, which is related to the $[A_A]$–matrix

$[C_s]$ is structural damping

$[K_s]$ is structural stiffness

If concentrated node masses are present they must be added to the diagonal elements of the mass matrix.

The right hand side of Eq. 6.2.11 gives rise to additional terms in the mass– and damping–matrices of the system EOM.

In order to prepare the assembling procedure, the matrix products in Eq. 6.2.11 are combined such that the deformation vectors are written as the usual 12×1 dimensional vector, corresponding to 6 DOFs at each node.

The following vectors and matrices are now defined

$$\left.\begin{array}{l} \left[\ [{}_iFD_{6A}]\ \middle|\ \left([{}_iFT2_{4A}]+[{}_iFT2_{5A}]+[{}_iFT2_{6A}]\right)\ \right]=[{}_iM_{TA}] \\ \left[\ [0]\qquad\ \middle|\ \left([{}_iFT1_{5A}]+[{}_iFT1_{6A}]\right)\ \right]=[{}_iC_{TA}] \\ \left\{{}_iFT^A_{4A}\right\}+\left\{{}_iFC0^A_{5A}\right\}+\left\{{}_iFC0^A_{6A}\right\}=\left\{{}_iF^A_{456A}\right\} \end{array}\right\} \quad (6.2.13)$$

By using these definitions the EOM for a shaft element (Eq. 6.2.11) may be written

$$[{}_iM_A]\left\{{}_i\ddot{q}^A_A\right\}+[{}_iC_A]\left\{{}_i\dot{q}^A_A\right\}+[{}_iK_A]\left\{{}_iq^A_A\right\}= \left\{{}_iF^A_A\right\}-\left\{{}_iF^A_{456A}\right\}-[{}_iM_{TA}]\left\{\ddot{q}^T_{T\ell}\right\}-[{}_iC_{TA}]\left\{\dot{q}^T_{T\ell}\right\} \quad (6.2.14)$$

where also the external force, $\left\{{}_iF^A_A\right\}$, has been included

$\left\{{}_iF^A_A\right\}$ is composed of all externally applied loads, including gravity and aerodynamic loads, consistently transformed to the nodes, as outlined in Sec. 4.10. Further, the vector includes the reactions at the boundary nodes.

Still, the resulting vectors are with reference to the shaft coordinate system, the A–system.

Assembling the element EOMs to the total substructure EOM reads

$$[M_A]\left\{\ddot{q}^A_A\right\}+[C_A]\left\{\dot{q}^A_A\right\}+[K_A]\left\{q^A_A\right\}= \left\{F^A_A\right\}-\left\{F^A_{456}\right\}-[M_{TA}]\left\{\ddot{q}^T_{T\ell}\right\}-[C_{TA}]\left\{\dot{q}^T_{T\ell}\right\} \quad (6.2.15)$$

To prepare the coupling of the shaft EOMs to the tower EOMs and the blade EOMs, respectively, Eq.6.2.15 is partitioned in order to facilitate the insight in the appropriate process. The result of the partitioning is

$$\begin{bmatrix} [M_{A11}] & [M_{1A}] & [M_{A1m}] \\ [M_{A1}] & [M_{AA}] & [M_{Am}] \\ [M_{Am1}] & [M_{mA}] & [M_{Amm}] \end{bmatrix} \begin{Bmatrix} \{\ddot{q}^A_{A1}\} \\ \{\ddot{q}^A_{AA}\} \\ \{\ddot{q}^A_{Am}\} \end{Bmatrix} + \begin{bmatrix} [C_{A11}] & [C_{1A}] & [C_{A1m}] \\ [C_{A1}] & [C_{AA}] & [C_{Am}] \\ [C_{Am1}] & [C_{mA}] & [C_{Amm}] \end{bmatrix} \begin{Bmatrix} \{\dot{q}^A_{A1}\} \\ \{\dot{q}^A_{AA}\} \\ \{\dot{q}^A_{Am}\} \end{Bmatrix}$$
$$+ \begin{bmatrix} [K_{A11}] & [K_{1A}] & [K_{A1m}] \\ [K_{A1}] & [K_{AA}] & [K_{Am}] \\ [K_{Am1}] & [K_{mA}] & [K_{Amm}] \end{bmatrix} \begin{Bmatrix} \{q^A_{A1}\} \\ \{q^A_{AA}\} \\ \{q^A_{Am}\} \end{Bmatrix} =$$
$$\begin{Bmatrix} \{F^A_{A1}\} \\ \{F^A_{AA}\} \\ \{F^A_{Am}\} \end{Bmatrix} - \begin{Bmatrix} \{F^A_{456A1}\} \\ \{F^A_{456AA}\} \\ \{F^A_{456Am}\} \end{Bmatrix} - \begin{bmatrix} [M_{TA1}] \\ [M_{TAA}] \\ [M_{TAm}] \end{bmatrix} \left\{\ddot{q}^T_{T\ell}\right\} - \begin{bmatrix} [C_{TA1}] \\ [C_{TAA}] \\ [C_{TAm}] \end{bmatrix} \left\{\dot{q}^T_{T\ell}\right\} \quad (6.2.16)$$

Before multiplication in Eq. 6.2.16 some simplifications are considered.

The definition of the moving shaft coordinate system with origo at node 1 of the shaft substructure implies that the substructure is considered clamped at node 1, such that

$$\left\{q^A_{A1}\right\} = \left\{\dot{q}^A_{A1}\right\} = \left\{\ddot{q}^A_{A1}\right\} = \{0\} \tag{6.2.17}$$

Using this equation, when carrying out the multiplications in the partitioned Eq. 6.2.16, we get for the first row (index E – external, index R – reaction)

$$\begin{aligned}[M_{1A}]\left\{\ddot{q}^A_{AA}\right\} + [C_{1A}]\left\{\dot{q}^A_{AA}\right\} + [K_{1A}]\left\{q^A_{AA}\right\} = \\ \left\{F^A_{A1E}\right\} + \left\{F^A_{A1R}\right\} - \left\{F^A_{456A1}\right\} - [M_{TA1}]\left\{\ddot{q}^T_{T\ell}\right\} - [C_{TA1}]\left\{\dot{q}^T_{T\ell}\right\}\end{aligned} \tag{6.2.18}$$

The second row in Eq. 6.2.16 gives after multiplication

$$\begin{aligned}[M_{AA}]\left\{\ddot{q}^A_{AA}\right\} + [M_{Am}]\left\{\ddot{q}^A_{Am}\right\} + [C_{AA}]\left\{\dot{q}^A_{AA}\right\} + [C_{Am}]\left\{\dot{q}^A_{Am}\right\} \\ + [K_{AA}]\left\{q^A_{AA}\right\} + [K_{Am}]\left\{q^A_{Am}\right\} = \\ \left\{F^A_{AA}\right\} - \left\{F^A_{456AA}\right\} - [M_{TAA}]\left\{\ddot{q}^T_{T\ell}\right\} - [C_{TAA}]\left\{\dot{q}^T_{T\ell}\right\}\end{aligned} \tag{6.2.19}$$

And finally the third row

$$\begin{aligned}[M_{mA}]\left\{\ddot{q}^A_{AA}\right\} + [M_{mm}]\left\{\ddot{q}^A_{Am}\right\} + [C_{mA}]\left\{\dot{q}^A_{AA}\right\} + [C_{mm}]\left\{\dot{q}^A_{Am}\right\} \\ + [K_{mA}]\left\{q^A_{AA}\right\} + [K_{mm}]\left\{q^A_{Am}\right\} = \\ \left\{F^A_{AmE}\right\} + \left\{F^A_{AmR}\right\} - \left\{F^A_{456Am}\right\} - [M_{TAm}]\left\{\ddot{q}^T_{T\ell}\right\} - [C_{TAm}]\left\{\dot{q}^T_{T\ell}\right\}\end{aligned} \tag{6.2.20}$$

Eq. 6.2.18 and Eq. 6.1.11 are the basis for coupling of the tower and the shaft EOMs. The actions at the tower node ℓ are equal in size and opposite directed to the reactions at the shaft node 1. This is expressed in the following equation, where the necessary transformation to common coordinates has taken place

$$\left\{F^T_{T\ell R}\right\} = -[T_{AT}]\left\{F^A_{A1R}\right\} \tag{6.2.21}$$

which by use of Eq. 6.1.11 and Eq. 6.2.18 is expressed as

$$\begin{aligned}&[M_{\ell T}]\left\{\ddot{q}^T_{TT}\right\} + [M_{\ell\ell}]\left\{\ddot{q}^T_{T\ell}\right\} + [C_{\ell T}]\left\{\dot{q}^T_{TT}\right\} \\ &+ [C_{\ell\ell}]\left\{\dot{q}^T_{T\ell}\right\} + [K_{\ell T}]\left\{q^T_{TT}\right\} + [K_{\ell\ell}]\left\{q^T_{T\ell}\right\} - \left\{F^T_{T\ell E}\right\} = \\ &\quad - [T_{AT}]\Big([M_{1A}]\left\{\ddot{q}^A_{AA}\right\} + [C_{1A}]\left\{\dot{q}^A_{AA}\right\} + [K_{1A}]\left\{q^A_{AA}\right\} \\ &\qquad + [M_{TA1}]\left\{\ddot{q}^T_{T\ell}\right\} + [C_{TA1}]\left\{\dot{q}^T_{T\ell}\right\} + \left\{F^A_{456A1}\right\} - \left\{F^A_{A1E}\right\}\Big)\end{aligned} \tag{6.2.22}$$

After rearranging we get

$$
\begin{aligned}
&[M_{\ell T}]\left\{\ddot{q}^T_{TT}\right\} + \Big([M_{\ell\ell}] + [M_{TA1}]\Big)\left\{\ddot{q}^T_{T\ell}\right\} \\
&+ [C_{\ell T}]\left\{\dot{q}^T_{TT}\right\} + \Big([C_{\ell\ell}] + [C_{TA1}]\Big)\left\{\dot{q}^T_{T\ell}\right\} \\
&+ [K_{\ell T}]\left\{q^T_{TT}\right\} + [K_{\ell\ell}]\left\{q^T_{T\ell}\right\} \\
&+ [T_{AT}][M_{1A}]\left\{\ddot{q}^A_{AA}\right\} + [T_{AT}][C_{1A}]\left\{\dot{q}^A_{AA}\right\} + [T_{AT}][K_{1A}]\left\{q^A_{AA}\right\} = \\
&\qquad\qquad \left\{F^T_{T\ell E}\right\} + [T_{AT}]\left\{F^A_{A1E}\right\} - [T_{AT}]\left\{F^A_{456A1}\right\} \qquad (6.2.23)
\end{aligned}
$$

Before arranging the equations in a common matrix equation, the EOM for the blade substructure shall be derived.

6.3 Derivation of EOM for the blade substructure.

This derivation is mainly identical to the one for the shaft substructure, and the steps can be identified in two almost parallel procedures.

The acceleration at a point on the blade substructure is with the actual DOFs written as

$$
\left\{\ddot{r}^B_{B0}\right\} = [A_B]\left\{s^B_B\right\} + [B_B]\left\{\dot{u}^B_B\right\} + [C_B]\left\{\ddot{u}^B_B\right\} + \left\{a^B_{Bc}\right\} \qquad (6.3.1)
$$

Here

$$
\begin{aligned}
\left\{a^B_{Bc}\right\} \;=\; & [D_B]\left\{\ddot{u}^T_{T\ell}\right\} + [E_B]\left\{\dot{\theta}^T_{T\ell}\right\} + [F_B]\left\{\ddot{\theta}^T_{T\ell}\right\} \\
& + [G_B]\left\{u^A_{Am}\right\} + [H_B]\left\{\dot{u}^A_{Am}\right\} + [R_B]\left\{\ddot{u}^A_{Am}\right\} \qquad (6.3.2)
\end{aligned}
$$

as derived by the kinematic analysis in Sec. 3 and the subsequent evaluation and decomposition as described in [Part 2, Sec. E].

Again, Eq. 4.11.39 is the basis for the derivation of the blade EOM, quite parallel to what was done for the shaft. From [Part 2, Sec. E.3] we use the result, where the angular accelerations have been extracted from the inertia vector $\left\{{}_iF^B_{4B}\right\}$ according to [Part 2, Eq. E.3.2]

$$
\left\{{}_iF^B_{4B}\right\} = [{}_iFT2_{4B}]\left\{\ddot{\theta}^T_{T\ell}\right\} + [{}_iFA2_{4B}]\left\{\ddot{\theta}^A_{Am}\right\} + \left\{{}_iFH2^B_{4B}\right\}\ddot{\theta}^H_{1H} + \left\{{}_iFT^B_{4B}\right\} \qquad (E.3.2)
$$

Further, for the blade substructure we have the decomposed matrix product

$$
\begin{aligned}
[A_B]\left\{{}_ir^B_j\right\} \;=\; & [{}_iBT2_j]\left\{\ddot{\theta}^T_{T\ell}\right\} + [{}_iBT1_j]\left\{\dot{\theta}^T_{T\ell}\right\} \\
& + [{}_iBS2_j]\left\{\ddot{\theta}^A_{Am}\right\} + [{}_iBS1_j]\left\{\dot{\theta}^A_{Am}\right\} + [{}_iBS0_j]\left\{\theta^A_{Am}\right\} \\
& + \left\{{}_iBH2^B_j\right\}\ddot{\theta}^H_1 + \left\{{}_iBH1^B_j\right\}\dot{\theta}^H_1 + \left\{{}_iBC0^B_j\right\} \qquad (6.3.3)
\end{aligned}
$$

where the coefficient matrices and vectors now are functions of the vector coordinates for $\{{}_ir_j^B\}$. The coefficient matrices and the vectors are listed in [Part 2, Sec. E.2].

For use in Eq. 4.11.39 line 3, the following matrices are defined, based on the expressions in Eq. 6.3.3.

First, in order to simplify the writing we introduce

$$[T_{EiB}^*]\,[{}_iF_5]\,[T_{EiB}]^T = [{}_iF_{5B}^*] \tag{6.3.4}$$

which is used in the following definitions

$$\left.\begin{array}{l}
[{}_iF_{5B}^*]\,[{}_iBT2_{12}] = [{}_iFT2_{5B}] \\
[{}_iF_{5B}^*]\,[{}_iBT1_{12}] = [{}_iFT1_{5B}] \\
[{}_iF_{5B}^*]\,[{}_iBS2_{12}] = [{}_iFS2_{5B}] \\
[{}_iF_{5B}^*]\,[{}_iBS1_{12}] = [{}_iFS1_{5B}] \\
[{}_iF_{5B}^*]\,[{}_iBS0_{12}] = [{}_iFS0_{5B}] \\
[{}_iF_{5B}^*]\,\{{}_iBH2_{12}^B\} = \{{}_iFH2_{5B}^B\} \\
[{}_iF_{5B}^*]\,\{{}_iBH1_{12}^B\} = \{{}_iFH1_{5B}^B\} \\
[{}_iF_{5B}^*]\,\{{}_iBC0_{12}^B\} = \{{}_iFC0_{5B}^B\}
\end{array}\right\} \tag{6.3.5}$$

Equivalently, for use in Eq. 4.11.39 line 4, the following matrices, related to Eq. 6.3.2 and Eq. 6.3.3, are defined, using the substitution

$$[T_{EiB}^*]\,[{}_iF_6]\,[T_{EiB}]^T = [{}_iF_{6B}^*] \tag{6.3.6}$$

Definitions related to Eq. 6.3.2 are

$$\left.\begin{array}{l}
[{}_iF_{6B}^*]\,[D_B] = [{}_iFD_{6B}] \\
[{}_iF_{6B}^*]\,[E_B] = [{}_iFE_{6B}] \\
[{}_iF_{6B}^*]\,[F_B] = [{}_iFF_{6B}] \\
[{}_iF_{6B}^*]\,[G_B] = [{}_iFG_{6B}] \\
[{}_iF_{6B}^*]\,[H_B] = [{}_iFH_{6B}] \\
[{}_iF_{6B}^*]\,[R_B] = [{}_iFR_{6B}]
\end{array}\right\} \tag{6.3.7}$$

and definitions related to Eq. 6.3.3 are

$$\left.\begin{array}{l}
[{}_iF_{6B}^*]\,[{}_iBT2_1] = [{}_iFT2_{6B}] \\
[{}_iF_{6B}^*]\,[{}_iBT1_1] = [{}_iFT1_{6B}] \\
[{}_iF_{6B}^*]\,[{}_iBS2_1] = [{}_iFS2_{6B}] \\
[{}_iF_{6B}^*]\,[{}_iBS1_1] = [{}_iFS1_{6B}] \\
[{}_iF_{6B}^*]\,[{}_iBS0_1] = [{}_iFS0_{6B}] \\
[{}_iF_{6B}^*]\,\{{}_iBH2_1^B\} = \{{}_iFH2_{6B}^B\} \\
[{}_iF_{6B}^*]\,\{{}_iBH1_1^B\} = \{{}_iFH1_{6B}^B\} \\
[{}_iF_{6B}^*]\,\{{}_iBC0_1^B\} = \{{}_iFC0_{6B}^B\}
\end{array}\right\} \tag{6.3.8}$$

Eq. 4.11.39 may now be rewritten, using Eqs. 6.3.5, 6.3.7, and 6.3.8, and further, for the moment assuming that the resulting inertia force is zero for convenience. The result is

$$
\begin{aligned}
[{}_iM_B]\left\{{}_i\ddot{q}_B^B\right\} + [{}_iC_{BC}]\left\{{}_i\dot{q}_B^B\right\} + [{}_iK_{BI}]\left\{{}_iq_B^B\right\} = \\
&-\left(\left\{{}_iFT_{4B}^B\right\} + \left\{{}_iFC0_{5B}^B\right\} + \left\{{}_iFC0_{6B}^B\right\}\right) \\
&-\left(\left\{{}_iFT2_{4B}^B\right\} + [{}_iFT2_{5B}] + [{}_iFT2_{6B}] + [{}_iFF_{6B}]\right)\left\{\ddot{\theta}_{T\ell}^T\right\} \\
&-\left([{}_iFT1_{5B}] + [{}_iFT1_{6B}] + [{}_iFE_{6B}]\right)\left\{\dot{\theta}_{T\ell}^T\right\} \\
&-\left([{}_iFA2_{4B}] + [{}_iFS2_{5B}] + [{}_iFS2_{6B}]\right)\left\{\ddot{\theta}_{Am}^A\right\} \\
&-\left([{}_iFS1_{5B}] + [{}_iFS1_{6B}]\right)\left\{\dot{\theta}_{Am}^A\right\} \\
&-\left([{}_iFS0_{5B}] + [{}_iFS0_{6B}]\right)\left\{\theta_{Am}^A\right\} \\
&-\left(\left\{{}_iFH2_{4B}^B\right\} + \left\{{}_iFH2_{5B}^B\right\} + \left\{{}_iFH2_{6B}^B\right\}\right)\ddot{\theta}_{1H}^H \\
&-\left(\left\{{}_iFH1_{5B}^B\right\} + \left\{{}_iFH1_{6B}^B\right\}\right)\dot{\theta}_{1H}^H \\
&-[{}_iFD_{6B}]\left\{\ddot{u}_{T\ell}^T\right\} \\
&-[{}_iFG_{6B}]\left\{u_{Am}^A\right\} \\
&-[{}_iFH_{6B}]\left\{\dot{u}_{Am}^A\right\} \\
&-[{}_iFR_{6B}]\left\{\ddot{u}_{Am}^A\right\}
\end{aligned}
\tag{6.3.9}
$$

In order to use the usual 12 dimensional DOF–vector, Eq. 6.3.9 is rearranged by using the following definitions

$$\left.\begin{array}{l}
\left[\ [{}_iFD_{6B}]\ \middle|\ \left([{}_iFT2_{4B}]+[{}_iFT2_{5B}]+[{}_iFT2_{6B}]+[{}_iFF_{6B}]\right)\ \right]=[{}_iM_{TB}]\\
\left[\ [0]\qquad\ \middle|\ \left([{}_iFT1_{5B}]+[{}_iFT1_{6B}]+[{}_iFE_{6B}]\right)\ \right]=[{}_iC_{TB}]\\
\left[\ [{}_iFR_{6B}]\ \middle|\ \left([{}_iFA2_{4B}]+[{}_iFS2_{5B}]+[{}_iFS2_{6B}]\right)\ \right]=[{}_iM_{AB}]\\
\left[\ [{}_iFH_{6B}]\ \middle|\ \left([{}_iFS1_{5B}]+[{}_iFS1_{6B}]\right)\ \right]=[{}_iC_{AB}]\\
\left[\ [{}_iFG_{6B}]\ \middle|\ \left([{}_iFS0_{5B}]+[{}_iFS0_{6B}]\right)\ \right]=[{}_iK_{AB}]\\
\left\{{}_iFH2^B_{4B}\right\}+\left\{{}_iFH2^B_{5B}\right\}+\left\{{}_iFH2^B_{6B}\right\}=\left\{{}_iM^B_{HB}\right\}\\
\left\{{}_iFH1^B_{5B}\right\}+\left\{{}_iFH1^B_{6B}\right\}=\left\{{}_iC^B_{HB}\right\}\\
\left\{{}_iFT^B_{4B}\right\}+\left\{{}_iFC0^B_{5B}\right\}+\left\{{}_iFC0^B_{6B}\right\}=\left\{{}_iF^B_{456B}\right\}
\end{array}\right\}\qquad(6.3.10)$$

Further, structural damping and structural stiffness, given by

$$\left.\begin{array}{l}[{}_iC_B]=[{}_iC_{BC}]+[{}_iC_s]\\ [{}_iK_B]=[{}_iK_{BI}]+[{}_iK_s]\end{array}\right\}\qquad(6.3.11)$$

are introduced into Eq. 6.3.9.

The indices refer to the origin of the matrix, which is inertia or structural properties

$[C_{BC}]$ is the Coriolis matrix, which is related to the $[B_B]$–matrix

$[K_{BI}]$ is the inertia stiffness or softening matrix, which is related to the $[A_B]$–matrix

$[C_s]$ is structural damping

$[K_s]$ is structural stiffness

If concentrated node masses are present, they have to be added to the mass matrix $[{}_iM_B]$, at the diagonal elements. Also, the external load vector is entered into the equation.

The result is the EOM for a blade element

$$\begin{aligned}
&[{}_iM_B]\left\{{}_i\ddot{q}^B_B\right\}+[{}_iC_B]\left\{{}_i\dot{q}^B_B\right\}+[{}_iK_B]\left\{{}_iq^B_B\right\}=\\
&\quad\left\{{}_iF^B_B\right\}-\left\{{}_iF^B_{456B}\right\}\\
&\quad-[{}_iM_{TB}]\left\{\ddot{q}^T_{T\ell}\right\}-[{}_iC_{TB}]\left\{\dot{q}^T_{T\ell}\right\}\\
&\quad-[{}_iM_{AB}]\left\{\ddot{q}^A_{Am}\right\}-[{}_iC_{AB}]\left\{\dot{q}^A_{Am}\right\}-[{}_iK_{AB}]\left\{q^A_{Am}\right\}\\
&\quad-\left\{{}_iM^B_{HB}\right\}\ddot{\theta}^H_{1H}-\left\{{}_iC^B_{HB}\right\}\dot{\theta}^H_{1H}
\end{aligned}\qquad(6.3.12)$$

where, analogous to the tower– and shaft–substructure

$\left\{{}_iF_B^B\right\}$ is composed of the externally applied loads, including gravity and aerodynamic loads, consistently transformed to the nodes, as prescribed in Sec. 4.10. For the coupling node to the shaft substructure the vector also includes the reactions.

When the blade EOM is assembled, the node numbering must be considered, because the structure is no longer a simple chain, as was the case for the tower and the shaft. To illustrate the preferred systematics, a general example with 3 blades is used. The difference between global node numbers for one element determines the band width of the coefficient matrices. Therefore, the following way of assigning node numbers is used.

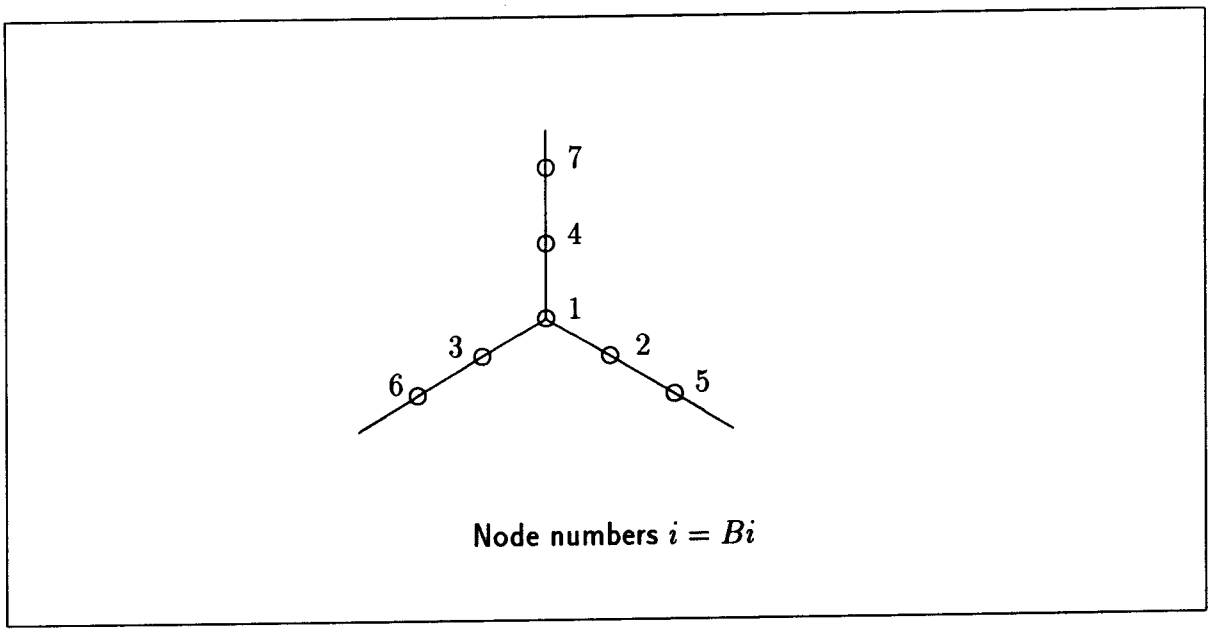

Figure 18: Node numbering for blades.

As illustrated in fig. 18, the node which couples the blades to the shaft is given number 1. The remaining nodes are numbered sequentially by chosing the node closest to the center node on one blade as node 2, and then step from blade to blade in the same direction, e.g. clock–wise, always taking the unnumbered node closest to the center as the next one in the sequence. This procedure results in a maximum node difference equal to the number of blades, and this number is also equal to the half band–width of the coefficient matrices.

The assembled EOM for the blade substructure is written

$$\begin{aligned}
&[M_B]\left\{\ddot{q}_B^B\right\} + [C_B]\left\{\dot{q}_B^B\right\} + [K_B]\left\{q_B^B\right\} = \\
&\quad \left\{F_B^B\right\} - \left\{F_{456B}^B\right\} \\
&\quad - [M_{TB}]\left\{\ddot{q}_{T\ell}^T\right\} - [C_{TB}]\left\{\dot{q}_{T\ell}^T\right\} \\
&\quad - [M_{AB}]\left\{\ddot{q}_{Am}^A\right\} - [C_{AB}]\left\{\dot{q}_{Am}^A\right\} - [K_{AB}]\left\{q_{Am}^A\right\} \\
&\quad - \left\{M_{HB}^B\right\}\ddot{\theta}_{1H}^H - \left\{C_{HB}^B\right\}\dot{\theta}_{1H}^H
\end{aligned} \tag{6.3.13}$$

Partitioning of Eq. 6.3.13 prepares the coupling of the shaft and the blade EOM

$$
\begin{aligned}
&\begin{bmatrix} [M_{B11}] & [M_{1B}] \\ [M_{B1}] & [M_{BB}] \end{bmatrix} \begin{Bmatrix} \{\ddot{q}^B_{B1}\} \\ \{\ddot{q}^B_{BB}\} \end{Bmatrix} + \begin{bmatrix} [C_{B11}] & [C_{1B}] \\ [C_{B1}] & [C_{BB}] \end{bmatrix} \begin{Bmatrix} \{\dot{q}^B_{B1}\} \\ \{\dot{q}^B_{BB}\} \end{Bmatrix} \\
&+ \begin{bmatrix} [K_{B11}] & [K_{1B}] \\ [K_{B1}] & [K_{BB}] \end{bmatrix} \begin{Bmatrix} \{q^B_{B1}\} \\ \{q^B_{BB}\} \end{Bmatrix} = \\
&\qquad \begin{Bmatrix} \{F^B_{B1E}\} + \{F^B_{B1R}\} - \{F^B_{456B1}\} \\ \{F^B_{BBE}\} - \{F^B_{456BB}\} \end{Bmatrix} \\
&\qquad - \begin{bmatrix} [M_{TB1}] \\ [M_{TBB}] \end{bmatrix} \{\ddot{q}^T_{T\ell}\} - \begin{bmatrix} [C_{TB1}] \\ [C_{TBB}] \end{bmatrix} \{\dot{q}^T_{T\ell}\} \\
&\qquad - \begin{bmatrix} [M_{AB1}] \\ [M_{ABB}] \end{bmatrix} \{\ddot{q}^A_{Am}\} - \begin{bmatrix} [C_{AB1}] \\ [C_{ABB}] \end{bmatrix} \{\dot{q}^A_{Am}\} - \begin{bmatrix} [K_{AB1}] \\ [K_{ABB}] \end{bmatrix} \{q^A_{Am}\} \\
&\qquad - \begin{Bmatrix} \{M^B_{HB1}\} \\ \{M^B_{HBB}\} \end{Bmatrix} \ddot{\theta}^H_{1H} - \begin{Bmatrix} \{C^B_{HB1}\} \\ \{C^B_{HBB}\} \end{Bmatrix} \dot{\theta}^H_{1H}
\end{aligned}
\tag{6.3.14}
$$

Here

$$
\{\ddot{q}^B_{B1}\} = \{\dot{q}^B_{B1}\} = \{q^B_{B1}\} = \{0\} \tag{6.3.15}
$$

this being an implication of the choice of coordinate system that has its origo at node 1, and follows the movements of the blade point.

The first partitioned row of Eq. 6.3.14 gives after multiplication and using Eq. 6.3.15 (index E – external, index R – reaction)

$$
\begin{aligned}
&[M_{1B}]\{\ddot{q}^B_{BB}\} + [C_{1B}]\{\dot{q}^B_{BB}\} + [K_{1B}]\{q^B_{BB}\} = \\
&\quad \{F^B_{B1E}\} + \{F^B_{B1R}\} - \{F^B_{456B1}\} \\
&\quad - [M_{TB1}]\{\ddot{q}^T_{T\ell}\} - [C_{TB1}]\{\dot{q}^T_{T\ell}\} \\
&\quad - [M_{AB1}]\{\ddot{q}^A_{Am}\} - [C_{AB1}]\{\dot{q}^A_{Am}\} - [K_{AB1}]\{q^A_{Am}\} \\
&\quad - \{M^B_{HB1}\}\ddot{\theta}^H_{1H} - \{C^B_{HB1}\}\dot{\theta}^H_{1H}
\end{aligned}
\tag{6.3.16}
$$

The reactions at the shaft node m, must be equal in size and opposite in direction to the reactions at blade node 1

$$
\{F^A_{AmR}\} = -[T_{BA}]\{F^B_{B1R}\} \tag{6.3.17}
$$

The reactions are isolated in eqs. 6.2.20 and 6.3.16, respectively, and substituted in Eq. 6.3.17

$$
\begin{aligned}
&[M_{mA}]\left\{\ddot{q}^A_{AA}\right\} + [M_{mm}]\left\{\ddot{q}^A_{Am}\right\} + [C_{mA}]\left\{\dot{q}^A_{AA}\right\} \\
&+ [C_{mm}]\left\{\dot{q}^A_{Am}\right\} + [K_{mA}]\left\{q^A_{AA}\right\} + [K_{mm}]\left\{q^A_{Am}\right\} \\
&+ [M_{TAm}]\left\{\ddot{q}^T_{T\ell}\right\} + [C_{TAm}]\left\{\dot{q}^T_{T\ell}\right\} + \left\{F^A_{456Am}\right\} - \left\{F^A_{AmE}\right\} = \\
&\qquad - [T_{BA}]\Big(\quad [M_{1B}]\left\{\ddot{q}^B_{BB}\right\} + [C_{1B}]\left\{\dot{q}^B_{BB}\right\} + [K_{1B}]\left\{q^B_{BB}\right\} \\
&\qquad\qquad + [M_{TB1}]\left\{\ddot{q}^T_{T\ell}\right\} + [C_{TB1}]\left\{\dot{q}^T_{T\ell}\right\} \\
&\qquad\qquad + [M_{AB1}]\left\{\ddot{q}^A_{Am}\right\} + [C_{AB1}]\left\{\dot{q}^A_{Am}\right\} + [K_{AB1}]\left\{q^A_{Am}\right\} \\
&\qquad\qquad + \left\{M^B_{HB1}\right\}\ddot{\theta}^H_{1H} + \left\{C^B_{HB1}\right\}\dot{\theta}^H_{1H} \\
&\qquad\qquad + \left\{F^B_{456B1}\right\} - \left\{F^B_{B1E}\right\} \quad \Big)
\end{aligned}
\tag{6.3.18}
$$

After rearranging we get the equation ready for combination in the system EOM

$$
\begin{aligned}
&[M_{mA}]\left\{\ddot{q}^A_{AA}\right\} + \Big([M_{mm}] + [T_{BA}]\,[M_{AB1}]\Big)\left\{\ddot{q}^A_{Am}\right\} \\
&+ [C_{mA}]\left\{\dot{q}^A_{AA}\right\} + \Big([C_{mm}] + [T_{BA}]\,[C_{AB1}]\Big)\left\{\dot{q}^A_{Am}\right\} \\
&+ [K_{mA}]\left\{q^A_{AA}\right\} + \Big([K_{mm}] + [T_{BA}]\,[K_{AB1}]\Big)\left\{q^A_{Am}\right\} \\
&+ \Big([M_{TAm}] + [T_{BA}]\,[M_{TB1}]\Big)\left\{\ddot{q}^T_{T\ell}\right\} \\
&+ \Big([C_{TAm}] + [T_{BA}]\,[C_{TB1}]\Big)\left\{\dot{q}^T_{T\ell}\right\} \\
&+ [T_{BA}]\left\{M^B_{HB1}\right\}\ddot{\theta}^H_{1H} + [T_{BA}]\left\{C^B_{HB1}\right\}\dot{\theta}^H_{1H} \\
&+ [T_{BA}]\,[M_{1B}]\left\{\ddot{q}^B_{BB}\right\} + [T_{BA}]\,[C_{1B}]\left\{\dot{q}^B_{BB}\right\} + [T_{BA}]\,[K_{1B}]\left\{q^B_{BB}\right\} = \\
&\qquad \left\{F^A_{AmE}\right\} + [T_{BA}]\left\{F^B_{B1E}\right\} - \left\{F^A_{456Am}\right\} - [T_{BA}]\left\{F^B_{456B1}\right\}
\end{aligned}
\tag{6.3.19}
$$

The EOM for the inner blade substructure is identified as the last row of the partitioned Eq. 6.3.14, which after introduction of Eq. 6.3.15 is written as

$$
\begin{aligned}
&[M_{BB}]\left\{\ddot{q}^B_{BB}\right\} + [C_{BB}]\left\{\dot{q}^B_{BB}\right\} + [K_{BB}]\left\{q^B_{BB}\right\} \\
&+ [M_{TBB}]\left\{\ddot{q}^T_{T\ell}\right\} + [C_{TBB}]\left\{\dot{q}^T_{T\ell}\right\} \\
&+ [M_{ABB}]\left\{\ddot{q}^A_{Am}\right\} + [C_{ABB}]\left\{\dot{q}^A_{Am}\right\} + [K_{ABB}]\left\{q^A_{Am}\right\} \\
&+ \left\{M^B_{HBB}\right\}\ddot{\theta}^H_{1H} + \left\{C^B_{HBB}\right\}\dot{\theta}^H_{1H} = \\
&\qquad\qquad \left\{F^B_{BBE}\right\} - \left\{F^B_{456BB}\right\}
\end{aligned}
\tag{6.3.20}
$$

This equation is also ready for assembly into the total system EOM.

6.4 Derivation of EOM for the teeter DOF.

The reactions at blade node 1 must be transformed to the teeter degree of freedom in order to derive the EOM for the teeter DOF.

Assuming that the teeter DOF has a stiffness and a damping given by

K_{1H} – teeter spring stiffness
C_{1H} – teeter damper

the EOM is written

$$
\begin{aligned}
&C_{1H}\dot{\theta}^H_{1H} + K_{1H}\theta^H_{1H} = \\
&\quad \text{row}_4\Big[-\Big([M_{1B}]\left\{\ddot{q}^B_{BB}\right\} + [C_{1B}]\left\{\dot{q}^B_{BB}\right\} + [K_{1B}]\left\{q^B_{BB}\right\} \\
&\qquad + [M_{TB1}]\left\{\ddot{q}^T_{T\ell}\right\}[C_{TB1}]\left\{\dot{q}^T_{T\ell}\right\} \\
&\qquad + [M_{AB1}]\left\{\ddot{q}^A_{Am}\right\} + [C_{AB1}]\left\{\dot{q}^A_{Am}\right\} + [K_{AB1}]\left\{q^A_{Am}\right\} \\
&\qquad + \left\{M^B_{HB1}\right\}\ddot{\theta}^H_{1H} + \left\{C^B_{HB1}\right\}\dot{\theta}^H_{1H} \\
&\qquad + \left\{F^B_{456B1}\right\} - \left\{F^B_{B1E}\right\}\Big)\Big]
\end{aligned}
\tag{6.4.1}
$$

where the symbol row_4 identifies a sort of operator, which indicates that only row number 4 of the resulting vector on the right hand side is part of the equation.

After minor rearrangements Eq. 6.4.1 can be directly combined with the other substructure EOMs into the total system EOM, where the teeter DOF then will appear as one single DOF.

6.5 Assembly of substructure EOMs to the system EOM.

In the previous sections, all the relevant substructure equations of motion have been derived, and the force compatibility conditions at the coupling nodes have been established.

The actual equations are

Eq.6.1.9 – Reactions at the tower support, corresponding tower DOF $\left\{q^T_{T1}\right\}$. May be determined, when the node displacements have been solved for.

Eq.6.1.10 – EOM for the inner tower DOFs $\left\{q^T_{TT}\right\}$.

Eq.6.2.23 – EOM for the coupling node between tower (node $T\ell$) and shaft (node $A1$) substructures, corresponding to DOF $\left\{q^T_{T\ell}\right\}$.

Eq.6.2.19 – EOM for the inner shaft DOFs $\left\{q^A_{AA}\right\}$.

Eq.6.3.19 – EOM for the coupling node between shaft (node Am) and blade (node $B1$) substructures, corresponding to DOF $\left\{q^A_{Am}\right\}$.

Although the teeter DOF, θ^H_{1H}, is at the same coupling node, the force compatibility still ensures that the coupling is correctly established, as the kinematic analysis has provided for the geometric compatibility.

Eq.6.4.1 – EOM for the teeter DOF, θ^H_{1H}.

Eq.6.3.20 – EOM for the inner DOFs of the blade substructure, $\left\{q^B_{BB}\right\}$.

Combination of these equations in a single system equation of motion gives

$$[M_S]\{\ddot{q}_S\} + [C_S]\{\dot{q}_S\} + ([K_S] + [K_{gS}])\{q_S\} = \{F_S\} \tag{6.5.1}$$

where

$$\{q_S\}^T = \left[\left\{q^T_{TT}\right\}^T, \left\{q^T_{T\ell}\right\}^T, \left\{q^A_{AA}\right\}^T, \left\{q^A_{Am}\right\}^T, \theta^H_{1H}, \left\{q^B_{BB}\right\}^T\right] \tag{6.5.2}$$

The geometric stiffness matrix $[K_{gS}]$ is shown separately in order to simplify the appearance of the matrices.

The following coefficient matrices are obtained:

The system mass matrix

$[M_S] =$

$\{\ddot{q}^T_{TT}\}$	$\{\ddot{q}^T_{T\ell}\}$	$\{\ddot{q}^A_{AA}\}$	$\{\ddot{q}^A_{Am}\}$	$\ddot{\theta}^H_{1H}$	$\{\ddot{q}^B_{BB}\}$
$[M_{TT}]$	$[M_{T\ell}]$	[0]	[0]	{0}	[0]
$[M_{\ell T}]$	$[M_{\ell\ell}]$ + $[T_{AT}]\,[M_{TA1}]$	$[T_{AT}]\,[M_{1A}]$	[0]	{0}	[0]
[0]	$[M_{TAA}]$	$[M_{AA}]$	$[M_{Am}]$	{0}	[0]
[0]	$[M_{TAm}]$ + $[T_{BA}]\,[M_{TB1}]$	$[M_{mA}]$	$[M_{mm}]$ + $[T_{BA}]\,[M_{AB1}]$	$[T_{BA}]\,\{M^B_{HB1}\}$	$[T_{BA}]\,[M_{1B}]$
0	$row_4\left([M_{TB1}]\right)$	0	$row_4\left([M_{AB1}]\right)$	$row_4\left(\{M^B_{HB1}\}\right)$	$row_4\left([M_{1B}]\right)$
[0]	$[M_{TBB}]$	[0]	$[M_{ABB}]$	$\{M^B_{HBB}\}$	$[M_{BB}]$

(6.5.3)

the system damping matrix

$$[C_S] =$$

$\{\dot{q}^T_{TT}\}$	$\{\dot{q}^T_{T\ell}\}$	$\{\dot{q}^A_{AA}\}$	$\{\dot{q}^A_{Am}\}$	$\dot{\theta}^H_{1H}$	$\{\dot{q}^B_{BB}\}$
$[C_{TT}]$	$[C_{T\ell}]$	[0]	[0]	{0}	[0]
$[C_{\ell T}]$	$[C_{\ell\ell}] + [T_{AT}]\,[C_{TA1}]$	$[T_{AT}]\,[C_{1A}]$	[0]	{0}	[0]
[0]	$[C_{TAA}]$	$[C_{AA}]$	$[C_{Am}]$	[0]	[0]
[0]	$[C_{TAm}] + [T_{BA}]\,[C_{TB1}]$	$[C_{mA}]$	$[C_{mm}] + [T_{BA}]\,[C_{AB1}]$	$[T_{BA}]\,\{C^B_{HB1}\}$	$[T_{BA}]\,[C_{1B}]$
0	$row_4\left([C_{TB1}]\right)$	0	$row_4\left([C_{AB1}]\right)$	$C_{1H} + row_4\left(\{C^B_{HB1}\}\right)$	$row_4\left([C_{1B}]\right)$
[0]	$[C_{TBB}]$	[0]	$[C_{ABB}]$	$\{C^B_{HBB}\}$	$[C_{BB}]$

(6.5.4)

the system stiffness matrix

$$[K_S] =$$

$\{q^T_{TT}\}$	$\{q^T_{T\ell}\}$	$\{q^A_{AA}\}$	$\{q^A_{Am}\}$	θ^H_{1H}	$\{q^B_{BB}\}$
$[K_{TT}]$	$[K_{T\ell}]$	[0]	[0]	{0}	[0]
$[K_{\ell T}]$	$[K_{\ell\ell}]$	$[T_{AT}]\,[K_{1A}]$	[0]	{0}	[0]
[0]	[0]	$[K_{AA}]$	$[K_{Am}]$	{0}	[0]
[0]	[0]	$[K_{mA}]$	$[K_{mm}] + [T_{BA}]\,[K_{AB1}]$	{0}	$[T_{BA}]\,[K_{1B}]$
0	0	0	$row_4\left([K_{AB1}]\right)$	K_{1H}	$row_4\left([K_{1B}]\right)$
[0]	[0]	[0]	$[K_{ABB}]$	{0}	$[K_{BB}]$

(6.5.5)

and the system geometric stiffness matrix

$$[K_{gS}] =$$

$\{q^T_{TT}\}$	$\{q^T_{T\ell}\}$	$\{q^A_{AA}\}$	$\{q^A_{Am}\}$	q^H_{1H}	$\{q^B_{BB}\}$
[0]	[0]	[0]	[0]	{0}	[0]
[0]	[0]	[0]	[0]	{0}	[0]
[0]	[0]	[0]	[0]	{0}	[0]
[0]	$[K_{gTA}]$	[0]	$[K_{gAA}]$	$\{K_{gHA}\}$	$[K_{gBA}]$
0	$\{K_{gTH}\}^T$	0	$\{K_{gAH}\}^T$	K_{gHH}	$\{K_{gBH}\}^T$
[0]	$[K_{gTB}]$	[0]	$[K_{gAB}]$	$\{K_{gHB}\}$	$[K_{gBB}]$

(6.5.6)

The geometric stiffness submatrices are not listed. Their derivation is based on the considerations in Sec. 5 and specifically Eq. 5.3.18.

The system load combines to

$$\{F_S\} = \begin{Bmatrix} \{F^T_{TT}\} \\ \{F^T_{T\ell E}\} + [T_{AT}]\{F^A_{A1E}\} - [T_{AT}]\{F^A_{456A1}\} \\ \{F^A_{AA}\} - \{F^A_{456A}\} \\ \{F^A_{AmE}\} - \{F^A_{456Am}\} + [T_{BA}]\{F^B_{B1E}\} - [T_{BA}]\{F^B_{456B1}\} \\ \text{row}_4\left(\{F^B_{B1E}\}\right) - \text{row}_4\left(\{F^B_{456B1}\}\right) \\ \{F^B_{BBE}\} - \{F^B_{456BB}\} \end{Bmatrix} \tag{6.5.7}$$

The program includes only the external loads on the blades $\{F^B_{BBE}\}$, combined of the gravity load as derived in Sec. 4.12 and the aerodynamic load as derived in [Part 2, Sec. F].

7 Solution procedures.

The mathematical model has resulted in a computer program written in Fortran 77. This closely follows the mathematical model and therefore a detailed description is omitted. The program allows for calculation of eigensolutions and time integration of the equations of motion.

The eigensolutions are found by a two step procedure. The first step involves calculation of eigenfrequencies by use of the Sturm-sequence property for symmetrical matrices and the method of bisection [M6, pp. 157-162]. The symmetric form of the equations of motion is established (see Sec. 5) including geometric stiffness (centrifugal stiffening) and the eigensolutions are calculated. These eigenvalues are then used in the second step as starting values in an inverse iteration performed on the nonsymmetric eigenvalue problem of the substructure formulation. The procedure works well as demonstrated in Sec. 8.

The time integration is performed by use of the Newmark implicit integration scheme [B1, pp. 549-552]. The sequence in the integration is shown in the diagram of Fig. 19, where also the

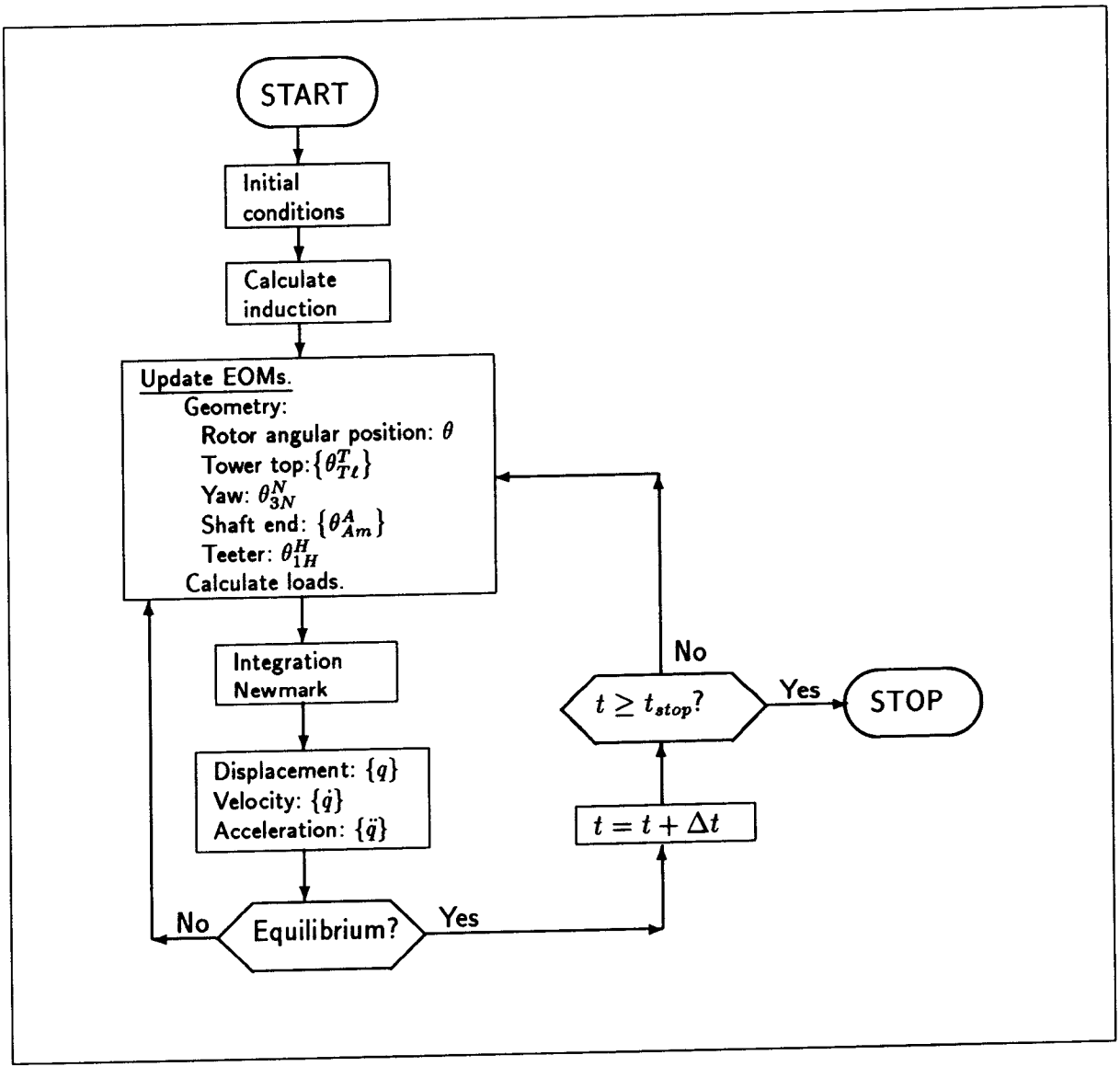

Figure 19: Solution of equations of motion.

step concerning updating of the geometry is shown. Due to the time dependent coefficient matrices, it is necessary to perform iterations in order to obtain equilibrium at each time step.

The Newton-Raphson iteration scheme is used [B1, pp. 490-491]. In genral no convergence problems arise when just an appropriate time step is chosen.

8 Results.

To illustrate some of the abilities of the model, simulations have been carried out on a three bladed rigid hub turbine. Initially the model parameters are established from known geometry and material parameters. A final adjustment of the model is carried out so that agreement is obtained between the measured and the model eigenfrequencies for the fundamental mode shapes.

The presented results concentrate on the dynamic characteristics. Initially, examples of deterministic response are presented. Due to omission of the tilt in the simulations and uncertainty on the tower interference and aerodynamic models, a realistic comparison of the shape and size of the deterministic response would require some transformations and adjustments and this tedious work has been avoided. Still, the comparison of the dynamics of the deterministic response is justified when only the relative distribution of energy on the frequencies, and not the actuel energy content, is compared.

Next, simulations including turbulence are compared with measurements. Again, the distribution on frequencies of the energy is the only characteristic where agreement can be expected, when the above mentioned adjustment of parameters have not been accomplished.

In all the simulations the gravity has been omitted in the model in order to elucidate the dynamics in the response variables, which otherwise would be dominated by the gravity.

8.1 Main data for the reference wind turbine.

The wind turbine used for the preliminary comparison of simulation results with measurements is the 180 kW Danwin [R1] of the stall regulated type. The main data for the turbine are listed in Table 1.

Finite element model.

A total of 14 elements have been used for the finite element model, corresponding to 84 degrees of freedom. The distribution of elements on the substructures and the node location in substructure coordinates are listed in Table 2.

Eigenfrequencies and mode shapes.

Initially, the fundamental eigenfrequencies and mode shapes have been calculated for the non-rotating turbine and the model parameters adjusted at the same time, in order to obtain agreement between the model and the measured eigenfrequencies. The tower model is based on the drawings. The blade model has been established with recourse to a similar model set up at the Test Station for Windmills at Risø. The shaft dimension is the basic parameter when the shaft-nacelle substructure is modelled. Final addition of mass and mass moment of inertia at the tower top node brings the frequencies to agree within approximately 2%. The centrifugal stiffening (geometric stiffness) is included when the simulations are carried out. For this case, the five lowest eigenfrequencies and the corresponding mode shapes are described below with reference to Fig. 20. Because the dominating displacements take place in the x- and y-directions, due to the slender tower and blade substructures, only the tower top and the blade tip displacements in the horizontal plane are reproduced in this description.

The rotor azimuthal position is with blade No. 1 vertical upward, i.e. $\theta = 180$ deg. The angular velocity of the rotor is $\omega = 4.95$ rad/sec corresponding to 47.3 RPM.

Table 1: Main data for Danwin 180 kW.

Rotor.	Rotor diameter:	22.2 m
	Number of blades:	3
	Position of rotor:	Upwind
	Rotaional speed:	46.5–47.5 RPM
	Cone angle :	0 deg
	Tilt angle :	5 deg
	Pitch angle :	−0.4 deg
Blade.	Glass fibre reinforced polyester.	
	Fundamental flapwise freq. :	3.2 Hz
	Chord at radius 2.2 m. :	1.445 m
	Chord at radius 11.1 m. :	0.565 m
	Twist :	16 deg
	Thickness variation :	32.0%–13.2%
	Total mass :	650 kg
	Center of gravity, radius :	3.12 m
	Mass moment of inertia :	11500 kgm^2
Tower.	Tapered tubular, steel.	
	Height :	29.8 m
	Diameter at top :	1.24 m
	Diameter at foundation :	2.10 m

Below, the number following the eigenfrequencies in parenthesis is the percentage increase due to the centrifugal stiffening. The mode shapes have been normalized. The units are $[m]$.

Mode 1.

Eigenfrequency = 0.886 Hz (+1.84%).
Mode shape displacements at tower top and blade tips:

$u_x^T =$	3.616E−12	$u_y^T =$	1.167E−02
$u_{1x}^B =$	−1.456E−13	$u_{1y}^B =$	1.722E−03
$u_{2x}^B =$	2.331E−05	$u_{2y}^B =$	1.619E−03
$u_{3x}^B =$	−2.331E−05	$u_{3y}^B =$	1.619E−03

It is characteristic for the mode that the deformations are mainly in the y-direction and that the tower top and blade tips are in *phase*. As regards the tower, the mode is comparable with the fundamental tower mode without rotor.

Table 2: Finite element model.

Substructure.	Node number.	Node coordinates [m]. x	y	z
Tower.	1	0.000E+00	0.000E+00	−1.070E+01
3 elements.	2	0.000E+00	0.000E+00	−1.870E+01
	3	0.000E+00	0.000E+00	−2.770E+01
Shaft.	4	0.000E+00	−1.500E+00	0.000E+01
2 elements.	5	0.000E+00	−2.000E+00	0.000E+01
Blades.	6	0.000E+00	0.000E+00	2.200E+00
9 elements,	7	1.905E+00	0.000E+00	−1.100E+00
3 per blade.	8	−1.905E+00	0.000E+00	−1.100E+00
	9	0.000E+00	0.000E+00	6.650E+00
	10	5.759E+00	0.000E+00	−3.325E+00
	11	−5.759E+00	0.000E+00	−3.325E+00
	12	0.000E+00	0.000E+00	1.110E+01
	13	9.613E+00	0.000E+00	−5.550E+00
	14	−9.613E+00	0.000E+00	−5.550E+00

Mode 2.

Eignefrequency = 0.888 Hz (+1.85%).
Mode shape displacements at tower top and blade tips:

$u_x^T =$	1.169E−02	$u_y^T =$	−2.345E−13
$u_{1x}^B =$	−4.706E−04	$u_{1y}^B =$	−3.461E−14
$u_{2x}^B =$	−9.455E−05	$u_{2y}^B =$	−4.452E−06
$u_{3x}^B =$	−9.455E−05	$u_{3y}^B =$	4.452E−06

The deformations are mainly in the x-direction and the tower top and the blade tips are in *phase*. This mode is tower dominated as it is the case with mode 1. This fact is also reflected in the almost identical eigenfrequencies.

Mode 3.

Eignefrequency = 2.67 Hz (+7.66%).
Mode shape displacements at tower top and blade tips:

$u_x^T =$	−7.739E−04	$u_y^T =$	−7.047E−18
$u_{1x}^B =$	−8.602E−04	$u_{1y}^B =$	4.012E−16
$u_{2x}^B =$	−3.094E−04	$u_{2y}^B =$	−1.006E−01
$u_{3x}^B =$	−3.094E−04	$u_{3y}^B =$	1.006E−01

The deformations are mainly in the x-direction and the tower top and the blade tips are in

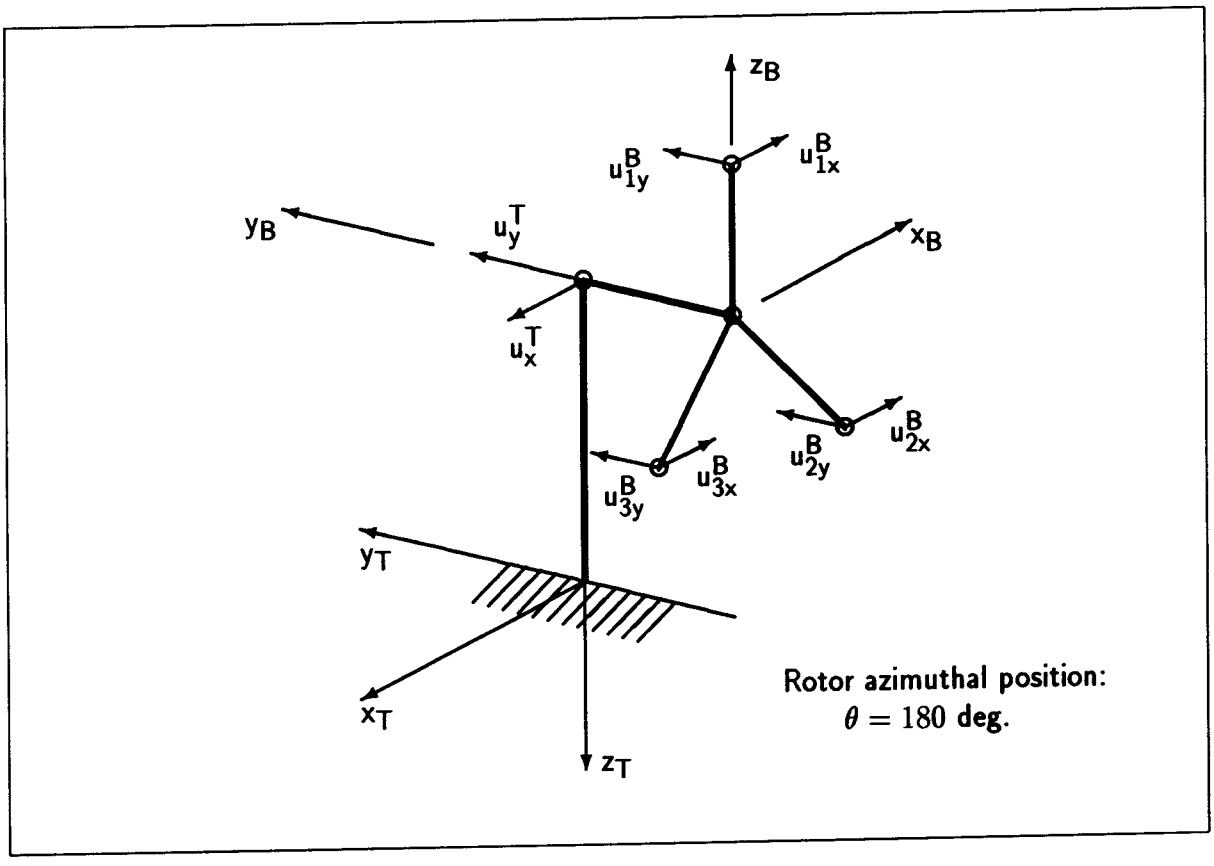

Figure 20: Coordinates for fundamental mode shapes.

counter phase in this direction. The tower is in a torsional motion (yaw). Blade 1 is almost at rest while blade 2 and 3 are in *counter phase* with respect to displacement in the y-direction. The rotor mode is often referred to as the asymmetrical mode.

Mode 4.

Eignefrequency = 2.78 Hz (+8.59%).
Mode shape displacements at tower top and blade tips:

$u_x^T =$	2.682E−18	$u_y^T =$	7.776E−04
$u_{1x}^B =$	−5.448E−18	$u_{1y}^B =$	1.182E−01
$u_{2x}^B =$	−2.762E−04	$u_{2y}^B =$	6.455E−02
$u_{3x}^B =$	2.762E−04	$u_{3y}^B =$	6.455E−02

The deformations are mainly in the y-direction. The tip ends of blade 2 and blade 3 are in *phase* with the tower top and blade 1 is in *counter phase*. The tower is in a bending motion (tilt). This rotor mode is also referred to as an asymmetrical mode. In fact, if the rotor was considered as an isolated structure, the rotor mode from mode shape 3 and this one correspond to a double eigenfrequency of the rotor.

Mode 5.

Eignefrequency = 3.39 Hz (+8.65%).
Mode shape displacements at tower top and blade tips:

$u_x^T =$	7.790E−18	$u_y^T =$	−2.132E−03
$u_{1x}^B =$	1.909E−17	$u_{1y}^B =$	1.118E−01
$u_{2x}^B =$	−4.863E−05	$u_{2y}^B =$	1.063E−01
$u_{3x}^B =$	4.863E−05	$u_{3y}^B =$	1.063E−01

The deformations are mainly in the y-direction. The blade tip ends are in *counter phase* with respect to the tower top. The eigenfrequency is close to the blade eigenfrequency.

8.2 Simulation of deterministic response.

The deterministic response has been simulated in a mean wind speed of 12 m/s, i.e. no turbulence is present. The wind shear corresponds to a surface roughness of 0.05 m. Two simulations have been run with and without tower interference represented, respectively. Wind shear is present in both cases.

The simulation is initiated with the structure static deflected, corresponding to the steady wind load, with blade 1 in zero azimuthal position. Initial deformation velocities and accelerations are zero. Therefore, the first revolutions show some transient response. The structural damping is set rather arbitrarily to approximately 5% of critical.

Generally, reasonable agreement is observed as regards the order of magnitude of measured and simulated response. In Fig. 21 the flap wise blade bending moment at radius 0 m is shown. The most dense curve with the square legends shows the response moment with tower interference included. It is evident that the blade dynamics is heavily influenced by the impulse from the tower. The lighter curve shows the response due to pure wind shear. The saw tooth is the signal corresponding to azimuthal position. A discrete Fourier transform (DFT) of the response shows the distribution of energy on the frequencies in Fig. 22. The peaks are at multiples of the rotor rotational frequency (1P = 4.95 rad/sec). The 4 first peaks are comparable in size, while the following peaks are significantly smaller. An equivalent analysis of a measured response [R1, p. 39] is shown in Fig. 23, where the same tendency can be observed. The reason for the discontinuity in peak heights at 4P is that the blade fundamental flap wise eigenfrequency is close to 4P.

The flap wise response with only wind shear present has been analysed in the same way. The result is shown in Fig. 24 where the energy is concentrated around the 1P frequency.

A similar analysis has been carried through for the blade moment in the lead lag direction. The simulated time response is shown in Fig. 25 and the Fourier transform in Fig. 26. An increase in the harmonic peaks around 6P is observed, due to the higher eigenfrequency of the blade in the lead lag direction. Measured results are not presented, but they show the same tendency [R1, p. 61].

The present treatment of the simulated deterministic response is concluded with presentation of some time series showing deformations and resulting loads corresponding to important degrees of freedom.

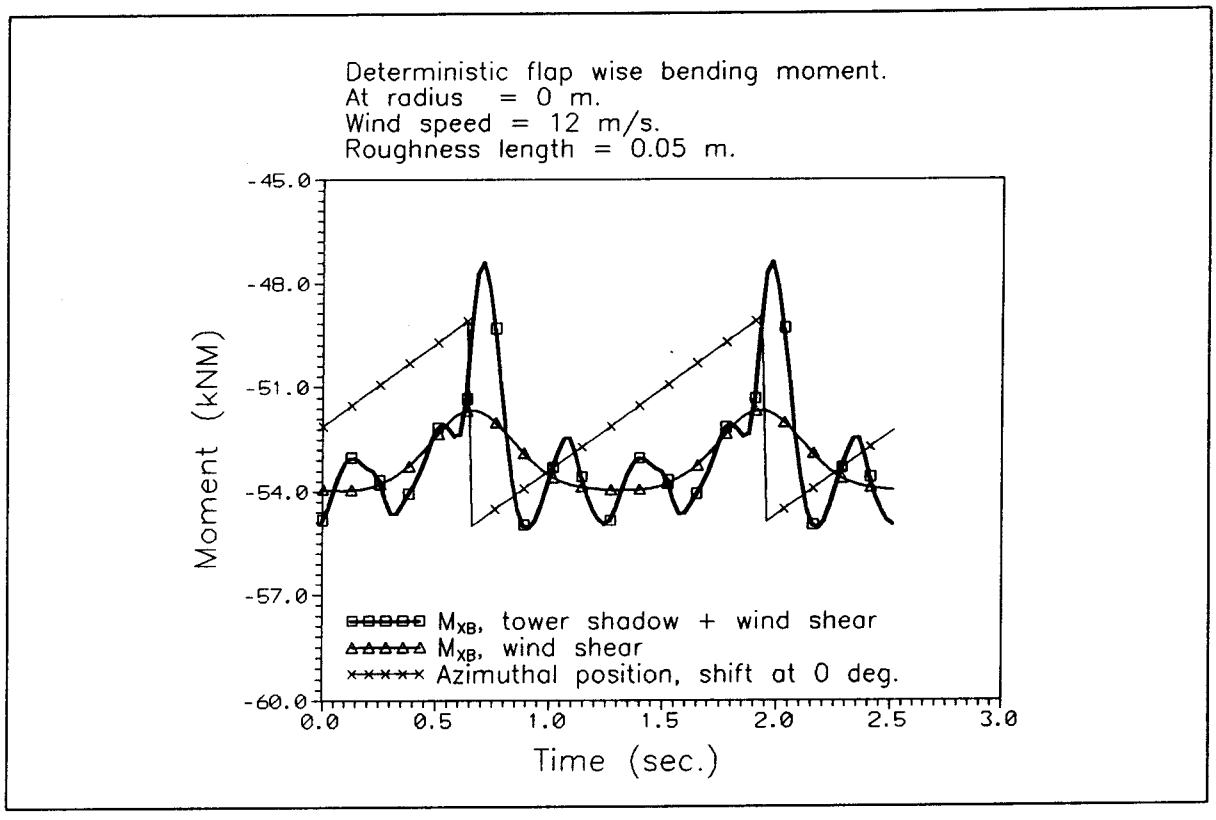

Figure 21: Blade flap wise bending moment. Deterministic.

The deflection of the blade tip in the x- and y-direction is shown in Fig. 28. The shape and the dynamic characteristics are very similar to the blade root moments described initially. In Fig. 29 some of the tower top deformations are shown. Generally, the transient response has died out after approximately 10 rotor revolutions. For deformations in the wind direction even before due to the aerodynamic damping. The tower top displacement in the across wind direction ($u^T_{xT\ell}$) is clearly lower damped than the displacement in the along wind direction ($u^T_{yT\ell}$). The 3P harmonic is observed in all the tower top signals. The DFT of the across wind displacement in Fig. 27 is presented as an example. Further, in this signal the lowest mode eigenfrequency is clearly present (0.88 Hz) due to the low aerodynamic damping in this direction and the harmonic input from 1P = 0.79 Hz. The lowest peak corresponds to the eigenfrequency and not 1P. The significant, higher harmonics are multiples of 3P. The rotor loads, thrust ($F^T_{yT\ell}$), tilt moment ($M^T_{xT\ell}$) and yaw moment ($M^T_{zT\ell}$), and further the power (P) presented in Fig. 30, show the same characteristic 3P content. These observations are in good agreement with the measurements.

8.3 Simulation of stochastic response.

A simulation has been carried out with the purpose of comparing with measurements and of illustrating the influence of turbulence on the response. The simulation parameters are chosen in agreement with the immediately available corresponding parameters for a measurement carried out in a mean wind speed of 8.1 m/s. Representative response characteristics of the simulation results are compared with the measured. The turbulence length scale has not been adjusted to the actual measured but is chosen to 150 m, which is known to be typical for the test site for similar conditions. The standard deviation of the measured wind speed is 1.04 m/s at hub height, corresponding to a turbulence intensity of 12.5%. Only flap wise blade bending

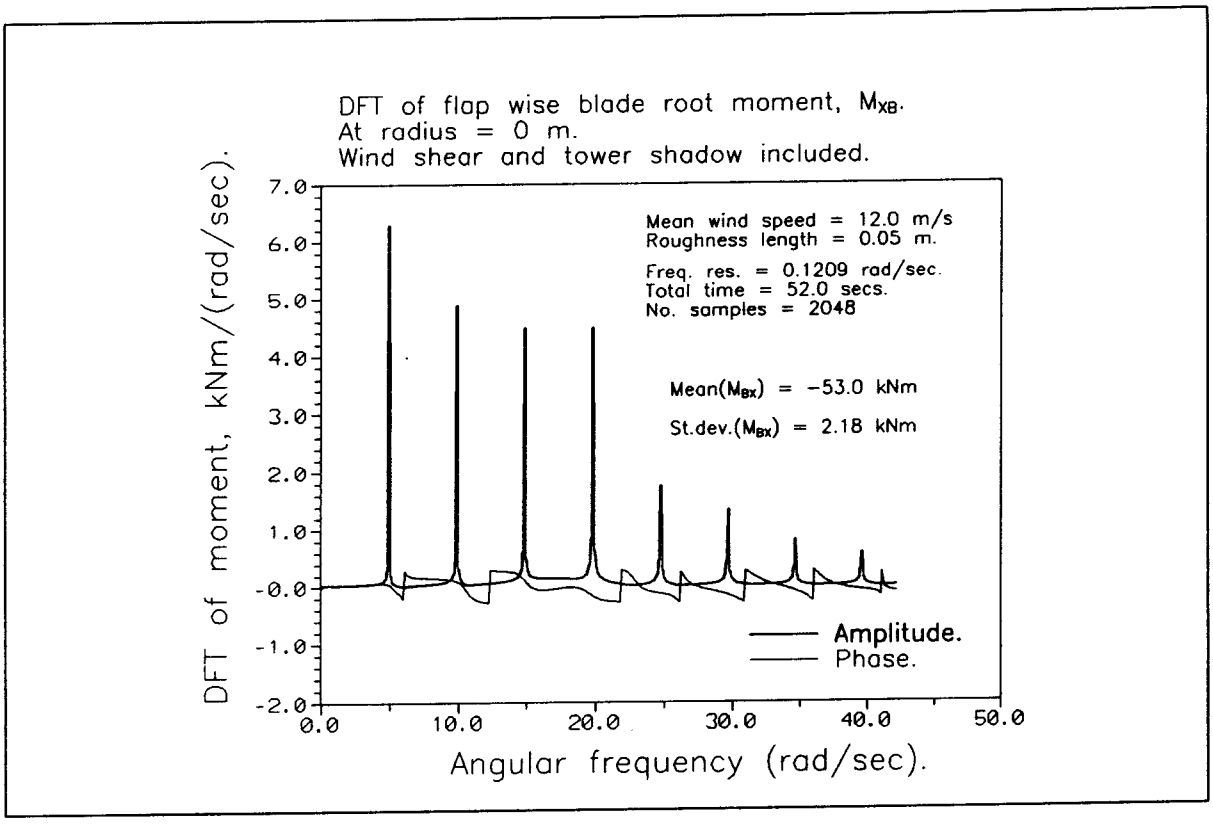

Figure 22: DFT of blade flap wise bending moment. Deterministic.

moment at radius 0.47 m is presented in the comparison.

The measured signal is sampled at a frequency of 25 Hz, and 8192 samples covering a time period of 328 secs are used. As mentioned previously, only the relative distribiution of energy on the frequencies and not the energy amount can be expected to agree when adjustment of the wind field model and the aerodynamic model has not been accomplished, and the actual energy content is not considered.

The simulation period covers a time period 52 secs with a sample rate of 39.4 Hz giving a total of 2048 samples. It corresponds to 50 samples per rotor revolution.

Initially, the blade root moments are compared, and the section concludes with a presentation of some characteristic response variables.

Fig. 31 and 33 show a 12 secs interval of the simulated and the measured blade root flap wise moments, respectively. The shapes of the time signals are very much the same. This is also reflected in the dynamic content, as shown in the PSD plots for the two signals in Figs. 32 and 34, respectively. The harmonics of the rotor angular frequency are clearly present. Partly due to the tower interference, as previously observed for the deterministic signal, but further the rotational sampling of turbulence influences the peaks. The simulated signal peaks are located at slightly higher frequencies than the measured, due to a too high rotational frequency in the simulation. The peaks of the simulated PSD are more distinct. Especially the measured 3P and 4P peaks are more "smeared out" than the simulated. Probably, this is mainly due to the time varying rotational angular velocity of the rotor, caused by the slip in the asynchronous generator. For the power variations appearing during the considered measurement period, the corresponding slip is approximately 1.5%. At the same time structural eigenfrequencies are close to the rotaional harmonics 3P and 4P and the energy "smear out" can be expected.

The influence of the rotational sampling of the turbulence on the wind speed felt by the blade

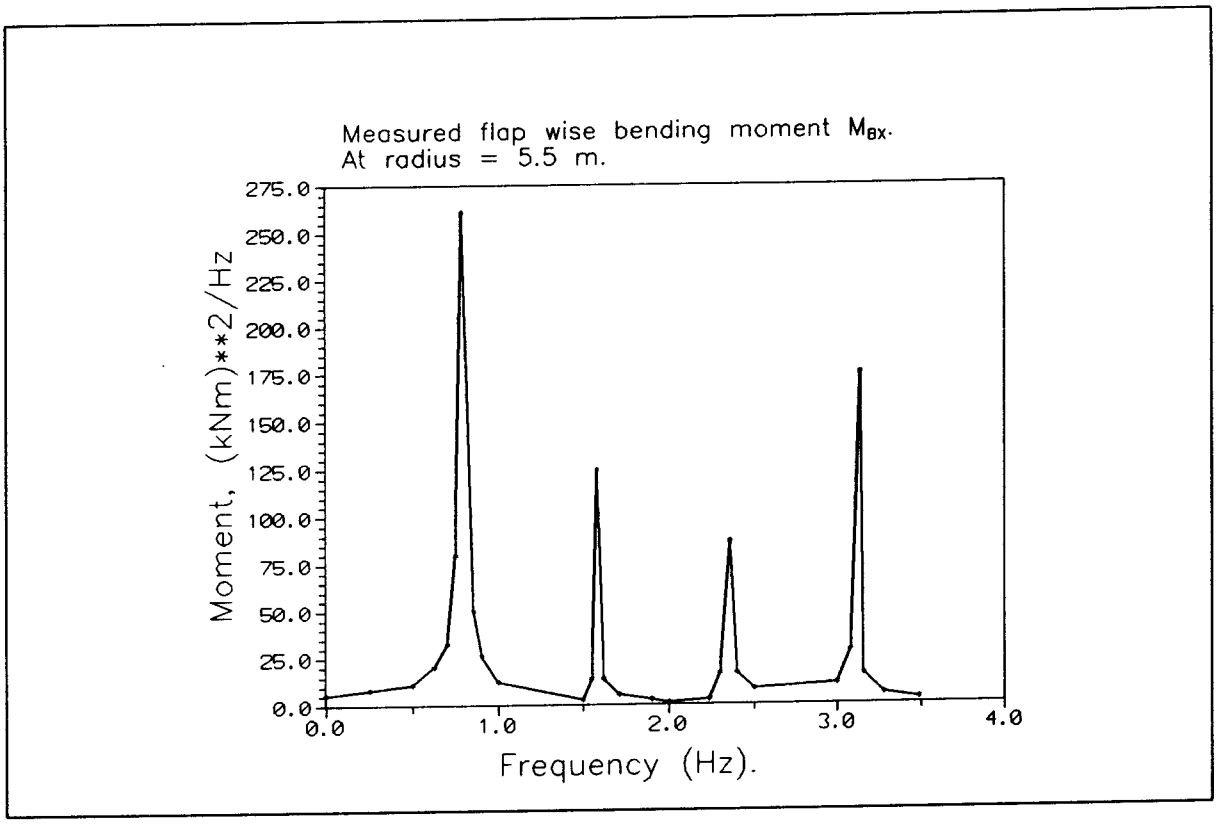

Figure 23: Fourier series resolution of measured signal.

is shown in Fig. 36, where the PSD of the sampled turbulence at the blade tip is presented. The energy is shifted from lower frequencies to harmonics of the rotational frequency. A time signal of the sampled turbulence is shown in Fig. 35. Some wind speed variance is lost during the simulation. The target spectrum has a variance of 1.1 $(m/s)^2$ while the sampled turbulence variance has decreased to 0.6 $(m/s)^2$. The explanation for this is partly the limited simulation time but also inherent in the turbulence simulation model as mentioned in [Part 2, Sec. F].

Other simulation variables are presented below in order to give a more complete picture of the dynamic response. In Fig. 37 some tower top deformations are shown. The PSD of the across wind tower displacement ($u^T_{xT\ell}$) is shown in Fig. 40. The lowest eigenfrequency (0.88 Hz) is again very significant in this signal. But generally, the 3P content is dominating for these deformations as it was the case for the deterministic response. Again it is observed that the damping in the along wind direction is higher than in the across wind direction.

In Fig. 38 the blade tip deflections are shown. Influence of the tower interference is still very clear. The relative energy distribution on frequencies is comparable to what is seen for the blade root response.

Simulated signals corresponding to rotor loads and power are shown in Fig. 39. In general, these variables are comparable with the corresponding signals for the deterministic response with tower influence included. The PSD of the yaw moment is shown in Fig. 41. The 3P harmonic is dominating.

The preliminary simulation results presented above show in general a reasonable agreement with corresponding measured results and experience. Allthough the material is rather limited and covers a wind turbine of the "rigid type" it is concluded that satisfactory model representation of the most important dynamic effects is achieved.

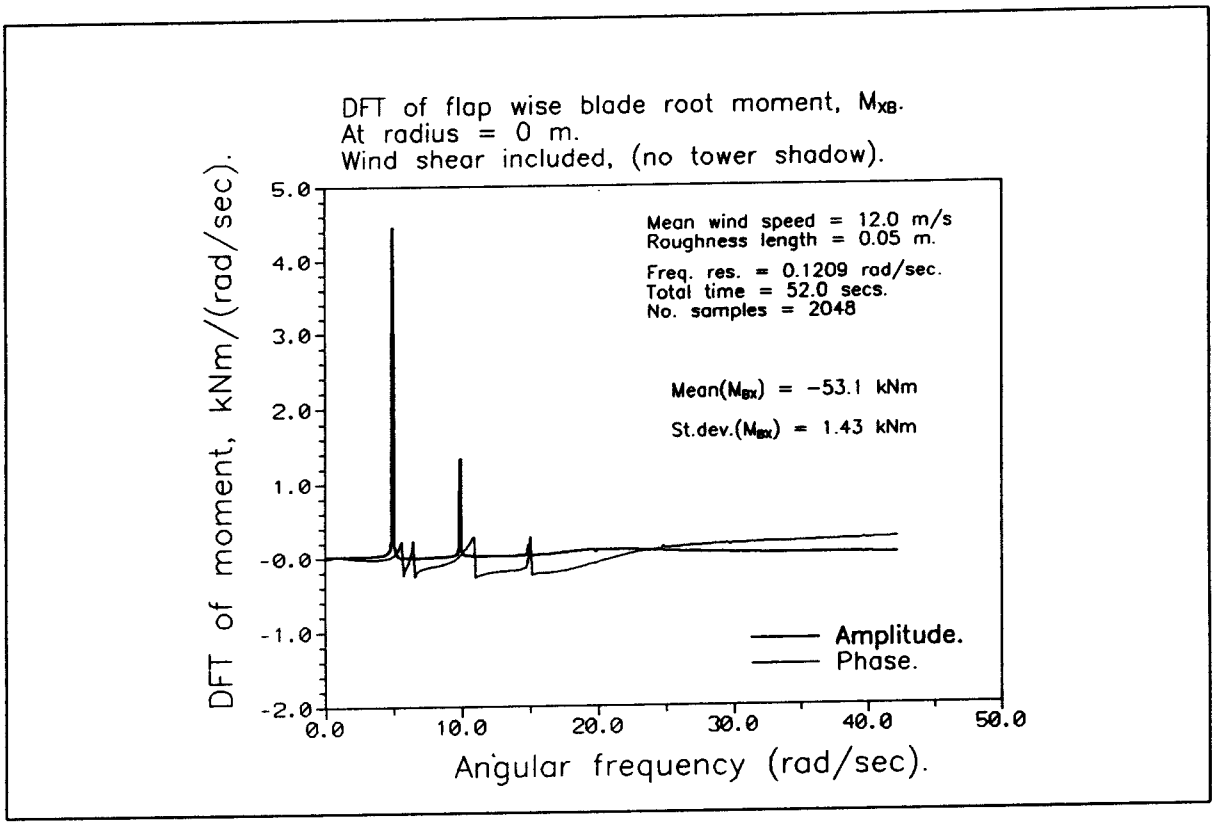

Figure 24: DFT of blade flap wise bending moment. Deterministic without tower shadow.

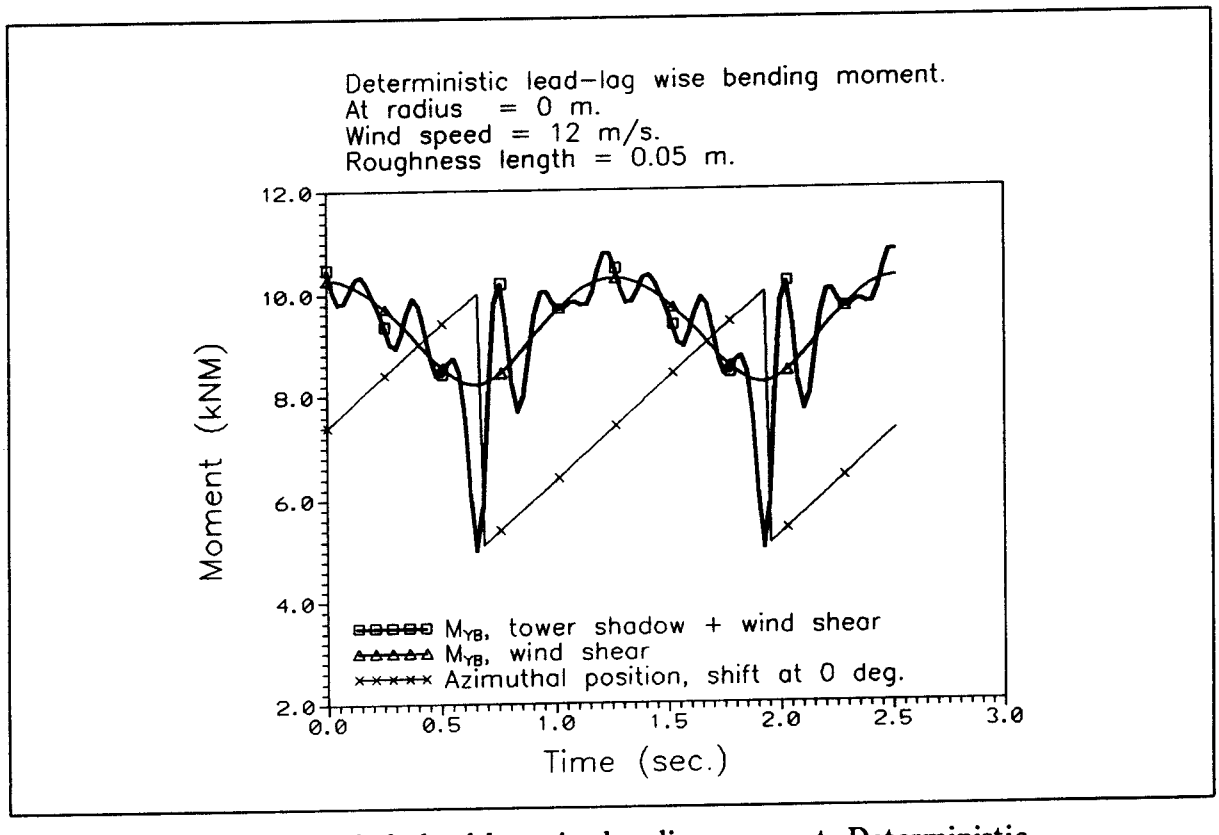

Figure 25: Blade lead-lag wise bending moment. Deterministic.

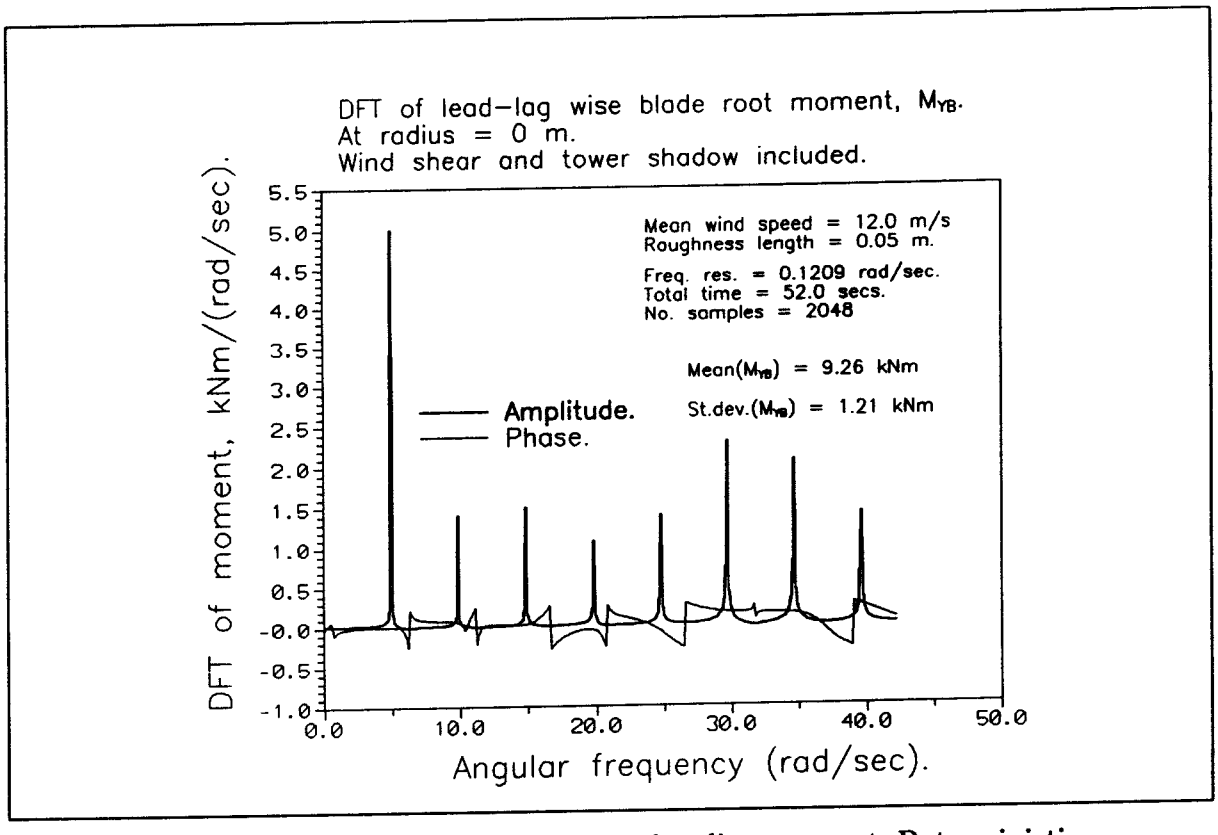

Figure 26: DFT of blade lead-lag wise bending moment. Deterministic.

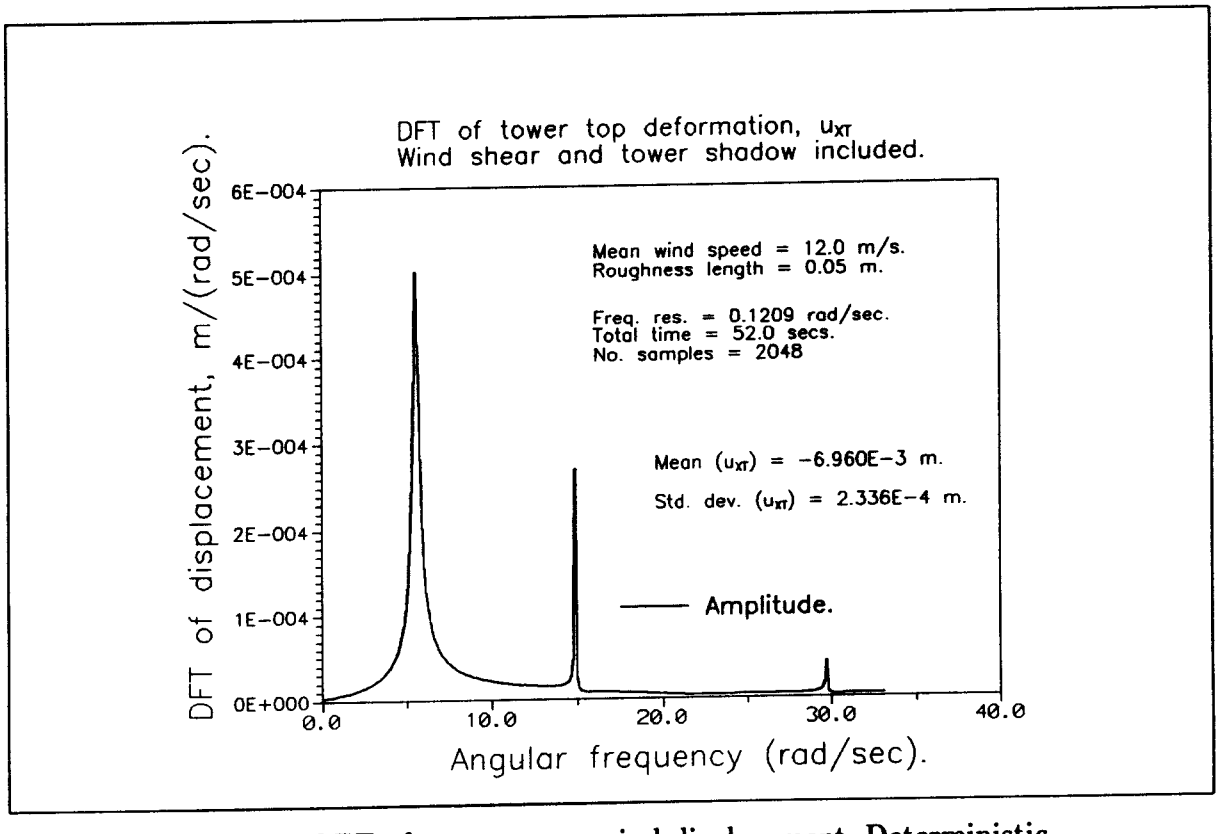

Figure 27: DFT of tower across wind displacement. Deterministic.

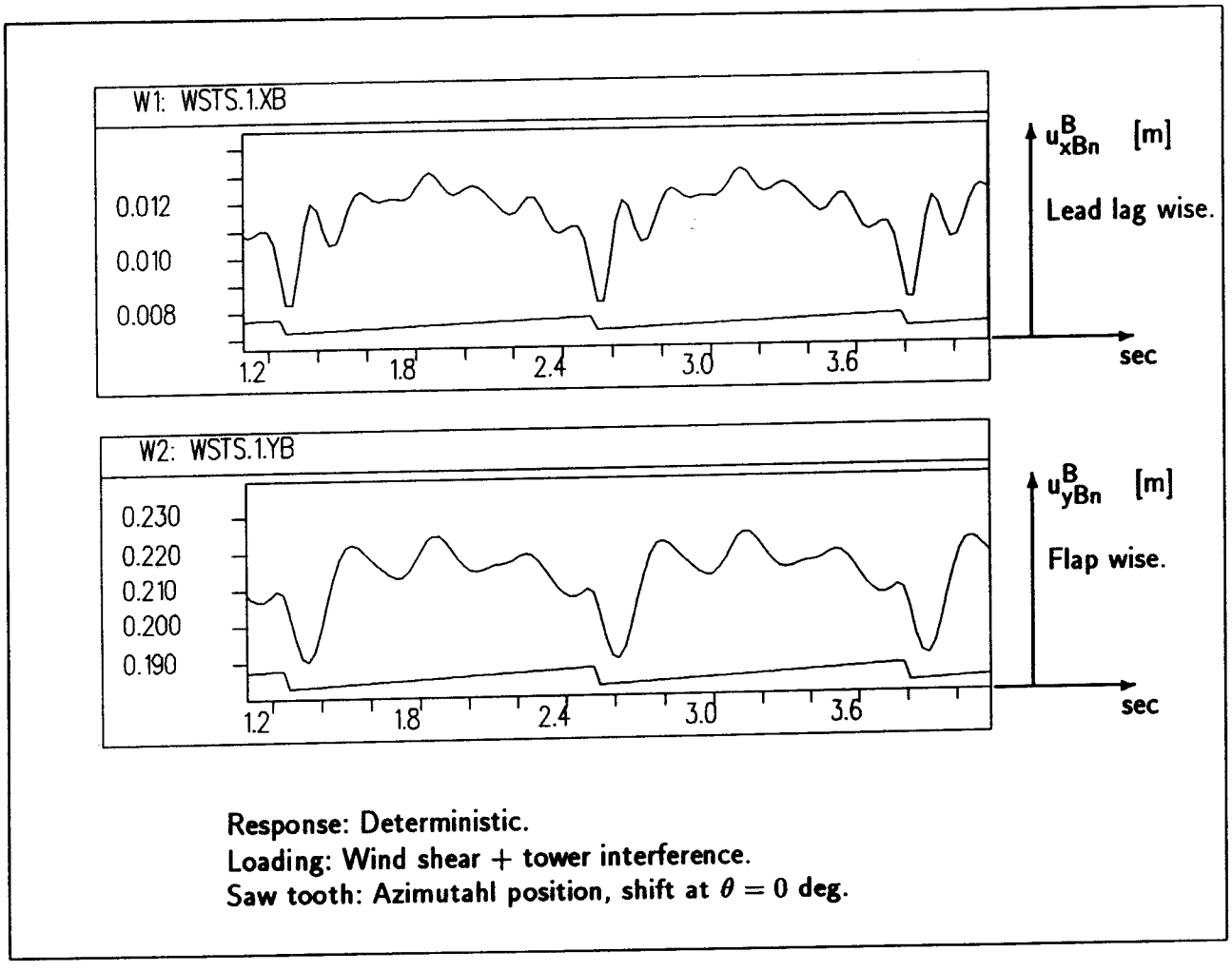

Figure 28: Blade tip deformation. Deterministic.

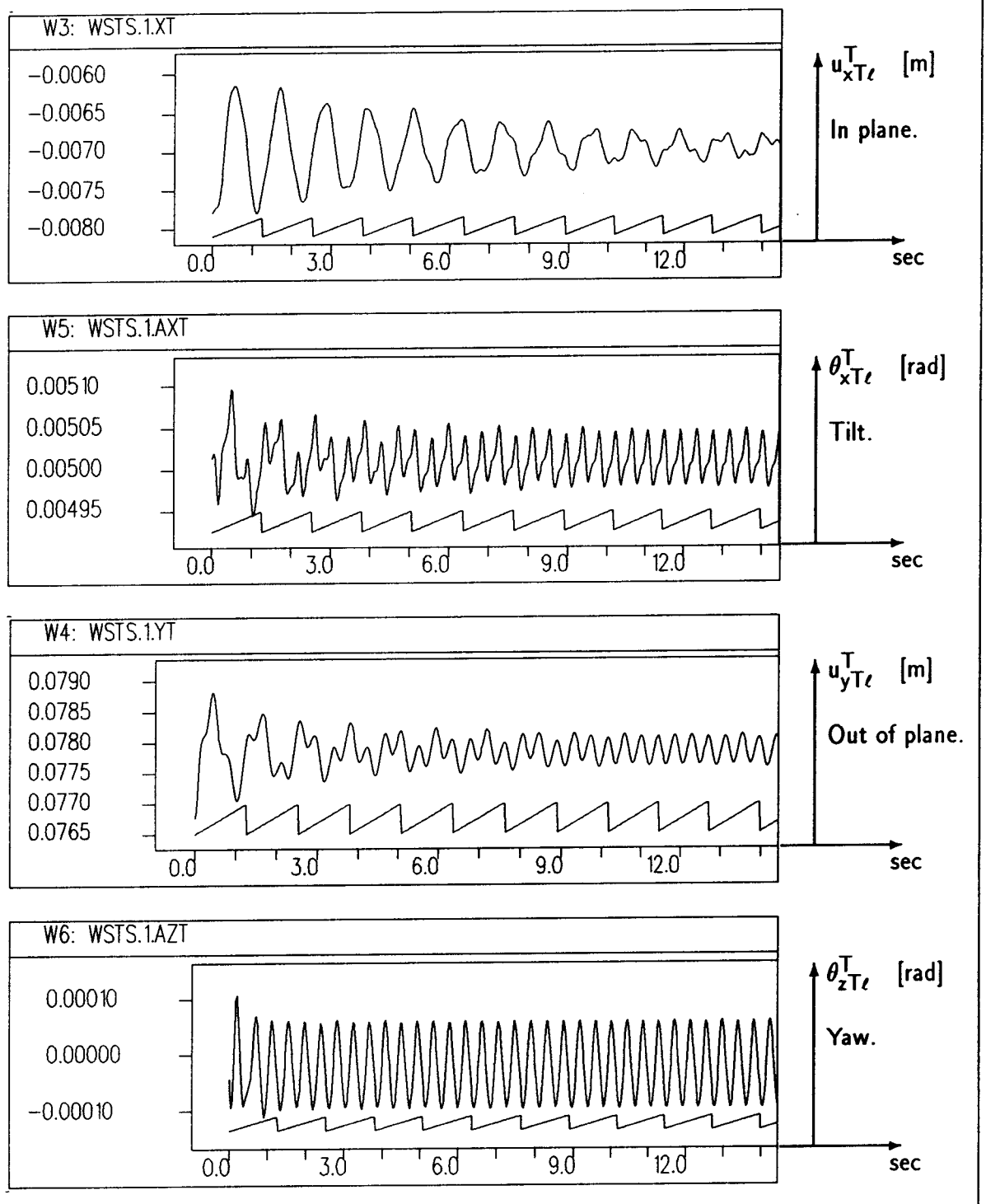

Figure 29: Tower top deformation. Deterministic.

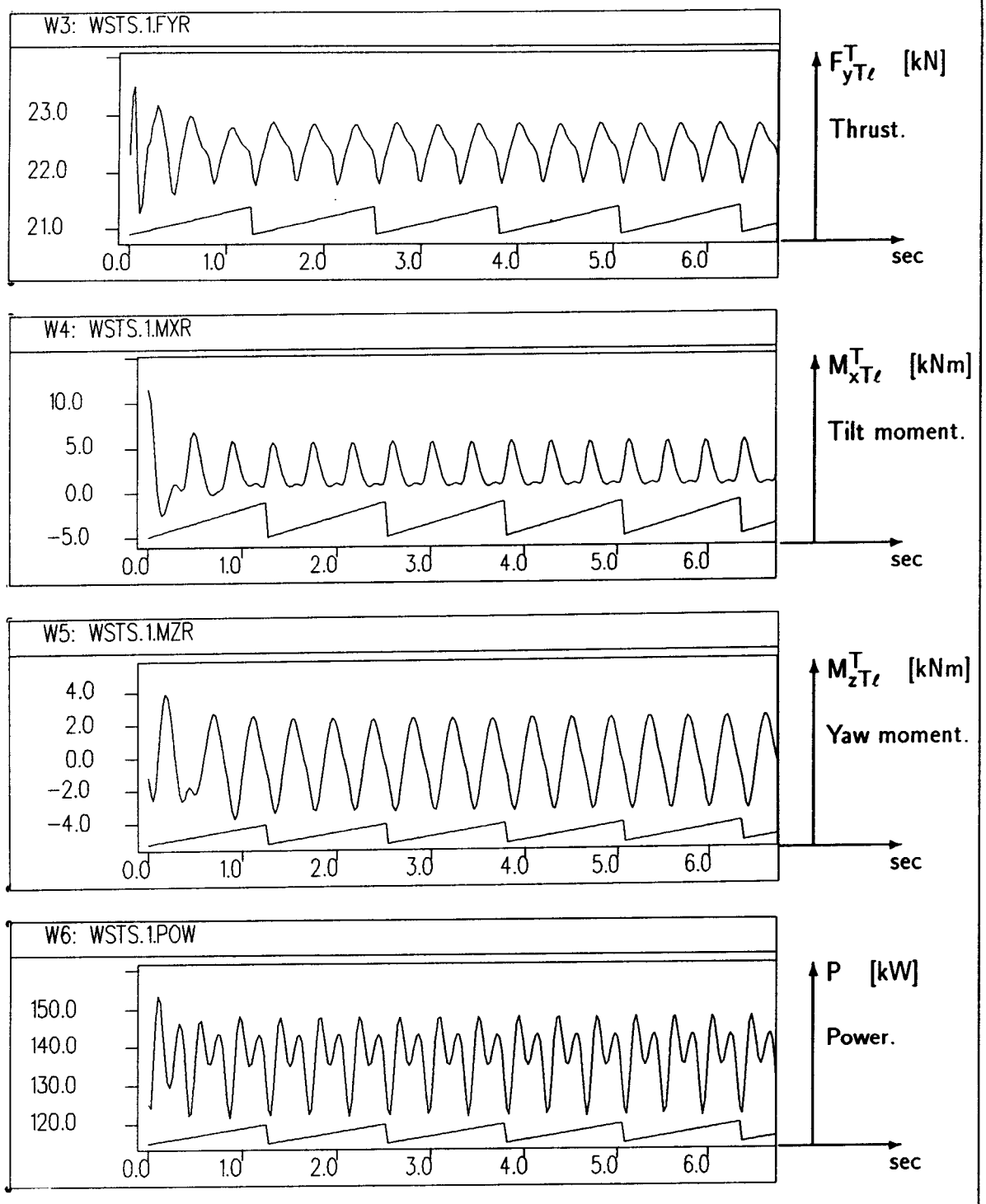

Figure 30: Tower top node loads (rotor loads). Deterministic.

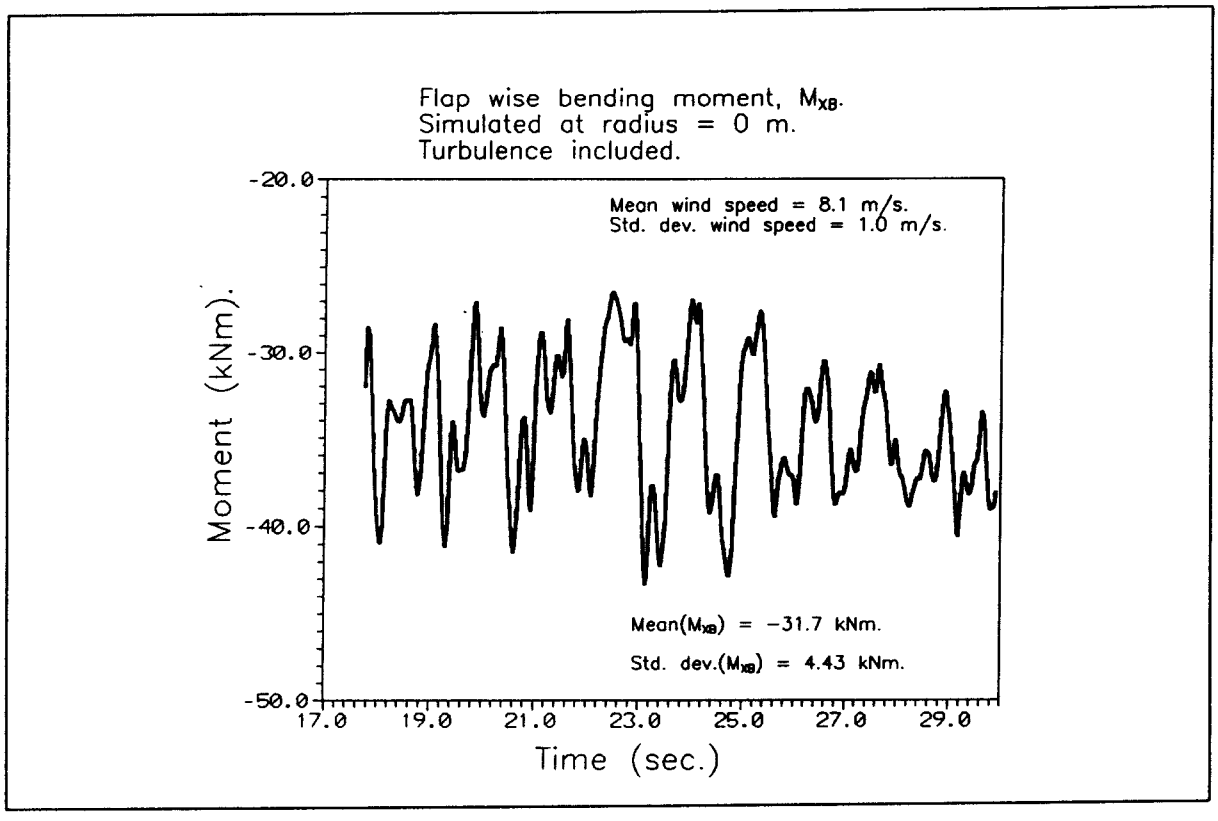

Figure 31: Blade flap wise bending moment. Simulated, stochastic.

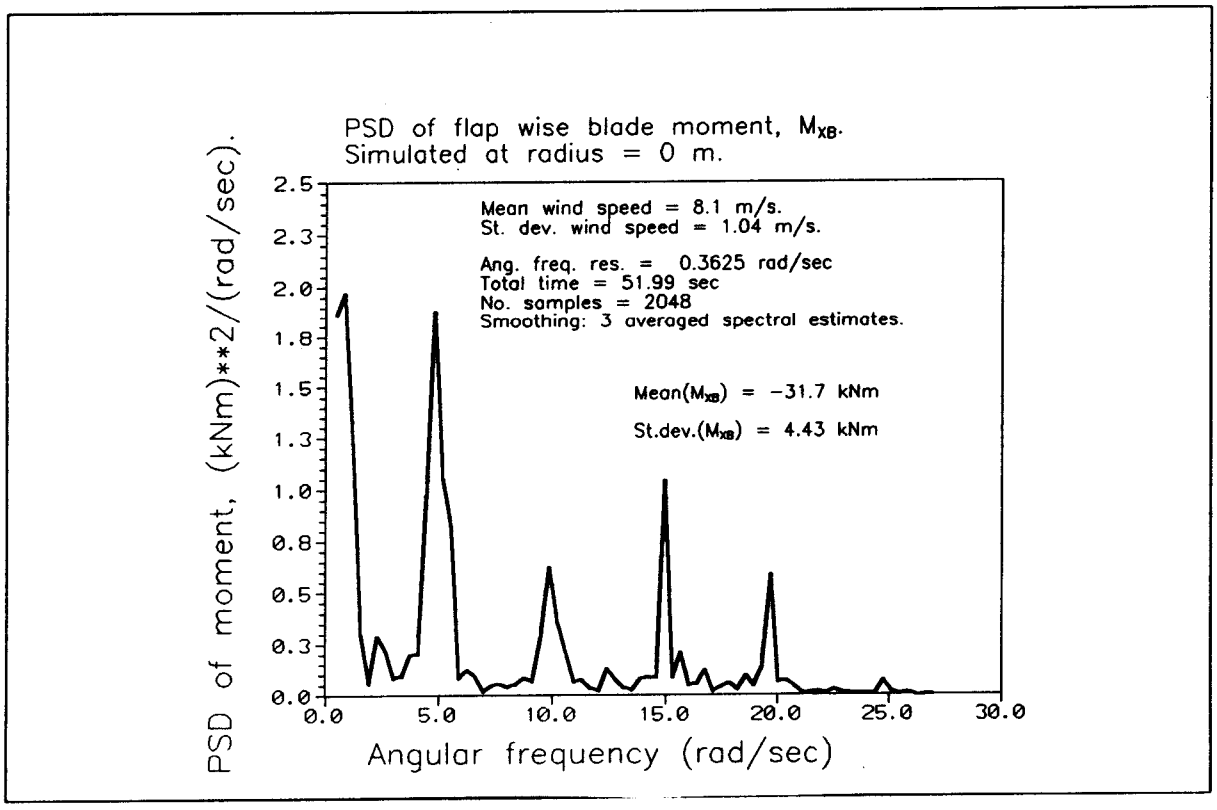

Figure 32: PSD of blade flap wise bending moment. Simulated, stochastic.

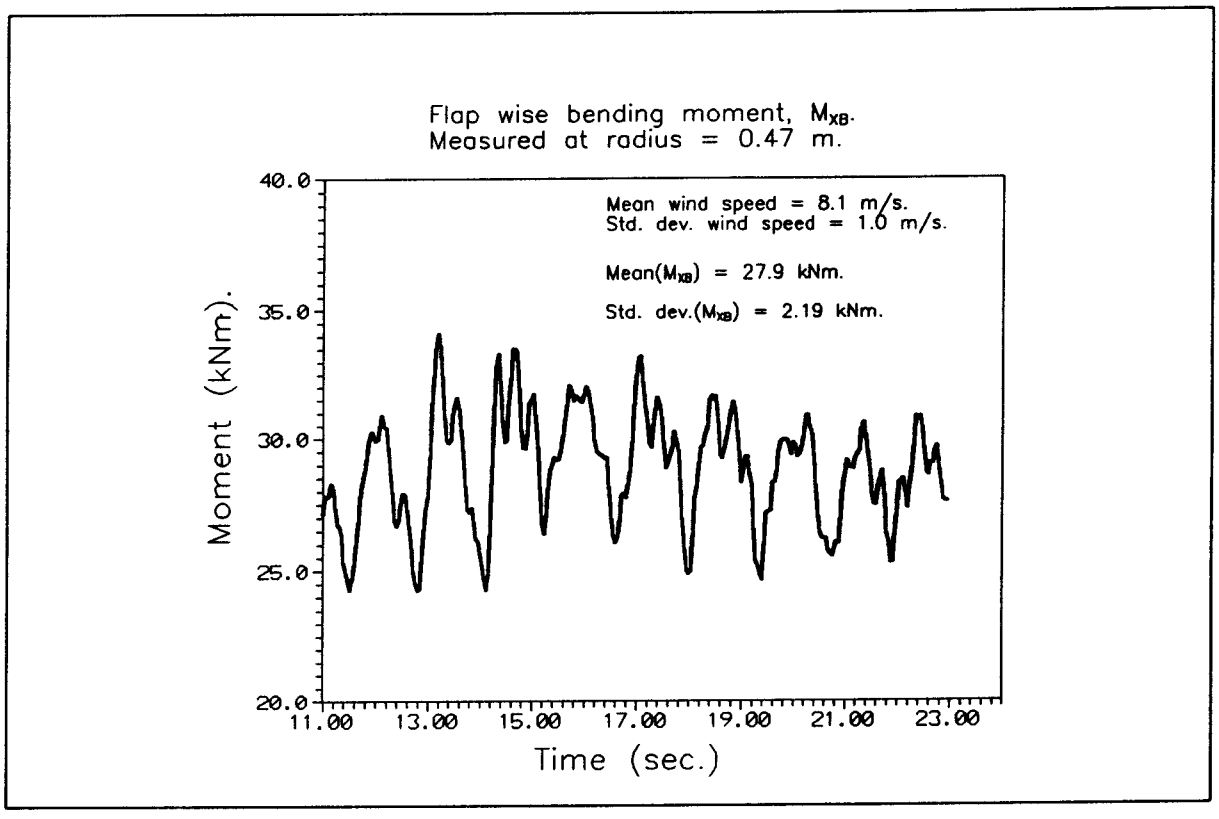

Figure 33: Blade flap wise bending moment. Measured.

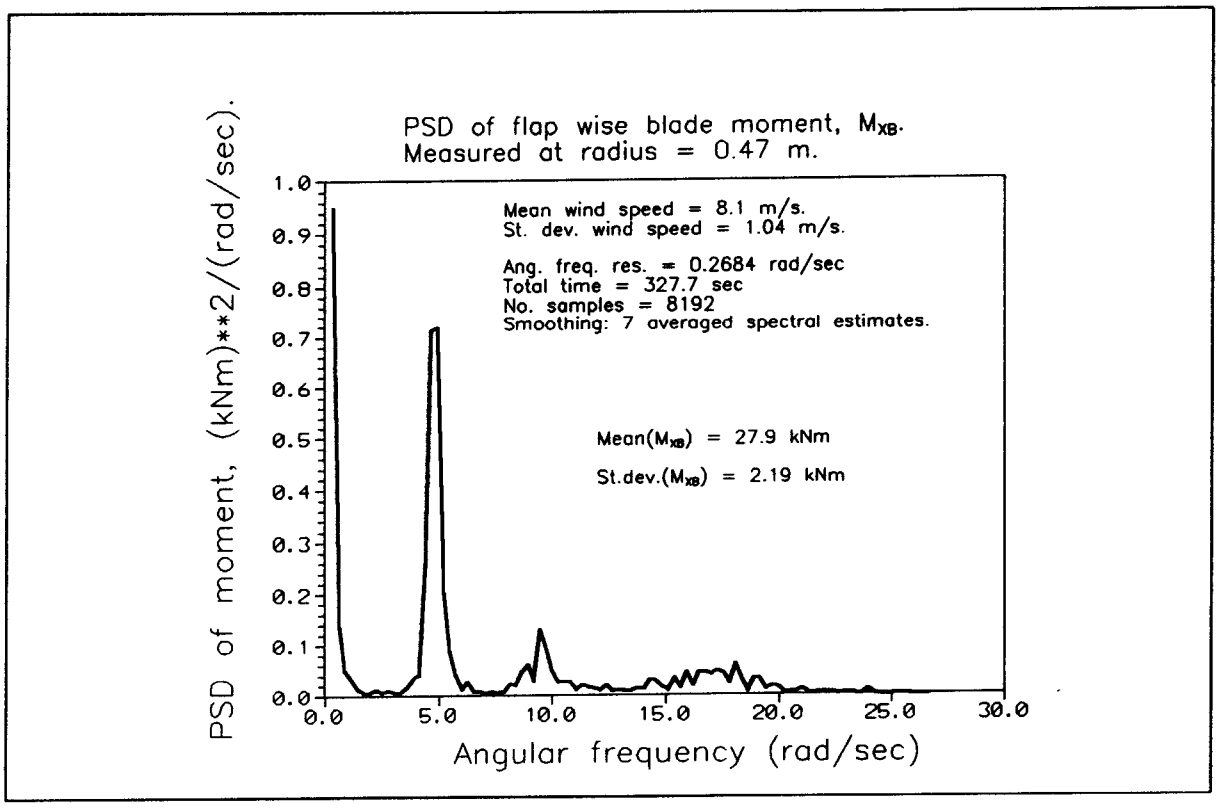

Figure 34: PSD of blade flap wise bending moment. Measured.

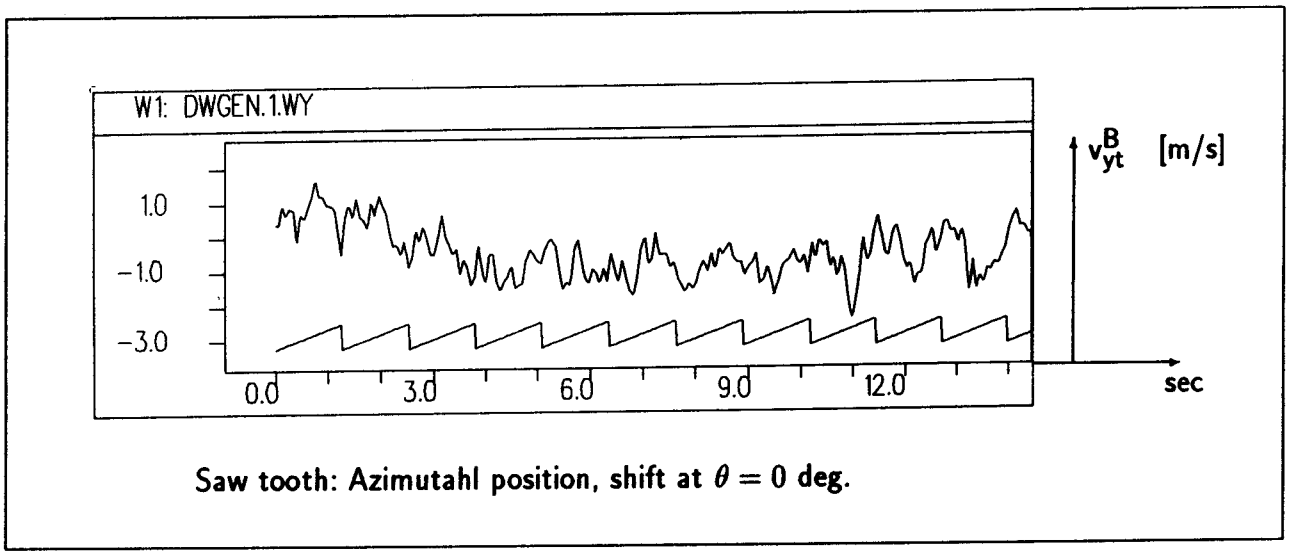

Figure 35: Sampled turbulence at blade tip.

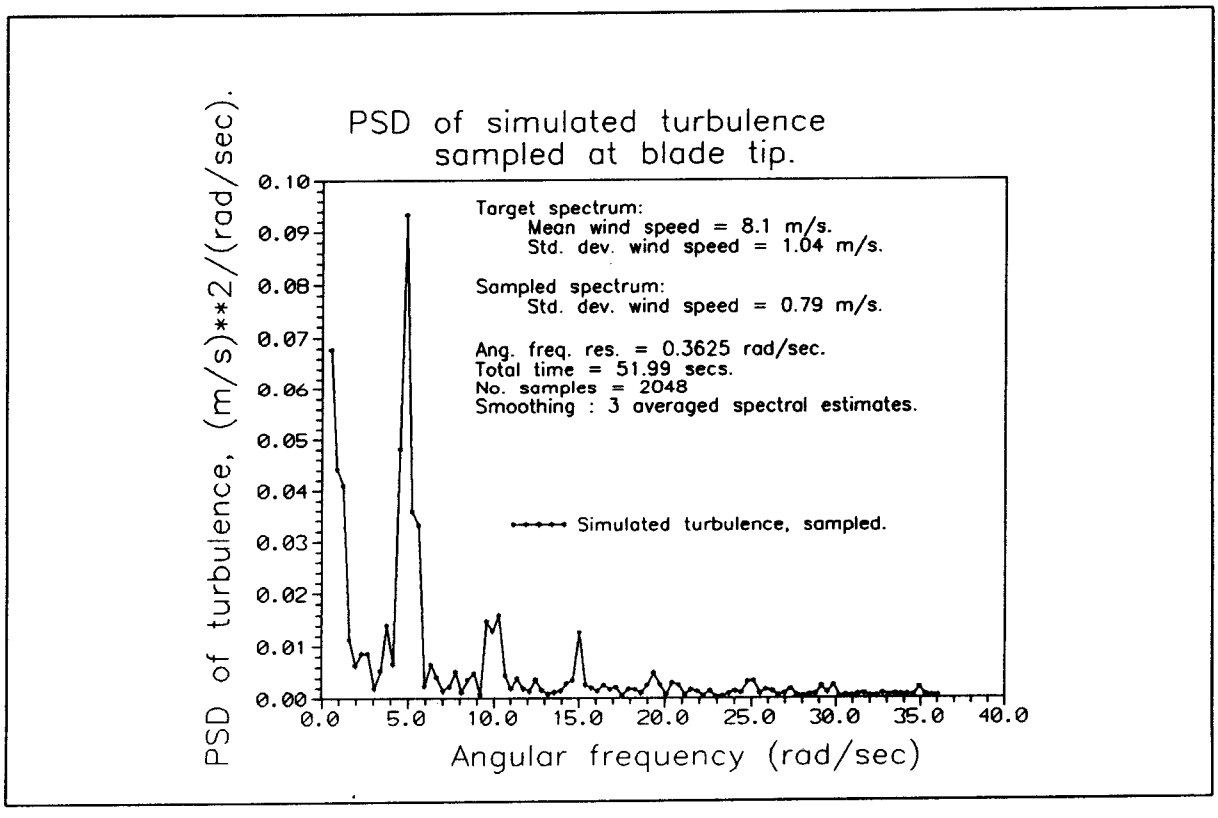

Figure 36: PSD of simulated turbulence, sampled at blade tip.

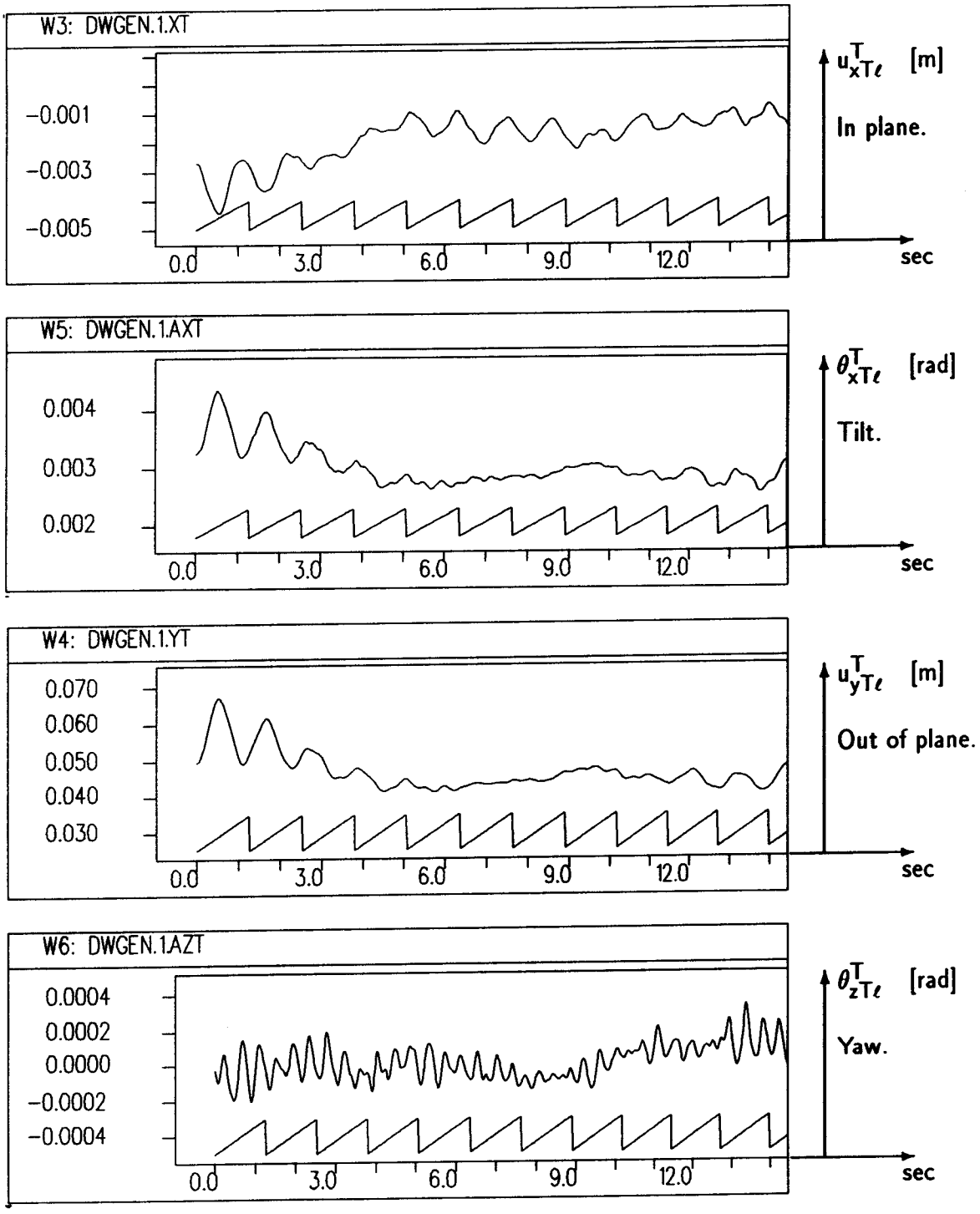

Figure 37: Tower top deformation. Simulated, stochastic.

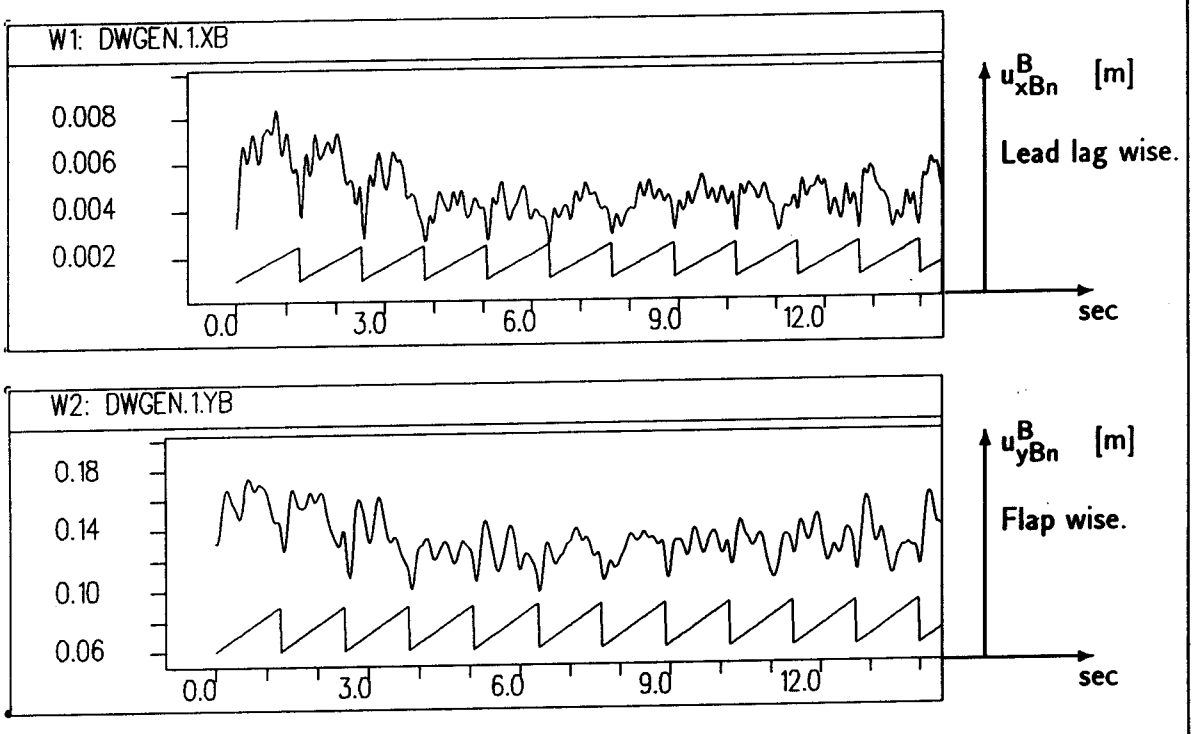

Response: Stochastic.
Loading: Wind shear + tower interference + turbulence.
Saw tooth: Azimutahl position, shift at $\theta = 0$ deg.

Figure 38: Blade tip deformation. Simulated, stochastic.

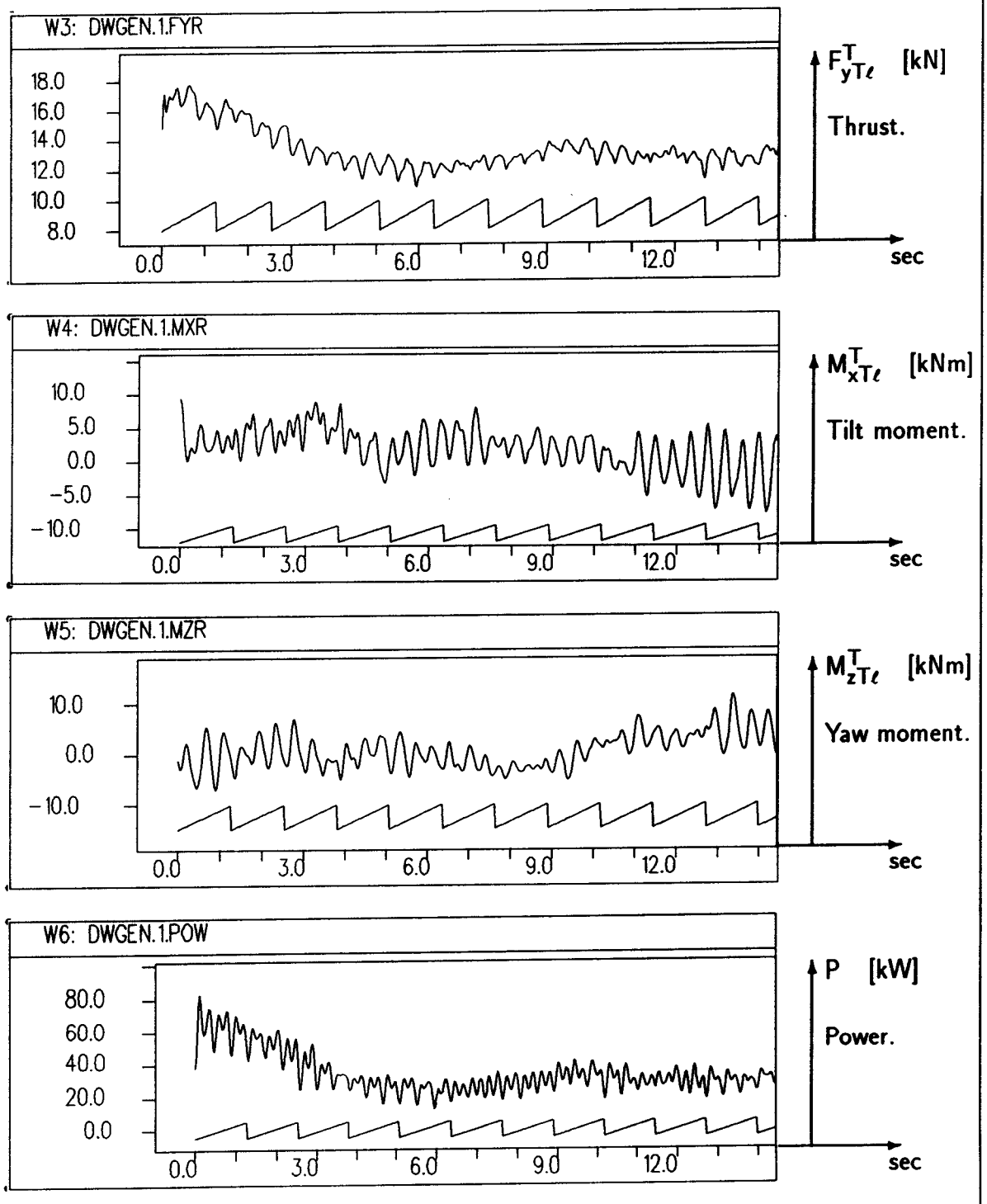

Figure 39: Tower top node loads (rotor loads) and power. Simulated, stochastic.

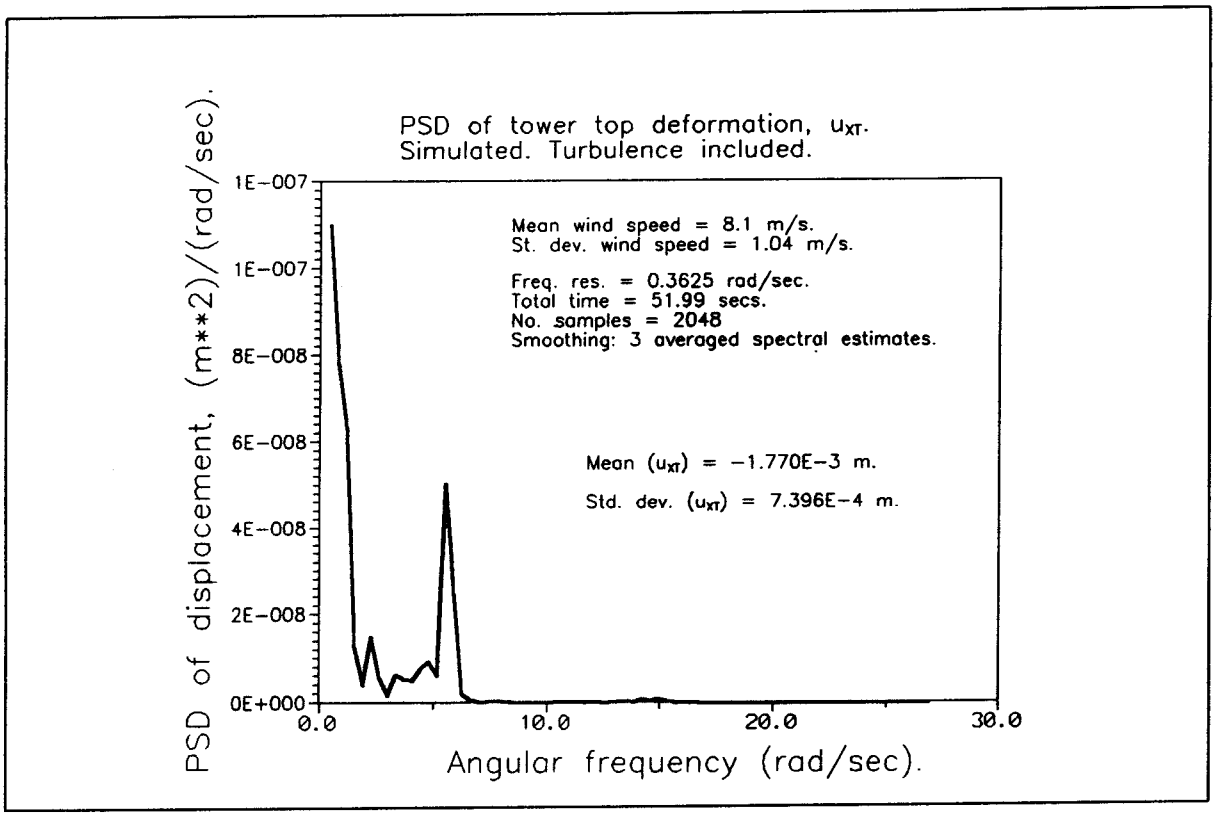

Figure 40: DFT of tower across wind displacement. Simulated, stochastic.

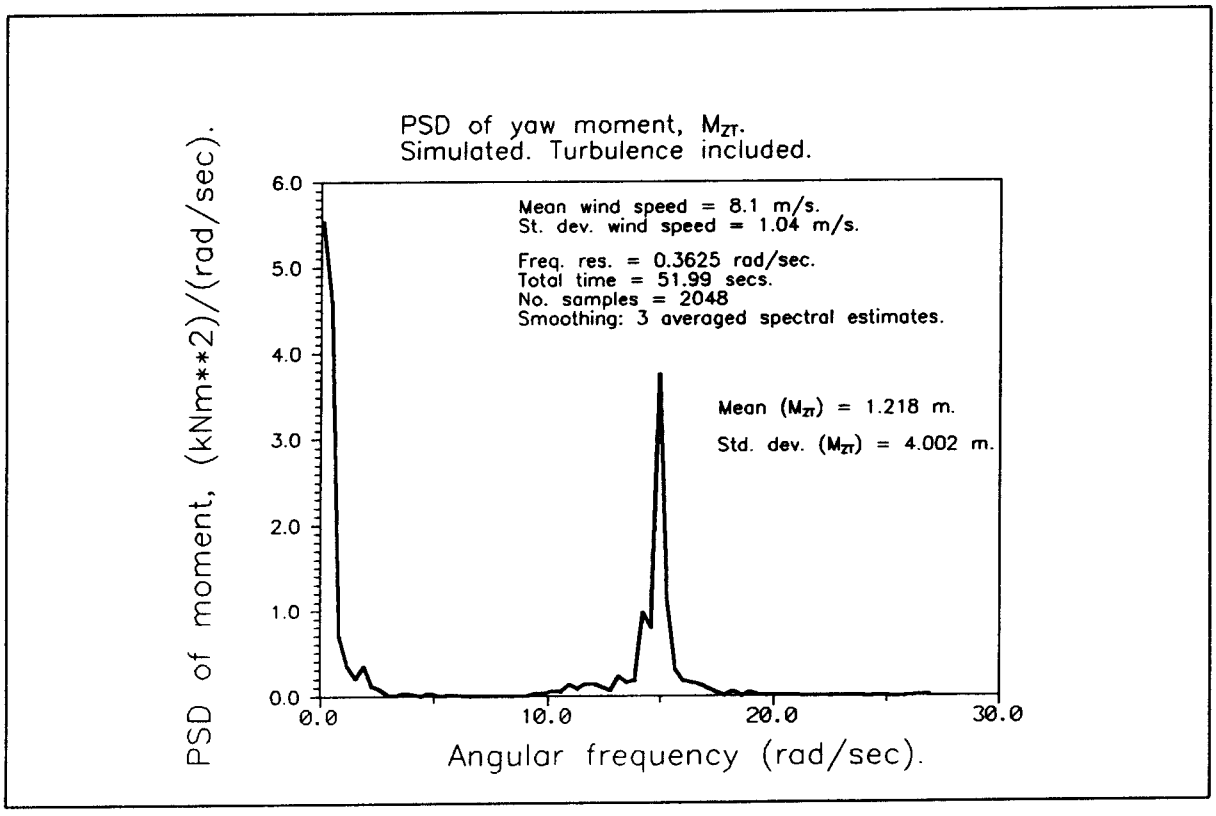

Figure 41: PSD of yaw moment. Simulated, stochastic.

9 Conclusion.

With the purpose to develop a tool which can support the choice of level of refinement in response calculations for horizontal axis wind turbines, a mathematical time domain model has been derived, and a corresponding computer program has been written.

The work concentrates on the representation of the inertia loads in the model. Depending on the stiffness of the structural elements, the appropriate model can be more or less simplified, in that the aim always is to use the simplest possible model that still provides the appropriate answer for use in designing the structural elements with the wanted safety. Therefore, the inertia loads have been represented in the model in a form which makes it possible to identify and isolate effects from selected degrees of freedom. If these effects are negligible the model can be simplified accordingly by omitting the degrees of freedom in question in the inertia expressions.

For one choice of degrees of freedom, expected to correspond to what would be important for the next generation of more flexible wind turbines, the final model equations have been derived and programmed. Only very limited linearizations of the kinematic terms have been introduced. With this model, time simulations have been carried out and the results used in preliminary comparisons with measurements. Good agreement has been found. Allthough the comparison covers a rather stiff turbine, it can be concluded that the model representation of the basic dynamic effects is satisfactory.

The more exciting testing of the model, when used on more flexible structures, still remains. If the work could be continued, a natural line to follow would be to concentrate on investigation of the next generation wind turbines of more flexible design. The model could then be optimized by including exactly the inertia loads which are important for the actual design.

In its present form, the model is well suited for supporting the development of the less complicated design tools and for providing information of the limitations of these tools as regards their ability to incorporate the inertia loads.

10 References.

[Part 2] Petersen, J.T. *Kinematically Nonlinear Finite Element Model of a Horizontal Axis Wind Turbine.*
This thesis, Part 2: Supplement. Inertia Matrices and Aerodynamic Model.
Dept. of Meteorology and Wind Energy.
Risø National Laboratory. Roskilde, Denmark, 1990.

[B1] Bathe, K-J. *Finite Element Procedures in Engineering Analysis.* Prentice-Hall, Englewood Cliffs, New Jersey, 1982.

[B2] Butterfield, C.P. *Three-Dimensional Airfoil Performance Measurements on a Rotating Wing.* Proceedings of the European Wind Energy Conference. Glasgow, Scotland, July 1989.

[C1] Clough, R.W. and Penzien, J. *Dynamics of Structures.* McGraw-Hill, New York, 1975.

[C2] Cowper, C.R. *The Shear Coefficient in Timoshenko's Beam Theory.* Journal of Applied Mechanics. June, 1966, pp. 335-340.

[D1] Davenport, A.G. *The Spectrum of Horizontal Gustiness near the Ground in High Winds.* Quart. Jr. Met. Soc., Vol. 87, 1961, pp. 194-211.

[F1] Fabian, O. *A new method for aeroelastic analysis of wind turbines.* Department of Fluid Mechanics. Technical University of Denmark. Lyngby, Denmark, 1981.

[G1] Garrad, A.D. *The Use of Finite Element Methods for Wind Turbine Dynamics.* Proceedings of the Ninth BWEA Wind Energy Association Conference. Edinburgh, England, April 1987, pp. 79-83.

[G2] Garrad, A.D. and Quarton, D.C. *Symbolic Computing as a Tool in Wind Turbine Dynamics.* Journal of Sound and Vibration. Vol. 109, No. 1, 1986, pp. 65-78.

[G3] Glauert, H. *Airplane Propellers. In: Aerodynamic Theory.* Ed. by W.F. Durand. Springer, Berlin, 1935.

[G4] Goldstein, H. *Classical Mechanics.* Addison-Wesley, Reading, Massachusetts, 1981.

[G5] Goyder, H.G.D. *A Novel Method for the Numerical Simulation of Turbulence.* Proceedings of the Tenth BWEA Wind Energy Association Conference. London, England, March 1988, pp. 121-127.

[H1] Hansen, K.S. and Larsen, A.M. *Hvirvelmodel til simulering af horisontalakslede vindturbiner.* Department of Fluid Mechanics. Technical University of Denmark. Lyngby, Denmark, 1981.

[H2] Hearn, A.C. *Reduce User's Manual.* Version 3.3, RAND Publication CP78 (Rev. 7/87). The RAND Corporation. Santa Monica, California, 1987.

[H3] Hemon, A., Zervos, A., and Huberson S. *Numerical Computation of Unsteady Forces on a Hawt.* Proceedings of the European Wind Energy Conference. Glasgow, Scotland, July 1989.

[H4] Holley, W.E., Thresher, R.W., and Lin, S.R. *Atmospheric Turbulence inputs for Horizontal Axis Wind Turbines.* Proceedings of the European Wind Energy Conference. Hamburg, West Germany, October 1984.

[J1] Janetzke, D.C. and Kaza, K.R.V. *Whirl Flutter Analysis of a Horizontal-Axis Wind Turbine with a Two-Bladed Teetering Rotor.* Proceedings of the Second DOE/NASA Wind Turbine Workshop. Cleveland, Ohio, 1981, pp. 201-210.

[K1] Kaimal, J.C. et al. *Spectral Characteristics of Surface Layer Turbulence.* Quart. Jr. Met. Soc., Vol. 98, 1972, pp. 563-589.

[K2] Krenk, S. and Jeppesen, B. *Calculation of Cross Section Properties of Wind Turbine Blades.* Proceedings of the European Community Wind Energy Conference. Herning, Denmark, June 1988, pp. 332-336.

[L1] Larsen, G.C., Frandsen, S., Sørensen, P., and Courtney, M.S. *Design Basis for Horizontal Axis Wind Turbines – Theoretical Background.* Risø report. M-2836. Risø National Laboratory. Roskilde, Denmark, 1989.

[L2] Lobitz, D.W. *A NASTRAN-Based Computer Program for Structural Dynamic Analysis of Horizontal Axis Wind Turbines.* Sandia report. SAND-84-0924C. Sandia National Laboratories. Albuquerque, New Mexico, 1984.

[L3] Lundsager, P., Frandsen, S., and Christensen, C.J. *The Measurements on the Gedser Windmill. 1977-1979.* Risø report. M-2250. Risø National Laboratory. Roskilde, Denmark, 1980.

[M1] Madsen, H.A. and Rasmussen, F. *Derivation of Three-Dimensional Airfoil Data on the Basis of Experiment and theory.* Paper presented at: Wind Power 1988. Honolulu, Hawaii, September, 1988 .

[M2] Madsen, H.A. *Measured Airfoil Characteristics of Three Blade Segments on a 19 M HAWT Rotor.* Paper presented at: The Thirteenth Annual Energy-Sources Technology Conference and Exhibition, New Orleans, Louisiana, January, 1990.

[M3] Madsen, P.H., and Rasmussen, F. *Rotor Loading on a Three-Bladed Wind Turbine.* Proceedings of the European Wind Energy Conference, EWEC'89. Glasgow, Scotland, July 1989.

[M4] Madsen, P.H., Frandsen, S., Holley, W.E., and Hansen, J.C. *Dynamics and Fatigue Damage of Wind Turbine Rotors during Steady Operation.* Risø National Laboratory. Roskilde , Denmark, 1984.

[M5] Madsen, P.H., Hock, S.M., and Hausfeld, T.E. *Turbulence Loads on the Howden 26 m Diameter Wind Turbine* Proceedings of Seventh ASME Wind Energy Symposium. New Orleans, Lousiana, January 1988, pp. 139-147.

[M6] Meirovitch, L. *Computational Methods in Structural Dynamics.* Sijthoff & Noordhoff. Alphen aan den Rijn, The Nederlands, 1980.

[M7] Meirovitch, L. *Methods of Analytical Dynamics.* McGraw-Hill, New York, 1970.

[P1] Patel, M.H. and Garrad, A.D. *Wind turbine tower and blade dynamics.* Proceedings of the Tenth BWEA Wind Energy Association Conference. London, England, March 1988, pp. 401-405.

[P2] Pedersen, B.M. and Nielsen, P. *Description of the two Danish 630 kW Wind Turbines, Nibe-A and Nibe-B, and some preliminary test results.* Proceedings of the 3rd International Symposium on Wind Energy Systems. Copenhagen, Denmark, August 1980. pp. 223-238.

[P3] Pedersen, P. *Et Notat om Elementanalyse for FEM (Finite Element Metoden).* Afdelingen for Faststofmekanik, Danmarks Tekniske Højskole. Lyngby, 1984, pp. 51-54.

[P4] Pedersen, P.T. and Jensen, J.J. *Styrkeberegning af Maritime Konstruktioner.* Del 2. Numeriske Metoder. Afdelingen for Skibs- of Havteknik, Danmarks Tekniske Højskole. Lyngby, 1983.

[P5] Petersen, J.T., Frandsen, S., and Courtney M. *Stall Induced Vibrations of Wind Turbine Blades.* Proceedings of the European Community Wind Energy Conference. Herning, Denmark, June 1988, pp. 246-250.

[P6] Przemieniecki, J.S. *Theory of Matrix Structural Analysis.* McGraw-Hill, New York, 1975.

[R1] Rasmussen, F., Petersen, S.M., Larsen, G., Kretz, A. and Andersen, P.D. *Investigations of Aerodynamics, Structural Dynamics and Fatigue on Danwin 180 kW.* Risø report. M-2727. Risø National Laboratory. Roskilde, Denmark, 1988.

[R2] Rosen, A. and Friedmann, P. *The Nonlinear Behaviour of Elastic Slender Straight Beams Undergoing Small Strains and Moderate Rotations.* Journal of Applied Mechanics. Vol. 46, March 1979, pp. 161-168.

[R3] Rosen, A. and Rand, O. *A General Model of the Dynamics of Moving and Rotating Rods.* Computers and Structures. Vol. 21, No.3, 1985, pp. 543-561.

[S1] Schöttl, Ch. and Wagner, S. *Dynamic and Aeroelastic Response of Wind Energy Converter to Aerodynamic Loads.* Proceedings of the European Community Wind Energy Conference. Herning, Denmark, June 1988, pp. 191-196.

[S2] Shinozuka, M. and Jan, C.-M. *Digital Simulation of Random Processes and its Applications.* Journal of Sound and Vibration, Vol. 25, No. 1, pp. 111-128. 1972

[T1] Thresher, R.W. and Hersberg, E.L. *Development of an Analytical Model and Code for the flapping Response of a HAWT Rotor Blade.* SERI. Solar Energy Research Institute. Golden, Colorado, 1985.

[T2] Thresher, R.W., Holley, W.E., and Jafaray, N. *Wind Response Characteristics of Horizontal Axis Wind Turbines.* Proceedings of the Second DOE/NASA Wind Turbine Workshop. Cleveland, Ohio, 1981, pp. 87-100.

[V1] Veers, P. *Three-dimensional wind simulation.* Sandia report. SAND88-015. Sandia National Laboratories. Albuquerque, New Mexico, 1988.

[V2] de Vries, O. *Fluid Dynamic Aspects of Wind Energy Conversion.* AGARDograph No. 243, AGARD 1979. Chapter 4.4.

[Y1] Yang, T.Y. *Matrix Displacement Solutions to Elastica Problems of Beams and Frames.* Int. Journal of Solids and Structures, Vol. 9, 1973, pp. 829-842.

[Ø1] Øye, S. *FIX. Dynamisk, Aeroelastisk Beregning af Vindmøllevinge.* Department of Fluid Mechanics. Technical University of Denmark. Lyngby, Denmark, 1983.

[Ø2] Øye, S. *CBEAM4. Beregning af Egensvingninger m.v. for Centrifugalbelastede Bjælker.* Department of Fluid Mechanics. Technical University of Denmark. Lyngby, Denmark, 1983.

A Notation.

The notation used in this report is explained below. All symbols are explained in the report, where they appear for the first time. The symbols that are used mainly in connection with local derivations, are not repeated in the present listing. Below, the general notation, used mainly for vectors and matrices, is explained in the first subsection. In the second subsection, the symbols are listed, and finally the meaning of important indices are explained in the third subsection.

A.1 General about vector and matrix notation.

$\{a\}$: Column vector.

$[A]$: Rectangular matrix.

The information which is related to the vector and matrix indices is explained next.

Meaning of vector indices.

$\left\{a_B^A\right\}$: The upper index refers to the coordinate system which is used as reference for the vector components. This index is always used when it is important to apply the correct coordinate reference.
The lower index or indices, as the B symbolizes the total lower right index which may be more than one character, is a part of the name. The only exception is the lower double index for the angular velocity vector mentioned next.

$\left\{\omega_{BC}^A\right\}$: The lower indices refer to two coordinate systems, the B- and the C-system. The vector represents the angular velocity of the B-coordinate system relative to the C-system. The opposite sequence of the indices is equivalent to a change of sign for the vector. The upper index refers to reference coordinate system as explained above and may be any system available.

$\{{}_i a\}$: Vector related to finite element No. i.

$\{a_{Si}\}$: Vector related to node No. i on substructure S.

Meaning of matrix indices.

$[T_{AB}]$: The matrix represents a coordinate transformation matrix. The lower inices indicate that the transformation is from the A- to the B-coordinate system.

$[{}_i A]$: Matrix related to finite element No. i.

General symbols.

$\dot{a}$, $\{\dot{a}\}$: Differentiation with respect to time.

a' : Differentiation with respect to position.

$\{a\}^T$, $[A]^T$: Transpose of vector and matrix.

$[A]^{-1}$: Inverse matrix.

A.2 Symbols.

$\{a_{Sc}\}$: Component of acceleration vector for point on substructure S, solely dependent on degrees of freedom outside the substructure.

A : Cross sectional area.

$[A]$: Inertia coefficient matrix to position vector.

$[B]$: Inertia coefficient matrix to velocity vector.

c : Length of profile chord.

$[C]$: Inertia coefficient matrix to acceleration vector.

$[C]$: Damping, Coriolis or gyroscopic matrix.

$[C_{\dot{\theta}}]$: Gyroscopic matrix.

C_D : Profile drag coefficient.

C_L : Profile lift coefficient.

$[C_s]$: Structural damping matrix.

$[C_{SC}]$: Coriolis matrix for element on substructure S.

C_{1H} : Teeter damping.

$\{e_i\}$: Coordinate axis unit vector, $i = 1,2,3$ or $i = x,y,z$.

e_{s1}, e_{s2} : x, y-components for shear center in element coordinates.

E : Modulus of elasticity.

E : Energy.

f_x, f_y, f_z : Components of distributed force.

f_i^a : Finite element interpolation function No. i corresponding to coordinate direction a, $a = x, y$.

$\{f_{pI}\}$: Inertia force on particle of infinitesimal volume.

$\{F\}$: Node load vector.

$\{F_{IS}\}$: Node inertia load for element on substructure S.

$\{F_{4S}\}$: Inertia vector for substructure S.

$[F_5]$: Mass matrix.

$[F_6]$: Mass matrix.

$\{g\}$: Gravity.

G : Modulus of elasticity in shear.

I_x, I_y : Principal area moments of inertia.

I_{zs} : Torsion constant.

$[I_{1LX}]$: General inertia matrix.

k_x, k_y : Form factor for shear.

$[K]$: Stiffness matrix.

$[K_g]$: Geometric stiffness matrix.

$[K_s]$: Structural stiffness matrix.

$[K_{SI}]$: Softening matrix for element on substructure S.

K_{1H} : Teeter stiffness.

ℓ : Element length.

ℓ_{shaft} : Shaft length.

m : Mass per unit length.

m_x, m_y, m_z : Components of distributed moment.

$[M]$: Mass matrix.

$[M_{\ddot{u}}]$: Mass matrix corresponding to rigid body translation.

$[M_{\ddot{\theta}}]$: Mass matrix corresponding to rigid body rotation.

$[N(z)]$: Finite element interpolation matrix.

$[N_{SB}(z)]$: Finite element interpolation matrix corresponding to inclusion of coupling between bending and torsion.

$[N_T(x,y)]$: Matrix, transforming between principal axes deformations and local deformations on cross section of finite element.

$\{q_{SS}\}$: Displacement vector corresponding to degrees of freedom for inner nodes (not on the boundary) of substructure S. The number of components is $6\times$(number of nodes).

$\{q_{Am}\}$: 6 component node displacement vector for shaft end node No. m. The displacements are 3 translations and 3 rotations.

$\{q_S\}$: 12 component node displacement vector for finite element on substructure S. The displacements are 3 translations and 3 rotations at each of the two nodes.

$\{q_{T\ell}\}$: 6 component node displacement vector for tower top node No. ℓ. The displacements are 3 translations and 3 rotations.

$\{r_1\}$: Substructure position vector to local node No. 1 for finite element.

$\{r_{12}\}$: Vector from local node No. 1 to local node No. 2 for finite element.

$\{r_p(x,y)\}$: Vector in cross sectional plane of finite element from the elastic axis to infinitesimal volume.

$\{r_{S0}\}$: Position vector from tower foundation (node $T1$) to point on substructure S.

$\{r_S\}$: Position vector from origin of substructure coordinate system (S) to point on the substructure in the undeformed state.

r_x : y-coordinate for center of mass.

r_{Ix} : Radius of inertia with respect to x-axis (measured in y-coordinate direction).

r_{Iy} : Radius of inertia with respect to y-axis (measured in x-coordinate direction).

r_y : x-coordinate for center of mass.

$\{s_S\}$: Position vector from origin of substructure coordinate system (S) to point on the substructure in the deformed state.

t : Time.

$\{u_S\}$: 3 component vector of translations at node on substructure S.

$\left\{u^A_{Am}\right\}$: 3 component vector of translations at shaft end node No. m.

$\left\{u^T_{T\ell}\right\}$: 3 component vector of translations at tower top node No. ℓ.

u_{iS} : Component of $\{u_S\}$, $i = 1,2,3$ or $i = x,y,z$.

W : Work.

x : Coordinate axis.

x_S, y_S, z_S : Coordinate axes belonging to system defined for substructure, coupling node, specific intermediate orientation of structural element or finite element, each identified by the corresponding index substituted for S.

y : Coordinate axis.

z : Coordinate axis.

δa : Virtual displacement or corresponding variation in energy or performed work, $a = u$, θ, W or E.

ε : Normalized coordinate along z-axis of finite element.

η_x, η_y : Ratio between element bending and shear parameters corresponding to principal bending axis.

θ : Rotor azimuthal position (θ^A_{2A} also used).

θ_{pitch} : Profile pitch angle.

$\{\theta_S\}$: 3 component vector of rotations at node on substructure S.

$\left\{\theta^A_{Am}\right\}$: 3 component vector of rotations at shaft end node No. m.

$\left\{\theta^T_{T\ell}\right\}$: 3 component vector of rotations at tower top node No. ℓ.

θ_{iS} : Component of $\{\theta_S\}$, $i = 1,2,3$ or $i = x,y,z$.

θ^A_{2A} : Rotor azimuthal position (θ also used, $2A$: y_A-axis).

θ^H_{1H} : Teeter rotation ($1H$: x_B-axis).

θ^N_{3N} : Yaw rotation ($3N$: z_N-axis).

θ^R_{1R} : Tilt angle ($1R$: x_R-axis).

ω : Angular velocity of rotor.

$\{\omega_{AB}\}$: Angular velocity of A- relative to B-coordinate system.

ϱ_i : Density of material for element No. i.

ϱ_x, ϱ_y : Scalar function of ratio between element bending and shear parameters (η_x, η_y) corresponding to principal bending axis.

A.3 Indices.

A : Shaft substructure coordinates.

Am : Shaft node No. m, coupling node to blades.

$A1$: Shaft node No. 1, coupling node to tower.

B : Blade substructure coordinates.

Bn : Blade node No. n, highest numbered blade node.

$B1$: Blade node No. 1, coupling node to shaft.

Ei : Blade element coordinates for element No. i.

N : Yaw rotation coordinates.

R : Tilt angle coordinates.

R^* : Tilt angle coordinates parallel displaced to shaft end.

S : Substructure, $S = T$, A or B.

S : System equations.

S' : Shaft end elastic deformation coordinates.

T : Tower substructure coordinates.

T' : Tower top elastic deformation coordinates.

$T\ell$: Tower node No. ℓ, tower top.

$T1$: Tower node No. 1, foundation.

B Formal representation of the blade inertia load

In the following a simplified expression for the blade inertia load is established, meant for use in the comparison with other models and in general for providing some insight in the present model.

Allthough the kinematic analysis in the present model includes deformation degrees of freedom (DOFs) at the shaft end and the teeter DOF as well as the yaw DOF at the tower top, only the tower top deformation DOFs will be included in the following survey and the azimuthal angular velocity is assumed constant, in order to keep the expressions in a reasonably clear form.

In order to prevent the reader from being too confused about the matrix and vector notation, it should be noted here that the notation in the following Eq. B.0.1 is not important for the considerations in this section. The notation is only retained here in order to maintain consistency with the sections which treat the general analysis.

The node inertia force from Eq. 6.3.9 for finite beam element No. i corresponding to the inclusion only of the tower top DOFs is expressed by

$$\begin{aligned}\left\{{}_iF^B_{IB}\right\} = & -[{}_iM_B]\left\{{}_i\ddot{q}^B_B\right\} - [{}_iC_{BC}]\left\{{}_i\dot{q}^B_B\right\} - [{}_iK_{BI}]\left\{{}_iq^B_B\right\} \\ & -\left(\left\{{}_iFT^B_{4B}\right\} + \left\{{}_iFC0^B_{5B}\right\} + \left\{{}_iFC0^B_{6B}\right\}\right) \\ & -\left([{}_iFT2_{4B}] + [{}_iFT2_{5B}] + [{}_iFT2_{6B}] + [{}_iFF_{6B}]\right)\left\{\ddot{\theta}^T_{T\ell}\right\} \\ & -\left([{}_iFT1_{5B}] + [{}_iFT1_{6B}] + [{}_iFE_{6B}]\right)\left\{\dot{\theta}^T_{T\ell}\right\} \\ & -[{}_iFD_{6B}]\left\{\ddot{u}^T_{T\ell}\right\} \end{aligned} \tag{B.0.1}$$

A dot over a variable indicates differentiation with respect to time.

With t denoting the time, the degrees of freedom are

$\left\{q^B_B\right\} = \left\{q^B_B(t)\right\}$ a 12 component column vector of node displacements for a finite element on the blade, as indicated by the lower index B. The vector coordinates are with reference to the blade substructure coordinate system, as indicated by the upper index B. The displacements are 3 translations and 3 rotations at each of the two nodes.

$\left\{u^T_{T\ell}\right\} = \left\{u^T_{T\ell}(t)\right\}$ a 3 component column vector of translations at the tower top node as indicated by the lower indices, where T means that we deal with tower DOFs and ℓ is the node number. The vector is with reference to the tower substructure coordinate system, as indicated by the upper index T.

$\left\{\theta^T_{T\ell}\right\} = \left\{\theta^T_{T\ell}(t)\right\}$ a 3 component column vector of rotations at the tower top node. The indices are equivalent to those for the tower top displacement just mentioned above.

As finite rotations cannot be expressed by a vector (see Sec. 2.1) it is necessary to impose limitations on the rotational degrees of freedom. The rotations must be small (strictly speaking

infinitesimal) in order to make the vector representation valid. In the present substructure representation it is sufficient to require, that the local rotations relative to the substructures are small. This means that the model is still able to work with non-infinitesimal, but still limited, rotations on the blade as measured relative to the fixed frame of reference, i.e. the tower support.

All matrices and vectors in Eq. B.0.1, except the mass matrix, are time dependent. This dependence is not stated explicitly below, unless it can help in clarifying the actual context.

It is the intention to write matrices and vectors formally as functions of degrees of freedom and geometric and material parameters.

With "formal" is here meant, that the introduced functional relations are not functions strictly in accordance with usual mathematical conventions, but rather a listing of the independent variables as arguments to the function in question. The purpose is only to show in a clear form, which DOFs and parameters the actual coefficient matrix or inertia-vector depends on.

One such formal function to be introduced is

$$ {}_ih_e = {}_ih_e\left(\varrho_i, S_{xi}, S_{yi}, I_{xi}, I_{yi}, E_i, G_i, k_{xi}, k_{yi}, \ell_i, e_{sxi}, e_{syi}\right) \tag{B.0.2} $$

with the independent variables being material parameters and geometric parameters for element No. i, (lower index i). This function is thus used to express, that the matrix or vector in question depends on these parameters, allthough the functional relationship may be different in different contexts.

The parameters in Eq. B.0.2 have the following meaning (omitting the element number i)

ϱ	mass density.
E	modulus of elasticity.
G	modulus of elasticity in shear.

and the geometric parameters are

S_x, S_y	1^{st} mass moment about x- and y-axis, respectively.
I_x, I_y	mass moment of inertia about x- and y-axis, respectively.
k_x, k_y	form factor for shear related to forces in x- and y-direction respectively.
e_{sx}, e_{sy}	coordinates for shear center.
ℓ	length of beam finite element.

The influence of transformation between the element coordinate system and the blade coordinate system, which depend on three direction cosines, is simply expressed by the functional symbol

$$ {}_if_e = {}_if_e\,(\text{direction cosines}) \tag{B.0.3} $$

Further, the following symbols are used below, apart from the DOFs listed above

$\theta = \theta\,(t)$	is the azimuthal position of the rotor.
$\omega = \dot{\theta}$	is the angular velocity of the rotor, which is assumed constant.

$r = 1, 2, 3$, $s = 1, 2, 3$, and $m = 1, 2, 3$ are lower indices, which correspond to the coordinate axis x, y, or z, along which the component in question has been resolved. In general these indices are independent, so they assume all combinations of values. Repeated indices are also independent and do not imply summation.

ℓ_{shaft} is the shaft length, equivalent to the distance from the tower top to the hub.

r_{m12} is the m^{th} component of the vector from node 1 to node 2 of the beam finite element, with reference to blade substructure coordinates.

r_{m1} is the m^{th} component of the vector from the origin of the blade coordinate system to node 1 of the beam finite element, with reference to blade substructure coordinates.

In the example calculation in Sec. 6 a limited linearization has been introduced in order to limit the number of terms in the integrated model, which also includes shaft and teeter DOFs. A detailed description of this linearization is given in Sec. 6. In the terms below this linearization has been omitted.

By use of the definitions above, the matrices and vectors from Eq. B.0.1 are now formally written as functions of degrees of freedom and geometric and material parameters.

The mass matrix.

The coefficient matrix to $\left\{\ddot{q}_B^B\right\}$ is the mass matrix for a beam finite element

$$[{}_iM_B] = [M_B\,({}_ih_e,\ {}_if_e)] \tag{B.0.4}$$

The matrix is composed solely of geometric and material parameters, in accordance with the principles chosen to transform the inertia loads to the nodes.

The Coriolis matrix.

The coefficient matrix to $\left\{\dot{q}_B^B\right\}$ is denoted the Coriolis matrix

$$[{}_iC_{BC}] = \left[C_{BC}\left(\omega, \dot{\theta}_{rT\ell}^T, \theta, \theta_{rT\ell}^T,\ {}_ih_e,\ {}_if_e\right)\right] \tag{B.0.5}$$

The matrix is skew-symmetric and the inertia force represents the inertial damping due to the local deformation velocity.

The softening matrix.

The coefficient matrix to $\left\{q_B^B\right\}$ is denoted the softening matrix

$$[{}_iK_{BI}] = \left[K_{BI}\left(\omega^2, \omega\dot{\theta}_{rT\ell}^T, \dot{\theta}_{rT\ell}^T\dot{\theta}_{sT\ell}^T, \ddot{\theta}_{rT\ell}^T, \theta, \theta_{rT\ell}^T, \theta_{rT\ell}^T\theta_{sT\ell}^T,\ {}_ih_e,\ {}_if_e,\right)\right] \tag{B.0.6}$$

The product of the stiffness like matrix and the DOF-vector accounts for the inertia force depending on change in local position. Due to the fact that the inertia force has the same sign as the deformation, the resulting effect is a softening, hence the name "softening matrix" of the coefficient matrix.

The inertia-vector.

The line of Eq. B.0.1 composed of vectors are combined to one formal vector function as follows

$$
\begin{aligned}
-\left\{{}_iF^B\right\} = & \\
& -\left(\left\{{}_iFT^B_{4B}\right\} + \left\{{}_iFC0^B_{5B}\right\} + \left\{{}_iFC0^B_{6B}\right\}\right) \\
= & -\left\{{}_iF^B\left(\omega^2, \omega\dot{\theta}^T_{rT\ell}, \dot{\theta}^T_{rT\ell}\dot{\omega}^T_{sT\ell}, \theta, \theta^T_{sT\ell}, \theta^T_{rT\ell}\theta^T_{sT\ell}, r_{m12}, r_{m1}, {}_ih_e, {}_if_e\right)\right\}
\end{aligned}
\tag{B.0.7}
$$

No general attempt shall be made here to relate these rather complicated expressions for inertia force to terms usually applied in the area, but a few notes shall be made about dominating terms.

The vector accounts for the dominating centrifugal force from the ω-rotation of the blades. Further the vector contains terms which give rise to damping, those dominating usually including the factor $\omega\dot{\theta}^T_{rT\ell}$. The damping terms are part of what is often denoted gyroscopic damping. It would be possible to extract the latter terms and include them in the $[C_{\dot{\theta}}]$-matrix described below. Considerations, regarding the final form, concern subjects such as computational efficiency and extent of work needed to prepare an actual representation of the equations. The extraction is a matter of algebraic manipulations, which in itself is straightforward, allthough rather involved. However, the resulting expressions might well require more basic arithmetic operations for evaluation than the original expression. The quality of the solution is usually not influenced by the actual choice here, at least not as long as numerical stability can be achieved.

$[M_{\ddot{\theta}}]$, coefficient-matrix to $\left\{\ddot{\theta}^T_{T\ell}\right\}$.

The sum of matrices, constituting the coefficient to $\left\{\ddot{\theta}^T_{T\ell}\right\}$, is combined to one formal matrix

$$
\begin{aligned}
-\left[{}_iM_{\ddot{\theta}}\right] &= -\left(\left[{}_iFT2_{4B}\right] + \left[{}_iFT2_{5B}\right] + \left[{}_iFT2_{6B}\right] + \left[{}_iFF_{6B}\right]\right) \\
&= -\left[M_{\ddot{\theta}}\left(\theta, \theta^T_{rT\ell}, \ell_{shaft}, r_{m12}, r_{m1}, {}_ih_e, {}_if_e\right)\right]
\end{aligned}
\tag{B.0.8}
$$

This term accounts for the inertia force resulting from rigid body accelerations of the beam finite element due to angular accelerations at the tower top.

$[C_{\dot{\theta}}]$, coefficient-matrix to $\left\{\dot{\theta}^T_{T\ell}\right\}$.

Following the same recipe for the next term in Eq. B.0.1, the sum of matrices, constituting the coefficient to $\left\{\dot{\theta}^T_{T\ell}\right\}$, is combined to one formal matrix

$$
\begin{aligned}
-\left[{}_iC_{\dot{\theta}}\right] &= -\left(\left[{}_iFT1_{5B}\right] + \left[{}_iFT1_{6B}\right] + \left[{}_iFE_{6B}\right]\right) \\
&= -\left[C_{\dot{\theta}}\left(\omega, \dot{\theta}^T_{rT\ell}, \theta, \theta^T_{rT\ell}, \theta^T_{rT\ell}\theta^T_{sT\ell}, \ell_{shaft}, r_{m12}, r_{m1}, {}_ih_e, {}_if_e\right)\right]
\end{aligned}
\tag{B.0.9}
$$

This term accounts for one part of the inertia force resulting from products of angular velocities. Another comparable contribution is embedded in the inertia vector $\left\{{}_iF^B\right\}$, as mentioned above.

Because more than one rotating frame of reference is involved, the expressions in the matrices above are composed of products of 4 different angular velocities, and the realtions to the well known case with one rotating frame of reference is no longer obvious. For that reason no further attempt shall be made to clarify the origin of the terms by comparing with the simpler case, only should it be mentioned that the effect of this inertia force will be a damping, which is often denoted gyroscopic damping.

$[M_{\ddot{u}}]$, coefficient-matrix to $\left\{\ddot{u}^T_{T\ell}\right\}$.

The coefficient matrix in the last term of Eq. B.0.1 is formally written

$$-\left[{}_iM_{\ddot{u}}\right] = -\left[{}_iFD_{6B}\right] = -\left[M_{\ddot{u}}\left(\theta, \theta^T_{rT\ell}, {}_ih_e, {}_if_e\right)\right] \tag{B.0.10}$$

This term accounts for rigid body translational acceleration of the beam finite element due to translational acceleration at the tower top.

Final expression for inertia force.

After introduction of these formal expressions in Eq. B.0.1 we get (omitting the element number i)

$$\begin{aligned}
\left\{F^B_{IB}\right\} = & \\
& -\left[M_B\left(h_e, f_e\right)\right]\left\{\ddot{q}^B_B\right\} \\
& -\left[C_{BC}\left(\omega, \dot{\theta}^T_{rT\ell}, \theta, \theta^T_{rT\ell}, h_e, f_e\right)\right]\left\{\dot{q}^B_B\right\} \\
& -\left[K_{BI}\left(\omega^2, \omega\dot{\theta}^T_{rT\ell}, \dot{\theta}^T_{rT\ell}\dot{\theta}^T_{sT\ell}, \ddot{\theta}^T_{rT\ell}, \theta, \theta^T_{rT\ell}, \theta^T_{rT\ell}\theta^T_{sT\ell}, h_e, f_e,\right)\right]\left\{q^B_B\right\} \\
& -\left\{F^B\left(\omega^2, \omega\dot{\theta}^T_{rT\ell}, \dot{\theta}^T_{rT\ell}\dot{\theta}^T_{sT\ell}, \theta, \theta^T_{sT\ell}, \theta^T_{rT\ell}\theta^T_{sT\ell}, r_{m12}, r_{m1}, h_e, f_e\right)\right\} \\
& -\left[M_{\ddot{\theta}}\left(\theta, \theta^T_{rT\ell}, \ell_{shaft}, r_{m12}, r_{m1}, h_e, f_e\right)\right]\left\{\ddot{\theta}^T_{T\ell}\right\} \\
& -\left[C_{\dot{\theta}}\left(\omega, \dot{\theta}^T_{rT\ell}, \theta, \theta^T_{rT\ell}, \theta^T_{rT\ell}\theta^T_{sT\ell}, \ell_{shaft}, r_{m12}, r_{m1}, h_e, f_e\right)\right]\left\{\dot{\theta}^T_{T\ell}\right\} \\
& -\left[M_{\ddot{u}}\left(\theta, \theta^T_{rT\ell}, h_e, f_e\right)\right]\left\{\ddot{u}^T_{T\ell}\right\}
\end{aligned} \tag{B.0.11}$$

It should be mentioned here, that the appearance of the elastic rotations at the tower top, $\theta^T_{rT\ell}$, in the equation, is due to the fact that the rotations are part of a coordinate transformation matrix, giving rise to an updating of the equations in accordance with the deformed geometry, quite parallel to the treatment of the azimuthal rotation θ, the only difference being, that the elastic rotations are part of the solution.

C Time derivation in rotating coordinate systems.

The differentiation with respect to time of a position vector to a point on a rotating structure is addressed in this section. The vector may be a sum of position vectors defined in local coordinate systems, and the expression for the vector will consist of product terms of time dependent transformation matrices and vectors. Without loss of generality only one such term is considered below. The time derivative of the transformation matrix is payed special attention. The general expression for the transformation matrix is derived. Another important purpose with the derivations is to establish a unique notation which helps managing the matrices and vectors correctly with respect to frame of reference.

Derivation of velocity and acceleration of a point on a rotating structure relative to an inertial coordinate system can be carried out basically in two different ways. Either by establishing the angular velocity vector of the rotating system and next use the well known vector product expressions for the final calculation. Or by establishing the position vector to the point in question and next obtain the final results by differentiation of this vector with respect to time. The latter method has been used in the present work, because it is found to be more safe and straightforward when more than one rotating frame of reference is involved.

Below the general transformation matrix is derived for transformations of vectors between coordinate systems that undergo finite rotations relative to each other. Finally, the matrix elements are linearized. The initial position of the system is denoted the A-system as indicated by the upper index in Fig. 42. The final position, for example corresponding to the deformed state of a structural element which the coordinate system follows, is denoted the D-position. Intermediate positions are marked by indices B and C. As finite rotations are considered initially, a sequence of the rotations must be prescribed. A sequence corresponding to the Euler xyz-convention is applied. The name arises from the fact that all three axes are involved in the rotations, ([G4, pp. 143-148], [M7, pp. 101-112]). The description is therefore appropriate for this situation where elastic rotations may be involved, and no axis can be assigned any preference.

The sequence of the rotations and the angles and axes involved in each rotation are (see Fig. 42)

1. θ_1^A about the x_1^A-axis
2. θ_2^B about the x_2^B-axis
3. θ_3^C about the x_3^C-axis

Considering the three transformation steps, we get the corresponding transformation matrices

$$[T_{AB}] = \begin{bmatrix} 1 & 0 & 0 \\ 0 & c\theta_1^A & s\theta_1^A \\ 0 & -s\theta_1^A & c\theta_1^A \end{bmatrix}, \quad [T_{BC}] = \begin{bmatrix} c\theta_2^B & 0 & -s\theta_2^B \\ 0 & 1 & 0 \\ s\theta_2^B & 0 & c\theta_2^B \end{bmatrix}, \text{ and } [T_{CD}] = \begin{bmatrix} c\theta_3^C & s\theta_3^C & 0 \\ -s\theta_3^C & c\theta_3^C & 0 \\ 0 & 0 & 1 \end{bmatrix} \quad \text{(C.0.1)}$$

where the abbreviations s for sin and c for cos have been introduced to save space.

The total transformation from A to D is expressed by the matrix product

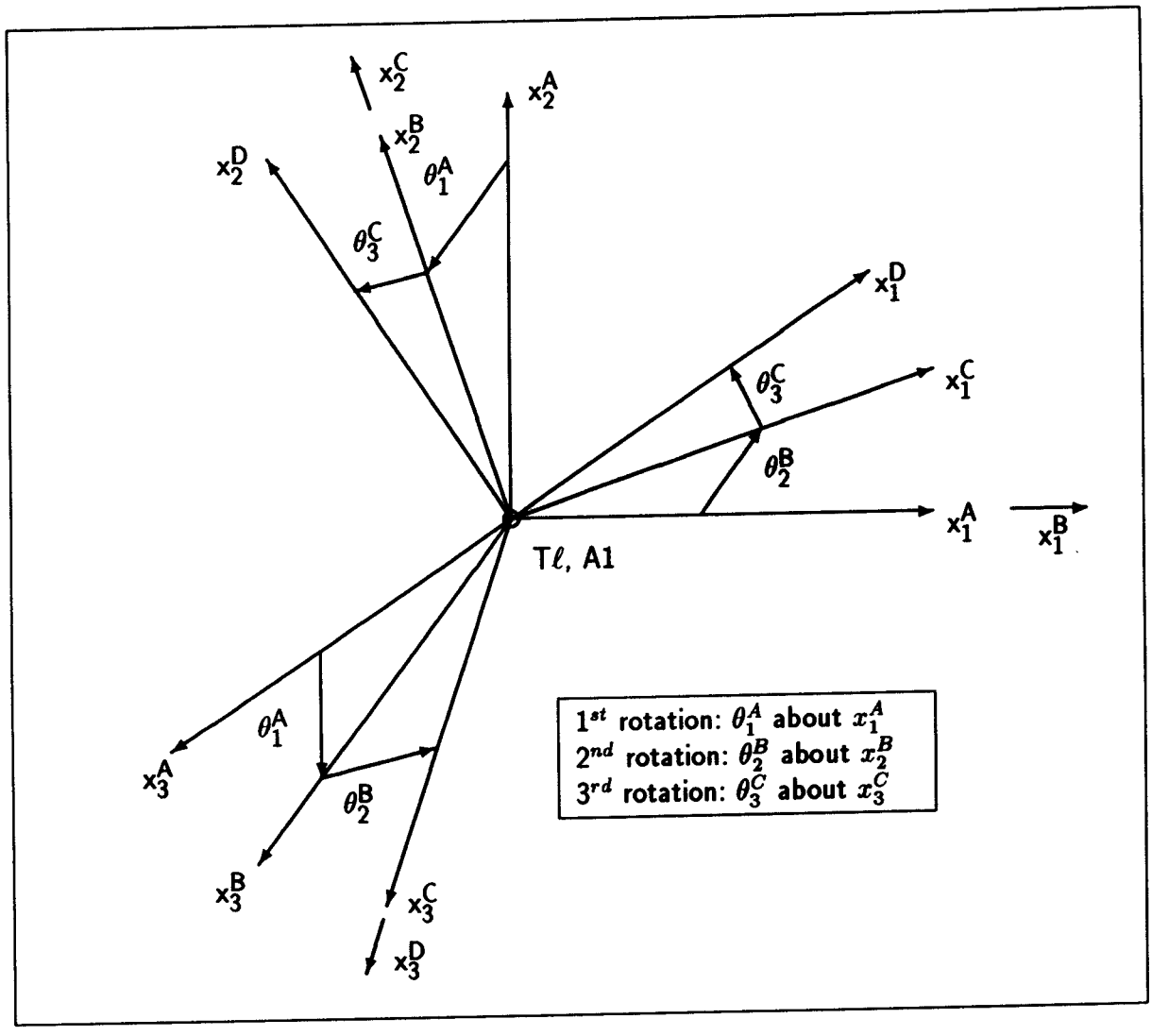

Figure 42: Finite transformation angles.

$$
\begin{aligned}
[T_{AD}] &= [T_{CD}]\,[T_{BC}]\,[T_{AB}] \\
&= \left[\begin{array}{c|c|c}
c\theta_2^B c\theta_3^C & s\theta_1^A s\theta_2^B c\theta_3^C + c\theta_1^A s\theta_3^C & -c\theta_1^A s\theta_2^B c\theta_3^C + s\theta_1^A s\theta_3^C \\
\hline
-c\theta_2^B s\theta_3^C & -s\theta_1^A s\theta_2^B s\theta_3^C + c\theta_1^A c\theta_3^C & c\theta_1^A s\theta_2^B s\theta_3^C + s\theta_1^A c\theta_3^C \\
\hline
s\theta_2^B & -s\theta_1^A c\theta_2^B & c\theta_1^A c\theta_2^B
\end{array}\right]
\end{aligned}
\tag{C.0.2}
$$

This matrix is orthonormal as rotation matrices in general, and the inverse can be found from

$$
[T_{AD}]^T = [T_{AD}]^{-1} = [T_{DA}] \tag{C.0.3}
$$

In the following derivation of angular velocity we will also need the partial transformation

$$
[T_{BD}] = [T_{CD}]\,[T_{BC}] = \left[\begin{array}{ccc}
c\theta_2^B c\theta_3^C & s\theta_3^C & -s\theta_2^B c\theta_3^C \\
-c\theta_2^B s\theta_3^C & c\theta_3^C & s\theta_2^B s\theta_3^C \\
s\theta_2^B & 0 & c\theta_2^B
\end{array}\right] \tag{C.0.4}
$$

If the rotations are time varying, the angular velocities will also be needed to describe the resulting angular velocity of the D-system relative to the A-system.

The angular velocities of the involved coordinate systems relative to each other can be described as vectors as follows

$$\left.\begin{array}{ll} \left\{\omega_{BA}^{B}\right\}^{T} = \left[\dot{\theta}_1^A, 0, 0\right] & B\text{- relative to } A\text{-system in } B\text{-coordinates} \\ \left\{\omega_{CB}^{C}\right\}^{T} = \left[0, \dot{\theta}_2^B, 0\right] & C\text{- relative to } B\text{-system in } C\text{-coordinates} \\ \left\{\omega_{DC}^{D}\right\}^{T} = \left[0, 0, \dot{\theta}_3^C\right] & D\text{- relative to } C\text{-system in } D\text{-coordinates} \end{array}\right\} \quad \text{(C.0.5)}$$

The resulting angular velocity of the D-system relative to the A-system in D-coordinates is obtained as the sum

$$\left\{\omega_{DA}^{D}\right\} = \left\{\omega_{DC}^{D}\right\} + [T_{CD}]\left\{\omega_{CB}^{C}\right\} + [T_{BD}]\left\{\omega_{BA}^{B}\right\} \quad \text{(C.0.6)}$$

where the local angular velocities have been transformed to the D-coordinates.

Carrying out the multiplications we arrive at

$$\left\{\omega_{DA}^{D}\right\} = \left\{\begin{array}{c} \dot{\theta}_1^A c\theta_2^B c\theta_3^C + \dot{\theta}_2^B s\theta_3^C \\ -\dot{\theta}_1^A c\theta_2^B s\theta_3^C + \dot{\theta}_2^B c\theta_3^C \\ \dot{\theta}_1^A s\theta_2^B + \dot{\theta}_3^C \end{array}\right\} \quad \text{(C.0.7)}$$

A problem arising in kinematic analysis is that the time derivative is needed of a position vector in a rotating coordinate system (D). The expression for the time derivative with respect to an inertial system (A) is the final need. The rotating position vector can be expressed in the inertial system by a transformation

$$\left\{r^A\right\} = [T_{DA}]\left\{r^D\right\} \quad \text{(C.0.8)}$$

where we can assume that the two coordinate systems have common origin without loss of generality. Fig. 42 illustrates this situation. The time derivative of the vector can now be obtained by differentiating in Eq. C.0.8 with respect to time, by use of the chain rule and we get

$$\left\{\dot{r}^{AA}\right\} = \frac{d}{dt}\left([T_{DA}]\right)\left\{r^D\right\} + [T_{DA}]\left\{\dot{r}^{DD}\right\} \quad \text{(C.0.9)}$$

Here the left upper index refers to the coordinate system with respect to which the time derivation is carried out. The right upper index refers to the system to which the components of the vector are referenced. It is important to be aware of these characteristics of the vectors, when they are manipulated in algebraic expressions. The left index is omitted in the kinematic analysis for the model, because the time derivatives of the substructure position vectors are taken consistently with respect to the substructure coordinate systems, and the time derivative of the resulting vector is taken with respect to the inertial system, so no doubt can arise here. However, the right index is retained, because the basis for the vectors are frequently changed.

The time derivative of the transformation matix is needed in Eq. C.0.9. It is found by differentiation of the matrix elements which yields

$$\frac{d}{dt}[T_{DA}] = \left[\begin{array}{c|c|c} -\dot{\theta}_2^B s\theta_2^B c\theta_3^C & +\dot{\theta}_2^B s\theta_2^B s\theta_3^C & +\dot{\theta}_2^B c\theta_2^B \\ -\dot{\theta}_3^C c\theta_2^B s\theta_3^C & -\dot{\theta}_3^C c\theta_2^B c\theta_3^C & \\ \hline + \dot{\theta}_1^A c\theta_1^A s\theta_2^B c\theta_3^C & -\dot{\theta}_1^A c\theta_1^A s\theta_2^B s\theta_3^C & \\ +\dot{\theta}_2^B s\theta_1^A c\theta_2^B c\theta_3^C & -\dot{\theta}_2^B s\theta_1^A c\theta_2^B s\theta_3^C & -\dot{\theta}_1^A c\theta_1^A c\theta_2^B \\ -\dot{\theta}_3^C s\theta_1^A s\theta_2^B s\theta_3^C & -\dot{\theta}_3^C s\theta_1^A s\theta_2^B c\theta_3^C & +\dot{\theta}_2^B s\theta_1^A s\theta_2^B \\ -\dot{\theta}_1^A s\theta_1^A s\theta_3^C & -\dot{\theta}_1^A s\theta_1^A c\theta_3^C & \\ +\dot{\theta}_3^C c\theta_1^A c\theta_3^C & -\dot{\theta}_3^C c\theta_1^A s\theta_3^C & \\ \hline + \dot{\theta}_1^A s\theta_1^A s\theta_2^B c\theta_3^C & -\dot{\theta}_1^A s\theta_1^A s\theta_2^B s\theta_3^C & \\ -\dot{\theta}_2^B c\theta_1^A c\theta_2^B c\theta_3^C & +\dot{\theta}_2^B c\theta_1^A c\theta_2^B s\theta_3^C & -\dot{\theta}_1^A s\theta_1^A c\theta_2^B \\ +\dot{\theta}_3^C c\theta_1^A s\theta_2^B s\theta_3^C & +\dot{\theta}_3^C c\theta_1^A s\theta_2^B c\theta_3^C & -\dot{\theta}_2^B c\theta_1^A s\theta_2^B \\ +\dot{\theta}_1^A c\theta_1^A s\theta_3^C & +\dot{\theta}_1^A c\theta_1^A c\theta_3^C & \\ +\dot{\theta}_3^C s\theta_1^A c\theta_3^C & -\dot{\theta}_3^C s\theta_1^A s\theta_3^C & \end{array}\right] \tag{C.0.10}$$

If the following skew symmetric matrix is formed by the components of the angular velocity vector from Eq. C.0.7

$$\begin{aligned} \left[\omega_{DA}^D\right] &= \left[\begin{array}{ccc} 0 & -\omega_{3DA}^D & -\omega_{2DA}^D \\ \omega_{3DA}^D & 0 & -\omega_{1DA}^D \\ -\omega_{2DA}^D & \omega_{1DA}^D & 0 \end{array}\right] \\ &= \left[\begin{array}{c|c|c} 0 & -\dot{\theta}_1^A s\theta_2^B - \dot{\theta}_3^C & -\dot{\theta}_1^A c\theta_2^B s\theta_3^C + \dot{\theta}_2^B c\theta_3^C \\ \hline \dot{\theta}_1^A s\theta_2^B + \dot{\theta}_3^C & 0 & -\dot{\theta}_1^A c\theta_2^B c\theta_3^C - \dot{\theta}_2^B s\theta_3^C \\ \hline \dot{\theta}_1^A c\theta_2^B s\theta_3^C - \dot{\theta}_2^B c\theta_3^C & \dot{\theta}_1^A c\theta_2^B c\theta_3^C + \dot{\theta}_2^B s\theta_3^C & 0 \end{array}\right] \end{aligned} \tag{C.0.11}$$

it can be seen by comparison ot the single terms that the following equation is valid

$$\frac{d}{dt}[T_{DA}] = [T_{DA}]\left[\omega_{DA}^D\right] \tag{C.0.12}$$

In this expression it is important to note that the angular velocity is of the D-system relative to the A-system. Especially when more than two coordinate systems are present there is a risk that the opposite vector is chosen. The notation serves to choose the correct vector. An equation equivalent to Eq. C.0.12 is found in [M7, p. 108], but derived by considering differentials.

The product of the skew symmetric matrix and a vector can further be written as a cross product

$$\left[\omega_{DA}^D\right]\left\{r^D\right\} = \left\{\omega_{DA}^D\right\} \times \left\{r^D\right\} \tag{C.0.13}$$

which can be seen easily by inspection.

By using the two last equations, the time derivative of the position vector in the rotating D-system with respect to the A-system (not necessarily an inertial system) can be derived as

$$\begin{aligned}\left\{\dot{r}^{AA}\right\} &= \frac{d}{dt}\left([T_{DA}]\right)\left\{r^D\right\} + [T_{DA}]\left\{\dot{r}^{DD}\right\} \\ &= [T_{DA}]\left[\left[\omega^D_{DA}\right]\left\{r^D\right\} + \left\{\dot{r}^{DD}\right\}\right] \\ &= [T_{DA}]\left[\left\{\omega^D_{DA}\right\} \times \left\{r^D\right\} + \left\{\dot{r}^{DD}\right\}\right] \end{aligned} \tag{C.0.14}$$

the last line expressing the well known rule for differentiation in a rotating frame of reference.

This equation is the recipe followed in the kinematic analysis, the starting point being the first line. It is often advantageous for simple systems to start with the last line. However, the chosen method is found to be more straightforward and safe when dealing with more than one rotating coordinate system.

If the transformation matrix is expressed as a product of matrices Eq. C.0.14 is still valid. In this case the differentiation can be carried out by application of the chain rule so that each time dependent matrix in the product is differentiated in accordance with Eq. C.0.12. For example, if we consider the $[T_{DA}]$-matrix as composed of the three transformation matrices defined previously, we get for the first term of Eq. C.0.14

$$\begin{aligned}\frac{d}{dt}\left([T_{DA}]\right)\left\{r^D\right\} &= \frac{d}{dt}\left([T_{BA}]\,[T_{CB}]\,[T_{DC}]\right)\left\{r^D\right\} \\ &= \left([T_{BA}]\left[\omega^B_{BA}\right][T_{DB}] + [T_{CA}]\left[\omega^C_{CB}\right][T_{DC}] + [T_{DA}]\left[\omega^D_{DC}\right]\right)\left\{r^D\right\} \\ &= [T_{BA}]\left[\left\{\omega^B_{BA}\right\} \times \left\{r^B\right\}\right] + [T_{CA}]\left[\left\{\omega^C_{CB}\right\} \times \left\{r^C\right\}\right] + [T_{DA}]\left[\left\{\omega^D_{DC}\right\} \times \left\{r^D\right\}\right] \end{aligned} \tag{C.0.15}$$

where the angular velocities of the participating coordinate systems now appear explicitly in the expression.

The linearization which is necessary in the present application is finally carried out in the transformation matrix from Eq. C.0.7. Assuming that the rotations are small, so that the approximations $\cos\theta \simeq 1$ and $\sin\theta \simeq \theta$ are valid, we get

$$[T_{DA}] = \begin{bmatrix} 1 & \theta^C_3 & -\theta^B_2 \\ -\theta^C_3 & 1 & \theta^A_1 \\ \theta^B_2 & -\theta^A_1 & 1 \end{bmatrix} \tag{C.0.16}$$

Linearization of the angular velocities is not necessary, because they are found in the model directly as part of the solution during the time integration.

Tryk: Grafisk Service, RISØ

Kinematically Nonlinear Finite Element Model of a Horizontal Axis Wind Turbine.

Part 2 : Supplement. Inertia Matrices and Aerodynamic Model.

Jørgen Thirstrup Petersen
Wind Engineering Section

Dept. of Meteorology and Wind Energy
Risø National Laboratory
DK-4000 Roskilde
Denmark

July 11, 1990

Kinematically Nonlinear Finite Element Model of a
Horizontal Axis Wind Turbine.

Part 2 : Supplement. Inertia Matrices and Aerodynamic Model.

Jørgen Thirstrup Petersen

Abstract.

This supplement contains some of the most space consuming inertia matrices derived for the mathematical model of a horizontal axis wind turbine. One is the general inertia matrix, from which the mass, Coriolis and softening matrices are derived. These matrices are coefficients to local substructure degrees of freedom.

Other matrices are resulting from extraction of degrees of freedom from inertia vectors, which originate directly from the consistent transformation of the inertia load to the nodes of the beam finite element. These matrices are coefficients to degrees of freedom outside the local substructure. They depend on the actual choice of degrees of freedom and the actual linearization introduced by cancelling of higher order product terms of the degrees of freedom and their time derivatives. The origin of the matrices is explained and some of the most important algebraic manipulations are shown.

Further, the complete description of the aerodynamic model is contained in this supplement. A procedure for time simulation of turbulence is part of the model.

Thesis submitted to the Technical University of Denmark in partial fulfilment of the requirements for the degree of Ph.D. (lic. techn.).

The thesis consists of 2 parts

Part 1 : Mathematical Model and Results.

Part 2 : Supplement. Inertia Matrices and Aerodynamic Model.

References to Part 1 are given, and the notation is in agreement with the notation of Part 1.

Contents

List of Figures

D General inertia matrix for the beam element.

The elements in the matrix $[I_{1LX}]$ are listed below. The matrix is the general expression for the mass, coriolis and softening matrices for the beam element, as derived in [Part 1, Sec. 4.11]. The respective matrix is achieved by substitution of the appropriate values for the T_{kl} terms, representing the unity matrix, angular velocities, and angular accelerations for the three cases, mentioned in corresponding order. Only the terms upon and above the diagonal of the 12×12 matrix are listed, because the terms below the diagonal can be found by the relation $I_{1LX(i,j)}(T_{kl}) = I_{1LX(j,i)}(T_{lk})$, which means that the lower triangle can be found from the upper by assuming symmetry and at the same time transposing the T_{kl} terms.

1^{st} row.

$$\begin{aligned} I_{1LX(1,1)} = -M\varrho_y^2 \Big[& T_{11}\left(1680\eta_y^2 + 294\eta_y + 13\right)\frac{1}{35} \\ & + (T_{13} + T_{31})\frac{r_y}{\ell}(12\eta_y + 1)\frac{1}{2} \\ & + T_{33}\left(\frac{r_{Iy}}{\ell}\right)^2 \frac{6}{5} \Big] \end{aligned} \tag{D.0.1}$$

$$\begin{aligned} I_{1LX(1,2)} = -M\varrho_x\varrho_y \Big[& T_{12}\left(1680\eta_x\eta_y + 147\left(\eta_x + \eta_y\right) + 13\right)\frac{1}{35} \\ & + T_{13}\frac{r_x}{\ell}(12\eta_y + 1)\frac{1}{2} \\ & + T_{32}\frac{r_y}{\ell}(12\eta_x + 1)\frac{1}{2} \Big] \end{aligned} \tag{D.0.2}$$

$$\begin{aligned} I_{1LX(1,3)} = -M\varrho_y \Big[& T_{13}(80\eta_y + 7)\frac{1}{20} \\ & + T_{33}\frac{r_y}{\ell}\frac{1}{2} \Big] \end{aligned} \tag{D.0.3}$$

$$\begin{aligned} I_{1LX(1,4)} = M\ell\varrho_x\varrho_y \Big[& T_{12}\left(1260\eta_x\eta_y + 105\eta_x + 126\eta_y + 11\right)\frac{1}{210} \\ & - T_{13}\frac{r_x}{\ell}\left(480\eta_x\eta_y + 42\eta_x + 10\eta_y + 1\right)\frac{1}{10} \\ & + T_{32}\frac{r_y}{\ell}(12\eta_x + 1)\frac{1}{10} \Big] \end{aligned} \tag{D.0.4}$$

$$\begin{aligned} I_{1LX(1,5)} = -M\ell\varrho_y^2 \Big[& T_{11}\left(1260\eta_y^2 + 231\eta_y + 11\right)\frac{1}{210} \\ & - T_{13}\frac{r_y}{\ell}\left(480\eta_y^2 + 52\eta_y + 1\right)\frac{1}{10} \\ & + T_{31}\frac{r_y}{\ell}(12\eta_y + 1)\frac{1}{10} \\ & - T_{33}\left(\frac{r_{Iy}}{\ell}\right)^2 (60\eta_y - 1)\frac{1}{10} \Big] \end{aligned} \tag{D.0.5}$$

$$
\begin{aligned}
I_{1LX(1,6)} = -M\varrho_y \Bigg[& -T_{11}\Bigg[e_{s2}\varrho_y\left(1680\eta_y^2+294\eta_y+13\right)\frac{1}{35} \\
& -(e_{s2}-r_x)\left(80\eta_y+7\right)\frac{1}{20}\Bigg] \\
& +T_{12}\Bigg[e_{s1}\varrho_x\left(1680\eta_x\eta_y+147\left(\eta_x+\eta_y\right)+13\right)\frac{1}{35} \\
& -(e_{s1}-r_y)\left(80\eta_y+7\right)\frac{1}{20}\Bigg] \\
& +T_{13}\left(e_{s1}\varrho_x\frac{r_x}{\ell}\left(12\eta_y+1\right)-e_{s2}\frac{r_y}{\ell}\right)\frac{1}{2} \\
& +T_{32}\ell\left(\frac{r_{Iy}}{\ell}\right)^2\frac{1}{2} \\
& -T_{33}e_{s2}\varrho_y\left(\frac{r_{Iy}}{\ell}\right)^2\frac{6}{5}\Bigg]
\end{aligned}
\tag{D.0.6}
$$

$$
\begin{aligned}
I_{1LX(1,7)} = -M\varrho_y^2\Bigg[& T_{11}\left(560\eta_y^2+84\eta_y+3\right)\frac{3}{70} \\
& -\left(T_{13}-T_{31}\right)\frac{r_y}{\ell}\left(12\eta_y+1\right)\frac{1}{2} \\
& -T_{33}\left(\frac{r_{Iy}}{\ell}\right)^2\frac{6}{5}\Bigg]
\end{aligned}
\tag{D.0.7}
$$

$$
\begin{aligned}
I_{1LX(1,8)} = -M\varrho_x\varrho_y\Bigg[& T_{12}\left(560\eta_x\eta_y+42\left(\eta_x+\eta_y\right)+3\right)\frac{3}{70} \\
& -T_{13}\frac{r_x}{\ell}\left(12\eta_y+1\right)\frac{1}{2} \\
& +T_{32}\frac{r_y}{\ell}\left(12\eta_x+1\right)\frac{1}{2}\Bigg]
\end{aligned}
\tag{D.0.8}
$$

$$
\begin{aligned}
I_{1LX(1,9)} = -M\varrho_y\Bigg[& T_{13}\left(40\eta_y+3\right)\frac{1}{20} \\
& +T_{33}\frac{r_y}{\ell}\frac{1}{2}\Bigg]
\end{aligned}
\tag{D.0.9}
$$

$$
\begin{aligned}
I_{1LX(1,10)} = -ML\varrho_x\varrho_y\Bigg[& T_{12}\left(2520\eta_x\eta_y+210\eta_x+168\eta_y+13\right)\frac{1}{420} \\
& +T_{13}\frac{r_x}{\ell}\left(240\eta_x\eta_y+18\eta_x-10\eta_y-1\right)\frac{1}{10} \\
& +T_{32}\frac{r_y}{\ell}\left(12\eta_x+1\right)\frac{1}{10}\Bigg]
\end{aligned}
\tag{D.0.10}
$$

$$
\begin{aligned}
I_{1LX(1,11)} = ML\varrho_y^2\Bigg[& T_{11}\left(2520\eta_y^2+378\eta_y+13\right)\frac{1}{420} \\
& +T_{13}\frac{r_y}{\ell}\left(240\eta_y^2+8\eta_y-1\right)\frac{1}{10} \\
& +T_{31}\frac{r_y}{\ell}\left(12\eta_y+1\right)\frac{1}{10} \\
& +T_{33}\left(\frac{r_{Iy}}{\ell}\right)^2\left(60\eta_y-1\right)\frac{1}{10}\Bigg]
\end{aligned}
\tag{D.0.11}
$$

$$
\begin{aligned}
I_{1LX(1,12)} \;=\; -M\varrho_y \Bigg[& -T_{11}\Bigg[e_{s2}\varrho_y\left(560\eta_y^2+84\eta_y+3\right)\frac{3}{70} \\
& \qquad -(e_{s2}-r_x)\,(40\eta_y+3)\,\frac{1}{20}\Bigg] \\
& +T_{12}\Bigg[e_{s1}\varrho_x\,(560\eta_x\eta_y+42\,(\eta_x+\eta_y)+3)\,\frac{3}{70} \\
& \qquad -(e_{s1}-r_y)\,(40\eta_y+3)\,\frac{1}{20}\Bigg] \\
& +T_{13}\left(e_{s2}\frac{r_y}{\ell}-e_{s1}\varrho_x\frac{r_x}{\ell}\,(12\eta_y+1)\right)\frac{1}{2} \\
& +T_{32}\ell\left(\frac{r_{Iy}}{\ell}\right)^2\frac{1}{2} \\
& +T_{33}e_{s2}\varrho_y\left(\frac{r_{Iy}}{\ell}\right)^2\frac{6}{5}\Bigg]
\end{aligned}
\tag{D.0.12}
$$

2nd row.

$$
\begin{aligned}
I_{1LX(2,2)} \;=\; -M\varrho_x^2\Bigg[& T_{22}\left(1680\eta_x^2+294\eta_x+13\right)\frac{1}{35} \\
& +(T_{23}+T_{32})\,\frac{r_x}{\ell}\,(12\eta_x+1)\,\frac{1}{2} \\
& +T_{33}\left(\frac{r_{Ix}}{\ell}\right)^2\frac{6}{5}\Bigg]
\end{aligned}
\tag{D.0.13}
$$

$$
\begin{aligned}
I_{1LX(2,3)} \;=\; -M\varrho_x\Bigg[& T_{23}\,(80\eta_x+7)\,\frac{1}{20} \\
& +T_{33}\frac{r_x}{\ell}\frac{1}{2}\Bigg]
\end{aligned}
\tag{D.0.14}
$$

$$
\begin{aligned}
I_{1LX(2,4)} \;=\; M\ell\varrho_x^2\Bigg[& T_{22}\left(1260\eta_x^2+231\eta_x+11\right)\frac{1}{210} \\
& -T_{23}\frac{r_x}{\ell}\left(480\eta_x^2+52\eta_x+1\right)\frac{1}{10} \\
& +T_{32}\frac{r_x}{\ell}\,(12\eta_x+1)\,\frac{1}{10} \\
& -T_{33}\left(\frac{r_{Ix}}{\ell}\right)^2(60\eta_x-1)\,\frac{1}{10}\Bigg]
\end{aligned}
\tag{D.0.15}
$$

$$
\begin{aligned}
I_{1LX(2,5)} \;=\; -M\ell\varrho_x\varrho_y\Bigg[& T_{21}\,(1260\eta_x\eta_y+126\eta_x+105\eta_y+11)\,\frac{1}{210} \\
& -T_{23}\frac{r_y}{\ell}\,(480\eta_x\eta_y+10\eta_x+42\eta_y+1)\,\frac{1}{10} \\
& +T_{31}\frac{r_x}{\ell}\,(12\eta_y+1)\,\frac{1}{10}\Bigg]
\end{aligned}
\tag{D.0.16}
$$

$$
\begin{aligned}
I_{1LX(2,6)} \;=\; -M\varrho_x \Bigg[& -T_{21}\Bigg[e_{s2}\varrho_y\left(1680\eta_x\eta_y+147\left(\eta_x+\eta_y\right)+13\right)\frac{1}{35} \\
& \qquad -\left(e_{s2}-r_x\right)\left(80\eta_x+7\right)\frac{1}{20}\Bigg] \\
& +T_{22}\Bigg[e_{s1}\varrho_x\left(1680\eta_x^2+294\eta_x+13\right)\frac{1}{35} \\
& \qquad -\left(e_{s1}-r_y\right)\left(80\eta_x+7\right)\frac{1}{20}\Bigg] \\
& +T_{23}\left[e_{s1}\frac{r_x}{\ell}-e_{s2}\varrho_y\frac{r_y}{\ell}\left(12\eta_x+1\right)\right]\frac{1}{2} \\
& -T_{31}\ell\left(\frac{r_{Ix}}{\ell}\right)^2\frac{1}{2} \\
& +T_{33}e_{s1}\varrho_x\left(\frac{r_{Ix}}{\ell}\right)^2\frac{6}{5}\Bigg]
\end{aligned}
\tag{D.0.17}
$$

$$
\begin{aligned}
I_{1LX(2,7)} \;=\; -M\varrho_x\varrho_y\Bigg[& T_{21}\left(560\eta_x\eta_y+42\left(\eta_x+\eta_y\right)+3\right)\frac{3}{70} \\
& -T_{23}\frac{r_y}{\ell}\left(12\eta_x+1\right)\frac{1}{2} \\
& +T_{31}\frac{r_x}{\ell}\left(12\eta_y+1\right)\frac{1}{2}\Bigg]
\end{aligned}
\tag{D.0.18}
$$

$$
\begin{aligned}
I_{1LX(2,8)} \;=\; -M\varrho_x^2\Bigg[& T_{22}\left(560\eta_x^2+84\eta_x+3\right)\frac{3}{70} \\
& -\left(T_{23}-T_{32}\right)\frac{r_x}{\ell}\left(12\eta_x+1\right)\frac{1}{2} \\
& -T_{33}\left(\frac{r_{Ix}}{\ell}\right)^2\frac{6}{5}\Bigg]
\end{aligned}
\tag{D.0.19}
$$

$$
\begin{aligned}
I_{1LX(2,9)} \;=\; -M\varrho_x\Bigg[& T_{23}\left(40\eta_x+3\right)\frac{1}{20} \\
& +T_{33}\frac{r_x}{\ell}\frac{1}{2}\Bigg]
\end{aligned}
\tag{D.0.20}
$$

$$
\begin{aligned}
I_{1LX(2,10)} \;=\; -M\ell\varrho_x^2\Bigg[& T_{22}\left(2520\eta_x^2+378\eta_x+13\right)\frac{1}{420} \\
& +T_{23}\frac{r_x}{\ell}\left(240\eta_x^2+8\eta_x-1\right)\frac{1}{10} \\
& +T_{32}\frac{r_x}{\ell}\left(12\eta_x+1\right)\frac{1}{10} \\
& +T_{33}\left(\frac{r_{Ix}}{\ell}\right)^2\left(60\eta_x-1\right)\frac{1}{10}\Bigg]
\end{aligned}
\tag{D.0.21}
$$

$$
\begin{aligned}
I_{1LX(2,11)} \;=\; M\ell\varrho_x\varrho_y\Bigg[& T_{21}\left(2520\eta_x\eta_y+168\eta_x+210\eta_y+13\right)\frac{1}{420} \\
& +T_{23}\frac{r_y}{\ell}\left(240\eta_x\eta_y-10\eta_x+18\eta_y-1\right)\frac{1}{10} \\
& +T_{31}\frac{r_x}{\ell}\left(12\eta_y+1\right)\frac{1}{10}\Bigg]
\end{aligned}
\tag{D.0.22}
$$

$$
\begin{aligned}
I_{1LX(2,12)} \;=\; -M\varrho_x \Bigg[& -T_{21}\Bigg[e_{s2}\varrho_y\left(560\eta_x\eta_y + 42\left(\eta_x+\eta_y\right)+3\right)\frac{3}{70} \\
& \qquad -\left(e_{s2}-r_x\right)\left(40\eta_x+3\right)\frac{1}{20}\Bigg] \\
& +T_{22}\Bigg[e_{s1}\varrho_x\left(560\eta_x^2+84\eta_x+3\right)\frac{3}{70} \\
& \qquad -\left(e_{s1}-r_y\right)\left(40\eta_x+3\right)\frac{1}{20}\Bigg] \\
& +T_{23}\left(e_{s2}\varrho_y\frac{r_y}{\ell}\left(12\eta_x+1\right)-e_{s1}\frac{r_x}{\ell}\right)\frac{1}{2} \\
& -T_{31}\ell\left(\frac{r_{Ix}}{\ell}\right)^2\frac{1}{2} \\
& -T_{33}e_{s1}\varrho_x\left(\frac{r_{Ix}}{\ell}\right)^2\frac{6}{5}\Bigg]
\end{aligned}
\tag{D.0.23}
$$

3rd row.

$$
I_{1LX(3,3)} = -MT_{33}\frac{1}{3} \tag{D.0.24}
$$

$$
\begin{aligned}
I_{1LX(3,4)} \;=\; M\ell\varrho_x \Bigg[& T_{32}\left(10\eta_x+1\right)\frac{1}{20} \\
& -T_{33}\frac{r_x}{\ell}\left(48\eta_x+1\right)\frac{1}{12}\Bigg]
\end{aligned}
\tag{D.0.25}
$$

$$
\begin{aligned}
I_{1LX(3,5)} \;=\; -M\ell\varrho_y \Bigg[& T_{31}\left(10\eta_y+1\right)\frac{1}{20} \\
& -T_{33}\frac{r_y}{\ell}\left(48\eta_y+1\right)\frac{1}{12}\Bigg]
\end{aligned}
\tag{D.0.26}
$$

$$
\begin{aligned}
I_{1LX(3,6)} \;=\; -M\Bigg[& -T_{31}\Bigg[e_{s2}\varrho_y\left(80\eta_y+7\right)\frac{1}{20}-\left(e_{s2}-r_x\right)\frac{1}{3}\Bigg] \\
& +T_{32}\Bigg[e_{s1}\varrho_x\left(80\eta_x+7\right)\frac{1}{20}-\left(e_{s1}-r_y\right)\frac{1}{3}\Bigg] \\
& +T_{33}\left(e_{s1}\varrho_x\frac{r_x}{\ell}-e_{s2}\varrho_y\frac{r_y}{\ell}\right)\frac{1}{2}\Bigg]
\end{aligned}
\tag{D.0.27}
$$

$$
\begin{aligned}
I_{1LX(3,7)} \;=\; -M\varrho_y \Bigg[& T_{31}\left(40\eta_y+3\right)\frac{1}{20} \\
& -T_{33}\frac{r_y}{\ell}\frac{1}{2}\Bigg]
\end{aligned}
\tag{D.0.28}
$$

$$
\begin{aligned}
I_{1LX(3,8)} \;=\; -M\varrho_x \Bigg[& T_{32}\left(40\eta_x+3\right)\frac{1}{20} \\
& -T_{33}\frac{r_x}{\ell}\frac{1}{2}\Bigg]
\end{aligned}
\tag{D.0.29}
$$

$$I_{1LX(3,9)} = -MT_{33}\frac{1}{6} \tag{D.0.30}$$

$$\begin{aligned} I_{1LX(3,10)} \;=\; -M\ell\varrho_x \Big[\;& T_{32}\left(15\eta_x+1\right)\frac{1}{30} \\ & +T_{33}\frac{r_x}{\ell}\left(24\eta_x-1\right)\frac{1}{12} \;\Big] \end{aligned} \tag{D.0.31}$$

$$\begin{aligned} I_{1LX(3,11)} \;=\; M\ell\varrho_y \Big[\;& T_{31}\left(15\eta_y+1\right)\frac{1}{30} \\ & +T_{33}\frac{r_y}{\ell}\left(24\eta_y-1\right)\frac{1}{12} \;\Big] \end{aligned} \tag{D.0.32}$$

$$\begin{aligned} I_{1LX(3,12)} \;=\; -M\Big[\;& -T_{31}\Big[\; e_{s2}\varrho_y\left(40\eta_y+3\right)\frac{1}{20}-\left(e_{s2}-r_x\right)\frac{1}{6} \;\Big] \\ & +T_{32}\Big[\; e_{s1}\varrho_x\left(40\eta_x+3\right)\frac{1}{20}-\left(e_{s1}-r_y\right)\frac{1}{6} \;\Big] \\ & -T_{33}\left(e_{s1}\varrho_x\frac{r_x}{\ell}-e_{s2}\varrho_y\frac{r_y}{\ell}\right)\frac{1}{2} \;\Big] \end{aligned} \tag{D.0.33}$$

4^{th} row.

$$\begin{aligned} I_{1LX(4,4)} \;=\; -M\ell^2\varrho_x^2\Big[\;& T_{22}\left(126\eta_x^2+21\eta_x+1\right)\frac{1}{105} \\ & -\left(T_{23}+T_{32}\right)\frac{r_x}{\ell}\eta_x\left(12\eta_x+1\right)\frac{1}{2} \\ & +T_{33}\left(\frac{r_{Ix}}{\ell}\right)^2\left(360\eta_x^2+15\eta_x+1\right)\frac{2}{15} \;\Big] \end{aligned} \tag{D.0.34}$$

$$\begin{aligned} I_{1LX(4,5)} \;=\; M\ell^2\varrho_x\varrho_y\Big[\;& T_{21}\left(252\eta_x\eta_y+21\left(\eta_x+\eta_y\right)+2\right)\frac{1}{210} \\ & -T_{23}\frac{r_y}{\ell}\left(60\eta_x\eta_y+6\eta_y-\eta_x\right)\frac{1}{10} \\ & -T_{31}\frac{r_x}{\ell}\left(60\eta_x\eta_y+6\eta_x-\eta_y\right)\frac{1}{10} \;\Big] \end{aligned} \tag{D.0.35}$$

$$\begin{aligned} I_{1LX(4,6)} \;=\; M\ell\varrho_x\Big[\;& -T_{21}\Big[\; e_{s2}\varrho_y\left(1260\eta_x\eta_y+105\eta_x+126\eta_y+11\right)\frac{1}{210} \\ & \qquad -\left(e_{s2}-r_x\right)\left(10\eta_x+1\right)\frac{1}{20} \;\Big] \\ & +T_{22}\Big[\; e_{s1}\varrho_x\left(1260\eta_x^2+231\eta_x+11\right)\frac{1}{210} \\ & \qquad -\left(e_{s1}-r_y\right)\left(10\eta_x+1\right)\frac{1}{20} \;\Big] \end{aligned}$$

$$
\begin{aligned}
&+T_{23}\left(e_{s1}\frac{r_x}{\ell}-e_{s2}\varrho_y\frac{r_y}{\ell}\left(12\eta_x+1\right)\right)\frac{1}{10}\\
&+T_{31}\Big[\ e_{s2}\varrho_y\frac{r_x}{\ell}\left(480\eta_x\eta_y+42\eta_x+10\eta_y+1\right)\frac{1}{10}\\
&\qquad+\left(\ell\left(\frac{r_{Ix}}{\ell}\right)^2-e_{s2}\frac{r_x}{\ell}\right)\left(48\eta_x+1\right)\frac{1}{12}\ \Big]\\
&-T_{32}e_{s1}\frac{r_x}{\ell}\Big[\ \varrho_x\left(480\eta_x^2+52\eta_x+1\right)\frac{1}{10}-\left(48\eta_x+1\right)\frac{1}{12}\ \Big]\\
&-T_{33}e_{s1}\varrho_x\left(\frac{r_{Ix}}{\ell}\right)^2\left(60\eta_x-1\right)\frac{1}{10}\ \Big]
\end{aligned}
\tag{D.0.36}
$$

$$
\begin{aligned}
I_{1LX(4,7)} \;=\; M\ell\varrho_x\varrho_y\Big[\ & T_{21}\left(2520\eta_x\eta_y+210\eta_x+168\eta_y+13\right)\frac{1}{420}\\
&-T_{23}\frac{r_y}{\ell}\left(12\eta_x+1\right)\frac{1}{10}\\
&-T_{31}\frac{r_x}{\ell}\left(240\eta_x\eta_y+18\eta_x-10\eta_y-1\right)\frac{1}{10}\ \Big]
\end{aligned}
\tag{D.0.37}
$$

$$
\begin{aligned}
I_{1LX(4,8)} \;=\; M\ell\varrho_x^2\Big[\ & T_{22}\left(2520\eta_x^2+378\eta_x+13\right)\frac{1}{420}\\
&-T_{23}\frac{r_x}{\ell}\left(12\eta_x+1\right)\frac{1}{10}\\
&-T_{32}\frac{r_x}{\ell}\left(240\eta_x^2+8\eta_x-1\right)\frac{1}{10}\\
&+T_{33}\left(\frac{r_{Ix}}{\ell}\right)^2\left(60\eta_x-1\right)\frac{1}{10}\ \Big]
\end{aligned}
\tag{D.0.38}
$$

$$
\begin{aligned}
I_{1LX(4,9)} \;=\; M\ell\varrho_x\Big[\ & T_{23}\left(15\eta_x+1\right)\frac{1}{30}\\
&-T_{33}\frac{r_x}{\ell}\left(24\eta_x-1\right)\frac{1}{12}\ \Big]
\end{aligned}
\tag{D.0.39}
$$

$$
\begin{aligned}
I_{1LX(4,10)} \;=\; M\ell^2\varrho_x^2\Big[\ & T_{22}\left(168\eta_x^2+28\eta_x+1\right)\frac{1}{140}\\
&+\left(T_{23}-T_{32}\right)\frac{r_x}{\ell}\left(360\eta_x^2+18\eta_x-1\right)\frac{1}{60}\\
&-T_{33}\left(\frac{r_{Ix}}{\ell}\right)^2\left(720\eta_x^2-60\eta_x-1\right)\frac{1}{30}\ \Big]
\end{aligned}
\tag{D.0.40}
$$

$$
\begin{aligned}
I_{1LX(4,11)} \;=\; -M\ell^2\varrho_x\varrho_y\Big[\ & T_{21}\left(168\eta_x\eta_y+14\left(\eta_x+\eta_y\right)+1\right)\frac{1}{140}\\
&+T_{23}\frac{r_y}{\ell}\left(360\eta_x\eta_y+24\eta_y-6\eta_x-1\right)\frac{1}{60}\\
&-T_{31}\frac{r_x}{\ell}\left(360\eta_x\eta_y+24\eta_x-6\eta_y-1\right)\frac{1}{60}\ \Big]
\end{aligned}
\tag{D.0.41}
$$

$$
\begin{aligned}
I_{1LX(4,12)} \;=\; M\ell\varrho_x \Bigg[& -T_{21}\Bigg[e_{s2}\varrho_y\left(2520\eta_x\eta_y+210\eta_x+168\eta_y+13\right)\frac{1}{420} \\
& \qquad -\left(e_{s2}-r_x\right)\left(15\eta_x+1\right)\frac{1}{30}\Bigg] \\
& +T_{22}\Bigg[e_{s1}\varrho_x\left(2520\eta_x^2+378\eta_x+13\right)\frac{1}{420} \\
& \qquad -\left(e_{s1}-r_y\right)\left(15\eta_x+1\right)\frac{1}{30}\Bigg] \\
& -T_{23}\left(e_{s1}\frac{r_x}{\ell}-e_{s2}\varrho_y\frac{r_y}{\ell}\left(12\eta_x+1\right)\right)\frac{1}{10} \\
& +T_{31}\Bigg[e_{s2}\varrho_y\frac{r_x}{\ell}\left(240\eta_x\eta_y+18\eta_x-10\eta_y-1\right)\frac{1}{10} \\
& \qquad +\left(\ell\left(\frac{r_{Ix}}{\ell}\right)^2-e_{s2}\frac{r_x}{\ell}\right)\left(24\eta_x-1\right)\frac{1}{12}\Bigg] \\
& -T_{32}e_{s1}\frac{r_x}{\ell}\Bigg[\varrho_x\left(240\eta_x^2+8\eta_x-1\right)\frac{1}{10}-\left(24\eta_x-1\right)\frac{1}{12}\Bigg] \\
& +T_{33}e_{s1}\varrho_x\left(\frac{r_{Ix}}{\ell}\right)^2\left(60\eta_x-1\right)\frac{1}{10}\Bigg]
\end{aligned}
\tag{D.0.42}
$$

5^{th} row.

$$
\begin{aligned}
I_{1LX(5,5)} \;=\; -M\ell^2\varrho_y^2\Bigg[& T_{11}\left(126\eta_y^2+21\eta_y+1\right)\frac{1}{105} \\
& -\left(T_{13}+T_{31}\right)\frac{r_y}{\ell}\eta_y\left(12\eta_y+1\right)\frac{1}{2} \\
& +T_{33}\left(\frac{r_{Iy}}{\ell}\right)^2\left(360\eta_y^2+15\eta_y+1\right)\frac{2}{15}\Bigg]
\end{aligned}
\tag{D.0.43}
$$

$$
\begin{aligned}
I_{1LX(5,6)} \;=\; -M\ell\varrho_y\Bigg[& -T_{11}\Bigg[e_{s2}\varrho_y\left(1260\eta_y^2+231\eta_y+11\right)\frac{1}{210} \\
& \qquad -\left(e_{s2}-r_x\right)\left(10\eta_y+1\right)\frac{1}{20}\Bigg] \\
& +T_{12}\Bigg[e_{s1}\varrho_x\left(1260\eta_x\eta_y+126\eta_x+105\eta_y+11\right)\frac{1}{210} \\
& \qquad -\left(e_{s1}-r_y\right)\left(10\eta_y+1\right)\frac{1}{20}\Bigg] \\
& +T_{13}\left(e_{s1}\varrho_x\frac{r_x}{\ell}\left(12\eta_y+1\right)-e_{s2}\frac{r_y}{\ell}\right)\frac{1}{10} \\
& +T_{31}\Bigg[e_{s2}\varrho_y\frac{r_y}{\ell}\left(480\eta_y^2+52\eta_y+1\right)\frac{1}{10}-e_{s2}\frac{r_y}{\ell}\left(48\eta_y+1\right)\frac{1}{12}\Bigg] \\
& -T_{32}\Bigg[e_{s1}\varrho_x\frac{r_y}{\ell}\left(480\eta_x\eta_y+10\eta_x+42\eta_y+1\right)\frac{1}{10} \\
& \qquad +\left(\ell\left(\frac{r_{Iy}}{\ell}\right)^2-e_{s1}\frac{r_y}{\ell}\right)\left(48\eta_y+1\right)\frac{1}{12}\Bigg] \\
& +T_{33}e_{s2}\varrho_y\left(\frac{r_{Iy}}{\ell}\right)^2\left(60\eta_y-1\right)\frac{1}{10}\Bigg]
\end{aligned}
\tag{D.0.44}
$$

$$I_{1LX(5,7)} = -M\ell\varrho_y^2\Big[\; T_{11}\left(2520\eta_y^2+378\eta_y+13\right)\frac{1}{420} - T_{13}\frac{r_y}{\ell}\left(12\eta_y+1\right)\frac{1}{10} - T_{31}\frac{r_y}{\ell}\left(240\eta_y^2+8\eta_y-1\right)\frac{1}{10} + T_{33}\left(\frac{r_{Iy}}{\ell}\right)^2\left(60\eta_y-1\right)\frac{1}{10}\;\Big] \tag{D.0.45}$$

$$I_{1LX(5,8)} = -M\ell\varrho_x\varrho_y\Big[\; T_{12}\left(2520\eta_x\eta_y+168\eta_x+210\eta_y+13\right)\frac{1}{420} - T_{13}\frac{r_x}{\ell}\left(12\eta_y+1\right)\frac{1}{10} - T_{32}\frac{r_y}{\ell}\left(240\eta_x\eta_y-10\eta_x+18\eta_y-1\right)\frac{1}{10}\;\Big] \tag{D.0.46}$$

$$I_{1LX(5,9)} = -M\ell\varrho_y\Big[\; T_{13}\left(15\eta_y+1\right)\frac{1}{30} - T_{33}\frac{r_y}{\ell}\left(24\eta_y-1\right)\frac{1}{12}\;\Big] \tag{D.0.47}$$

$$I_{1LX(5,10)} = -M\ell^2\varrho_x\varrho_y\Big[\; T_{12}\left(168\eta_x\eta_y+14\left(\eta_x+\eta_y\right)+1\right)\frac{1}{140} + T_{13}\frac{r_x}{\ell}\left(360\eta_x\eta_y+24\eta_x-6\eta_y-1\right)\frac{1}{60} - T_{32}\frac{r_y}{\ell}\left(360\eta_x\eta_y+24\eta_y-6\eta_x-1\right)\frac{1}{60}\;\Big] \tag{D.0.48}$$

$$I_{1LX(5,11)} = M\ell^2\varrho_y^2\Big[\; T_{11}\left(168\eta_y^2+28\eta_y+1\right)\frac{1}{140} + \left(T_{13}-T_{31}\right)\frac{r_y}{\ell}\left(360\eta_y^2+18\eta_y-1\right)\frac{1}{60} - T_{33}\left(\frac{r_{Iy}}{\ell}\right)^2\left(720\eta_y^2-60\eta_y-1\right)\frac{1}{30}\;\Big] \tag{D.0.49}$$

$$\begin{aligned} I_{1LX(5,12)} = -M\ell\varrho_y\Big[& -T_{11}\Big[\; e_{s2}\varrho_y\left(2520\eta_y^2+378\eta_y+13\right)\frac{1}{420} - \left(e_{s2}-r_x\right)\left(15\eta_y+1\right)\frac{1}{30}\;\Big] \\ & +T_{12}\Big[\; e_{s1}\varrho_x\left(2520\eta_x\eta_y+168\eta_x+210\eta_y+13\right)\frac{1}{420} - \left(e_{s1}-r_y\right)\left(15\eta_y+1\right)\frac{1}{30}\;\Big] \\ & -T_{13}\left(e_{s1}\varrho_x\frac{r_x}{\ell}\left(12\eta_y+1\right)-e_{s2}\frac{r_y}{\ell}\right)\frac{1}{10} \\ & +T_{31}e_{s2}\frac{r_y}{\ell}\Big[\; \varrho_y\left(240\eta_y^2+8\eta_y-1\right)\frac{1}{10}-\left(24\eta_y-1\right)\frac{1}{12}\;\Big]\Big] \end{aligned}$$

$$
\begin{aligned}
&-T_{32}\left[\; e_{s1}\varrho_x\frac{r_y}{\ell}\left(240\eta_x\eta_y-10\eta_x+18\eta_y-1\right)\frac{1}{10}\right.\\
&\qquad\left.+\left(\ell\left(\frac{r_{Iy}}{\ell}\right)^2-e_{s1}\frac{r_y}{\ell}\right)\left(24\eta_y-1\right)\frac{1}{12}\;\right]\\
&-T_{33}e_{s2}\varrho_y\left(\frac{r_{Iy}}{\ell}\right)^2\left(60\eta_y-1\right)\frac{1}{10}\;\Bigg]
\end{aligned}
\tag{D.0.50}
$$

6^{th} row.

$$
\begin{aligned}
I_{1LX(6,6)} \;=\; -M\Bigg[\;& T_{11}\left[\; e_{s2}^2\varrho_y^2\left(1680\eta_y^2+294\eta_y+13\right)\frac{1}{35}\right.\\
&-\left(e_{s2}-r_x\right)e_{s2}\varrho_y\left(80\eta_y+7\right)\frac{1}{10}\\
&\left.+\left(e_{s2}^2-2e_{s2}r_x+\ell^2\left(\frac{r_{Ix}}{\ell}\right)^2\right)\frac{1}{3}\;\right]\\
&+\left(T_{12}+T_{21}\right)\left[\;-e_{s1}e_{s2}\varrho_x\varrho_y\left(1680\eta_x\eta_y+147\left(\eta_x+\eta_y\right)+13\right)\frac{1}{35}\right.\\
&\qquad+e_{s1}\varrho_x\left(e_{s2}-r_x\right)\left(80\eta_x+7\right)\frac{1}{20}\\
&\qquad+e_{s2}\varrho_y\left(e_{s1}-r_y\right)\left(80\eta_y+7\right)\frac{1}{20}\\
&\qquad\left.+\left(e_{s1}r_x-e_{s1}e_{s2}+e_{s2}r_y\right)\frac{1}{3}\;\right]\\
&+T_{22}\left[\; e_{s1}^2\varrho_x^2\left(1680\eta_x^2+294\eta_x+13\right)\frac{1}{35}\right.\\
&-\left(e_{s1}-r_y\right)e_{s1}\varrho_x\left(80\eta_x+7\right)\frac{1}{10}\\
&\left.+\left(e_{s1}^2-2e_{s1}r_y+\ell^2\left(\frac{r_{Iy}}{\ell}\right)^2\right)\frac{1}{3}\;\right]\\
&-\left(T_{13}+T_{31}\right)\ell e_{s1}\varrho_x\left(\frac{r_{Ix}}{\ell}\right)^2\frac{1}{2}\\
&-\left(T_{23}+T_{32}\right)\ell e_{s2}\varrho_y\left(\frac{r_{Iy}}{\ell}\right)^2\frac{1}{2}\\
&+T_{33}\left(e_{s1}^2\varrho_x^2\left(\frac{r_{Ix}}{\ell}\right)^2+e_{s2}^2\varrho_y^2\left(\frac{r_{Iy}}{\ell}\right)^2\right)\frac{6}{5}\;\Bigg]
\end{aligned}
\tag{D.0.51}
$$

$$
\begin{aligned}
I_{1LX(6,7)} \;=\; -M\varrho_y\Bigg[\;& -T_{11}\left[\; e_{s2}\varrho_y\left(560\eta_y^2+84\eta_y+3\right)\frac{3}{70}\right.\\
&\left.-\left(e_{s2}-r_x\right)\left(40\eta_y+3\right)\frac{1}{20}\;\right]\\
&+T_{21}\left[\; e_{s1}\varrho_x\left(560\eta_x\eta_y+42\left(\eta_x+\eta_y\right)+3\right)\frac{3}{70}\right.\\
&\left.-\left(e_{s1}-r_y\right)\left(40\eta_y+3\right)\frac{1}{20}\;\right]\\
&-T_{23}\ell\left(\frac{r_{Iy}}{\ell}\right)^2\frac{1}{2}
\end{aligned}
$$

$$
\begin{aligned}
&+T_{31}\left[\; e_{s1}\varrho_x\frac{r_x}{\ell}\left(12\eta_y+1\right)\frac{1}{2}-e_{s2}\frac{r_y}{\ell}\frac{1}{2}\;\right]\\
&+T_{33}e_{s2}\varrho_y\left(\frac{r_{Iy}}{\ell}\right)^2\frac{6}{5}\;\Bigg]
\end{aligned}
\tag{D.0.52}
$$

$$
\begin{aligned}
I_{1LX(6,8)} \;=\; -M\varrho_x\Bigg[\; &-T_{12}\left[\; e_{s2}\varrho_y\left(560\eta_x\eta_y+42\left(\eta_x+\eta_y\right)+3\right)\frac{3}{70}\right.\\
&\qquad\left.-\left(e_{s2}-r_x\right)\left(40\eta_x+3\right)\frac{1}{20}\;\right]\\
&+T_{13}\ell\left(\frac{r_{Ix}}{\ell}\right)^2\frac{1}{2}\\
&+T_{22}\left[\; e_{s1}\varrho_x\left(560\eta_x^2+84\eta_x+3\right)\frac{3}{70}\right.\\
&\qquad\left.-\left(e_{s1}-r_y\right)\left(40\eta_x+3\right)\frac{1}{20}\;\right]\\
&+T_{32}\left(e_{s1}\frac{r_x}{\ell}-e_{s2}\varrho_y\frac{r_y}{\ell}\left(12\eta_x+1\right)\right)\frac{1}{2}\\
&-T_{33}e_{s1}\varrho_x\left(\frac{r_{Ix}}{\ell}\right)^2\frac{6}{5}\;\Bigg]
\end{aligned}
\tag{D.0.53}
$$

$$
\begin{aligned}
I_{1LX(6,9)} \;=\; -M\Bigg[\; &-T_{13}\left[\; e_{s2}\varrho_y\left(40\eta_y+3\right)\frac{1}{20}-\left(e_{s2}-r_x\right)\frac{1}{6}\;\right]\\
&+T_{23}\left[\; e_{s1}\varrho_x\left(40\eta_x+3\right)\frac{1}{20}-\left(e_{s1}-r_y\right)\frac{1}{6}\;\right]\\
&+T_{33}\left(e_{s1}\varrho_x\frac{r_x}{\ell}-e_{s2}\varrho_y\frac{r_y}{\ell}\right)\frac{1}{2}\;\Bigg]
\end{aligned}
\tag{D.0.54}
$$

$$
\begin{aligned}
I_{1LX(6,10)} \;=\; -M\ell\varrho_x\Bigg[\; &-T_{12}\left[\; e_{s2}\varrho_y\left(2520\eta_x\eta_y+210\eta_x+168\eta_y+13\right)\frac{1}{420}\right.\\
&\qquad\left.-\left(e_{s2}-r_x\right)\left(15\eta_x+1\right)\frac{1}{30}\;\right]\\
&-T_{13}\left[\; e_{s2}\varrho_y\frac{r_x}{\ell}\left(240\eta_x\eta_y+18\eta_x-10\eta_y-1\right)\frac{1}{10}\right.\\
&\qquad\left.+\left(\ell\left(\frac{r_{Ix}}{\ell}\right)^2-e_{s2}\frac{r_x}{\ell}\right)\left(24\eta_x-1\right)\frac{1}{12}\;\right]\\
&+T_{22}\left[\; e_{s1}\varrho_x\left(2520\eta_x^2+378\eta_x+13\right)\frac{1}{420}\right.\\
&\qquad\left.-\left(e_{s1}-r_y\right)\left(15\eta_x+1\right)\frac{1}{30}\;\right]\\
&+T_{23}e_{s1}\frac{r_x}{\ell}\left[\; \varrho_x\left(240\eta_x^2+8\eta_x-1\right)\frac{1}{10}-\left(24\eta_x-1\right)\frac{1}{12}\;\right]\\
&+T_{32}\left(e_{s1}\frac{r_x}{\ell}-e_{s2}\varrho_y\frac{r_y}{\ell}\left(12\eta_x+1\right)\right)\frac{1}{10}\\
&+T_{33}e_{s1}\varrho_x\left(\frac{r_{Ix}}{\ell}\right)^2\left(60\eta_x-1\right)\frac{1}{10}\;\Bigg]
\end{aligned}
\tag{D.0.55}
$$

$$
I_{1LX(6,11)} \;=\; M\ell\varrho_y\Bigg[\; -T_{11}\left[\; e_{s2}\varrho_y\left(2520\eta_y^2+378\eta_y+13\right)\frac{1}{420}\right.
$$

$$
\begin{aligned}
&\quad -(e_{s2}-r_x)(15\eta_y+1)\frac{1}{30}\ \Big] \\
&-T_{13}e_{s2}\frac{r_y}{\ell}\Big[\ \varrho_y\left(240\eta_y^2+8\eta_y-1\right)\frac{1}{10}-(24\eta_y-1)\frac{1}{12}\ \Big] \\
&+T_{21}\Big[\ e_{s1}\varrho_x\,(2520\eta_x\eta_y+168\eta_x+210\eta_y+13)\frac{1}{420} \\
&\quad -(e_{s1}-r_y)(15\eta_y+1)\frac{1}{30}\ \Big] \\
&+T_{23}\Big[\ e_{s1}\varrho_x\frac{r_y}{\ell}(240\eta_x\eta_y-10\eta_x+18\eta_y-1)\frac{1}{10} \\
&\quad +\left(\ell\left(\frac{r_{Iy}}{\ell}\right)^2-e_{s1}\frac{r_y}{\ell}\right)(24\eta_y-1)\frac{1}{12}\ \Big] \\
&+T_{31}\left(e_{s1}\varrho_x\frac{r_x}{\ell}(12\eta_y+1)-e_{s2}\frac{r_y}{\ell}\right)\frac{1}{10} \\
&-T_{33}e_{s2}\varrho_y\left(\frac{r_{Iy}}{\ell}\right)^2(60\eta_y-1)\frac{1}{10}\ \Big]
\end{aligned}
\tag{D.0.56}
$$

$$
\begin{aligned}
I_{1LX(6,12)} \;=\; -M\Big[\ & T_{11}\Big[\ e_{s2}^2\varrho_y^2\left(560\eta_y^2+84\eta_y+3\right)\frac{3}{70} \\
&\quad -(e_{s2}-r_x)\,e_{s2}\varrho_y\,(40\eta_y+3)\frac{1}{10} \\
&\quad +\left(e_{s2}^2-2e_{s2}r_x+\ell^2\left(\frac{r_{Ix}}{\ell}\right)^2\right)\frac{1}{6}\ \Big] \\
&-(T_{12}+T_{21})\Big[\ e_{s1}e_{s2}\varrho_x\varrho_y\,(560\eta_x\eta_y+42\,(\eta_x+\eta_y)+3)\frac{3}{70} \\
&\qquad -(e_{s2}-r_x)\,e_{s1}\varrho_x\,(40\eta_x+3)\frac{1}{20} \\
&\qquad -(e_{s1}-r_y)\,e_{s2}\varrho_y\,(40\eta_y+3)\frac{1}{20} \\
&\qquad +(e_{s1}e_{s2}-e_{s1}r_x-e_{s2}r_y)\frac{1}{6}\ \Big] \\
&+T_{22}\Big[\ e_{s1}^2\varrho_x^2\left(560\eta_x^2+84\eta_x+3\right)\frac{3}{70} \\
&\quad -(e_{s1}-r_y)\,e_{s1}\varrho_x\,(40\eta_x+3)\frac{1}{10} \\
&\quad +\left(e_{s1}^2-2e_{s1}r_y+\ell^2\left(\frac{r_{Iy}}{\ell}\right)^2\right)\frac{1}{6}\ \Big] \\
&+(T_{13}-T_{31})\,\ell e_{s1}\varrho_x\left(\frac{r_{Ix}}{\ell}\right)^2\frac{1}{2} \\
&+(T_{23}-T_{32})\,\ell e_{s2}\varrho_y\left(\frac{r_{Iy}}{\ell}\right)^2\frac{1}{2} \\
&-T_{33}\left(e_{s1}^2\varrho_x^2\left(\frac{r_{Ix}}{\ell}\right)^2+e_{s2}^2\varrho_y^2\left(\frac{r_{Iy}}{\ell}\right)^2\right)\frac{6}{5}\ \Big]
\end{aligned}
\tag{D.0.57}
$$

7^{th} row.

$$I_{1LX(7,7)} = -M\varrho_y^2\Big[\; T_{11}\left(1680\eta_y^2+294\eta_y+13\right)\frac{1}{35} - \left(T_{13}+T_{31}\right)\frac{r_y}{\ell}\left(12\eta_y+1\right)\frac{1}{2} + T_{33}\left(\frac{r_{Iy}}{\ell}\right)^2\frac{6}{5}\;\Big] \tag{D.0.58}$$

$$I_{1LX(7,8)} = -M\varrho_x\varrho_y\Big[\; T_{12}\left(1680\eta_x\eta_y+147\left(\eta_x+\eta_y\right)+13\right)\frac{1}{35} - T_{13}\frac{r_x}{\ell}\left(12\eta_y+1\right)\frac{1}{2} - T_{32}\frac{r_y}{\ell}\left(12\eta_x+1\right)\frac{1}{2}\;\Big] \tag{D.0.59}$$

$$I_{1LX(7,9)} = -M\varrho_y\Big[\; T_{13}\left(80\eta_y+7\right)\frac{1}{20} - T_{33}\frac{r_y}{\ell}\frac{1}{2}\;\Big] \tag{D.0.60}$$

$$I_{1LX(7,10)} = -M\ell\varrho_x\varrho_y\Big[\; T_{12}\left(1260\eta_x\eta_y+105\eta_x+126\eta_y+11\right)\frac{1}{210} + T_{13}\frac{r_x}{\ell}\left(480\eta_x\eta_y+42\eta_x+10\eta_y+1\right)\frac{1}{10} - T_{32}\frac{r_y}{\ell}\left(12\eta_x+1\right)\frac{1}{10}\;\Big] \tag{D.0.61}$$

$$I_{1LX(7,11)} = M\ell\varrho_y^2\Big[\; T_{11}\left(1260\eta_y^2+231\eta_y+11\right)\frac{1}{210} + T_{13}\frac{r_y}{\ell}\left(480\eta_y^2+52\eta_y+1\right)\frac{1}{10} - T_{31}\frac{r_y}{\ell}\left(12\eta_y+1\right)\frac{1}{10} - T_{33}\left(\frac{r_{Iy}}{\ell}\right)^2\left(60\eta_y-1\right)\frac{1}{10}\;\Big] \tag{D.0.62}$$

$$I_{1LX(7,12)} = -M\varrho_y\Big[-T_{11}\Big[\; e_{s2}\varrho_y\left(1680\eta_y^2+294\eta_y+13\right)\frac{1}{35} - \left(e_{s2}-r_x\right)\left(80\eta_y+7\right)\frac{1}{20}\;\Big] + T_{12}\Big[\; e_{s1}\varrho_x\left(1680\eta_x\eta_y+147\left(\eta_x+\eta_y\right)+13\right)\frac{1}{35} - \left(e_{s1}-r_y\right)\left(80\eta_y+7\right)\frac{1}{20}\;\Big] - T_{13}\left(e_{s1}\varrho_x\frac{r_x}{\ell}\left(12\eta_y+1\right)-e_{s2}\frac{r_y}{\ell}\right)\frac{1}{2} - T_{32}\ell\left(\frac{r_{Iy}}{\ell}\right)^2\frac{1}{2} - T_{33}e_{s2}\varrho_y\left(\frac{r_{Iy}}{\ell}\right)^2\frac{6}{5}\;\Big] \tag{D.0.63}$$

8^{th} row.

$$
\begin{aligned}
I_{1LX(8,8)} \;=\; -M\varrho_x^2\Big[\;& T_{22}\left(1680\eta_x^2+294\eta_x+13\right)\frac{1}{35}\\
&-\left(T_{23}+T_{32}\right)\frac{r_x}{\ell}\left(12\eta_x+1\right)\frac{1}{2}\\
&+T_{33}\left(\frac{r_{Ix}}{\ell}\right)^2\frac{6}{5}\;\Big]
\end{aligned}
\tag{D.0.64}
$$

$$
\begin{aligned}
I_{1LX(8,9)} \;=\; -M\varrho_x\Big[\;& T_{23}\left(80\eta_x+7\right)\frac{1}{20}\\
&-T_{33}\frac{r_x}{\ell}\frac{1}{2}\;\Big]
\end{aligned}
\tag{D.0.65}
$$

$$
\begin{aligned}
I_{1LX(8,10)} \;=\; -M\ell\varrho_x^2\Big[\;& T_{22}\left(1260\eta_x^2+231\eta_x+11\right)\frac{1}{210}\\
&+T_{23}\frac{r_x}{\ell}\left(480\eta_x^2+52\eta_x+1\right)\frac{1}{10}\\
&-T_{32}\frac{r_x}{\ell}\left(12\eta_x+1\right)\frac{1}{10}\\
&-T_{33}\left(\frac{r_{Ix}}{\ell}\right)^2\left(60\eta_x-1\right)\frac{1}{10}\;\Big]
\end{aligned}
\tag{D.0.66}
$$

$$
\begin{aligned}
I_{1LX(8,11)} \;=\; M\ell\varrho_x\varrho_y\Big[\;& T_{21}\left(1260\eta_x\eta_y+126\eta_x+105\eta_y+11\right)\frac{1}{210}\\
&+T_{23}\frac{r_y}{\ell}\left(480\eta_x\eta_y+10\eta_x+42\eta_y+1\right)\frac{1}{10}\\
&-T_{31}\frac{r_x}{\ell}\left(12\eta_y+1\right)\frac{1}{10}\;\Big]
\end{aligned}
\tag{D.0.67}
$$

$$
\begin{aligned}
I_{1LX(8,12)} \;=\; -M\varrho_x\Big[\;& -T_{21}\Big[\;e_{s2}\varrho_y\left(1680\eta_x\eta_y+147\left(\eta_x+\eta_y\right)+13\right)\frac{1}{35}\\
&\qquad-\left(e_{s2}-r_x\right)\left(80\eta_x+7\right)\frac{1}{20}\;\Big]\\
&+T_{22}\Big[\;e_{s1}\varrho_x\left(1680\eta_x^2+294\eta_x+13\right)\frac{1}{35}\\
&\qquad-\left(e_{s1}-r_y\right)\left(80\eta_x+7\right)\frac{1}{20}\;\Big]\\
&-T_{23}\Big[\;\left(e_{s1}\frac{r_x}{\ell}-e_{s2}\varrho_y\frac{r_y}{\ell}\left(12\eta_x+1\right)\right)\frac{1}{2}\;\Big]\\
&+T_{31}\ell\left(\frac{r_{Ix}}{\ell}\right)^2\frac{1}{2}\\
&+T_{33}e_{s1}\varrho_x\left(\frac{r_{Ix}}{\ell}\right)^2\frac{6}{5}\;\Big]
\end{aligned}
\tag{D.0.68}
$$

9^{th} row.

$$I_{1LX(9,9)} = -MT_{33}\frac{1}{3} \tag{D.0.69}$$

$$\begin{aligned} I_{1LX(9,10)} &= -M\ell\varrho_x \Big[\; T_{32}\left(10\eta_x+1\right)\frac{1}{20} \\ &\qquad +T_{33}\frac{r_x}{\ell}\left(48\eta_x+1\right)\frac{1}{12} \; \Big] \end{aligned} \tag{D.0.70}$$

$$\begin{aligned} I_{1LX(9,11)} &= M\ell\varrho_y \Big[\; T_{31}\left(10\eta_y+1\right)\frac{1}{20} \\ &\qquad +T_{33}\frac{r_y}{\ell}\left(48\eta_y+1\right)\frac{1}{12} \; \Big] \end{aligned} \tag{D.0.71}$$

$$\begin{aligned} I_{1LX(9,12)} &= -M\Big[-T_{31}\Big[\; e_{s2}\varrho_y\left(80\eta_y+7\right)\frac{1}{20} - \left(e_{s2}-r_x\right)\frac{1}{3} \; \Big] \\ &\qquad +T_{32}\Big[\; e_{s1}\varrho_x\left(80\eta_x+7\right)\frac{1}{20} - \left(e_{s1}-r_y\right)\frac{1}{3} \; \Big] \\ &\qquad -T_{33}\left(e_{s1}\varrho_x\frac{r_x}{\ell} - e_{s2}\varrho_y\frac{r_y}{\ell}\right)\frac{1}{2} \; \Big] \end{aligned} \tag{D.0.72}$$

<u>10^{th} row.</u>

$$\begin{aligned} I_{1LX(10,10)} &= -M\ell^2\varrho_x^2 \Big[\; T_{22}\left(126\eta_x^2+21\eta_x+1\right)\frac{1}{105} \\ &\qquad +\left(T_{23}+T_{32}\right)\frac{r_x}{\ell}\eta_x\left(12\eta_x+1\right)\frac{1}{2} \\ &\qquad +T_{33}\left(\frac{r_{Ix}}{\ell}\right)^2\left(360\eta_x^2+15\eta_x+1\right)\frac{2}{15} \; \Big] \end{aligned} \tag{D.0.73}$$

$$\begin{aligned} I_{1LX(10,11)} &= M\ell^2\varrho_x\varrho_y \Big[\; T_{21}\left(252\eta_x\eta_y+21\left(\eta_x+\eta_y\right)+2\right)\frac{1}{210} \\ &\qquad +T_{23}\frac{r_y}{\ell}\left(60\eta_x\eta_y+6\eta_y-\eta_x\right)\frac{1}{10} \\ &\qquad +T_{31}\frac{r_x}{\ell}\left(60\eta_x\eta_y+6\eta_x-\eta_y\right)\frac{1}{10} \; \Big] \end{aligned} \tag{D.0.74}$$

$$\begin{aligned} I_{1LX(10,12)} &= -M\ell\varrho_x\Big[-T_{21}\Big[\; e_{s2}\varrho_y\left(1260\eta_x\eta_y+105\eta_x+126\eta_y+11\right)\frac{1}{210} \\ &\qquad -\left(e_{s2}-r_x\right)\left(10\eta_x+1\right)\frac{1}{20} \; \Big] \\ &\qquad +T_{22}\Big[\; e_{s1}\varrho_x\left(1260\eta_x^2+231\eta_x+11\right)\frac{1}{210} \\ &\qquad -\left(e_{s1}-r_y\right)\left(10\eta_x+1\right)\frac{1}{20} \; \Big] \end{aligned}$$

$$
\begin{aligned}
&+T_{23}\left(e_{s2}\varrho_y\frac{r_y}{\ell}\left(12\eta_x+1\right)-e_{s1}\frac{r_x}{\ell}\right)\frac{1}{10}\\
&-T_{31}\left[\ e_{s2}\varrho_y\frac{r_x}{\ell}\left(480\eta_x\eta_y+42\eta_x+10\eta_y+1\right)\frac{1}{10}\right.\\
&\qquad\left.+\left(\ell\left(\frac{r_{Ix}}{\ell}\right)^2-e_{s2}\frac{r_x}{\ell}\right)\left(48\eta_x+1\right)\frac{1}{12}\ \right]\\
&+T_{32}e_{s1}\frac{r_x}{\ell}\left[\ \varrho_x\left(480\eta_x^2+52\eta_x+1\right)\frac{1}{10}-\left(48\eta_x+1\right)\frac{1}{12}\ \right]\\
&-T_{33}e_{s1}\varrho_x\left(\frac{r_{Ix}}{\ell}\right)^2\left(60\eta_x-1\right)\frac{1}{10}\ \Bigg]
\end{aligned}
\tag{D.0.75}
$$

11^{th} row.

$$
\begin{aligned}
I_{1LX(11,11)} \;=\; -M\ell^2\varrho_y^2\Bigg[\ & T_{11}\left(126\eta_y^2+21\eta_y+1\right)\frac{1}{105}\\
&+\left(T_{13}+T_{31}\right)\frac{r_y}{\ell}\eta_y\left(12\eta_y+1\right)\frac{1}{2}\\
&+T_{33}\left(\frac{r_{Iy}}{\ell}\right)^2\left(360\eta_y^2+15\eta_y+1\right)\frac{2}{15}\ \Bigg]
\end{aligned}
\tag{D.0.76}
$$

$$
\begin{aligned}
I_{1LX(11,12)} \;=\; M\ell\varrho_y\Bigg[& -T_{11}\left[\ e_{s2}\varrho_y\left(1260\eta_y^2+231\eta_y+11\right)\frac{1}{210}\right.\\
&\qquad\left.-\left(e_{s2}-r_x\right)\left(10\eta_y+1\right)\frac{1}{20}\ \right]\\
&+T_{12}\left[\ e_{s1}\varrho_x\left(1260\eta_x\eta_y+126\eta_x+105\eta_y+11\right)\frac{1}{210}\right.\\
&\qquad\left.-\left(e_{s1}-r_y\right)\left(10\eta_y+1\right)\frac{1}{20}\ \right]\\
&-T_{13}\left(e_{s1}\varrho_x\frac{r_x}{\ell}\left(12\eta_y+1\right)-e_{s2}\varrho_y\frac{r_y}{\ell}\right)\frac{1}{10}\\
&-T_{31}e_{s2}\frac{r_y}{\ell}\left[\ \varrho_y\left(480\eta_y^2+52\eta_y+1\right)\frac{1}{10}-\left(48\eta_y+1\right)\frac{1}{12}\ \right]\\
&+T_{32}\left[\ e_{s1}\varrho_x\frac{r_y}{\ell}\left(480\eta_x\eta_y+10\eta_x+42\eta_y+1\right)\frac{1}{10}\right.\\
&\qquad\left.+\left(\ell\left(\frac{r_{Iy}}{\ell}\right)^2-e_{s1}\frac{r_y}{\ell}\right)\left(48\eta_y+1\right)\frac{1}{12}\ \right]\\
&+T_{33}e_{s2}\varrho_y\left(\frac{r_{Iy}}{\ell}\right)^2\left(60\eta_y-1\right)\frac{1}{10}\ \Bigg]
\end{aligned}
\tag{D.0.77}
$$

12^{th} row.

$$
I_{1LX(12,12)} \;=\; -M\Bigg[\ T_{11}\left[\ e_{s2}^2\varrho_y^2\left(1680\eta_y^2+294\eta_y+13\right)\frac{1}{35}\right.
$$

$$
\begin{aligned}
&\quad - (e_{s2} - r_x)\, e_{s2} \varrho_y \,(80\eta_y + 7)\, \frac{1}{10} \\
&\quad + \left(e_{s2}^2 - 2 e_{s2} r_x + \ell^2 \left(\frac{r_{Ix}}{\ell} \right)^2 \right) \frac{1}{3} \; \Big] \\
&- (T_{12} + T_{21}) \Big[\; e_{s1} e_{s2} \varrho_y \varrho_y \,(1680 \eta_x \eta_y + 147\,(\eta_x + \eta_y) + 13)\, \frac{1}{35} \\
&\qquad\qquad - (e_{s2} - r_x)\, e_{s1} \varrho_x \,(80\eta_x + 7)\, \frac{1}{20} \\
&\qquad\qquad - (e_{s1} - r_y)\, e_{s2} \varrho_y \,(80\eta_y + 7)\, \frac{1}{20} \\
&\qquad\qquad + (e_{s1} e_{s2} - e_{s1} r_x - e_{s2} r_y)\, \frac{1}{3} \; \Big] \\
&+ (T_{13} + T_{31})\, \ell e_{s1} \varrho_x \left(\frac{r_{Ix}}{\ell} \right)^2 \frac{1}{2} \\
&+ T_{22} \Big[\; e_{s1}^2 \varrho_x^2 \left(1680 \eta_x^2 + 294 \eta_x + 13 \right) \frac{1}{35} \\
&\qquad - (e_{s1} - r_y)\, e_{s1} \varrho_x \,(80\eta_x + 7)\, \frac{1}{10} \\
&\qquad + \left(e_{s1}^2 - 2 e_{s1} r_y + \ell^2 \left(\frac{r_{Iy}}{\ell} \right)^2 \right) \frac{1}{3} \; \Big] \\
&+ (T_{23} + T_{32})\, \ell e_{s2} \varrho_y \left(\frac{r_{Iy}}{\ell} \right)^2 \frac{1}{2} \\
&+ T_{33} \left(e_{s1}^2 \varrho_x^2 \left(\frac{r_{Ix}}{\ell} \right)^2 + e_{s2}^2 \varrho_y^2 \left(\frac{r_{Iy}}{\ell} \right)^2 \right) \frac{6}{5} \; \Big]
\end{aligned}
\tag{D.0.78}
$$

E Acceleration coefficient matrices for a specific choice of degrees of freedom.

As described in [Part 1, Sec. 3.4], the expressions for acceleration on the substructures are calculated by use of Reduce [H2], where also the chosen cancelling of product terms is introduced. A subsequent filtering of the Reduce output results in the matrices listed in this section. The degrees of freedom, retained in the model are described in [Part 1, Sec. 6].

The angular rotor velocity (ω) is assumed constant and the yaw degree of freedom (θ^N_{3N}) is set to zero. Further, the tilt angle has been omitted.

In Reduce a weight is assigned to each variable and a weight level is assigned to the calculation. The weight of a product is calculated as the sum of the weights of the factors. When the product weight exceeds the weight level, the product term is cancelled.

The calculation weight level is chosen to 6, and the following weights are assigned to the remaining degrees of freedom

Tower top displacement:
$$u^T_{T\ell} = 2, \quad \dot{u}^T_{T\ell} = 2, \quad \ddot{u}^T_{T\ell} = 2$$
$$\theta^T_{T\ell} = 4, \quad \dot{\theta}^T_{T\ell} = 2, \quad \ddot{\theta}^T_{T\ell} = 2$$

Shaft end displacement:
$$u^A_{Am} = 2, \quad \dot{u}^A_{Am} = 2, \quad \ddot{u}^A_{Am} = 2$$
$$\theta^A_{Am} = 4, \quad \dot{\theta}^A_{Am} = 2, \quad \ddot{\theta}^A_{Am} = 2$$

Teeter:
$$\theta^H_{1H} = 2, \quad \dot{\theta}^H_{1H} = 2, \quad \ddot{\theta}^H_{1H} = 2$$

where the weights for the elastic deformations at tower top and shaft end cover all three coordinate directions.

These cancelling directions mean that for example products including one of the terms $\theta^T_{T\ell}\theta^T_{T\ell}$ or $\theta^A_{Am}\theta^T_{T\ell}$ are cancelled. No attempt has been made yet to estimate the influence of this linearization on the accuracy of the calculations. The choice is based primarily on the intention to restrict the linearization as much as possible and at the same time obtaining reasonable inertia expressions that do not grow too much. A thorough investigation of directions for linearization would be a natural part of further development of the model.

Where partly symmetry and skew–symmetry is a dominating characteristics of a matrix, a decomposition in two matrix addends, having either of these properties and a third addend containing the remaining terms, is carried through, and the resulting matrix is then the sum of these addends.

E.1 Coefficient matrices for the shaft substructure.

The matrices consist partly of the coefficients in [Part 1, Eq. 6.2.1], which is the general expression, partly of the coefficient matrices in the expansion for the acceleration vector, $\left\{a^A_{Ac}\right\}$, [Part 1, Eq. 6.2.2], and partly of the matrices in the expression for the decomposition of the matrix product $[A_A]\left\{{}_ir^A_j\right\}$, [Part 1, Eq. 6.2.3].

The actual equations for the shaft substructure are repeated below in order to support the continuity in reading the expressions

$$\left\{\ddot{r}^A_{A0}\right\} = [A_A]\left\{s^A_A\right\} + [B_A]\left\{\dot{u}^A_A\right\} + [C_A]\left\{\ddot{u}^A_A\right\} + \left\{a^A_{Ac}\right\} \tag{6.2.1}$$

$$\left\{a^A_{Ac}\right\} = [D_A]\left\{\ddot{u}^T_{T\ell}\right\} \tag{6.2.2}$$

$$[A_A]\left\{{}_ir^A_j\right\} = [{}_iAT2_j]\left\{\ddot{\theta}^T_{T\ell}\right\} + [{}_iAT1_j]\left\{\dot{\theta}^T_{T\ell}\right\} + \left\{{}_iAC0^A_j\right\} \tag{6.2.3}$$

The matrices are listed in the following, in general without further comments. The most space demanding matrices are listed in component form for typographical reasons.

The left subscript i is retained on the resulting terms, which are element dependent, in order to stress this dependency. It results from the spatial vectors

${}_ir_{kj}$ where i refers to element number
$k = 1, 2, 3$ is vector component number and
j refers to the type of spatial vector:
$j = 1$ position vector to node 1 of element i
$j = 12$ vector from node 1 to node 2 of element i
In order to simplify the writing, the subscript i is cancelled on the vector components in the following.

The $[A_A]$–matrix.

The matrix is found as the sum

$$[A_A] = [A_A]_{sym} + [A_A]_{skewsym} + [A_A]_{nosym} \tag{E.1.1}$$

where the addends are

$[A_A]_{sym} =$

$$\left[\begin{array}{c|c|c}
\begin{array}{l}-(\omega)^2 - 2\omega\dot{\theta}^T_{2T\ell} \\ -\sin^2(\theta)\left(\dot{\theta}^T_{1T\ell}\right)^2 - \left(\dot{\theta}^T_{2T\ell}\right)^2 \\ -\cos^2(\theta)\left(\dot{\theta}^T_{3T\ell}\right)^2 \\ -2\cos(\theta)\sin(\theta)\dot{\theta}^T_{1T\ell}\dot{\theta}^T_{3T\ell}\end{array} & +\cos(\theta)\dot{\theta}^T_{1T\ell}\dot{\theta}^T_{2T\ell} - \sin(\theta)\dot{\theta}^T_{2T\ell}\dot{\theta}^T_{3T\ell} & \begin{array}{l}\cos(\theta)\sin(\theta)\left(\dot{\theta}^T_{1T\ell}\right)^2 \\ -\cos(\theta)\sin(\theta)\left(\dot{\theta}^T_{3T\ell}\right)^2 \\ +\left(\cos^2(\theta) - \sin^2(\theta)\right)\dot{\theta}^T_{1T\ell}\dot{\theta}^T_{3T\ell}\end{array} \\ \hline
\cos(\theta)\dot{\theta}^T_{1T\ell}\dot{\theta}^T_{2T\ell} - \sin(\theta)\dot{\theta}^T_{2T\ell}\dot{\theta}^T_{3T\ell} & -\left(\dot{\theta}^T_{1T\ell}\right)^2 - \left(\dot{\theta}^T_{3T\ell}\right)^2 & \left(\sin(\theta)\dot{\theta}^T_{1T\ell} + \cos(\theta)\dot{\theta}^T_{3T\ell}\right)\dot{\theta}^T_{2T\ell} \\ \hline
\begin{array}{l}\cos(\theta)\sin(\theta)\left(\dot{\theta}^T_{1T\ell}\right)^2 \\ -\cos(\theta)\sin(\theta)\left(\dot{\theta}^T_{3T\ell}\right)^2 \\ +\left(\cos^2(\theta) - \sin^2(\theta)\right)\dot{\theta}^T_{1T\ell}\dot{\theta}^T_{3T\ell}\end{array} & \left(\sin(\theta)\dot{\theta}^T_{1T\ell} + \cos(\theta)\dot{\theta}^T_{3T\ell}\right)\dot{\theta}^T_{2T\ell} & \begin{array}{l}-(\omega)^2 - 2\omega\dot{\theta}^T_{2T\ell} \\ -\cos^2(\theta)\left(\dot{\theta}^T_{1T\ell}\right)^2 - \left(\dot{\theta}^T_{2T\ell}\right)^2 \\ -\sin^2(\theta)\left(\dot{\theta}^T_{3T\ell}\right)^2 \\ +2\cos(\theta)\sin(\theta)\dot{\theta}^T_{1T\ell}\dot{\theta}^T_{3T\ell}\end{array}
\end{array}\right] \tag{E.1.2}$$

$[A_A]_{skewsym} =$

$$\left[\begin{array}{c|c|c} 0 & \begin{array}{l} -\left(\sin(\theta)+\cos(\theta)\,\theta^T_{2T\ell}\right)\ddot{\theta}^T_{1T\ell} \\ +\cos(\theta)\left(\theta^T_{1T\ell}-\sin(\theta)\,\theta^T_{3T\ell}\right)\ddot{\theta}^T_{2T\ell} \\ -\left(\cos(\theta)-\sin(\theta)\,\theta^T_{2T\ell}\right)\ddot{\theta}^T_{3T\ell} \end{array} & -\theta^T_{3T\ell}\ddot{\theta}^T_{1T\ell}+\ddot{\theta}^T_{2T\ell}+\theta^T_{1T\ell}\ddot{\theta}^T_{3T\ell} \\ \hline \begin{array}{l} \left(\sin(\theta)+\cos(\theta)\,\theta^T_{2T\ell}\right)\ddot{\theta}^T_{1T\ell} \\ -\cos(\theta)\left(\theta^T_{1T\ell}-\sin(\theta)\,\theta^T_{3T\ell}\right)\ddot{\theta}^T_{2T\ell} \\ +\left(\cos(\theta)-\sin(\theta)\,\theta^T_{2T\ell}\right)\ddot{\theta}^T_{3T\ell} \end{array} & 0 & \begin{array}{l} -\left(\cos(\theta)-\sin(\theta)\,\theta^T_{2T\ell}\right)\ddot{\theta}^T_{1T\ell} \\ -\left(\sin(\theta)\,\theta^T_{1T\ell}+\cos(\theta)\,\theta^T_{3T\ell}\right)\ddot{\theta}^T_{2T\ell} \\ +\left(\sin(\theta)+\cos(\theta)\,\theta^T_{2T\ell}\right)\ddot{\theta}^T_{3T\ell} \end{array} \\ \hline \theta^T_{3T\ell}\ddot{\theta}^T_{1T\ell}-\ddot{\theta}^T_{2T\ell}-\theta^T_{1T\ell}\ddot{\theta}^T_{3T\ell} & \begin{array}{l} \left(\cos(\theta)-\sin(\theta)\,\theta^T_{2T\ell}\right)\ddot{\theta}^T_{1T\ell} \\ +\left(\sin(\theta)\,\theta^T_{1T\ell}+\cos(\theta)\,\theta^T_{3T\ell}\right)\ddot{\theta}^T_{2T\ell} \\ -\left(\sin(\theta)+\cos(\theta)\,\theta^T_{2T\ell}\right)\ddot{\theta}^T_{3T\ell} \end{array} & 0 \end{array}\right] \tag{E.1.3}$$

$[A_A]_{nosym} =$

$$\left[\begin{array}{c|c|c} 0 & 0 & 0 \\ \hline 2\omega\left(\cos(\theta)\,\dot{\theta}^T_{1T\ell}-\sin(\theta)\,\dot{\theta}^T_{3T\ell}\right) & 0 & 2\omega\left(\sin(\theta)\,\dot{\theta}^T_{1T\ell}+\cos(\theta)\,\dot{\theta}^T_{3T\ell}\right) \\ \hline 0 & 0 & 0 \end{array}\right] \tag{E.1.4}$$

The $[B_A]$–matrix.

$[B_A] =$

$$2\begin{bmatrix} 0 & \begin{matrix} -\left(\sin(\theta)+\cos(\theta)\,\theta^T_{2T\ell}\right)\dot{\theta}^T_{1T\ell} \\ +\left(\cos(\theta)\,\theta^T_{1T\ell}-\sin(\theta)\,\theta^T_{3T\ell}\right)\dot{\theta}^T_{2T\ell} \\ -\left(\cos(\theta)-\sin(\theta)\,\theta^T_{2T\ell}\right)\dot{\theta}^T_{3T\ell} \end{matrix} & \dot{\theta}-\theta^T_{3T\ell}\dot{\theta}^T_{1T\ell}+\dot{\theta}^T_{2T\ell}+\theta^T_{1T\ell}\dot{\theta}^T_{3T\ell} \\ \begin{matrix} \left(\sin(\theta)+\cos(\theta)\,\theta^T_{2T\ell}\right)\dot{\theta}^T_{1T\ell} \\ -\left(\cos(\theta)\,\theta^T_{1T\ell}-\sin(\theta)\,\theta^T_{3T\ell}\right)\dot{\theta}^T_{2T\ell} \\ +\left(\cos(\theta)-\sin(\theta)\,\theta^T_{2T\ell}\right)\dot{\theta}^T_{3T\ell} \end{matrix} & 0 & \begin{matrix} -\left(\cos(\theta)-\sin(\theta)\,\theta^T_{2T\ell}\right)\dot{\theta}^T_{1T\ell} \\ -\left(\sin(\theta)\,\theta^T_{1T\ell}+\cos(\theta)\,\theta^T_{3T\ell}\right)\dot{\theta}^T_{2T\ell} \\ +\left(\sin(\theta)+\cos(\theta)\,\theta^T_{2T\ell}\right)\dot{\theta}^T_{3T\ell} \end{matrix} \\ -\dot{\theta}+\theta^T_{3T\ell}\dot{\theta}^T_{1T\ell}-\dot{\theta}^T_{2T\ell}-\theta^T_{1T\ell}\dot{\theta}^T_{3T\ell} & \begin{matrix} \left(\cos(\theta)-\sin(\theta)\,\theta^T_{2T\ell}\right)\dot{\theta}^T_{1T\ell} \\ +\left(\sin(\theta)\,\theta^T_{1T\ell}+\cos(\theta)\,\theta^T_{3T\ell}\right)\dot{\theta}^T_{2T\ell} \\ -\left(\sin(\theta)+\cos(\theta)\,\theta^T_{2T\ell}\right)\dot{\theta}^T_{3T\ell} \end{matrix} & 0 \end{bmatrix} \tag{E.1.5}$$

The matrix is skew–symmetric.

The $[D_A]$–matrix.

$[D_A] =$

$$\begin{bmatrix} \cos(\theta)-\sin(\theta)\,\theta^T_{2T\ell} & \cos(\theta)\,\theta^T_{3T\ell}+\sin(\theta)\,\theta^T_{1T\ell} & -\cos(\theta)\,\theta^T_{2T\ell}-\sin(\theta) \\ -\theta^T_{3T\ell} & 1 & \theta^T_{1T\ell} \\ \cos(\theta)\,\theta^T_{2T\ell}+\sin(\theta) & -\cos(\theta)\,\theta^T_{1T\ell}+\sin(\theta)\,\theta^T_{3T\ell} & \cos(\theta)-\sin(\theta)\,\theta^T_{2T\ell} \end{bmatrix} \tag{E.1.6}$$

The $[{}_iAT2_j]$–matrix.

$[{}_iAT2_j] =$

$$\left[\begin{array}{c|c|c}
\begin{array}{l} -r_{2j}\sin(\theta) \\ -r_{2j}\cos(\theta)\,\theta^T_{2T\ell} \\ -r_{3j}\theta^T_{3T\ell} \end{array} & \begin{array}{l} +r_{3j} \\ +r_{2j}\cos(\theta)\,\theta^T_{1T\ell} \\ -r_{2j}\sin(\theta)\,\theta^T_{3T\ell} \end{array} & \begin{array}{l} -r_{2j}\cos(\theta) \\ +r_{3j}\theta^T_{1T\ell} \\ +r_{2j}\sin(\theta)\,\theta^T_{2T\ell} \end{array} \\ \hline
\begin{array}{l} +r_{1j}\sin(\theta) - r_{3j}\cos(\theta) \\ +\Big(r_{1j}\cos(\theta) + r_{3j}\sin(\theta)\Big)\theta^T_{2T\ell} \end{array} & \begin{array}{l} -\Big(r_{1j}\cos(\theta) + r_{3j}\sin(\theta)\Big)\theta^T_{1T\ell} \\ +\Big(r_{1j}\sin(\theta) - r_{3j}\cos(\theta)\Big)\theta^T_{3T\ell} \end{array} & \begin{array}{l} +r_{1j}\cos(\theta) + r_{3j}\sin(\theta) \\ -\Big(r_{1j}\sin(\theta) - r_{3j}\cos(\theta)\Big)\theta^T_{2T\ell} \end{array} \\ \hline
\begin{array}{l} +r_{2j}\cos(\theta) \\ -r_{2j}\sin(\theta)\,\theta^T_{2T\ell} \\ +r_{1j}\theta^T_{3T\ell} \end{array} & \begin{array}{l} -r_{1j} \\ +r_{2j}\sin(\theta)\,\theta^T_{1T\ell} \\ +r_{2j}\cos(\theta)\,\theta^T_{3T\ell} \end{array} & \begin{array}{l} -r_{2j}\sin(\theta) \\ -r_{1j}\theta^T_{1T\ell} \\ -r_{2j}\cos(\theta)\,\theta^T_{2T\ell} \end{array}
\end{array}\right] \tag{E.1.7}$$

The $[{}_iAT1_j]$–matrix.

$[{}_iAT1_j] =$

$$\left[\begin{array}{c|c|c}
\begin{array}{l} -\Big(r_{1j}\sin^2(\theta) - r_{3j}\cos(\theta)\sin(\theta)\Big)\dot{\theta}^T_{1T\ell} \\ +r_{2j}\cos(\theta)\,\dot{\theta}^T_{2T\ell} \\ -\Big[2r_{1j}\cos(\theta)\sin(\theta) \\ \quad - r_{3j}\Big(\cos^2(\theta) - \sin^2(\theta)\Big)\Big]\dot{\theta}^T_{3T\ell} \end{array} & \begin{array}{l} -2\omega r_{1j} \\ -r_{1j}\dot{\theta}^T_{2T\ell} \\ -r_{2j}\sin(\theta)\,\dot{\theta}^T_{3T\ell} \end{array} & \begin{array}{l} -\Big(r_{1j}\cos^2(\theta) \\ \quad +r_{3j}\cos(\theta)\sin(\theta)\Big)\dot{\theta}^T_{3T\ell} \end{array} \\ \hline
\begin{array}{l} 2\omega\Big(r_{1j}\cos(\theta) + r_{3j}\sin(\theta)\Big) \\ -r_{2j}\dot{\theta}^T_{1T\ell} + \Big(r_{1j}\cos(\theta) + r_{3j}\sin(\theta)\Big)\dot{\theta}^T_{2T\ell} \end{array} & -\Big(r_{1j}\sin(\theta) - r_{3j}\cos(\theta)\Big)\dot{\theta}^T_{3T\ell} & \begin{array}{l} -2\omega\Big(r_{1j}\sin(\theta) - r_{3j}\cos(\theta)\Big) \\ -r_{2j}\theta^T_{3T\ell} \end{array} \\ \hline
\begin{array}{l} \Big(r_{1j}\cos(\theta)\sin(\theta) - r_{3j}\cos^2(\theta)\Big)\dot{\theta}^T_{1T\ell} \\ +r_{2j}\sin(\theta)\,\dot{\theta}^T_{2T\ell} \\ +\Big[r_{1j}\Big(\cos^2(\theta) - \sin^2(\theta)\Big) \\ \quad + 2r_{3j}\cos(\theta)\sin(\theta)\Big]\dot{\theta}^T_{3T\ell} \end{array} & \begin{array}{l} -2\omega r_{3j} \\ -r_{3j}\dot{\theta}^T_{2T\ell} \\ +r_{2j}\cos(\theta)\,\dot{\theta}^T_{3T\ell} \end{array} & \begin{array}{l} -\Big(r_{1j}\cos(\theta)\sin(\theta) \\ \quad +r_{3j}\sin^2(\theta)\Big)\dot{\theta}^T_{3T\ell} \end{array}
\end{array}\right] \tag{E.1.8}$$

The $\left\{{}_iAC0^A_j\right\}$–vector.

$$\left\{{}_iAC0^A_j\right\} = (\omega)^2 \left\{ \begin{array}{c} -r_{1j} \\ 0 \\ -r_{3j} \end{array} \right\} \tag{E.1.9}$$

E.2 Coefficient matrices for the blade substructure.

For the blade substructure the relevant matrix expressions are found from [Part 1, Sec. 6.3]. These equations are repeated below

$$\left\{\ddot{r}^B_{B0}\right\} = [A_B]\left\{s^B_B\right\} + [B_B]\left\{\dot{u}^B_B\right\} + [C_B]\left\{\ddot{u}^B_B\right\} + \left\{a^B_{Bc}\right\} \tag{6.3.1}$$

$$\begin{aligned}\left\{a^B_{Bc}\right\} &= [D_B]\left\{\ddot{u}^T_{T\ell}\right\} + [E_B]\left\{\dot{\theta}^T_{T\ell}\right\} + [F_B]\left\{\ddot{\theta}^T_{T\ell}\right\} \\ &\quad + [G_B]\left\{u^A_{Am}\right\} + [H_B]\left\{\dot{u}^A_{Am}\right\} + [R_B]\left\{\ddot{u}^A_{Am}\right\}\end{aligned} \tag{6.3.2}$$

$$\begin{aligned}[A_B]\left\{{}_ir^B_j\right\} &= [{}_iBT2_j]\left\{\ddot{\theta}^T_{T\ell}\right\} + [{}_iBT1_j]\left\{\dot{\theta}^T_{T\ell}\right\} \\ &\quad + [{}_iBS2_j]\left\{\ddot{\theta}^A_{Am}\right\} + [{}_iBS1_j]\left\{\dot{\theta}^A_{Am}\right\} + [{}_iBS0_j]\left\{\theta^A_{Am}\right\} \\ &\quad + \left\{{}_iBH2^B_j\right\}\ddot{\theta}^H_1 + \left\{{}_iBH1^B_j\right\}\dot{\theta}^H_1 + \left\{{}_iBC0^B_j\right\}\end{aligned} \tag{6.3.3}$$

The $[A_B]$–matrix.

The resulting matrix is found as

$$\begin{aligned}
A_B(1,1) &= A_B(1,1)_{sym} \\
A_B(1,2) &= A_B(1,2)_{sym} + A_B(1,2)_{skewsym} + A_B(1,2)_{nosym} \\
A_B(1,3) &= A_B(1,3)_{sym} + A_B(1,3)_{skewsym} + A_B(1,3)_{nosym} \\
A_B(2,1) &= A_B(1,2)_{sym} - A_B(1,2)_{skewsym} + A_B(2,1)_{nosym} \\
A_B(2,2) &= A_B(22,33)_{sym} + A_B(22,33)_{skewsym} + A_B(2,2)_{nosym} \\
A_B(2,3) &= A_B(2,3)_{sym} + A_B(2,3)_{skewsym} + A_B(2,3)_{nosym} \\
A_B(3,1) &= A_B(1,3)_{sym} - A_B(1,3)_{skewsym} + A_B(3,1)_{nosym} \\
A_B(3,2) &= A_B(2,3)_{sym} - A_B(2,3)_{skewsym} + A_B(3,2)_{nosym} \\
A_B(3,3) &= A_B(22,33)_{sym} - A_B(22,33)_{skewsym} + A_B(3,3)_{nosym}
\end{aligned}$$

where the single terms are given below

$$
\begin{aligned}
A_B\,(1,1)_{sym} = \\
&-(\omega)^2 \\
&+2\omega\Big[-\dot{\theta}^T_{2T\ell} - \dot{\theta}^A_{2Am} + \theta^T_{3T\ell}\dot{\theta}^T_{1T\ell} - \theta^T_{1T\ell}\dot{\theta}^T_{3T\ell} \\
&\qquad + \cos(\theta)\,\theta^A_{3Am}\dot{\theta}^T_{1T\ell} - \sin(\theta)\,\theta^A_{3Am}\dot{\theta}^T_{3T\ell} \\
&\qquad + \theta^A_{3Am}\dot{\theta}^A_{1Am}\Big] \\
&-\sin^2(\theta)\left(\dot{\theta}^T_{1T\ell}\right)^2 - \left(\dot{\theta}^T_{2T\ell}\right)^2 - \cos^2(\theta)\left(\dot{\theta}^T_{3T\ell}\right)^2 \\
&-\left(\dot{\theta}^A_{2Am}\right)^2 - \left(\dot{\theta}^A_{3Am}\right)^2 \\
&-2\cos(\theta)\sin(\theta)\,\dot{\theta}^T_{1T\ell}\dot{\theta}^T_{3T\ell} \\
&-2\sin(\theta)\,\dot{\theta}^A_{3Am}\dot{\theta}^T_{1T\ell} - 2\dot{\theta}^A_{2Am}\dot{\theta}^T_{2T\ell} - 2\cos(\theta)\,\dot{\theta}^A_{3Am}\dot{\theta}^T_{3T\ell}
\end{aligned}
\tag{E.2.10}
$$

$$
\begin{aligned}
A_B\,(1,2)_{sym} = \\
&(\omega)^2\cos\left(\theta^H_{1H}\right)\theta^A_{3Am} \\
&+2\omega\Big[\cos\left(\theta^H_{1H}\right)\theta^A_{3Am}\dot{\theta}^T_{2T\ell} + \cos\left(\theta^H_{1H}\right)\theta^A_{3Am}\dot{\theta}^A_{2Am}\Big] \\
&+\cos(\theta)\sin(\theta)\sin\left(\theta^H_{1H}\right)\left(\dot{\theta}^T_{1T\ell}\right)^2 - \cos(\theta)\sin(\theta)\sin\left(\theta^H_{1H}\right)\left(\dot{\theta}^T_{3T\ell}\right)^2 \\
&+\cos(\theta)\cos\left(\theta^H_{1H}\right)\dot{\theta}^T_{1T\ell}\dot{\theta}^T_{2T\ell} + \cos^2(\theta)\sin\left(\theta^H_{1H}\right)\dot{\theta}^T_{1T\ell}\dot{\theta}^T_{3T\ell} \\
&\quad -\sin^2(\theta)\sin\left(\theta^H_{1H}\right)\dot{\theta}^T_{1T\ell}\dot{\theta}^T_{3T\ell} - \sin(\theta)\cos\left(\theta^H_{1H}\right)\dot{\theta}^T_{2T\ell}\dot{\theta}^T_{3T\ell} \\
&+\cos\left(\theta^H_{1H}\right)\dot{\theta}^A_{1Am}\dot{\theta}^A_{2Am} + \sin\left(\theta^H_{1H}\right)\dot{\theta}^A_{1Am}\dot{\theta}^A_{3Am}
\end{aligned}
\tag{E.2.11}
$$

$$
\begin{aligned}
A_B\,(1,2)_{skewsym} = \\
&-\sin(\theta)\cos\left(\theta^H_{1H}\right)\ddot{\theta}^T_{1T\ell} + \sin\left(\theta^H_{1H}\right)\ddot{\theta}^T_{2T\ell} - \cos(\theta)\cos\left(\theta^H_{1H}\right)\ddot{\theta}^T_{3T\ell} \\
&+\sin\left(\theta^H_{1H}\right)\ddot{\theta}^A_{2Am} - \cos\left(\theta^H_{1H}\right)\ddot{\theta}^A_{3Am} \\
&-\cos(\theta)\cos\left(\theta^H_{1H}\right)\theta^T_{2T\ell}\ddot{\theta}^T_{1T\ell} - \sin\left(\theta^H_{1H}\right)\theta^T_{3T\ell}\ddot{\theta}^T_{1T\ell} + \cos(\theta)\cos\left(\theta^H_{1H}\right)\theta^T_{1T\ell}\ddot{\theta}^T_{2T\ell} \\
&\quad -\sin(\theta)\cos\left(\theta^H_{1H}\right)\theta^T_{3T\ell}\ddot{\theta}^T_{2T\ell} + \sin\left(\theta^H_{1H}\right)\theta^T_{1T\ell}\ddot{\theta}^T_{3T\ell} + \sin(\theta)\cos\left(\theta^H_{1H}\right)\theta^T_{2T\ell}\ddot{\theta}^T_{3T\ell} \\
&+\sin(\theta)\sin\left(\theta^H_{1H}\right)\theta^A_{1Am}\ddot{\theta}^T_{1T\ell} - \cos(\theta)\cos\left(\theta^H_{1H}\right)\theta^A_{2Am}\ddot{\theta}^T_{1T\ell} \\
&\quad -\cos(\theta)\sin\left(\theta^H_{1H}\right)\theta^A_{3Am}\ddot{\theta}^T_{1T\ell} + \cos\left(\theta^H_{1H}\right)\theta^A_{1Am}\ddot{\theta}^T_{2T\ell} \\
&\quad +\cos(\theta)\sin\left(\theta^H_{1H}\right)\theta^A_{1Am}\ddot{\theta}^T_{3T\ell} + \sin(\theta)\cos\left(\theta^H_{1H}\right)\theta^A_{2Am}\ddot{\theta}^T_{3T\ell} \\
&\quad +\sin(\theta)\sin\left(\theta^H_{1H}\right)\theta^A_{3Am}\ddot{\theta}^T_{3T\ell} \\
&-\cos\left(\theta^H_{1H}\right)\theta^A_{2Am}\ddot{\theta}^A_{1Am} - \sin\left(\theta^H_{1H}\right)\theta^A_{3Am}\ddot{\theta}^A_{1Am} \\
&\quad +\cos\left(\theta^H_{1H}\right)\theta^A_{1Am}\ddot{\theta}^A_{2Am} + \sin\left(\theta^H_{1H}\right)\theta^A_{1Am}\ddot{\theta}^A_{3Am}
\end{aligned}
\tag{E.2.12}
$$

$$
\begin{aligned}
&A_B\,(1,2)_{nosym} = \\
&\quad 2\omega\Big[\cos\left(\theta^H_{1H}\right)\dot{\theta}^A_{1Am} + \cos\left(\theta^H_{1H}\right)\dot{\theta}^H_{1H} \\
&\qquad + \sin\left(\theta\right)\sin\left(\theta^H_{1H}\right)\theta^A_{3Am}\dot{\theta}^T_{1T\ell} + \cos\left(\theta\right)\sin\left(\theta^H_{1H}\right)\theta^A_{3Am}\dot{\theta}^T_{3T\ell} \\
&\qquad - \sin\left(\theta^H_{1H}\right)\theta^A_{1Am}\dot{\theta}^A_{1Am} - \cos\left(\theta^H_{1H}\right)\theta^A_{2Am}\dot{\theta}^A_{3Am} \\
&\qquad - \sin\left(\theta^H_{1H}\right)\theta^A_{1Am}\dot{\theta}^H_{1H}\Big] \\
&\quad + 2\cos\left(\theta^H_{1H}\right)\dot{\theta}^H_{1H}\dot{\theta}^A_{2Am} + 2\sin\left(\theta^H_{1H}\right)\dot{\theta}^H_{1H}\dot{\theta}^A_{3Am} \\
&\quad + 2\sin\left(\theta\right)\sin\left(\theta^H_{1H}\right)\dot{\theta}^A_{1Am}\dot{\theta}^T_{1T\ell} + 2\cos\left(\theta^H_{1H}\right)\dot{\theta}^A_{1Am}\dot{\theta}^T_{2T\ell} + 2\cos\left(\theta\right)\sin\left(\theta^H_{1H}\right)\dot{\theta}^A_{1Am}\dot{\theta}^T_{3T\ell} \\
&\quad + 2\sin\left(\theta\right)\sin\left(\theta^H_{1H}\right)\dot{\theta}^H_{1H}\dot{\theta}^T_{1T\ell} + 2\cos\left(\theta^H_{1H}\right)\dot{\theta}^H_{1H}\dot{\theta}^T_{2T\ell} + 2\cos\left(\theta\right)\sin\left(\theta^H_{1H}\right)\dot{\theta}^H_{1H}\dot{\theta}^T_{3T\ell}
\end{aligned}
\tag{E.2.13}
$$

$$
\begin{aligned}
&A_B\,(1,3)_{sym} = \\
&\quad -\left(\omega\right)^2\sin\left(\theta^H_{1H}\right)\theta^A_{3Am} \\
&\quad -2\omega\sin\left(\theta^H_{1H}\right)\theta^A_{3Am}\dot{\theta}^T_{2T\ell} \\
&\quad + \cos\left(\theta\right)\sin\left(\theta\right)\cos\left(\theta^H_{1H}\right)\left(\dot{\theta}^T_{1T\ell}\right)^2 - \cos\left(\theta\right)\sin\left(\theta\right)\cos\left(\theta^H_{1H}\right)\left(\dot{\theta}^T_{3T\ell}\right)^2 \\
&\quad - \cos\left(\theta\right)\sin\left(\theta^H_{1H}\right)\dot{\theta}^T_{1T\ell}\dot{\theta}^T_{2T\ell} + \cos^2\left(\theta\right)\cos\left(\theta^H_{1H}\right)\dot{\theta}^T_{1T\ell}\dot{\theta}^T_{3T\ell} \\
&\qquad - \sin^2\left(\theta\right)\cos\left(\theta^H_{1H}\right)\dot{\theta}^T_{1T\ell}\dot{\theta}^T_{3T\ell} + \sin\left(\theta\right)\sin\left(\theta^H_{1H}\right)\dot{\theta}^T_{2T\ell}\dot{\theta}^T_{3T\ell} \\
&\quad - \sin\left(\theta^H_{1H}\right)\dot{\theta}^A_{1Am}\dot{\theta}^A_{2Am} + \cos\left(\theta^H_{1H}\right)\dot{\theta}^A_{1Am}\dot{\theta}^A_{3Am}
\end{aligned}
\tag{E.2.14}
$$

$$
\begin{aligned}
&A_B\,(1,3)_{skewsym} = \\
&\quad \sin\left(\theta\right)\sin\left(\theta^H_{1H}\right)\ddot{\theta}^T_{1T\ell} + \cos\left(\theta^H_{1H}\right)\ddot{\theta}^T_{2T\ell} + \cos\left(\theta\right)\sin\left(\theta^H_{1H}\right)\ddot{\theta}^T_{3T\ell} \\
&\quad + \cos\left(\theta^H_{1H}\right)\ddot{\theta}^A_{2Am} + \sin\left(\theta^H_{1H}\right)\ddot{\theta}^A_{3Am} \\
&\quad + \cos\left(\theta\right)\sin\left(\theta^H_{1H}\right)\theta^T_{2T\ell}\ddot{\theta}^T_{1T\ell} - \cos\left(\theta^H_{1H}\right)\theta^T_{3T\ell}\ddot{\theta}^T_{1T\ell} - \cos\left(\theta\right)\sin\left(\theta^H_{1H}\right)\theta^T_{1T\ell}\ddot{\theta}^T_{2T\ell} \\
&\qquad + \sin\left(\theta\right)\sin\left(\theta^H_{1H}\right)\theta^T_{3T\ell}\ddot{\theta}^T_{2T\ell} + \cos\left(\theta^H_{1H}\right)\theta^T_{1T\ell}\ddot{\theta}^T_{3T\ell} - \sin\left(\theta\right)\sin\left(\theta^H_{1H}\right)\theta^T_{2T\ell}\ddot{\theta}^T_{3T\ell} \\
&\quad + \sin\left(\theta\right)\cos\left(\theta^H_{1H}\right)\theta^A_{1Am}\ddot{\theta}^T_{1T\ell} + \cos\left(\theta\right)\sin\left(\theta^H_{1H}\right)\theta^A_{2Am}\ddot{\theta}^T_{1T\ell} \\
&\qquad - \cos\left(\theta\right)\cos\left(\theta^H_{1H}\right)\theta^A_{3Am}\ddot{\theta}^T_{1T\ell} - \sin\left(\theta^H_{1H}\right)\theta^A_{1Am}\ddot{\theta}^T_{2T\ell} \\
&\qquad + \cos\left(\theta\right)\cos\left(\theta^H_{1H}\right)\theta^A_{1Am}\ddot{\theta}^T_{3T\ell} - \sin\left(\theta\right)\sin\left(\theta^H_{1H}\right)\theta^A_{2Am}\ddot{\theta}^T_{3T\ell} \\
&\qquad + \sin\left(\theta\right)\cos\left(\theta^H_{1H}\right)\theta^A_{3Am}\ddot{\theta}^T_{3T\ell} \\
&\quad + \sin\left(\theta^H_{1H}\right)\theta^A_{2Am}\ddot{\theta}^A_{1Am} - \cos\left(\theta^H_{1H}\right)\theta^A_{3Am}\ddot{\theta}^A_{1Am} \\
&\qquad - \sin\left(\theta^H_{1H}\right)\theta^A_{1Am}\ddot{\theta}^A_{2Am} + \cos\left(\theta^H_{1H}\right)\theta^A_{1Am}\ddot{\theta}^A_{3Am}
\end{aligned}
\tag{E.2.15}
$$

$$
\begin{aligned}
&A_B\,(1,3)_{nosym} = \\
&\quad 2\omega\Big[-\sin\left(\theta^H_{1H}\right)\dot{\theta}^A_{1Am} - \sin\left(\theta^H_{1H}\right)\dot{\theta}^H_{1H} \\
&\qquad +\sin(\theta)\cos\left(\theta^H_{1H}\right)\theta^A_{3Am}\dot{\theta}^T_{1T\ell} + \cos(\theta)\cos\left(\theta^H_{1H}\right)\theta^A_{3Am}\dot{\theta}^T_{3T\ell} \\
&\qquad -\cos\left(\theta^H_{1H}\right)\theta^A_{1Am}\dot{\theta}^A_{1Am} - \sin\left(\theta^H_{1H}\right)\theta^A_{3Am}\dot{\theta}^A_{2Am} + \sin\left(\theta^H_{1H}\right)\theta^A_{2Am}\dot{\theta}^A_{3Am} \\
&\qquad -\cos\left(\theta^H_{1H}\right)\theta^A_{1Am}\dot{\theta}^H_{1H}\Big] \\
&\quad -2\sin\left(\theta^H_{1H}\right)\dot{\theta}^H_{1H}\dot{\theta}^A_{2Am} + 2\cos\left(\theta^H_{1H}\right)\dot{\theta}^H_{1H}\dot{\theta}^A_{3Am} \\
&\quad +2\sin(\theta)\cos\left(\theta^H_{1H}\right)\dot{\theta}^A_{1Am}\dot{\theta}^T_{1T\ell} - 2\sin\left(\theta^H_{1H}\right)\dot{\theta}^A_{1Am}\dot{\theta}^T_{2T\ell} + 2\cos(\theta)\cos\left(\theta^H_{1H}\right)\dot{\theta}^A_{1Am}\dot{\theta}^T_{3T\ell} \\
&\quad +2\sin(\theta)\cos\left(\theta^H_{1H}\right)\dot{\theta}^H_{1H}\dot{\theta}^T_{1T\ell} - 2\sin\left(\theta^H_{1H}\right)\dot{\theta}^H_{1H}\dot{\theta}^T_{2T\ell} \\
&\qquad +2\cos(\theta)\cos\left(\theta^H_{1H}\right)\dot{\theta}^H_{1H}\dot{\theta}^T_{3T\ell}
\end{aligned}
\tag{E.2.16}
$$

$$
\begin{aligned}
&A_B\,(2,1)_{nosym} = \\
&\quad 2\omega\Big[\cos(\theta)\cos\left(\theta^H_{1H}\right)\dot{\theta}^T_{1T\ell} - \sin(\theta)\cos\left(\theta^H_{1H}\right)\dot{\theta}^T_{3T\ell} \\
&\qquad -\sin(\theta)\cos\left(\theta^H_{1H}\right)\theta^T_{2T\ell}\dot{\theta}^T_{1T\ell} + \sin(\theta)\cos\left(\theta^H_{1H}\right)\theta^T_{1T\ell}\dot{\theta}^T_{2T\ell} \\
&\qquad\quad +\cos(\theta)\cos\left(\theta^H_{1H}\right)\theta^T_{3T\ell}\dot{\theta}^T_{2T\ell} - \cos(\theta)\cos\left(\theta^H_{1H}\right)\theta^T_{2T\ell}\dot{\theta}^T_{3T\ell} \\
&\qquad -\cos(\theta)\sin\left(\theta^H_{1H}\right)\theta^A_{1Am}\dot{\theta}^T_{1T\ell} - \sin(\theta)\cos\left(\theta^H_{1H}\right)\theta^A_{2Am}\dot{\theta}^T_{1T\ell} \\
&\qquad\quad +\sin(\theta)\sin\left(\theta^H_{1H}\right)\theta^A_{1Am}\dot{\theta}^T_{3T\ell} - \cos(\theta)\cos\left(\theta^H_{1H}\right)\theta^A_{2Am}\dot{\theta}^T_{3T\ell} \\
&\qquad +\sin\left(\theta^H_{1H}\right)\theta^A_{3Am}\dot{\theta}^A_{3Am}\Big] \\
&\quad +2\cos(\theta)\cos\left(\theta^H_{1H}\right)\dot{\theta}^A_{2Am}\dot{\theta}^T_{1T\ell} + 2\cos(\theta)\sin\left(\theta^H_{1H}\right)\dot{\theta}^A_{3Am}\dot{\theta}^T_{1T\ell} \\
&\qquad -2\sin(\theta)\cos\left(\theta^H_{1H}\right)\dot{\theta}^A_{2Am}\dot{\theta}^T_{3T\ell} - 2\sin(\theta)\sin\left(\theta^H_{1H}\right)\dot{\theta}^A_{3Am}\dot{\theta}^T_{3T\ell}
\end{aligned}
\tag{E.2.17}
$$

$$
\begin{aligned}
&A_B\,(22,33)_{sym} = \\
&\quad -2\omega\theta^A_{3Am}\dot{\theta}^H_{1H} \\
&\quad -\left(\dot{\theta}^T_{1T\ell}\right)^2 - \left(\dot{\theta}^T_{3T\ell}\right)^2 \\
&\quad -\left(\dot{\theta}^A_{1Am}\right)^2 \\
&\quad -\left(\dot{\theta}^H_{1H}\right)^2 \\
&\quad -2\cos(\theta)\dot{\theta}^A_{1Am}\dot{\theta}^T_{1T\ell} \\
&\quad +2\sin(\theta)\dot{\theta}^A_{1Am}\dot{\theta}^T_{3T\ell} \\
&\quad -2\cos(\theta)\dot{\theta}^H_{1H}\dot{\theta}^T_{1T\ell} + 2\sin(\theta)\dot{\theta}^H_{1H}\dot{\theta}^T_{3T\ell} \\
&\quad -2\dot{\theta}^H_{1H}\dot{\theta}^A_{1Am}
\end{aligned}
\tag{E.2.18}
$$

$$
\begin{aligned}
&A_B\,(22,33)_{skewsym} = \\
&\quad -2\,(\omega)^2 \cos\left(\theta^H_{1H}\right) \sin\left(\theta^H_{1H}\right) \theta^A_{1Am} \\
&\quad +2\omega\Big[\sin(\theta) \cos\left(\theta^H_{1H}\right) \sin\left(\theta^H_{1H}\right) \dot\theta^T_{1T\ell} + \cos(\theta) \cos\left(\theta^H_{1H}\right) \sin\left(\theta^H_{1H}\right) \dot\theta^T_{3T\ell} \\
&\qquad\quad + \cos\left(\theta^H_{1H}\right) \sin\left(\theta^H_{1H}\right) \dot\theta^A_{3Am} \\
&\qquad\quad + \cos(\theta) \cos\left(\theta^H_{1H}\right) \sin\left(\theta^H_{1H}\right) \theta^T_{2T\ell}\dot\theta^T_{1T\ell} - \cos(\theta) \cos\left(\theta^H_{1H}\right) \sin\left(\theta^H_{1H}\right) \theta^T_{1T\ell}\dot\theta^T_{2T\ell} \\
&\qquad\qquad + \sin(\theta) \cos\left(\theta^H_{1H}\right) \sin\left(\theta^H_{1H}\right) \theta^T_{3T\ell}\dot\theta^T_{2T\ell} - \sin(\theta) \cos\left(\theta^H_{1H}\right) \sin\left(\theta^H_{1H}\right) \theta^T_{2T\ell}\dot\theta^T_{3T\ell} \\
&\qquad\quad + \sin(\theta) \cos^2\left(\theta^H_{1H}\right) \theta^A_{1Am}\dot\theta^T_{1T\ell} - \sin(\theta) \sin^2\left(\theta^H_{1H}\right) \theta^A_{1Am}\dot\theta^T_{1T\ell} \\
&\qquad\qquad + \cos(\theta) \cos\left(\theta^H_{1H}\right) \sin\left(\theta^H_{1H}\right) \theta^A_{2Am}\dot\theta^T_{1T\ell} - 2\cos\left(\theta^H_{1H}\right) \sin\left(\theta^H_{1H}\right) \theta^A_{1Am}\dot\theta^T_{2T\ell} \\
&\qquad\qquad + \cos(\theta) \cos^2\left(\theta^H_{1H}\right) \theta^A_{1Am}\dot\theta^T_{3T\ell} - \cos(\theta) \sin^2\left(\theta^H_{1H}\right) \theta^A_{1Am}\dot\theta^T_{3T\ell} \\
&\qquad\qquad - \sin(\theta) \cos\left(\theta^H_{1H}\right) \sin\left(\theta^H_{1H}\right) \theta^A_{2Am}\dot\theta^T_{3T\ell} \\
&\qquad\quad + \cos\left(\theta^H_{1H}\right) \sin\left(\theta^H_{1H}\right) \theta^A_{2Am}\dot\theta^A_{1Am} - 2\cos\left(\theta^H_{1H}\right) \sin\left(\theta^H_{1H}\right) \theta^A_{1Am}\dot\theta^A_{2Am} \\
&\qquad\qquad + \cos^2\left(\theta^H_{1H}\right) \theta^A_{1Am}\dot\theta^A_{3Am} - \sin^2\left(\theta^H_{1H}\right) \theta^A_{1Am}\dot\theta^A_{3Am} \quad \Big] \\
&\quad +2\sin(\theta) \cos\left(\theta^H_{1H}\right) \sin\left(\theta^H_{1H}\right) \dot\theta^T_{1T\ell}\dot\theta^T_{2T\ell} + 2\cos(\theta) \cos\left(\theta^H_{1H}\right) \sin\left(\theta^H_{1H}\right) \dot\theta^T_{2T\ell}\dot\theta^T_{3T\ell} \\
&\quad +2\cos\left(\theta^H_{1H}\right) \sin\left(\theta^H_{1H}\right) \dot\theta^A_{2Am}\dot\theta^A_{3Am} \\
&\quad +2\sin(\theta) \cos\left(\theta^H_{1H}\right) \sin\left(\theta^H_{1H}\right) \dot\theta^A_{2Am}\dot\theta^T_{1T\ell} + 2\cos\left(\theta^H_{1H}\right) \sin\left(\theta^H_{1H}\right) \dot\theta^A_{3Am}\dot\theta^T_{2T\ell} \\
&\qquad +2\cos(\theta) \cos\left(\theta^H_{1H}\right) \sin\left(\theta^H_{1H}\right) \dot\theta^A_{2Am}\dot\theta^T_{3T\ell}
\end{aligned}
\tag{E.2.19}
$$

$$
\begin{aligned}
&A_B\,(2,2)_{nosym} = \\
&\quad -(\omega)^2 \sin^2\left(\theta^H_{1H}\right) \\
&\quad +2\omega\Big[-\sin^2\left(\theta^H_{1H}\right) \dot\theta^T_{2T\ell} \\
&\qquad\quad -\sin^2\left(\theta^H_{1H}\right) \dot\theta^A_{2Am} \\
&\qquad\quad +\sin^2\left(\theta^H_{1H}\right) \theta^T_{3T\ell}\dot\theta^T_{1T\ell} - \sin^2\left(\theta^H_{1H}\right) \theta^T_{1T\ell}\dot\theta^T_{3T\ell} \\
&\qquad\quad -\cos(\theta) \cos^2\left(\theta^H_{1H}\right) \theta^A_{3Am}\dot\theta^T_{1T\ell} + \sin(\theta) \cos^2\left(\theta^H_{1H}\right) \theta^A_{3Am}\dot\theta^T_{3T\ell} \\
&\qquad\quad -\cos^2\left(\theta^H_{1H}\right) \theta^A_{3Am}\dot\theta^A_{1Am} \quad \Big] \\
&\quad +\sin^2(\theta) \sin^2\left(\theta^H_{1H}\right) \left(\dot\theta^T_{1T\ell}\right)^2 - \sin^2\left(\theta^H_{1H}\right) \left(\dot\theta^T_{2T\ell}\right)^2 + \cos^2(\theta) \sin^2\left(\theta^H_{1H}\right) \left(\dot\theta^T_{3T\ell}\right)^2 \\
&\quad -\sin^2\left(\theta^H_{1H}\right) \left(\dot\theta^A_{2Am}\right)^2 - \cos^2\left(\theta^H_{1H}\right) \left(\dot\theta^A_{3Am}\right)^2 \\
&\quad +2\cos(\theta) \sin(\theta) \sin^2\left(\theta^H_{1H}\right) \dot\theta^T_{1T\ell}\dot\theta^T_{3T\ell} \\
&\quad -2\sin(\theta) \cos^2\left(\theta^H_{1H}\right) \dot\theta^A_{3Am}\dot\theta^T_{1T\ell} - 2\sin^2\left(\theta^H_{1H}\right) \dot\theta^A_{2Am}\dot\theta^T_{2T\ell} \\
&\qquad -2\cos(\theta) \cos^2\left(\theta^H_{1H}\right) \dot\theta^A_{3Am}\dot\theta^T_{3T\ell}
\end{aligned}
\tag{E.2.20}
$$

$$
\begin{aligned}
A_B(2,3)_{sym} = \\
&-(\omega)^2 \cos\left(\theta^H_{1H}\right) \sin\left(\theta^H_{1H}\right) \\
&-(\omega)^2 \cos^2\left(\theta^H_{1H}\right) \theta^A_{1Am} + (\omega)^2 \sin^2\left(\theta^H_{1H}\right) \theta^A_{1Am} \\
&+2\omega \Big[-\cos\left(\theta^H_{1H}\right) \sin\left(\theta^H_{1H}\right) \dot{\theta}^T_{2T\ell} - \cos\left(\theta^H_{1H}\right) \sin\left(\theta^H_{1H}\right) \dot{\theta}^A_{2Am} \\
&\quad + \cos\left(\theta^H_{1H}\right) \sin\left(\theta^H_{1H}\right) \theta^T_{3T\ell} \dot{\theta}^T_{1T\ell} - \cos\left(\theta^H_{1H}\right) \sin\left(\theta^H_{1H}\right) \theta^T_{1T\ell} \dot{\theta}^T_{3T\ell} \\
&\quad -2 \sin(\theta) \cos\left(\theta^H_{1H}\right) \sin\left(\theta^H_{1H}\right) \theta^A_{1Am} \dot{\theta}^T_{1T\ell} + \cos(\theta) \cos\left(\theta^H_{1H}\right) \sin\left(\theta^H_{1H}\right) \theta^A_{3Am} \dot{\theta}^T_{1T\ell} \\
&\quad\quad - \cos^2\left(\theta^H_{1H}\right) \theta^A_{1Am} \dot{\theta}^T_{2T\ell} + \sin^2\left(\theta^H_{1H}\right) \theta^A_{1Am} \dot{\theta}^T_{2T\ell} \\
&\quad\quad -2 \cos(\theta) \cos\left(\theta^H_{1H}\right) \sin\left(\theta^H_{1H}\right) \theta^A_{1Am} \dot{\theta}^T_{3T\ell} - \sin(\theta) \cos\left(\theta^H_{1H}\right) \sin\left(\theta^H_{1H}\right) \theta^A_{3Am} \dot{\theta}^T_{3T\ell} \\
&\quad + \cos\left(\theta^H_{1H}\right) \sin\left(\theta^H_{1H}\right) \theta^A_{3Am} \dot{\theta}^A_{1Am} - \cos^2\left(\theta^H_{1H}\right) \theta^A_{1Am} \dot{\theta}^A_{2Am} + \sin^2\left(\theta^H_{1H}\right) \theta^A_{1Am} \dot{\theta}^A_{2Am} \\
&\quad\quad -2 \cos\left(\theta^H_{1H}\right) \sin\left(\theta^H_{1H}\right) \theta^A_{1Am} \dot{\theta}^A_{3Am} \Big] \\
&+ \sin^2(\theta) \cos\left(\theta^H_{1H}\right) \sin\left(\theta^H_{1H}\right) \left(\dot{\theta}^T_{1T\ell}\right)^2 - \cos\left(\theta^H_{1H}\right) \sin\left(\theta^H_{1H}\right) \left(\dot{\theta}^T_{2T\ell}\right)^2 \\
&\quad + \cos^2(\theta) \cos\left(\theta^H_{1H}\right) \sin\left(\theta^H_{1H}\right) \left(\dot{\theta}^T_{3T\ell}\right)^2 \\
&- \cos\left(\theta^H_{1H}\right) \sin\left(\theta^H_{1H}\right) \left(\dot{\theta}^A_{2Am}\right)^2 + \cos\left(\theta^H_{1H}\right) \sin\left(\theta^H_{1H}\right) \left(\dot{\theta}^A_{3Am}\right)^2 \\
&+ \sin(\theta) \cos^2\left(\theta^H_{1H}\right) \dot{\theta}^T_{1T\ell} \dot{\theta}^T_{2T\ell} - \sin(\theta) \sin^2\left(\theta^H_{1H}\right) \dot{\theta}^T_{1T\ell} \dot{\theta}^T_{2T\ell} \\
&\quad +2 \cos(\theta) \sin(\theta) \cos\left(\theta^H_{1H}\right) \sin\left(\theta^H_{1H}\right) \dot{\theta}^T_{1T\ell} \dot{\theta}^T_{3T\ell} + \cos(\theta) \cos^2\left(\theta^H_{1H}\right) \dot{\theta}^T_{2T\ell} \dot{\theta}^T_{3T\ell} \\
&\quad - \cos(\theta) \sin^2\left(\theta^H_{1H}\right) \dot{\theta}^T_{2T\ell} \dot{\theta}^T_{3T\ell} \\
&+2 \sin(\theta) \cos\left(\theta^H_{1H}\right) \sin\left(\theta^H_{1H}\right) \dot{\theta}^A_{3Am} \dot{\theta}^T_{1T\ell} - 2 \cos\left(\theta^H_{1H}\right) \sin\left(\theta^H_{1H}\right) \dot{\theta}^A_{2Am} \dot{\theta}^T_{2T\ell} \\
&\quad +2 \cos(\theta) \cos\left(\theta^H_{1H}\right) \sin\left(\theta^H_{1H}\right) \dot{\theta}^A_{3Am} \dot{\theta}^T_{3T\ell} \\
&+ \cos^2\left(\theta^H_{1H}\right) \dot{\theta}^A_{2Am} \dot{\theta}^A_{3Am} - \sin^2\left(\theta^H_{1H}\right) \dot{\theta}^A_{2Am} \dot{\theta}^A_{3Am}
\end{aligned}
\tag{E.2.21}
$$

$$
\begin{aligned}
A_B(2,3)_{skewsym} = \\
&-\cos(\theta) \ddot{\theta}^T_{1T\ell} + \sin(\theta) \ddot{\theta}^T_{3T\ell} \\
&-\ddot{\theta}^A_{1Am} \\
&-\ddot{\theta}^H_{1H} \\
&+\sin(\theta) \theta^T_{2T\ell} \ddot{\theta}^T_{1T\ell} - \sin(\theta) \theta^T_{1T\ell} \ddot{\theta}^T_{2T\ell} - \cos(\theta) \theta^T_{3T\ell} \ddot{\theta}^T_{2T\ell} + \cos(\theta) \theta^T_{2T\ell} \ddot{\theta}^T_{3T\ell} \\
&+\sin(\theta) \theta^A_{2Am} \ddot{\theta}^T_{1T\ell} - \theta^A_{3Am} \ddot{\theta}^T_{2T\ell} + \cos(\theta) \theta^A_{2Am} \ddot{\theta}^T_{3T\ell} \\
&+\theta^A_{2Am} \ddot{\theta}^A_{3Am} - \theta^A_{3Am} \ddot{\theta}^A_{2Am}
\end{aligned}
\tag{E.2.22}
$$

$$
\begin{aligned}
&A_B\,(2,3)_{nosym} = \\
&\quad 2\omega\Big[\sin(\theta)\cos^2\left(\theta^H_{1H}\right)\dot{\theta}^T_{1T\ell} + \cos(\theta)\cos^2\left(\theta^H_{1H}\right)\dot{\theta}^T_{3T\ell} \\
&\qquad -\sin^2\left(\theta^H_{1H}\right)\dot{\theta}^A_{3Am} \\
&\qquad +\cos(\theta)\cos^2\left(\theta^H_{1H}\right)\theta^T_{2T\ell}\dot{\theta}^T_{1T\ell} - \cos(\theta)\cos^2\left(\theta^H_{1H}\right)\theta^T_{1T\ell}\dot{\theta}^T_{2T\ell} \\
&\qquad\quad +\sin(\theta)\cos^2\left(\theta^H_{1H}\right)\theta^T_{3T\ell}\dot{\theta}^T_{2T\ell} - \sin(\theta)\cos^2\left(\theta^H_{1H}\right)\theta^T_{2T\ell}\dot{\theta}^T_{3T\ell} \\
&\qquad +\cos(\theta)\cos^2\left(\theta^H_{1H}\right)\theta^A_{2Am}\dot{\theta}^T_{1T\ell} - \sin(\theta)\cos^2\left(\theta^H_{1H}\right)\theta^A_{2Am}\dot{\theta}^T_{3T\ell} \\
&\qquad -\sin^2\left(\theta^H_{1H}\right)\theta^A_{2Am}\dot{\theta}^A_{1Am}\Big] \\
&\quad +2\sin(\theta)\cos^2\left(\theta^H_{1H}\right)\dot{\theta}^A_{2Am}\dot{\theta}^T_{1T\ell} - 2\sin^2\left(\theta^H_{1H}\right)\dot{\theta}^A_{3Am}\dot{\theta}^T_{2T\ell} \\
&\qquad +2\cos(\theta)\cos^2\left(\theta^H_{1H}\right)\dot{\theta}^A_{2Am}\dot{\theta}^T_{3T\ell}
\end{aligned}
\tag{E.2.23}
$$

$$
\begin{aligned}
&A_B\,(3,1)_{nosym} = \\
&\quad 2\omega\Big[-\cos(\theta)\sin\left(\theta^H_{1H}\right)\dot{\theta}^T_{1T\ell} + \sin(\theta)\sin\left(\theta^H_{1H}\right)\dot{\theta}^T_{3T\ell} \\
&\qquad +\sin(\theta)\sin\left(\theta^H_{1H}\right)\theta^T_{2T\ell}\dot{\theta}^T_{1T\ell} - \sin(\theta)\sin\left(\theta^H_{1H}\right)\theta^T_{1T\ell}\dot{\theta}^T_{2T\ell} \\
&\qquad\quad -\cos(\theta)\sin\left(\theta^H_{1H}\right)\theta^T_{3T\ell}\dot{\theta}^T_{2T\ell} + \cos(\theta)\sin\left(\theta^H_{1H}\right)\theta^T_{2T\ell}\dot{\theta}^T_{3T\ell} \\
&\qquad -\cos(\theta)\cos\left(\theta^H_{1H}\right)\theta^A_{1Am}\dot{\theta}^T_{1T\ell} + \sin(\theta)\sin\left(\theta^H_{1H}\right)\theta^A_{2Am}\dot{\theta}^T_{1T\ell} \\
&\qquad +\sin(\theta)\cos\left(\theta^H_{1H}\right)\theta^A_{1Am}\dot{\theta}^T_{3T\ell} + \cos(\theta)\sin\left(\theta^H_{1H}\right)\theta^A_{2Am}\dot{\theta}^T_{3T\ell} \\
&\qquad -\sin\left(\theta^H_{1H}\right)\theta^A_{3Am}\dot{\theta}^A_{2Am} + \cos\left(\theta^H_{1H}\right)\theta^A_{3Am}\dot{\theta}^A_{3Am}\Big] \\
&\quad -2\cos(\theta)\sin\left(\theta^H_{1H}\right)\dot{\theta}^A_{2Am}\dot{\theta}^T_{1T\ell} + 2\cos(\theta)\cos\left(\theta^H_{1H}\right)\dot{\theta}^A_{3Am}\dot{\theta}^T_{1T\ell} \\
&\qquad +2\sin(\theta)\sin\left(\theta^H_{1H}\right)\dot{\theta}^A_{2Am}\dot{\theta}^T_{3T\ell} - 2\sin(\theta)\cos\left(\theta^H_{1H}\right)\dot{\theta}^A_{3Am}\dot{\theta}^T_{3T\ell}
\end{aligned}
\tag{E.2.24}
$$

$$
\begin{aligned}
&A_B\,(3,2)_{nosym} = \\
&\quad 2\omega\Big[-\sin(\theta)\sin^2\left(\theta^H_{1H}\right)\dot{\theta}^T_{1T\ell} - \cos(\theta)\sin^2\left(\theta^H_{1H}\right)\dot{\theta}^T_{3T\ell} \\
&\qquad +\cos^2\left(\theta^H_{1H}\right)\dot{\theta}^A_{3Am} \\
&\qquad -\cos(\theta)\sin^2\left(\theta^H_{1H}\right)\theta^T_{2T\ell}\dot{\theta}^T_{1T\ell} + \cos(\theta)\sin^2\left(\theta^H_{1H}\right)\theta^T_{1T\ell}\dot{\theta}^T_{2T\ell} \\
&\qquad\quad -\sin(\theta)\sin^2\left(\theta^H_{1H}\right)\theta^T_{3T\ell}\dot{\theta}^T_{2T\ell} + \sin(\theta)\sin^2\left(\theta^H_{1H}\right)\theta^T_{2T\ell}\dot{\theta}^T_{3T\ell} \\
&\qquad -\cos(\theta)\sin^2\left(\theta^H_{1H}\right)\theta^A_{2Am}\dot{\theta}^T_{1T\ell} + \sin(\theta)\sin^2\left(\theta^H_{1H}\right)\theta^A_{2Am}\dot{\theta}^T_{3T\ell} \\
&\qquad +\cos^2\left(\theta^H_{1H}\right)\theta^A_{2Am}\dot{\theta}^A_{1Am}\Big] \\
&\quad -2\sin(\theta)\sin^2\left(\theta^H_{1H}\right)\dot{\theta}^A_{2Am}\dot{\theta}^T_{1T\ell} + 2\cos^2\left(\theta^H_{1H}\right)\dot{\theta}^A_{3Am}\dot{\theta}^T_{2T\ell} \\
&\qquad -2\cos(\theta)\sin^2\left(\theta^H_{1H}\right)\dot{\theta}^A_{2Am}\dot{\theta}^T_{3T\ell}
\end{aligned}
\tag{E.2.25}
$$

$$
\begin{aligned}
&A_B\,(3,3)_{nosym} = \\
&\quad -(\omega)^2 \cos^2\left(\theta^H_{1H}\right) \\
&\quad +2\omega\Big[-\cos^2\left(\theta^H_{1H}\right)\dot{\theta}^T_{2T\ell} \\
&\qquad\qquad -\cos^2\left(\theta^H_{1H}\right)\dot{\theta}^A_{2Am} \\
&\qquad\qquad +\cos^2\left(\theta^H_{1H}\right)\theta^T_{3T\ell}\dot{\theta}^T_{1T\ell} - \cos^2\left(\theta^H_{1H}\right)\theta^T_{1T\ell}\dot{\theta}^T_{3T\ell} \\
&\qquad\qquad -\cos(\theta)\sin^2\left(\theta^H_{1H}\right)\theta^A_{3Am}\dot{\theta}^T_{1T\ell} + \sin(\theta)\sin^2\left(\theta^H_{1H}\right)\theta^A_{3Am}\dot{\theta}^T_{3T\ell} \\
&\qquad\qquad -\sin^2\left(\theta^H_{1H}\right)\theta^A_{3Am}\dot{\theta}^A_{1Am}\Big] \\
&\quad +\sin^2(\theta)\cos\left(\theta^H_{1H}\right)\cos\left(\theta^H_{1H}\right)\left(\dot{\theta}^T_{1T\ell}\right)^2 - \cos^2\left(\theta^H_{1H}\right)\left(\dot{\theta}^T_{2T\ell}\right)^2 \\
&\qquad +\cos^2(\theta)\cos\left(\theta^H_{1H}\right)\cos\left(\theta^H_{1H}\right)\left(\dot{\theta}^T_{3T\ell}\right)^2 \\
&\quad -\cos^2\left(\theta^H_{1H}\right)\left(\dot{\theta}^A_{2Am}\right)^2 - \sin^2\left(\theta^H_{1H}\right)\left(\dot{\theta}^A_{3Am}\right)^2 \\
&\quad +2\cos(\theta)\sin(\theta)\cos^2\left(\theta^H_{1H}\right)\dot{\theta}^T_{1T\ell}\dot{\theta}^T_{3T\ell} \\
&\quad -2\sin(\theta)\sin^2\left(\theta^H_{1H}\right)\dot{\theta}^A_{3Am}\dot{\theta}^T_{1T\ell} - 2\cos^2\left(\theta^H_{1H}\right)\dot{\theta}^A_{2Am}\dot{\theta}^T_{2T\ell} \\
&\qquad -2\cos(\theta)\sin^2\left(\theta^H_{1H}\right)\dot{\theta}^A_{3Am}\dot{\theta}^T_{3T\ell}
\end{aligned}
\tag{E.2.26}
$$

The $[B_B]$–matrix.

The skew–symmetric matrix is listed in component form, where only the three elements above the diagonal are given

$$
\begin{aligned}
B_B\,(1,2) = \\
2\Big[&\omega \sin\left(\theta^H_{1H}\right) + \omega \cos\left(\theta^H_{1H}\right) \theta^A_{1Am} \\
&- \sin(\theta) \cos\left(\theta^H_{1H}\right) \dot{\theta}^T_{1T\ell} + \sin\left(\theta^H_{1H}\right) \dot{\theta}^T_{2T\ell} - \cos(\theta) \cos\left(\theta^H_{1H}\right) \dot{\theta}^T_{3T\ell} \\
&+ \sin\left(\theta^H_{1H}\right) \dot{\theta}^A_{2Am} - \cos\left(\theta^H_{1H}\right) \dot{\theta}^A_{3Am} \\
&- \Big(\cos(\theta) \cos\left(\theta^H_{1H}\right) \theta^T_{2T\ell} + \sin\left(\theta^H_{1H}\right) \theta^T_{3T\ell}\Big) \dot{\theta}^T_{1T\ell} \\
&\quad + \Big(\cos(\theta) \cos\left(\theta^H_{1H}\right) \theta^T_{1T\ell} - \sin(\theta) \cos\left(\theta^H_{1H}\right) \theta^T_{3T\ell}\Big) \dot{\theta}^T_{2T\ell} \\
&\quad + \Big(\sin\left(\theta^H_{1H}\right) \theta^T_{1T\ell} + \sin(\theta) \cos\left(\theta^H_{1H}\right) \theta^T_{2T\ell}\Big) \dot{\theta}^T_{3T\ell} \\
&+ \Big(\sin(\theta) \sin\left(\theta^H_{1H}\right) \theta^A_{1Am} - \cos(\theta) \cos\left(\theta^H_{1H}\right) \theta^A_{2Am} - \cos(\theta) \sin\left(\theta^H_{1H}\right) \theta^A_{3Am}\Big) \dot{\theta}^T_{1T\ell} \\
&\quad + \cos\left(\theta^H_{1H}\right) \theta^A_{1Am} \dot{\theta}^T_{2T\ell} \\
&\quad + \Big(\cos(\theta) \sin\left(\theta^H_{1H}\right) \theta^A_{1Am} + \sin(\theta) \cos\left(\theta^H_{1H}\right) \theta^A_{2Am} + \sin(\theta) \sin\left(\theta^H_{1H}\right) \theta^A_{3Am}\Big) \dot{\theta}^T_{3T\ell} \\
&- \Big(\cos\left(\theta^H_{1H}\right) \theta^A_{2Am} + \sin\left(\theta^H_{1H}\right) \theta^A_{3Am}\Big) \dot{\theta}^A_{1Am} \\
&\quad + \cos\left(\theta^H_{1H}\right) \theta^A_{1Am} \dot{\theta}^A_{2Am} + \sin\left(\theta^H_{1H}\right) \theta^A_{1Am} \dot{\theta}^A_{3Am}\Big]
\end{aligned}
\tag{E.2.27}
$$

$$
\begin{aligned}
B_B(1,3) = \\
2\Big[&\omega\cos\left(\theta^H_{1H}\right) - \omega\sin\left(\theta^H_{1H}\right)\theta^A_{1Am} \\
&+\sin(\theta)\sin\left(\theta^H_{1H}\right)\dot{\theta}^T_{1T\ell} + \cos\left(\theta^H_{1H}\right)\dot{\theta}^T_{2T\ell} + \cos(\theta)\sin\left(\theta^H_{1H}\right)\dot{\theta}^T_{3T\ell} \\
&+\cos\left(\theta^H_{1H}\right)\dot{\theta}^A_{2Am} + \sin\left(\theta^H_{1H}\right)\dot{\theta}^A_{3Am} \\
&+\Big(\cos(\theta)\sin\left(\theta^H_{1H}\right)\theta^T_{2T\ell} - \cos\left(\theta^H_{1H}\right)\theta^T_{3T\ell}\Big)\dot{\theta}^T_{1T\ell} \\
&\quad-\Big(\cos(\theta)\sin\left(\theta^H_{1H}\right)\theta^T_{1T\ell} - \sin(\theta)\sin\left(\theta^H_{1H}\right)\theta^T_{3T\ell}\Big)\dot{\theta}^T_{2T\ell} \\
&\quad+\Big(\cos\left(\theta^H_{1H}\right)\theta^T_{1T\ell} - \sin(\theta)\sin\left(\theta^H_{1H}\right)\theta^T_{2T\ell}\Big)\dot{\theta}^T_{3T\ell} \\
&+\Big(\sin(\theta)\cos\left(\theta^H_{1H}\right)\theta^A_{1Am} + \cos(\theta)\sin\left(\theta^H_{1H}\right)\theta^A_{2Am} - \cos(\theta)\cos\left(\theta^H_{1H}\right)\theta^A_{3Am}\Big)\dot{\theta}^T_{1T\ell} \\
&\quad-\sin\left(\theta^H_{1H}\right)\theta^A_{1Am}\dot{\theta}^T_{2T\ell} \\
&\quad+\Big(\cos(\theta)\cos\left(\theta^H_{1H}\right)\theta^A_{1Am} - \sin(\theta)\sin\left(\theta^H_{1H}\right)\theta^A_{2Am} + \sin(\theta)\cos\left(\theta^H_{1H}\right)\theta^A_{3Am}\Big)\dot{\theta}^T_{3T\ell} \\
&+\Big(\sin\left(\theta^H_{1H}\right)\theta^A_{2Am} - \cos\left(\theta^H_{1H}\right)\theta^A_{3Am}\Big)\dot{\theta}^A_{1Am} \\
&\quad-\sin\left(\theta^H_{1H}\right)\theta^A_{1Am}\dot{\theta}^A_{2Am} + \cos\left(\theta^H_{1H}\right)\theta^A_{1Am}\dot{\theta}^A_{3Am}\Big]
\end{aligned}
\tag{E.2.28}
$$

$$
\begin{aligned}
B_B(2,3) = \\
2\Big[&-\omega\theta^A_{3Am} - \cos(\theta)\dot{\theta}^T_{1T\ell} + \sin(\theta)\dot{\theta}^T_{3T\ell} - \dot{\theta}^A_{1Am} - \dot{\theta}^H_{1H} \\
&+\sin(\theta)\theta^T_{2T\ell}\dot{\theta}^T_{1T\ell} - \Big(\sin(\theta)\theta^T_{1T\ell} + \cos(\theta)\theta^T_{3T\ell}\Big)\dot{\theta}^T_{2T\ell} + \cos(\theta)\theta^T_{2T\ell}\dot{\theta}^T_{3T\ell} \\
&+\sin(\theta)\theta^A_{2Am}\dot{\theta}^T_{1T\ell} - \theta^A_{3Am}\dot{\theta}^T_{2T\ell} + \cos(\theta)\theta^A_{2Am}\dot{\theta}^T_{3T\ell} \\
&-\theta^A_{3Am}\dot{\theta}^A_{2Am} + \theta^A_{2Am}\dot{\theta}^A_{3Am}\Big]
\end{aligned}
\tag{E.2.29}
$$

The $[D_B]$–matrix.

$$D_B(1,1) = \cos(\theta) - \sin(\theta)\,\theta^T_{2T\ell} - \sin(\theta)\,\theta^A_{2Am} \tag{E.2.30}$$

$$D_B(1,2) = \sin(\theta)\,\theta^T_{1T\ell} + \cos(\theta)\,\theta^T_{3T\ell} + \theta^A_{3Am} \tag{E.2.31}$$

$$D_B(1,3) = -\sin(\theta) - \cos(\theta)\,\theta^T_{2T\ell} - \cos(\theta)\,\theta^A_{2Am} \tag{E.2.32}$$

$$\begin{aligned} D_B(2,1) = {} & \sin(\theta)\sin\left(\theta^H_{1H}\right) \\ & + \cos(\theta)\sin\left(\theta^H_{1H}\right)\theta^T_{2T\ell} - \cos\left(\theta^H_{1H}\right)\theta^T_{3T\ell} \\ & + \sin(\theta)\cos\left(\theta^H_{1H}\right)\theta^A_{1Am} + \cos(\theta)\sin\left(\theta^H_{1H}\right)\theta^A_{2Am} - \cos(\theta)\cos\left(\theta^H_{1H}\right)\theta^A_{3Am} \end{aligned} \tag{E.2.33}$$

$$\begin{aligned} D_B(2,2) = {} & \cos\left(\theta^H_{1H}\right) \\ & - \cos(\theta)\sin\left(\theta^H_{1H}\right)\theta^T_{1T\ell} + \sin(\theta)\sin\left(\theta^H_{1H}\right)\theta^T_{3T\ell} \\ & - \sin\left(\theta^H_{1H}\right)\theta^A_{1Am} \end{aligned} \tag{E.2.34}$$

$$\begin{aligned} D_B(2,3) = {} & \cos(\theta)\sin\left(\theta^H_{1H}\right) \\ & + \cos\left(\theta^H_{1H}\right)\theta^T_{1T\ell} - \sin(\theta)\sin\left(\theta^H_{1H}\right)\theta^T_{2T\ell} \\ & + \cos(\theta)\cos\left(\theta^H_{1H}\right)\theta^A_{1Am} - \sin(\theta)\sin\left(\theta^H_{1H}\right)\theta^A_{2Am} + \sin(\theta)\cos\left(\theta^H_{1H}\right)\theta^A_{3Am} \end{aligned} \tag{E.2.35}$$

$$\begin{aligned} D_B(3,1) = {} & \sin(\theta)\cos\left(\theta^H_{1H}\right) \\ & + \cos(\theta)\cos\left(\theta^H_{1H}\right)\theta^T_{2T\ell} + \sin\left(\theta^H_{1H}\right)\theta^T_{3T\ell} \\ & - \sin(\theta)\sin\left(\theta^H_{1H}\right)\theta^A_{1Am} + \cos(\theta)\cos\left(\theta^H_{1H}\right)\theta^A_{2Am} + \cos(\theta)\sin\left(\theta^H_{1H}\right)\theta^A_{3Am} \end{aligned} \tag{E.2.36}$$

$$\begin{aligned} D_B(3,2) = {} & -\sin\left(\theta^H_{1H}\right) \\ & - \cos(\theta)\cos\left(\theta^H_{1H}\right)\theta^T_{1T\ell} + \sin(\theta)\cos\left(\theta^H_{1H}\right)\theta^T_{3T\ell} \\ & - \cos\left(\theta^H_{1H}\right)\theta^A_{1Am} \end{aligned} \tag{E.2.37}$$

$$
\begin{aligned}
D_B(3,3) = & \\
& \cos(\theta)\cos\left(\theta_{1H}^{H}\right) \\
& -\sin\left(\theta_{1H}^{H}\right)\theta_{1T\ell}^{T} - \sin(\theta)\cos\left(\theta_{1H}^{H}\right)\theta_{2T\ell}^{T} \\
& -\cos(\theta)\sin\left(\theta_{1H}^{H}\right)\theta_{1Am}^{A} - \sin(\theta)\cos\left(\theta_{1H}^{H}\right)\theta_{2Am}^{A} - \sin(\theta)\sin\left(\theta_{1H}^{H}\right)\theta_{3Am}^{A}
\end{aligned}
\tag{E.2.38}
$$

The $[E_B]$–matrix.

$$
\begin{aligned}
E_B(1,1) = \\
&-2\sin(\theta)\,\dot{u}^A_{2Am} \\
&-\ell_{shaft}\cos(\theta)\,\dot{\theta}^T_{2T\ell} \\
&+2\omega\theta^T_{3T\ell}u^A_{1Am} \\
&+2\omega\cos(\theta)\,\theta^A_{3Am}u^A_{1Am} + 2\omega\sin(\theta)\,\theta^A_{3Am}u^A_{3Am} \\
&-\sin^2(\theta)\,\dot{\theta}^T_{1T\ell}u^A_{1Am} + \cos(\theta)\sin(\theta)\,\dot{\theta}^T_{1T\ell}u^A_{3Am} + \cos(\theta)\,\dot{\theta}^T_{2T\ell}u^A_{2Am} \\
&\quad -2\cos(\theta)\sin(\theta)\,\dot{\theta}^T_{3T\ell}u^A_{1Am} + \cos^2(\theta)\,\dot{\theta}^T_{3T\ell}u^A_{3Am} - \sin^2(\theta)\,\dot{\theta}^T_{3T\ell}u^A_{3Am} \\
&-2\cos(\theta)\,\theta^T_{2T\ell}\dot{u}^A_{2Am} - 2\theta^T_{3T\ell}\dot{u}^A_{3Am} \\
&+2\sin(\theta)\,\theta^A_{3Am}\dot{u}^A_{1Am} - 2\cos(\theta)\,\theta^A_{2Am}\dot{u}^A_{2Am} - 2\cos(\theta)\,\theta^A_{3Am}\dot{u}^A_{3Am}
\end{aligned}
\tag{E.2.39}
$$

$$
\begin{aligned}
E_B(1,2) = \\
&-2\omega u^A_{1Am} \\
&+\ell_{shaft}\sin(\theta)\,\dot{\theta}^T_{3T\ell} \\
&+2\dot{u}^A_{3Am} \\
&+2\omega\theta^A_{2Am}u^A_{3Am} \\
&-\dot{\theta}^T_{2T\ell}u^A_{1Am} - \sin(\theta)\,\dot{\theta}^T_{3T\ell}u^A_{2Am} \\
&+2\cos(\theta)\,\theta^T_{1T\ell}\dot{u}^A_{2Am} - 2\sin(\theta)\,\theta^T_{3T\ell}\dot{u}^A_{2Am} \\
&+2\theta^A_{2Am}\dot{u}^A_{1Am}
\end{aligned}
\tag{E.2.40}
$$

$$
\begin{aligned}
E_B(1,3) = \\
&-2\cos(\theta)\,\dot{u}^A_{2Am} \\
&-2\omega\theta^T_{1T\ell}u^A_{1Am} \\
&-2\omega\sin(\theta)\,\theta^A_{3Am}u^A_{1Am} + 2\omega\cos(\theta)\,\theta^A_{3Am}u^A_{3Am} \\
&-\cos^2(\theta)\,\dot{\theta}^T_{3T\ell}u^A_{1Am} - \cos(\theta)\sin(\theta)\,\dot{\theta}^T_{3T\ell}u^A_{3Am} \\
&+2\sin(\theta)\,\theta^T_{2T\ell}\dot{u}^A_{2Am} + 2\theta^T_{1T\ell}\dot{u}^A_{3Am} \\
&+2\cos(\theta)\,\theta^A_{3Am}\dot{u}^A_{1Am} + 2\sin(\theta)\,\theta^A_{2Am}\dot{u}^A_{2Am} + 2\sin(\theta)\,\theta^A_{3Am}\dot{u}^A_{3Am}
\end{aligned}
\tag{E.2.41}
$$

$$
\begin{aligned}
E_B(2,1) = \\
&+2\omega\cos(\theta)\cos\left(\theta_{1H}^H\right)u_{1Am}^A + 2\omega\sin(\theta)\cos\left(\theta_{1H}^H\right)u_{3Am}^A \\
&+\ell_{shaft}\cos\left(\theta_{1H}^H\right)\dot{\theta}_{1T\ell}^T - \ell_{shaft}\sin(\theta)\sin\left(\theta_{1H}^H\right)\dot{\theta}_{2T\ell}^T \\
&-2\omega\sin(\theta)\cos\left(\theta_{1H}^H\right)\theta_{2T\ell}^T u_{1Am}^A + 2\omega\cos(\theta)\cos\left(\theta_{1H}^H\right)\theta_{2T\ell}^T u_{3Am}^A + 2\omega\sin\left(\theta_{1H}^H\right)\theta_{3T\ell}^T u_{3Am}^A \\
&-2\omega\cos(\theta)\sin\left(\theta_{1H}^H\right)\theta_{1Am}^A u_{1Am}^A - 2\omega\sin(\theta)\sin\left(\theta_{1H}^H\right)\theta_{1Am}^A u_{3Am}^A \\
&+2\sin(\theta)\cos\left(\theta_{1H}^H\right)\dot{u}_{1Am}^A + 2\cos(\theta)\sin\left(\theta_{1H}^H\right)\dot{u}_{2Am}^A - 2\cos(\theta)\cos\left(\theta_{1H}^H\right)\dot{u}_{3Am}^A \\
&+\cos(\theta)\sin(\theta)\sin\left(\theta_{1H}^H\right)\dot{\theta}_{1T\ell}^T u_{1Am}^A + \cos(\theta)\cos\left(\theta_{1H}^H\right)\dot{\theta}_{2T\ell}^T u_{1Am}^A \\
&\quad+\cos^2(\theta)\sin\left(\theta_{1H}^H\right)\dot{\theta}_{3T\ell}^T u_{1Am}^A - \sin^2(\theta)\sin\left(\theta_{1H}^H\right)\dot{\theta}_{3T\ell}^T u_{1Am}^A \\
&\quad-\cos\left(\theta_{1H}^H\right)\dot{\theta}_{1T\ell}^T u_{2Am}^A + \sin(\theta)\sin\left(\theta_{1H}^H\right)\dot{\theta}_{2T\ell}^T u_{2Am}^A \\
&\quad-\cos^2(\theta)\sin\left(\theta_{1H}^H\right)\dot{\theta}_{1T\ell}^T u_{3Am}^A + \sin(\theta)\cos\left(\theta_{1H}^H\right)\dot{\theta}_{2T\ell}^T u_{3Am}^A \\
&\quad+2\cos(\theta)\sin(\theta)\sin\left(\theta_{1H}^H\right)\dot{\theta}_{3T\ell}^T u_{3Am}^A \\
&+2\cos(\theta)\cos\left(\theta_{1H}^H\right)\theta_{2T\ell}^T\dot{u}_{1Am}^A + 2\sin\left(\theta_{1H}^H\right)\theta_{3T\ell}^T\dot{u}_{1Am}^A \\
&\quad-2\sin(\theta)\sin\left(\theta_{1H}^H\right)\theta_{2T\ell}^T\dot{u}_{2Am}^A + 2\sin(\theta)\cos\left(\theta_{1H}^H\right)\theta_{2T\ell}^T\dot{u}_{3Am}^A \\
&-2\sin(\theta)\sin\left(\theta_{1H}^H\right)\theta_{1Am}^A\dot{u}_{1Am}^A + 2\cos(\theta)\cos\left(\theta_{1H}^H\right)\theta_{1Am}^A\dot{u}_{2Am}^A \\
&\quad-2\sin(\theta)\sin\left(\theta_{1H}^H\right)\theta_{2Am}^A\dot{u}_{2Am}^A + 2\sin(\theta)\cos\left(\theta_{1H}^H\right)\theta_{3Am}^A\dot{u}_{2Am}^A \\
&\quad+2\cos(\theta)\sin\left(\theta_{1H}^H\right)\theta_{1Am}^A\dot{u}_{3Am}^A
\end{aligned}
\tag{E.2.42}
$$

$$
\begin{aligned}
E_B(2,2) = \\
&-2\omega\sin\left(\theta_{1H}^H\right)u_{3Am}^A \\
&-\ell_{shaft}\cos(\theta)\sin\left(\theta_{1H}^H\right)\dot{\theta}_{3T\ell}^T \\
&-2\sin\left(\theta_{1H}^H\right)\dot{u}_{1Am}^A \\
&+2\omega\sin(\theta)\cos\left(\theta_{1H}^H\right)\theta_{1T\ell}^T u_{1Am}^A + 2\omega\cos(\theta)\cos\left(\theta_{1H}^H\right)\theta_{3T\ell}^T u_{1Am}^A \\
&\quad-2\omega\cos(\theta)\cos\left(\theta_{1H}^H\right)\theta_{1T\ell}^T u_{3Am}^A + 2\omega\sin(\theta)\cos\left(\theta_{1H}^H\right)\theta_{3T\ell}^T u_{3Am}^A \\
&-2\omega\sin\left(\theta_{1H}^H\right)\theta_{2Am}^A u_{1Am}^A + 2\omega\cos\left(\theta_{1H}^H\right)\theta_{3Am}^A u_{1Am}^A - 2\omega\cos\left(\theta_{1H}^H\right)\theta_{1Am}^A u_{3Am}^A \\
&-\sin(\theta)\cos\left(\theta_{1H}^H\right)\dot{\theta}_{3T\ell}^T u_{1Am}^A + \cos(\theta)\sin\left(\theta_{1H}^H\right)\dot{\theta}_{3T\ell}^T u_{2Am}^A \\
&\quad-\sin\left(\theta_{1H}^H\right)\dot{\theta}_{2T\ell}^T u_{3Am}^A + \cos(\theta)\cos\left(\theta_{1H}^H\right)\dot{\theta}_{3T\ell}^T u_{3Am}^A \\
&-2\cos(\theta)\cos\left(\theta_{1H}^H\right)\theta_{1T\ell}^T\dot{u}_{1Am}^A + 2\sin(\theta)\cos\left(\theta_{1H}^H\right)\theta_{3T\ell}^T\dot{u}_{1Am}^A \\
&\quad+2\sin(\theta)\sin\left(\theta_{1H}^H\right)\theta_{1T\ell}^T\dot{u}_{2Am}^A + 2\cos(\theta)\sin\left(\theta_{1H}^H\right)\theta_{3T\ell}^T\dot{u}_{2Am}^A \\
&\quad-2\sin(\theta)\cos\left(\theta_{1H}^H\right)\theta_{1T\ell}^T\dot{u}_{3Am}^A - 2\cos(\theta)\cos\left(\theta_{1H}^H\right)\theta_{3T\ell}^T\dot{u}_{3Am}^A \\
&-2\cos\left(\theta_{1H}^H\right)\theta_{1Am}^A\dot{u}_{1Am}^A + 2\sin\left(\theta_{1H}^H\right)\theta_{2Am}^A\dot{u}_{3Am}^A \\
&\quad-2\cos\left(\theta_{1H}^H\right)\theta_{3Am}^A\dot{u}_{3Am}^A
\end{aligned}
\tag{E.2.43}
$$

$$
\begin{aligned}
&E_B(2,3) = \\
&\quad -2\omega \sin(\theta) \cos\left(\theta_{1H}^H\right) u_{1Am}^A + 2\omega \cos(\theta) \cos\left(\theta_{1H}^H\right) u_{3Am}^A \\
&\quad +\ell_{shaft} \cos\left(\theta_{1H}^H\right) \dot{\theta}_{3T\ell}^T \\
&\quad +2 \cos(\theta) \cos\left(\theta_{1H}^H\right) \dot{u}_{1Am}^A - 2 \sin(\theta) \sin\left(\theta_{1H}^H\right) \dot{u}_{2Am}^A + 2 \sin(\theta) \cos\left(\theta_{1H}^H\right) \dot{u}_{3Am}^A \\
&\quad -2\omega \cos(\theta) \cos\left(\theta_{1H}^H\right) \theta_{2T\ell}^T u_{1Am}^A - 2\omega \sin\left(\theta_{1H}^H\right) \theta_{1T\ell}^T u_{3Am}^A - 2\omega \sin(\theta) \cos\left(\theta_{1H}^H\right) \theta_{2T\ell}^T u_{3Am}^A \\
&\quad +2\omega \sin(\theta) \sin\left(\theta_{1H}^H\right) \theta_{1Am}^A u_{1Am}^A - 2\omega \cos(\theta) \sin\left(\theta_{1H}^H\right) \theta_{1Am}^A u_{3Am}^A \\
&\qquad -2\omega \sin(\theta) \sin\left(\theta_{1H}^H\right) \theta_{3Am}^A u_{3Am}^A + 2\omega \sin(\theta) \sin\left(\theta_{1H}^H\right) \theta_{3Am}^A u_{3Am}^A \\
&\quad -\cos(\theta) \sin(\theta) \sin\left(\theta_{1H}^H\right) \dot{\theta}_{3T\ell}^T u_{1Am}^A - \cos\left(\theta_{1H}^H\right) \dot{\theta}_{3T\ell}^T u_{2Am}^A - \sin^2(\theta) \sin\left(\theta_{1H}^H\right) \dot{\theta}_{3T\ell}^T u_{3Am}^A \\
&\quad -2 \sin\left(\theta_{1H}^H\right) \theta_{1T\ell}^T \dot{u}_{1Am}^A - 2 \sin(\theta) \cos\left(\theta_{1H}^H\right) \theta_{2T\ell}^T \dot{u}_{1Am}^A \\
&\qquad -2 \cos(\theta) \sin\left(\theta_{1H}^H\right) \theta_{2T\ell}^T \dot{u}_{2Am}^A + 2 \cos(\theta) \cos\left(\theta_{1H}^H\right) \theta_{2T\ell}^T \dot{u}_{3Am}^A \\
&\quad -2 \cos(\theta) \sin\left(\theta_{1H}^H\right) \theta_{1Am}^A \dot{u}_{1Am}^A - 2 \sin(\theta) \cos\left(\theta_{1H}^H\right) \theta_{1Am}^A \dot{u}_{2Am}^A \\
&\qquad -2 \cos(\theta) \sin\left(\theta_{1H}^H\right) \theta_{2Am}^A \dot{u}_{2Am}^A + 2 \cos(\theta) \cos\left(\theta_{1H}^H\right) \theta_{3Am}^A \dot{u}_{2Am}^A \\
&\qquad -2 \sin(\theta) \sin\left(\theta_{1H}^H\right) \theta_{1Am}^A \dot{u}_{3Am}^A
\end{aligned}
\tag{E.2.44}
$$

$$
\begin{aligned}
&E_B(3,1) = \\
&\quad -2\omega \cos(\theta) \sin\left(\theta_{1H}^H\right) u_{1Am}^A - 2\omega \sin(\theta) \sin\left(\theta_{1H}^H\right) u_{3Am}^A \\
&\quad -\ell_{shaft} \sin\left(\theta_{1H}^H\right) \dot{\theta}_{1T\ell}^T - \ell_{shaft} \sin(\theta) \cos\left(\theta_{1H}^H\right) \dot{\theta}_{2T\ell}^T \\
&\quad -2 \sin(\theta) \sin\left(\theta_{1H}^H\right) \dot{u}_{1Am}^A + 2 \cos(\theta) \cos\left(\theta_{1H}^H\right) \dot{u}_{2Am}^A + 2 \cos(\theta) \sin\left(\theta_{1H}^H\right) \dot{u}_{3Am}^A \\
&\quad +2\omega \sin(\theta) \sin\left(\theta_{1H}^H\right) \theta_{2T\ell}^T u_{1Am}^A - 2\omega \cos(\theta) \sin\left(\theta_{1H}^H\right) \theta_{2T\ell}^T u_{3Am}^A + 2\omega \cos\left(\theta_{1H}^H\right) \theta_{3T\ell}^T u_{3Am}^A \\
&\quad -2\omega \cos(\theta) \cos\left(\theta_{1H}^H\right) \theta_{1Am}^A u_{1Am}^A - 2\omega \sin(\theta) \cos\left(\theta_{1H}^H\right) \theta_{1Am}^A u_{3Am}^A \\
&\quad +\cos(\theta) \sin(\theta) \cos\left(\theta_{1H}^H\right) \dot{\theta}_{1T\ell}^T u_{1Am}^A - \cos(\theta) \sin\left(\theta_{1H}^H\right) \dot{\theta}_{2T\ell}^T u_{1Am}^A \\
&\qquad +\cos^2(\theta) \cos\left(\theta_{1H}^H\right) \dot{\theta}_{3T\ell}^T u_{1Am}^A - \sin^2(\theta) \cos\left(\theta_{1H}^H\right) \dot{\theta}_{3T\ell}^T u_{1Am}^A \\
&\qquad +\sin\left(\theta_{1H}^H\right) \dot{\theta}_{1T\ell}^T u_{2Am}^A + \sin(\theta) \cos\left(\theta_{1H}^H\right) \dot{\theta}_{2T\ell}^T u_{2Am}^A \\
&\qquad -\cos^2(\theta) \cos\left(\theta_{1H}^H\right) \dot{\theta}_{1T\ell}^T u_{3Am}^A - \sin(\theta) \sin\left(\theta_{1H}^H\right) \dot{\theta}_{2T\ell}^T u_{3Am}^A \\
&\qquad +2 \cos(\theta) \sin(\theta) \cos\left(\theta_{1H}^H\right) \dot{\theta}_{3T\ell}^T u_{3Am}^A \\
&\quad -2 \cos(\theta) \sin\left(\theta_{1H}^H\right) \theta_{2T\ell}^T \dot{u}_{1Am}^A + 2 \cos\left(\theta_{1H}^H\right) \theta_{3T\ell}^T \dot{u}_{1Am}^A \\
&\qquad -2 \sin(\theta) \cos\left(\theta_{1H}^H\right) \theta_{2T\ell}^T \dot{u}_{2Am}^A - 2 \sin(\theta) \sin\left(\theta_{1H}^H\right) \theta_{2T\ell}^T \dot{u}_{3Am}^A \\
&\quad -2 \sin(\theta) \cos\left(\theta_{1H}^H\right) \theta_{1Am}^A \dot{u}_{1Am}^A - 2 \cos(\theta) \sin\left(\theta_{1H}^H\right) \theta_{1Am}^A \dot{u}_{2Am}^A \\
&\qquad -2 \sin(\theta) \cos\left(\theta_{1H}^H\right) \theta_{2Am}^A \dot{u}_{2Am}^A - 2 \sin(\theta) \sin\left(\theta_{1H}^H\right) \theta_{3Am}^A \dot{u}_{2Am}^A \\
&\qquad +2 \cos(\theta) \cos\left(\theta_{1H}^H\right) \theta_{1Am}^A \dot{u}_{3Am}^A
\end{aligned}
\tag{E.2.45}
$$

$$
\begin{aligned}
E_B(3,2) = \\
&-2\omega\cos\left(\theta_{1H}^H\right) u_{3Am}^A \\
&-\ell_{shaft}\cos\left(\theta\right)\cos\left(\theta_{1H}^H\right)\dot{\theta}_{3T\ell}^T \\
&-2\cos\left(\theta_{1H}^H\right)\dot{u}_{1Am}^A \\
&-2\omega\sin\left(\theta\right)\sin\left(\theta_{1H}^H\right)\theta_{1T\ell}^T u_{1Am}^A - 2\omega\cos\left(\theta\right)\sin\left(\theta_{1H}^H\right)\theta_{3T\ell}^T u_{1Am}^A \\
&\quad +2\omega\cos\left(\theta\right)\sin\left(\theta_{1H}^H\right)\theta_{1T\ell}^T u_{3Am}^A - 2\omega\sin\left(\theta\right)\sin\left(\theta_{1H}^H\right)\theta_{3T\ell}^T u_{3Am}^A \\
&-2\omega\cos\left(\theta_{1H}^H\right)\theta_{2Am}^A u_{1Am}^A - 2\omega\sin\left(\theta_{1H}^H\right)\theta_{3Am}^A u_{1Am}^A \\
&\quad +2\omega\sin\left(\theta_{1H}^H\right)\theta_{1Am}^A u_{3Am}^A \\
&+\sin\left(\theta\right)\sin\left(\theta_{1H}^H\right)\dot{\theta}_{3T\ell}^T u_{1Am}^A + \cos\left(\theta\right)\cos\left(\theta_{1H}^H\right)\dot{\theta}_{3T\ell}^T u_{2Am}^A \\
&\quad -\cos\left(\theta_{1H}^H\right)\dot{\theta}_{2T\ell}^T u_{3Am}^A - \cos\left(\theta\right)\sin\left(\theta_{1H}^H\right)\dot{\theta}_{3T\ell}^T u_{3Am}^A \\
&+2\cos\left(\theta\right)\sin\left(\theta_{1H}^H\right)\theta_{1T\ell}^T\dot{u}_{1Am}^A - 2\sin\left(\theta\right)\sin\left(\theta_{1H}^H\right)\theta_{3T\ell}^T\dot{u}_{1Am}^A \\
&\quad +2\sin\left(\theta\right)\cos\left(\theta_{1H}^H\right)\theta_{1T\ell}^T\dot{u}_{2Am}^A + 2\cos\left(\theta\right)\cos\left(\theta_{1H}^H\right)\theta_{3T\ell}^T\dot{u}_{2Am}^A \\
&\quad +2\sin\left(\theta\right)\sin\left(\theta_{1H}^H\right)\theta_{1T\ell}^T\dot{u}_{3Am}^A + 2\cos\left(\theta\right)\sin\left(\theta_{1H}^H\right)\theta_{3T\ell}^T\dot{u}_{3Am}^A \\
&+2\sin\left(\theta_{1H}^H\right)\theta_{1Am}^A\dot{u}_{1Am}^A + 2\cos\left(\theta_{1H}^H\right)\theta_{2Am}^A\dot{u}_{3Am}^A \\
&\quad +2\sin\left(\theta_{1H}^H\right)\theta_{3Am}^A\dot{u}_{3Am}^A
\end{aligned}
\tag{E.2.46}
$$

$$
\begin{aligned}
E_B(3,3) = \\
&+2\omega\sin\left(\theta\right)\sin\left(\theta_{1H}^H\right)u_{1Am}^A - 2\omega\cos\left(\theta\right)\sin\left(\theta_{1H}^H\right)u_{3Am}^A \\
&-2\cos\left(\theta\right)\sin\left(\theta_{1H}^H\right)\dot{u}_{1Am}^A - 2\sin\left(\theta\right)\cos\left(\theta_{1H}^H\right)\dot{u}_{2Am}^A - 2\sin\left(\theta\right)\sin\left(\theta_{1H}^H\right)\dot{u}_{3Am}^A \\
&-\ell_{shaft}\sin\left(\theta_{1H}^H\right)\dot{\theta}_{3T\ell}^T \\
&+2\omega\cos\left(\theta\right)\sin\left(\theta_{1H}^H\right)\theta_{2T\ell}^T u_{1Am}^A - 2\omega\cos\left(\theta_{1H}^H\right)\theta_{1T\ell}^T u_{3Am}^A + 2\omega\sin\left(\theta\right)\sin\left(\theta_{1H}^H\right)\theta_{2T\ell}^T u_{3Am}^A \\
&+2\omega\sin\left(\theta\right)\cos\left(\theta_{1H}^H\right)\theta_{1Am}^A u_{1Am}^A - 2\omega\cos\left(\theta\right)\cos\left(\theta_{1H}^H\right)\theta_{1Am}^A u_{3Am}^A \\
&-\cos\left(\theta\right)\sin\left(\theta\right)\cos\left(\theta_{1H}^H\right)\dot{\theta}_{3T\ell}^T u_{1Am}^A + \sin\left(\theta_{1H}^H\right)\dot{\theta}_{3T\ell}^T u_{2Am}^A - \sin^2\left(\theta\right)\cos\left(\theta_{1H}^H\right)\dot{\theta}_{3T\ell}^T u_{3Am}^A \\
&-2\cos\left(\theta_{1H}^H\right)\theta_{1T\ell}^T\dot{u}_{1Am}^A + 2\sin\left(\theta\right)\sin\left(\theta_{1H}^H\right)\theta_{2T\ell}^T\dot{u}_{1Am}^A \\
&\quad -2\cos\left(\theta\right)\cos\left(\theta_{1H}^H\right)\theta_{2T\ell}^T\dot{u}_{2Am}^A - 2\cos\left(\theta\right)\sin\left(\theta_{1H}^H\right)\theta_{2T\ell}^T\dot{u}_{3Am}^A \\
&-2\cos\left(\theta\right)\cos\left(\theta_{1H}^H\right)\theta_{1Am}^A\dot{u}_{1Am}^A + 2\sin\left(\theta\right)\sin\left(\theta_{1H}^H\right)\theta_{1Am}^A\dot{u}_{2Am}^A \\
&\quad -2\cos\left(\theta\right)\cos\left(\theta_{1H}^H\right)\theta_{2Am}^A\dot{u}_{2Am}^A - 2\cos\left(\theta\right)\sin\left(\theta_{1H}^H\right)\theta_{3Am}^A\dot{u}_{2Am}^A \\
&\quad -2\sin\left(\theta\right)\cos\left(\theta_{1H}^H\right)\theta_{1Am}^A\dot{u}_{3Am}^A
\end{aligned}
\tag{E.2.47}
$$

The $[F_B]$–matrix.

$$
\begin{aligned}
F_B(1,1) = \\
&\ell_{shaft}\sin(\theta) \\
&+\ell_{shaft}\cos(\theta)\,\theta^T_{2T\ell} \\
&+\ell_{shaft}\cos(\theta)\,\theta^A_{2Am} \\
&-\sin(\theta)\,u^A_{2Am} \\
&-\cos(\theta)\,\theta^T_{2T\ell}u^A_{2Am} - \theta^T_{3T\ell}u^A_{3Am} \\
&+\sin(\theta)\,\theta^A_{3Am}u^A_{1Am} - \cos(\theta)\,\theta^A_{2Am}u^A_{2Am} - \cos(\theta)\,\theta^A_{3Am}u^A_{3Am}
\end{aligned}
\tag{E.2.48}
$$

$$
\begin{aligned}
F_B(1,2) = \\
&u^A_{3Am} \\
&-\ell_{shaft}\cos(\theta)\,\theta^T_{1T\ell} + \ell_{shaft}\sin(\theta)\,\theta^T_{3T\ell} \\
&+\cos(\theta)\,\theta^T_{1T\ell}u^A_{2Am} - \sin(\theta)\,\theta^T_{3T\ell}u^A_{2Am} \\
&+\theta^A_{2Am}u^A_{1Am}
\end{aligned}
\tag{E.2.49}
$$

$$
\begin{aligned}
F_B(1,3) = \\
&\ell_{shaft}\cos(\theta) \\
&-\ell_{shaft}\sin(\theta)\,\theta^T_{2T\ell} \\
&-\ell_{shaft}\sin(\theta)\,\theta^A_{2Am} \\
&-\cos(\theta)\,u^A_{2Am} \\
&+\sin(\theta)\,\theta^T_{2T\ell}u^A_{2Am} + \theta^T_{1T\ell}u^A_{3Am} \\
&+\cos(\theta)\,\theta^A_{3Am}u^A_{1Am} + \sin(\theta)\,\theta^A_{2Am}u^A_{2Am} + \sin(\theta)\,\theta^A_{3Am}u^A_{3Am}
\end{aligned}
\tag{E.2.50}
$$

$$
\begin{aligned}
F_B(2,1) = \\
&-\ell_{shaft}\cos(\theta)\sin\left(\theta^H_{1H}\right) \\
&+\ell_{shaft}\sin(\theta)\sin\left(\theta^H_{1H}\right)\theta^T_{2T\ell} \\
&-\ell_{shaft}\cos(\theta)\cos\left(\theta^H_{1H}\right)\theta^A_{1Am} + \ell_{shaft}\sin(\theta)\sin\left(\theta^H_{1H}\right)\theta^A_{2Am} - \ell_{shaft}\sin(\theta)\cos\left(\theta^H_{1H}\right)\theta^A_{3Am} \\
&+\sin(\theta)\cos\left(\theta^H_{1H}\right)u^A_{1Am} + \cos(\theta)\sin\left(\theta^H_{1H}\right)u^A_{2Am} - \cos(\theta)\cos\left(\theta^H_{1H}\right)u^A_{3Am} \\
&+\cos(\theta)\cos\left(\theta^H_{1H}\right)\theta^T_{2T\ell}u^A_{1Am} + \sin\left(\theta^H_{1H}\right)\theta^T_{3T\ell}u^A_{1Am} \\
&\quad -\sin(\theta)\sin\left(\theta^H_{1H}\right)\theta^T_{2T\ell}u^A_{2Am} + \sin(\theta)\cos\left(\theta^H_{1H}\right)\theta^T_{2T\ell}u^A_{3Am} \\
&-\sin(\theta)\sin\left(\theta^H_{1H}\right)\theta^A_{1Am}u^A_{1Am} + \cos(\theta)\cos\left(\theta^H_{1H}\right)\theta^A_{1Am}u^A_{2Am} \\
&\quad -\sin(\theta)\sin\left(\theta^H_{1H}\right)\theta^A_{2Am}u^A_{2Am} + \sin(\theta)\cos\left(\theta^H_{1H}\right)\theta^A_{3Am}u^A_{2Am} \\
&\quad +\cos(\theta)\sin\left(\theta^H_{1H}\right)\theta^A_{1Am}u^A_{3Am}
\end{aligned}
\tag{E.2.51}
$$

$$
\begin{aligned}
F_B(2,2) = \\
&-\ell_{shaft}\sin(\theta)\sin\left(\theta^H_{1H}\right)\theta^T_{1T\ell} - \ell_{shaft}\cos(\theta)\sin\left(\theta^H_{1H}\right)\theta^T_{3T\ell} \\
&-\sin\left(\theta^H_{1H}\right)u^A_{1Am} \\
&-\cos(\theta)\cos\left(\theta^H_{1H}\right)\theta^T_{1T\ell}u^A_{1Am} + \sin(\theta)\cos\left(\theta^H_{1H}\right)\theta^T_{3T\ell}u^A_{1Am} \\
&\quad+\sin(\theta)\sin\left(\theta^H_{1H}\right)\theta^T_{1T\ell}u^A_{2Am} + \cos(\theta)\sin\left(\theta^H_{1H}\right)\theta^T_{3T\ell}u^A_{2Am} \\
&\quad-\sin(\theta)\cos\left(\theta^H_{1H}\right)\theta^T_{1T\ell}u^A_{3Am} - \cos(\theta)\cos\left(\theta^H_{1H}\right)\theta^T_{3T\ell}u^A_{3Am} \\
&-\cos\left(\theta^H_{1H}\right)\theta^A_{1Am}u^A_{1Am} + \sin\left(\theta^H_{1H}\right)\theta^A_{2Am}u^A_{3Am} \\
&\quad-\cos\left(\theta^H_{1H}\right)\theta^A_{3Am}u^A_{3Am}
\end{aligned}
\tag{E.2.52}
$$

$$
\begin{aligned}
F_B(2,3) = \\
&\ell_{shaft}\sin(\theta)\sin\left(\theta^H_{1H}\right) \\
&+\ell_{shaft}\cos(\theta)\sin\left(\theta^H_{1H}\right)\theta^T_{2T\ell} \\
&+\ell_{shaft}\sin(\theta)\cos\left(\theta^H_{1H}\right)\theta^A_{1Am} + \ell_{shaft}\cos(\theta)\sin\left(\theta^H_{1H}\right)\theta^A_{2Am} - \ell_{shaft}\cos(\theta)\cos\left(\theta^H_{1H}\right)\theta^A_{3Am} \\
&+\cos(\theta)\cos\left(\theta^H_{1H}\right)u^A_{1Am} - \sin(\theta)\sin\left(\theta^H_{1H}\right)u^A_{2Am} + \sin(\theta)\cos\left(\theta^H_{1H}\right)u^A_{3Am} \\
&-\sin\left(\theta^H_{1H}\right)\theta^T_{1T\ell}u^A_{1Am} - \sin(\theta)\cos\left(\theta^H_{1H}\right)\theta^T_{2T\ell}u^A_{1Am} \\
&\quad-\cos(\theta)\sin\left(\theta^H_{1H}\right)\theta^T_{2T\ell}u^A_{2Am} + \cos(\theta)\cos\left(\theta^H_{1H}\right)\theta^T_{2T\ell}u^A_{3Am} \\
&-\cos(\theta)\sin\left(\theta^H_{1H}\right)\theta^A_{1Am}u^A_{1Am} - \sin(\theta)\cos\left(\theta^H_{1H}\right)\theta^A_{1Am}u^A_{2Am} \\
&\quad-\cos(\theta)\sin\left(\theta^H_{1H}\right)\theta^A_{2Am}u^A_{2Am} + \cos(\theta)\cos\left(\theta^H_{1H}\right)\theta^A_{3Am}u^A_{2Am} \\
&\quad-\sin(\theta)\sin\left(\theta^H_{1H}\right)\theta^A_{1Am}u^A_{3Am}
\end{aligned}
\tag{E.2.53}
$$

$$
\begin{aligned}
F_B(3,1) = \\
&-\ell_{shaft}\cos(\theta)\cos\left(\theta^H_{1H}\right) \\
&+\ell_{shaft}\sin(\theta)\cos\left(\theta^H_{1H}\right)\theta^T_{2T\ell} \\
&+\ell_{shaft}\cos(\theta)\sin\left(\theta^H_{1H}\right)\theta^A_{1Am} + \ell_{shaft}\sin(\theta)\cos\left(\theta^H_{1H}\right)\theta^A_{2Am} + \ell_{shaft}\sin(\theta)\sin\left(\theta^H_{1H}\right)\theta^A_{3Am} \\
&-\sin(\theta)\sin\left(\theta^H_{1H}\right)u^A_{1Am} + \cos(\theta)\cos\left(\theta^H_{1H}\right)u^A_{2Am} + \cos(\theta)\sin\left(\theta^H_{1H}\right)u^A_{3Am} \\
&-\cos(\theta)\sin\left(\theta^H_{1H}\right)\theta^T_{2T\ell}u^A_{1Am} + \cos\left(\theta^H_{1H}\right)\theta^T_{3T\ell}u^A_{1Am} \\
&\quad-\sin(\theta)\cos\left(\theta^H_{1H}\right)\theta^T_{2T\ell}u^A_{2Am} - \sin(\theta)\sin\left(\theta^H_{1H}\right)\theta^T_{2T\ell}u^A_{3Am} \\
&-\sin\left(\theta^H_{1H}\right)\cos\left(\theta^H_{1H}\right)\theta^A_{1Am}u^A_{1Am} - \cos(\theta)\sin\left(\theta^H_{1H}\right)\theta^A_{1Am}u^A_{2Am} \\
&\quad-\sin(\theta)\sin\left(\theta^H_{1H}\right)\theta^A_{3Am}u^A_{2Am} - \sin(\theta)\cos\left(\theta^H_{1H}\right)\theta^A_{2Am}u^A_{2Am} \\
&\quad+\cos(\theta)\cos\left(\theta^H_{1H}\right)\theta^A_{1Am}u^A_{3Am}
\end{aligned}
\tag{E.2.54}
$$

$$
\begin{aligned}
F_B(3,2) = \\
&-\ell_{shaft}\sin(\theta)\cos\left(\theta^H_{1H}\right)\theta^T_{1T\ell} - \ell_{shaft}\cos(\theta)\cos\left(\theta^H_{1H}\right)\theta^T_{3T\ell} \\
&-\cos\left(\theta^H_{1H}\right)u^A_{1Am} \\
&+\cos(\theta)\sin\left(\theta^H_{1H}\right)\theta^T_{1T\ell}u^A_{1Am} - \sin(\theta)\sin\left(\theta^H_{1H}\right)\theta^T_{3T\ell}u^A_{1Am} \\
&\quad+\sin(\theta)\cos\left(\theta^H_{1H}\right)\theta^T_{1T\ell}u^A_{2Am} + \cos(\theta)\cos\left(\theta^H_{1H}\right)\theta^T_{3T\ell}u^A_{2Am} \\
&\quad+\sin(\theta)\sin\left(\theta^H_{1H}\right)\theta^T_{1T\ell}u^A_{3Am} + \cos(\theta)\sin\left(\theta^H_{1H}\right)\theta^T_{3T\ell}u^A_{3Am} \\
&+\sin\left(\theta^H_{1H}\right)\theta^A_{1Am}u^A_{1Am} + \cos\left(\theta^H_{1H}\right)\theta^A_{2Am}u^A_{3Am} \\
&\quad+\sin\left(\theta^H_{1H}\right)\theta^A_{3Am}u^A_{3Am}
\end{aligned}
\tag{E.2.55}
$$

$$
\begin{aligned}
F_B(3,3) = \\
&\ell_{shaft} \sin(\theta) \cos\left(\theta_{1H}^H\right) \\
&+\ell_{shaft} \cos(\theta) \cos\left(\theta_{1H}^H\right) \theta_{2T\ell}^T \\
&-\ell_{shaft} \sin(\theta) \sin\left(\theta_{1H}^H\right) \theta_{1Am}^A + \ell_{shaft} \cos(\theta) \cos\left(\theta_{1H}^H\right) \theta_{2Am}^A + \ell_{shaft} \cos(\theta) \sin\left(\theta_{1H}^H\right) \theta_{3Am}^A \\
&- \cos(\theta) \sin\left(\theta_{1H}^H\right) u_{1Am}^A - \sin(\theta) \cos\left(\theta_{1H}^H\right) u_{2Am}^A - \sin(\theta) \sin\left(\theta_{1H}^H\right) u_{3Am}^A \\
&- \cos\left(\theta_{1H}^H\right) \theta_{1T\ell}^T u_{1Am}^A + \sin(\theta) \sin\left(\theta_{1H}^H\right) \theta_{2T\ell}^T u_{1Am}^A \\
&\quad - \cos(\theta) \cos\left(\theta_{1H}^H\right) \theta_{2T\ell}^T u_{2Am}^A - \cos(\theta) \sin\left(\theta_{1H}^H\right) \theta_{2T\ell}^T u_{3Am}^A \\
&- \cos(\theta) \cos\left(\theta_{1H}^H\right) \theta_{1Am}^A u_{1Am}^A + \sin(\theta) \sin\left(\theta_{1H}^H\right) \theta_{1Am}^A u_{2Am}^A \\
&\quad - \cos(\theta) \cos\left(\theta_{1H}^H\right) \theta_{2Am}^A u_{2Am}^A - \cos(\theta) \sin\left(\theta_{1H}^H\right) \theta_{3Am}^A u_{2Am}^A \\
&\quad - \sin(\theta) \cos\left(\theta_{1H}^H\right) \theta_{1Am}^A u_{3Am}^A
\end{aligned}
\tag{E.2.56}
$$

The $[G_B]$–matrix.

$$
[G_B] = (\omega)^2 \begin{bmatrix}
-1.0 & 0 & \theta_{2Am}^A \\
-\sin\left(\theta_{1H}^H\right) \theta_{2Am}^A + \cos\left(\theta_{1H}^H\right) \theta_{3Am}^A & 0 & -\sin\left(\theta_{1H}^H\right) - \cos\left(\theta_{1H}^H\right) \theta_{1Am}^A \\
-\cos\left(\theta_{1H}^H\right) \theta_{2Am}^A - \sin\left(\theta_{1H}^H\right) \theta_{3Am}^A & 0 & -\cos\left(\theta_{1H}^H\right) + \sin\left(\theta_{1H}^H\right) \theta_{1Am}^A
\end{bmatrix}
\tag{E.2.57}
$$

The $[H_B]$–matrix.

$$
[H_B] = 2\omega \begin{bmatrix}
\theta_{2Am}^A & 0 & 1.0 \\
-\sin\left(\theta_{1H}^H\right) - \cos\left(\theta_{1H}^H\right) \theta_{1Am}^A & 0 & \sin\left(\theta_{1H}^H\right) \theta_{2Am}^A - \cos\left(\theta_{1H}^H\right) \theta_{3Am}^A \\
-\cos\left(\theta_{1H}^H\right) + \sin\left(\theta_{1H}^H\right) \theta_{1Am}^A & 0 & \cos\left(\theta_{1H}^H\right) \theta_{2Am}^A + \sin\left(\theta_{1H}^H\right) \theta_{3Am}^A
\end{bmatrix}
\tag{E.2.58}
$$

The $[R_B]$–matrix.

$[R_B] =$

$$\left[\begin{array}{c|c|c} 1.0 & \theta^A_{3Am} & -\theta^A_{2Am} \\ \hline \sin\left(\theta^H_{1H}\right)\theta^A_{2Am} - \cos\left(\theta^H_{1H}\right)\theta^A_{3Am} & \cos\left(\theta^H_{1H}\right) - \sin\left(\theta^H_{1H}\right)\theta^A_{1Am} & \sin\left(\theta^H_{1H}\right) + \cos\left(\theta^H_{1H}\right)\theta^A_{1Am} \\ \hline \cos\left(\theta^H_{1H}\right)\theta^A_{2Am} + \sin\left(\theta^H_{1H}\right)\theta^A_{3Am} & -\sin\left(\theta^H_{1H}\right) - \cos\left(\theta^H_{1H}\right)\theta^A_{1Am} & \cos\left(\theta^H_{1H}\right) - \sin\left(\theta^H_{1H}\right)\theta^A_{1Am} \end{array}\right] \tag{E.2.59}$$

The $[{}_iBT2_j]$–matrix.

$$
\begin{aligned}
{}_iBT2_j\,(1,1) = \\
&-r_{2j}\sin(\theta)\cos\left(\theta_{1H}^{H}\right) + r_{3j}\sin(\theta)\sin\left(\theta_{1H}^{H}\right) \\
&-\left(r_{2j}\cos(\theta)\cos\left(\theta_{1H}^{H}\right) - r_{3j}\cos(\theta)\sin\left(\theta_{1H}^{H}\right)\right)\theta_{2T\ell}^{T} \\
&\quad -\left(r_{2j}\sin\left(\theta_{1H}^{H}\right) + r_{3j}\cos\left(\theta_{1H}^{H}\right)\right)\theta_{3T\ell}^{T} \\
&+\left(r_{2j}\sin(\theta)\sin\left(\theta_{1H}^{H}\right) + r_{3j}\sin(\theta)\cos\left(\theta_{1H}^{H}\right)\right)\theta_{1Am}^{A} \\
&\quad -\left(r_{2j}\cos(\theta)\cos\left(\theta_{1H}^{H}\right) - r_{3j}\cos(\theta)\sin\left(\theta_{1H}^{H}\right)\right)\theta_{2Am}^{A} \\
&\quad -\left(r_{2j}\cos(\theta)\sin\left(\theta_{1H}^{H}\right) + r_{3j}\cos(\theta)\cos\left(\theta_{1H}^{H}\right)\right)\theta_{3Am}^{A}
\end{aligned}
\tag{E.2.60}
$$

$$
\begin{aligned}
{}_iBT2_j\,(1,2) = \\
&+r_{2j}\sin\left(\theta_{1H}^{H}\right) + r_{3j}\cos\left(\theta_{1H}^{H}\right) \\
&+\left(r_{2j}\cos(\theta)\cos\left(\theta_{1H}^{H}\right) - r_{3j}\cos(\theta)\sin\left(\theta_{1H}^{H}\right)\right)\theta_{1T\ell}^{T} \\
&\quad -\left(r_{2j}\sin(\theta)\cos\left(\theta_{1H}^{H}\right) - r_{3j}\sin(\theta)\sin\left(\theta_{1H}^{H}\right)\right)\theta_{3T\ell}^{T} \\
&+\left(r_{2j}\cos\left(\theta_{1H}^{H}\right) - r_{3j}\sin\left(\theta_{1H}^{H}\right)\right)\theta_{1Am}^{A}
\end{aligned}
\tag{E.2.61}
$$

$$
\begin{aligned}
{}_iBT2_j\,(1,3) = \\
&-r_{2j}\cos(\theta)\cos\left(\theta_{1H}^{H}\right) + r_{3j}\cos(\theta)\sin\left(\theta_{1H}^{H}\right) \\
&+\left(r_{2j}\sin\left(\theta_{1H}^{H}\right) + r_{3j}\cos\left(\theta_{1H}^{H}\right)\right)\theta_{1T\ell}^{T} \\
&\quad +\left(r_{2j}\sin(\theta)\cos\left(\theta_{1H}^{H}\right) - r_{3j}\sin(\theta)\sin\left(\theta_{1H}^{H}\right)\right)\theta_{2T\ell}^{T} \\
&+\left(r_{2j}\cos(\theta)\sin\left(\theta_{1H}^{H}\right) + r_{3j}\cos(\theta)\cos\left(\theta_{1H}^{H}\right)\right)\theta_{1Am}^{A} \\
&\quad +\left(r_{2j}\sin(\theta)\cos\left(\theta_{1H}^{H}\right) - r_{3j}\sin(\theta)\sin\left(\theta_{1H}^{H}\right)\right)\theta_{2Am}^{A} \\
&\quad +\left(r_{2j}\sin(\theta)\sin\left(\theta_{1H}^{H}\right) + r_{3j}\sin(\theta)\cos\left(\theta_{1H}^{H}\right)\right)\theta_{3Am}^{A}
\end{aligned}
\tag{E.2.62}
$$

$$
\begin{aligned}
{}_iBT2_j\,(2,1) = \\
&+r_{1j}\sin(\theta)\cos\left(\theta_{1H}^{H}\right) - r_{3j}\cos(\theta) \\
&+\left(r_{1j}\cos(\theta)\cos\left(\theta_{1H}^{H}\right) + r_{3j}\sin(\theta)\right)\theta_{2T\ell}^{T} + r_{1j}\sin\left(\theta_{1H}^{H}\right)\theta_{3T\ell}^{T} \\
&-r_{1j}\sin(\theta)\sin\left(\theta_{1H}^{H}\right)\theta_{1Am}^{A} \\
&\quad +\left(r_{1j}\cos(\theta)\cos\left(\theta_{1H}^{H}\right) + r_{3j}\sin(\theta)\right)\theta_{2Am}^{A} \\
&\quad +r_{1j}\cos(\theta)\sin\left(\theta_{1H}^{H}\right)\theta_{3Am}^{A}
\end{aligned}
\tag{E.2.63}
$$

$$
\begin{aligned}
{}_iBT2_j\,(2,2) = \\
&-r_{1j}\sin\left(\theta^H_{1H}\right) \\
&-\Big(r_{1j}\cos\left(\theta\right)\cos\left(\theta^H_{1H}\right)+r_{3j}\sin\left(\theta\right)\Big)\theta^T_{1T\ell} \\
&\quad+\Big(r_{1j}\sin\left(\theta\right)\cos\left(\theta^H_{1H}\right)-r_{3j}\cos\left(\theta\right)\Big)\theta^T_{3T\ell} \\
&-r_{1j}\cos\left(\theta^H_{1H}\right)\theta^A_{1Am}-r_{3j}\theta^A_{3Am}
\end{aligned}
\tag{E.2.64}
$$

$$
\begin{aligned}
{}_iBT2_j\,(2,3) = \\
&+r_{1j}\cos\left(\theta\right)\cos\left(\theta^H_{1H}\right)+r_{3j}\sin\left(\theta\right) \\
&-r_{1j}\sin\left(\theta^H_{1H}\right)\theta^T_{1T\ell}-\Big(r_{1j}\sin\left(\theta\right)\cos\left(\theta^H_{1H}\right)-r_{3j}\cos\left(\theta\right)\Big)\theta^T_{2T\ell} \\
&-r_{1j}\cos\left(\theta\right)\sin\left(\theta^H_{1H}\right)\theta^A_{1Am} \\
&\quad-\Big(r_{1j}\sin\left(\theta\right)\cos\left(\theta^H_{1H}\right)-r_{3j}\cos\left(\theta\right)\Big)\theta^A_{2Am} \\
&\quad-r_{1j}\sin\left(\theta\right)\sin\left(\theta^H_{1H}\right)\theta^A_{3Am}
\end{aligned}
\tag{E.2.65}
$$

$$
\begin{aligned}
{}_iBT2_j\,(3,1) = \\
&-r_{1j}\sin\left(\theta\right)\sin\left(\theta^H_{1H}\right)+r_{2j}\cos\left(\theta\right) \\
&-\Big(r_{1j}\cos\left(\theta\right)\sin\left(\theta^H_{1H}\right)+r_{2j}\sin\left(\theta\right)\Big)\theta^T_{2T\ell}+r_{1j}\cos\left(\theta^H_{1H}\right)\theta^T_{3T\ell} \\
&-r_{1j}\sin\left(\theta\right)\cos\left(\theta^H_{1H}\right)\theta^A_{1Am} \\
&\quad-\Big(r_{1j}\cos\left(\theta\right)\sin\left(\theta^H_{1H}\right)+r_{2j}\sin\left(\theta\right)\Big)\theta^A_{2Am} \\
&\quad+r_{1j}\cos\left(\theta\right)\cos\left(\theta^H_{1H}\right)\theta^A_{3Am}
\end{aligned}
\tag{E.2.66}
$$

$$
\begin{aligned}
{}_iBT2_j\,(3,2) = \\
&-r_{1j}\cos\left(\theta^H_{1H}\right) \\
&+\Big(r_{1j}\cos\left(\theta\right)\sin\left(\theta^H_{1H}\right)+r_{2j}\sin\left(\theta\right)\Big)\theta^T_{1T\ell} \\
&\quad-\Big(r_{1j}\sin\left(\theta\right)\sin\left(\theta^H_{1H}\right)-r_{2j}\cos\left(\theta\right)\Big)\theta^T_{3T\ell} \\
&+r_{1j}\sin\left(\theta^H_{1H}\right)\theta^A_{1Am}+r_{2j}\theta^A_{3Am}
\end{aligned}
\tag{E.2.67}
$$

$$
\begin{aligned}
{}_iBT2_j\,(3,3) = \\
&-r_{1j}\cos\left(\theta\right)\sin\left(\theta^H_{1H}\right)-r_{2j}\sin\left(\theta\right) \\
&-r_{1j}\cos\left(\theta^H_{1H}\right)\theta^T_{1T\ell}+\Big(r_{1j}\sin\left(\theta\right)\sin\left(\theta^H_{1H}\right)-r_{2j}\cos\left(\theta\right)\Big)\theta^T_{2T\ell} \\
&-r_{1j}\cos\left(\theta\right)\cos\left(\theta^H_{1H}\right)\theta^A_{1Am} \\
&\quad+\Big(r_{1j}\sin\left(\theta\right)\sin\left(\theta^H_{1H}\right)-r_{2j}\cos\left(\theta\right)\Big)\theta^A_{2Am} \\
&\quad-r_{1j}\sin\left(\theta\right)\cos\left(\theta^H_{1H}\right)\theta^A_{3Am}
\end{aligned}
\tag{E.2.68}
$$

The $[{}_iBT1_j]$–matrix.

$$
\begin{aligned}
&{}_iBT1_j(1,1) = \\
&\quad 2\omega r_{1j}\theta^T_{3T\ell} \\
&\quad +2\omega\Big(r_{1j}\cos(\theta)+r_{2j}\sin(\theta)\sin\left(\theta^H_{1H}\right)+r_{3j}\sin(\theta)\cos\left(\theta^H_{1H}\right)\Big)\theta^A_{3Am} \\
&\quad -\Big(r_{1j}\sin^2(\theta)-r_{2j}\cos(\theta)\sin(\theta)\sin\left(\theta^H_{1H}\right)-r_{3j}\cos\left(\theta^H_{1H}\right)\cos(\theta)\sin(\theta)\Big)\dot\theta^T_{1T\ell} \\
&\qquad +\Big(r_{2j}\cos(\theta)\cos\left(\theta^H_{1H}\right)-r_{3j}\cos(\theta)\sin\left(\theta^H_{1H}\right)\Big)\dot\theta^T_{2T\ell} \\
&\qquad -\Big[2r_{1j}\cos(\theta)\sin(\theta)-r_{2j}\Big(\cos^2(\theta)\sin\left(\theta^H_{1H}\right)-\sin^2(\theta)\sin\left(\theta^H_{1H}\right)\Big) \\
&\qquad\quad -r_{3j}\Big(\cos^2(\theta)\cos\left(\theta^H_{1H}\right)-\sin^2(\theta)\cos\left(\theta^H_{1H}\right)\Big)\Big]\dot\theta^T_{3T\ell} \\
&\quad +2\Big(r_{2j}\sin(\theta)\sin\left(\theta^H_{1H}\right)+r_{3j}\sin(\theta)\cos\left(\theta^H_{1H}\right)\Big)\dot\theta^A_{1Am}-2r_{1j}\sin(\theta)\,\dot\theta^A_{3Am} \\
&\quad +2\Big(r_{2j}\sin(\theta)\sin\left(\theta^H_{1H}\right)+r_{3j}\sin(\theta)\cos\left(\theta^H_{1H}\right)\Big)\dot\theta^H_{1H}
\end{aligned}
\tag{E.2.69}
$$

$$
\begin{aligned}
&{}_iBT1_j(1,2) = \\
&\quad -2\omega r_{1j} \\
&\quad +2\omega\Big(r_{2j}\cos\left(\theta^H_{1H}\right)-r_{3j}\sin\left(\theta^H_{1H}\right)\Big)\theta^A_{3Am} \\
&\quad -r_{1j}\dot\theta^T_{2T\ell}-\Big(r_{2j}\sin(\theta)\cos\left(\theta^H_{1H}\right)-r_{3j}\sin(\theta)\sin\left(\theta^H_{1H}\right)\Big)\dot\theta^T_{3T\ell} \\
&\quad +2\Big(r_{2j}\cos\left(\theta^H_{1H}\right)-r_{3j}\sin\left(\theta^H_{1H}\right)\Big)\dot\theta^A_{1Am}-2r_{1j}\dot\theta^A_{2Am} \\
&\quad +2\Big(r_{2j}\cos\left(\theta^H_{1H}\right)-r_{3j}\sin\left(\theta^H_{1H}\right)\Big)\dot\theta^H_{1H}
\end{aligned}
\tag{E.2.70}
$$

$$
\begin{aligned}
&{}_iBT1_j(1,3) = \\
&\quad -2\omega r_{1j}\theta^T_{1T\ell} \\
&\quad -2\omega\Big(r_{1j}\sin(\theta)-r_{2j}\cos(\theta)\sin\left(\theta^H_{1H}\right)-r_{3j}\cos(\theta)\cos\left(\theta^H_{1H}\right)\Big)\theta^A_{3Am} \\
&\quad -\Big(r_{1j}\cos^2(\theta)+r_{2j}\cos(\theta)\sin(\theta)\sin\left(\theta^H_{1H}\right)+r_{3j}\cos\left(\theta^H_{1H}\right)\cos(\theta)\sin(\theta)\Big)\dot\theta^T_{3T\ell} \\
&\quad +2\Big(r_{2j}\cos(\theta)\sin\left(\theta^H_{1H}\right)+r_{3j}\cos(\theta)\cos\left(\theta^H_{1H}\right)\Big)\dot\theta^A_{1Am}-2r_{1j}\cos(\theta)\,\dot\theta^A_{3Am} \\
&\quad +2\Big(r_{2j}\cos(\theta)\sin\left(\theta^H_{1H}\right)+r_{3j}\cos(\theta)\cos\left(\theta^H_{1H}\right)\Big)\dot\theta^H_{1H}
\end{aligned}
\tag{E.2.71}
$$

$$
\begin{aligned}
{}_iBT1_j(2,1) = \\
&2\omega\Big(r_{1j}\cos(\theta)\cos\left(\theta_{1H}^H\right) + r_{2j}\sin(\theta)\cos\left(\theta_{1H}^H\right)\sin\left(\theta_{1H}^H\right) + r_{3j}\sin(\theta)\cos^2\left(\theta_{1H}^H\right)\Big) \\
&-2\omega\Big(r_{1j}\sin(\theta)\cos\left(\theta_{1H}^H\right) - r_{2j}\cos(\theta)\cos\left(\theta_{1H}^H\right)\sin\left(\theta_{1H}^H\right) - r_{3j}\cos(\theta)\cos^2\left(\theta_{1H}^H\right)\Big)\theta_{2T\ell}^T \\
&\quad +2\omega\Big(r_{2j}\sin^2\left(\theta_{1H}^H\right) + r_{3j}\cos\left(\theta_{1H}^H\right)\sin\left(\theta_{1H}^H\right)\Big)\theta_{3T\ell}^T \\
&-2\omega\Big(r_{1j}\cos(\theta)\sin\left(\theta_{1H}^H\right) - r_{2j}\sin(\theta)\cos^2\left(\theta_{1H}^H\right) \\
&\quad +r_{2j}\sin(\theta)\sin^2\left(\theta_{1H}^H\right) + 2r_{3j}\sin(\theta)\cos\left(\theta_{1H}^H\right)\sin\left(\theta_{1H}^H\right)\Big)\theta_{1Am}^A \\
&\quad -2\omega\Big[r_{1j}\sin(\theta)\cos\left(\theta_{1H}^H\right) - r_{2j}\Big(\cos(\theta)\cos\left(\theta_{1H}^H\right)\sin\left(\theta_{1H}^H\right) - \cos(\theta)\cos^2\left(\theta_{1H}^H\right)\Big) \\
&\qquad -r_{3j}\Big(\cos(\theta)\cos^2\left(\theta_{1H}^H\right) + \cos(\theta)\cos\left(\theta_{1H}^H\right)\sin\left(\theta_{1H}^H\right)\Big)\Big]\theta_{3Am}^A \\
&+\Big[r_{1j}\cos(\theta)\sin(\theta)\sin\left(\theta_{1H}^H\right) + r_{2j}\Big(\sin^2(\theta)\sin^2\left(\theta_{1H}^H\right) - 1\Big) \\
&\quad +r_{3j}\sin\left(\theta_{1H}^H\right)\sin^2(\theta)\cos\left(\theta_{1H}^H\right)\Big]\dot{\theta}_{1T\ell}^T \\
&\quad +\Big[r_{1j}\cos(\theta)\cos\left(\theta_{1H}^H\right) + 2r_{2j}\sin(\theta)\cos\left(\theta_{1H}^H\right)\sin\left(\theta_{1H}^H\right) \\
&\qquad +r_{3j}\Big(\sin(\theta)\cos^2\left(\theta_{1H}^H\right) - \sin(\theta)\sin^2\left(\theta_{1H}^H\right)\Big)\Big]\dot{\theta}_{2T\ell}^T \\
&\quad +\Big[r_{1j}\Big(\cos^2(\theta)\sin\left(\theta_{1H}^H\right) - \sin^2(\theta)\sin\left(\theta_{1H}^H\right)\Big) + 2r_{2j}\cos(\theta)\sin(\theta)\sin^2\left(\theta_{1H}^H\right) \\
&\qquad +2r_{3j}\cos(\theta)\sin(\theta)\cos\left(\theta_{1H}^H\right)\sin\left(\theta_{1H}^H\right)\Big]\dot{\theta}_{3T\ell}^T \\
&-2r_{2j}\cos(\theta)\dot{\theta}_{1Am}^A \\
&\quad +2\Big(r_{1j}\cos(\theta)\cos\left(\theta_{1H}^H\right) + r_{2j}\sin(\theta)\cos\left(\theta_{1H}^H\right)\sin\left(\theta_{1H}^H\right) + r_{3j}\sin(\theta)\cos^2\left(\theta_{1H}^H\right)\Big)\dot{\theta}_{2Am}^A \\
&\quad +2\Big(r_{1j}\cos(\theta)\sin\left(\theta_{1H}^H\right) - r_{2j}\sin(\theta)\cos^2\left(\theta_{1H}^H\right) + r_{3j}\sin(\theta)\cos\left(\theta_{1H}^H\right)\sin\left(\theta_{1H}^H\right)\Big)\dot{\theta}_{3Am}^A \\
&-2r_{2j}\cos(\theta)\dot{\theta}_{1H}^H
\end{aligned}
\tag{E.2.72}
$$

$$
\begin{aligned}
{}_iBT1_j(2,2) = \\
&-2\omega\Big(r_{2j}\sin^2\left(\theta_{1H}^H\right) + r_{3j}\cos\left(\theta_{1H}^H\right)\sin\left(\theta_{1H}^H\right)\Big) \\
&+2\omega\Big(r_{1j}\sin(\theta)\cos\left(\theta_{1H}^H\right) - r_{2j}\cos(\theta)\cos\left(\theta_{1H}^H\right)\sin\left(\theta_{1H}^H\right) - r_{3j}\cos(\theta)\cos^2\left(\theta_{1H}^H\right)\Big)\theta_{1T\ell}^T \\
&\quad +2\omega\Big(r_{1j}\cos(\theta)\cos\left(\theta_{1H}^H\right) + r_{2j}\sin(\theta)\cos\left(\theta_{1H}^H\right)\sin\left(\theta_{1H}^H\right) + r_{3j}\sin(\theta)\cos^2\left(\theta_{1H}^H\right)\Big)\theta_{3T\ell}^T \\
&-2\omega\Big[2r_{2j}\cos\left(\theta_{1H}^H\right)\sin\left(\theta_{1H}^H\right) + r_{3j}\Big(\cos^2\left(\theta_{1H}^H\right) - \sin^2\left(\theta_{1H}^H\right)\Big)\Big]\theta_{1Am}^A \\
&\quad +2\omega r_{1j}\cos\left(\theta_{1H}^H\right)\theta_{3Am}^A \\
&-\Big(r_{2j}\sin^2\left(\theta_{1H}^H\right) + r_{3j}\cos\left(\theta_{1H}^H\right)\sin\left(\theta_{1H}^H\right)\Big)\dot{\theta}_{2T\ell}^T \\
&\quad -\Big[r_{1j}\sin(\theta)\cos\left(\theta_{1H}^H\right) - 2r_{2j}\cos(\theta)\cos\left(\theta_{1H}^H\right)\sin\left(\theta_{1H}^H\right) \\
&\qquad -r_{3j}\Big(\cos(\theta)\cos^2\left(\theta_{1H}^H\right) - \cos(\theta)\ sin^2\left(\theta_{1H}^H\right)\Big)\Big]\dot{\theta}_{3T\ell}^T \\
&-2\Big(r_{2j}\sin^2\left(\theta_{1H}^H\right) + r_{3j}\cos\left(\theta_{1H}^H\right)\sin\left(\theta_{1H}^H\right)\Big)\dot{\theta}_{2Am}^A \\
&\quad +2\Big(r_{2j}\cos\left(\theta_{1H}^H\right)\sin\left(\theta_{1H}^H\right) - r_{3j}\sin^2\left(\theta_{1H}^H\right)\Big)\dot{\theta}_{3Am}^A
\end{aligned}
\tag{E.2.73}
$$

$$
\begin{aligned}
{}_iBT1_j(2,3) = \\
&-2\omega\Big(r_{1j}\sin(\theta)\cos\left(\theta_{1H}^H\right) - r_{2j}\cos(\theta)\cos\left(\theta_{1H}^H\right)\sin\left(\theta_{1H}^H\right) - r_{3j}\cos(\theta)\cos^2\left(\theta_{1H}^H\right)\Big) \\
&-2\omega\Big(r_{2j}\sin^2\left(\theta_{1H}^H\right) + r_{3j}\cos\left(\theta_{1H}^H\right)\sin\left(\theta_{1H}^H\right)\Big)\theta_{1T\ell}^T \\
&-2\omega\Big(r_{1j}\cos(\theta)\cos\left(\theta_{1H}^H\right) + r_{2j}\sin(\theta)\cos\left(\theta_{1H}^H\right)\sin\left(\theta_{1H}^H\right) + r_{3j}\sin(\theta)\cos^2\left(\theta_{1H}^H\right)\Big)\theta_{2T\ell}^T \\
&+2\omega\Big[r_{1j}\sin(\theta)\sin\left(\theta_{1H}^H\right) + r_{2j}\Big(\cos(\theta)\cos^2\left(\theta_{1H}^H\right) - \cos(\theta)\sin^2\left(\theta_{1H}^H\right)\Big) \\
&\qquad -2r_{3j}\cos(\theta)\cos\left(\theta_{1H}^H\right)\sin\left(\theta_{1H}^H\right)\Big]\theta_{1Am}^A \\
&\quad -2\omega\Big(r_{1j}\cos(\theta)\cos\left(\theta_{1H}^H\right) + r_{2j}\sin(\theta)\cos\left(\theta_{1H}^H\right)\sin\left(\theta_{1H}^H\right) + r_{3j}\sin(\theta)\cos^2\left(\theta_{1H}^H\right)\Big)\theta_{2Am}^A \\
&\quad +2\omega\Big(r_{2j}\sin(\theta)\cos^2\left(\theta_{1H}^H\right) - r_{3j}\sin(\theta)\cos\left(\theta_{1H}^H\right)\sin\left(\theta_{1H}^H\right)\Big)\theta_{3Am}^A \\
&-\Big[r_{1j}\cos(\theta)\sin(\theta)\sin\left(\theta_{1H}^H\right) + r_{2j}\Big(1-\cos^2(\theta)\sin^2\left(\theta_{1H}^H\right)\Big) \\
&\quad -r_{3j}\sin\left(\theta_{1H}^H\right)\cos^2(\theta)\cos\left(\theta_{1H}^H\right)\Big]\dot{\theta}_{3T\ell}^T \\
&+2r_{2j}\sin(\theta)\,\dot{\theta}_{1Am}^A \\
&\quad -2\Big(r_{1j}\sin(\theta)\cos\left(\theta_{1H}^H\right) - r_{2j}\cos(\theta)\cos\left(\theta_{1H}^H\right)\sin\left(\theta_{1H}^H\right) - r_{3j}\cos(\theta)\cos^2\left(\theta_{1H}^H\right)\Big)\dot{\theta}_{2Am}^A \\
&\quad -2\Big(r_{1j}\sin(\theta)\sin\left(\theta_{1H}^H\right) + r_{2j}\cos(\theta)\cos^2\left(\theta_{1H}^H\right) - r_{3j}\cos(\theta)\cos\left(\theta_{1H}^H\right)\sin\left(\theta_{1H}^H\right)\Big)\dot{\theta}_{3Am}^A \\
&+2r_{2j}\sin(\theta)\,\dot{\theta}_{1H}^H
\end{aligned}
\tag{E.2.74}
$$

$$
\begin{aligned}
&{}_iBT1_j(3,1) = \\
&\quad -2\omega\Big(r_{1j}\cos(\theta)\sin\left(\theta_{1H}^H\right) + r_{2j}\sin(\theta)\sin^2\left(\theta_{1H}^H\right) + r_{3j}\sin(\theta)\cos\left(\theta_{1H}^H\right)\sin\left(\theta_{1H}^H\right)\Big) \\
&\quad +2\omega\Big(r_{1j}\sin(\theta)\sin\left(\theta_{1H}^H\right) - r_{2j}\cos(\theta)\sin^2\left(\theta_{1H}^H\right) - r_{3j}\cos(\theta)\cos\left(\theta_{1H}^H\right)\sin\left(\theta_{1H}^H\right)\Big)\theta_{2T\ell}^T \\
&\qquad +2\omega\Big(r_{2j}\cos\left(\theta_{1H}^H\right)\sin\left(\theta_{1H}^H\right) + r_{3j}\cos^2\left(\theta_{1H}^H\right)\Big)\theta_{3T\ell}^T \\
&\quad -2\omega\Big[r_{1j}\cos(\theta)\cos\left(\theta_{1H}^H\right) + 2r_{2j}\sin(\theta)\cos\left(\theta_{1H}^H\right)\sin\left(\theta_{1H}^H\right) \\
&\qquad +r_{3j}\Big(\sin(\theta)\cos^2\left(\theta_{1H}^H\right) - \sin(\theta)\sin^2\left(\theta_{1H}^H\right)\Big)\Big]\theta_{1Am}^A \\
&\qquad +2\omega\Big(r_{1j}\sin(\theta)\sin\left(\theta_{1H}^H\right) - r_{2j}\cos(\theta)\sin^2\left(\theta_{1H}^H\right) - r_{3j}\cos(\theta)\cos\left(\theta_{1H}^H\right)\sin\left(\theta_{1H}^H\right)\Big)\theta_{2Am}^A \\
&\qquad +2\omega\Big(r_{2j}\cos(\theta)\cos\left(\theta_{1H}^H\right)\sin\left(\theta_{1H}^H\right) - r_{3j}\cos(\theta)\sin^2\left(\theta_{1H}^H\right)\Big)\theta_{3Am}^A \\
&\quad +\Big[r_{1j}\cos\left(\theta_{1H}^H\right)\cos(\theta)\sin(\theta) + r_{2j}\sin\left(\theta_{1H}^H\right)\sin^2(\theta)\cos\left(\theta_{1H}^H\right) \\
&\qquad +r_{3j}\Big(\cos\left(\theta_{1H}^H\right)\sin^2(\theta)\cos\left(\theta_{1H}^H\right) - 1\Big)\Big]\dot{\theta}_{1T\ell}^T \\
&\qquad -\Big[r_{1j}\cos(\theta)\sin\left(\theta_{1H}^H\right) - r_{2j}\Big(\sin(\theta)\cos^2\left(\theta_{1H}^H\right) - \sin(\theta)\sin^2\left(\theta_{1H}^H\right)\Big) \\
&\qquad\quad +2r_{3j}\sin(\theta)\cos\left(\theta_{1H}^H\right)\sin\left(\theta_{1H}^H\right)\Big]\dot{\theta}_{2T\ell}^T \\
&\qquad +\Big[r_{1j}\Big(\cos^2(\theta)\cos\left(\theta_{1H}^H\right) - \sin^2(\theta)\cos\left(\theta_{1H}^H\right)\Big) + 2r_{2j}\cos(\theta)\sin(\theta)\cos\left(\theta_{1H}^H\right)\sin\left(\theta_{1H}^H\right) \\
&\qquad\quad +2r_{3j}\cos(\theta)\sin(\theta)\cos^2\left(\theta_{1H}^H\right)\Big]\dot{\theta}_{3T\ell}^T \\
&\quad -2\cos(\theta)\dot{\theta}_{1Am}^A \\
&\qquad -2\Big(r_{1j}\cos(\theta)\sin\left(\theta_{1H}^H\right) + r_{2j}\sin(\theta)\sin^2\left(\theta_{1H}^H\right) + r_{3j}\sin(\theta)\cos\left(\theta_{1H}^H\right)\sin\left(\theta_{1H}^H\right)\Big)\dot{\theta}_{2Am}^A \\
&\qquad +2\Big(r_{1j}\cos(\theta)\cos\left(\theta_{1H}^H\right) + r_{2j}\sin(\theta)\cos\left(\theta_{1H}^H\right)\sin\left(\theta_{1H}^H\right) - r_{3j}\sin(\theta)\sin^2\left(\theta_{1H}^H\right)\Big)\dot{\theta}_{3Am}^A \\
&\quad -2r_{3j}\cos(\theta)\dot{\theta}_{1H}^H
\end{aligned}
\tag{E.2.75}
$$

$$
\begin{aligned}
&{}_iBT1_j(3,2) = \\
&\quad -2\omega\Big(r_{2j}\cos\left(\theta_{1H}^H\right)\sin\left(\theta_{1H}^H\right) + r_{3j}\cos^2\left(\theta_{1H}^H\right)\Big) \\
&\quad -2\omega\Big(r_{1j}\sin\left(\theta\right)\sin\left(\theta_{1H}^H\right) - r_{2j}\cos\left(\theta\right)\sin^2\left(\theta_{1H}^H\right) - r_{3j}\cos\left(\theta\right)\cos\left(\theta_{1H}^H\right)\sin\left(\theta_{1H}^H\right)\Big)\theta_{1T\ell}^T \\
&\qquad -2\omega\Big(r_{1j}\cos\left(\theta\right)\sin\left(\theta_{1H}^H\right) + r_{2j}\sin\left(\theta\right)\sin^2\left(\theta_{1H}^H\right) + r_{3j}\sin\left(\theta\right)\cos\left(\theta_{1H}^H\right)\sin\left(\theta_{1H}^H\right)\Big)\theta_{3T\ell}^T \\
&\quad -2\omega\Big[r_{2j}\Big(\cos^2\left(\theta_{1H}^H\right) - \sin^2\left(\theta_{1H}^H\right)\Big) - 2r_{3j}\cos\left(\theta_{1H}^H\right)\sin\left(\theta_{1H}^H\right)\Big]\theta_{1Am}^A - 2\omega r_{1j}\sin\left(\theta_{1H}^H\right)\theta_{3Am}^A \\
&\quad -\Big(r_{2j}\cos\left(\theta_{1H}^H\right)\sin\left(\theta_{1H}^H\right) + r_{3j}\cos^2\left(\theta_{1H}^H\right)\Big)\dot{\theta}_{2T\ell}^T \\
&\qquad +\Big[r_{1j}\sin\left(\theta\right)\sin\left(\theta_{1H}^H\right) + r_{2j}\Big(\cos\left(\theta\right)\cos^2\left(\theta_{1H}^H\right) - \cos\left(\theta\right)\sin^2\left(\theta_{1H}^H\right)\Big) \\
&\qquad\quad -2r_{3j}\cos\left(\theta\right)\cos\left(\theta_{1H}^H\right)\sin\left(\theta_{1H}^H\right)\Big]\dot{\theta}_{3T\ell}^T \\
&\quad -2\Big[r_{2j}\Big(\cos\left(\theta_{1H}^H\right)\sin\left(\theta_{1H}^H\right) - \cos^2\left(\theta_{1H}^H\right)\Big) \\
&\qquad +r_{3j}\Big(\cos^2\left(\theta_{1H}^H\right) + \cos\left(\theta_{1H}^H\right)\sin\left(\theta_{1H}^H\right)\Big)\Big]\dot{\theta}_{3Am}^A
\end{aligned}
\tag{E.2.76}
$$

$$
\begin{aligned}
&{}_iBT1_j(3,3) = \\
&\quad +2\omega\Big(r_{1j}\sin\left(\theta\right)\sin\left(\theta_{1H}^H\right) - r_{2j}\cos\left(\theta\right)\sin^2\left(\theta_{1H}^H\right) - r_{3j}\cos\left(\theta\right)\cos\left(\theta_{1H}^H\right)\sin\left(\theta_{1H}^H\right)\Big) \\
&\quad -2\omega\Big(r_{2j}\cos\left(\theta_{1H}^H\right)\sin\left(\theta_{1H}^H\right) + r_{3j}\cos^2\left(\theta_{1H}^H\right)\Big)\theta_{1T\ell}^T \\
&\qquad +2\omega\Big(r_{1j}\cos\left(\theta\right)\sin\left(\theta_{1H}^H\right) + r_{2j}\sin\left(\theta\right)\sin^2\left(\theta_{1H}^H\right) + r_{3j}\sin\left(\theta\right)\cos\left(\theta_{1H}^H\right)\sin\left(\theta_{1H}^H\right)\Big)\theta_{2T\ell}^T \\
&\quad +2\omega\Big[r_{1j}\sin\left(\theta\right)\cos\left(\theta_{1H}^H\right) - 2r_{2j}\cos\left(\theta\right)\cos\left(\theta_{1H}^H\right)\sin\left(\theta_{1H}^H\right) \\
&\qquad\quad -r_{3j}\Big(\cos\left(\theta\right)\cos^2\left(\theta_{1H}^H\right) - \cos\left(\theta\right)\sin^2\left(\theta_{1H}^H\right)\Big)\Big]\theta_{1Am}^A \\
&\qquad +2\omega\Big(r_{1j}\cos\left(\theta\right)\sin\left(\theta_{1H}^H\right) + r_{2j}\sin\left(\theta\right)\sin^2\left(\theta_{1H}^H\right) + r_{3j}\sin\left(\theta\right)\cos\left(\theta_{1H}^H\right)\sin\left(\theta_{1H}^H\right)\Big)\theta_{2Am}^A \\
&\qquad -2\omega\Big(r_{2j}\sin\left(\theta\right)\cos\left(\theta_{1H}^H\right)\sin\left(\theta_{1H}^H\right) - r_{3j}\sin\left(\theta\right)\sin^2\left(\theta_{1H}^H\right)\Big)\theta_{3Am}^A \\
&\quad -\Big[r_{1j}\cos\left(\theta_{1H}^H\right)\cos\left(\theta\right)\sin\left(\theta\right) - r_{2j}\sin\left(\theta_{1H}^H\right)\cos^2\left(\theta\right)\cos\left(\theta_{1H}^H\right) \\
&\qquad\quad -r_{3j}\Big(\cos\left(\theta_{1H}^H\right)\cos^2\left(\theta\right)\cos\left(\theta_{1H}^H\right) - 1\Big)\Big]\dot{\theta}_{3T\ell}^T \\
&\quad +2r_{3j}\sin\left(\theta\right)\dot{\theta}_{1Am}^A \\
&\qquad +2\Big(r_{1j}\sin\left(\theta\right)\sin\left(\theta_{1H}^H\right) - r_{2j}\cos\left(\theta\right)\sin^2\left(\theta_{1H}^H\right) - r_{3j}\cos\left(\theta\right)\cos\left(\theta_{1H}^H\right)\sin\left(\theta_{1H}^H\right)\Big)\dot{\theta}_{2Am}^A \\
&\qquad -2\Big(r_{1j}\sin\left(\theta\right)\cos\left(\theta_{1H}^H\right) - r_{2j}\cos\left(\theta\right)\cos\left(\theta_{1H}^H\right)\sin\left(\theta_{1H}^H\right) + r_{3j}\cos\left(\theta\right)\sin^2\left(\theta_{1H}^H\right)\Big)\dot{\theta}_{3Am}^A \\
&\quad +2r_{3j}\sin\left(\theta\right)\dot{\theta}_{1H}^H
\end{aligned}
\tag{E.2.77}
$$

The $[{}_iBS2_j]$–matrix.

$$[{}_iBS2_j] =$$

$$\left[\begin{array}{c|c|c}
\begin{array}{l} -\left(-r_{2j}\cos\left(\theta^H_{1H}\right) - r_{3j}\sin\left(\theta^H_{1H}\right)\right)\theta^A_{2Am} \\ -\left(r_{2j}\sin\left(\theta^H_{1H}\right) + r_{3j}\cos\left(\theta^H_{1H}\right)\right)\theta^A_{3Am} \end{array} & \begin{array}{l} r_{2j}\sin\left(\theta^H_{1H}\right) + r_{3j}\cos\left(\theta^H_{1H}\right) \\ +\left(r_{2j}\cos\left(\theta^H_{1H}\right) - r_{3j}\sin\left(\theta^H_{1H}\right)\right)\theta^A_{1Am} \end{array} & \begin{array}{l} -r_{2j}\cos\left(\theta^H_{1H}\right) + r_{3j}\sin\left(\theta^H_{1H}\right) \\ +\left(r_{2j}\sin\left(\theta^H_{1H}\right) + r_{3j}\cos\left(\theta^H_{1H}\right)\right)\theta^A_{1Am} \end{array} \\ \hline
\begin{array}{l} -r_{3j} \\ +r_{1j}\cos\left(\theta^H_{1H}\right)\theta^A_{2Am} + r_{1j}\sin\left(\theta^H_{1H}\right)\theta^A_{3Am} \end{array} & \begin{array}{l} -r_{1j}\sin\left(\theta^H_{1H}\right) \\ -r_{1j}\cos\left(\theta^H_{1H}\right)\theta^A_{1Am} - r_{3j}\theta^A_{3Am} \end{array} & \begin{array}{l} +r_{1j}\cos\left(\theta^H_{1H}\right) \\ -r_{1j}\sin\left(\theta^H_{1H}\right)\theta^A_{1Am} + r_{3j}\theta^A_{2Am} \end{array} \\ \hline
\begin{array}{l} +r_{2j} \\ -r_{1j}\sin\left(\theta^H_{1H}\right)\theta^A_{2Am} + r_{1j}\cos\left(\theta^H_{1H}\right)\theta^A_{3Am} \end{array} & \begin{array}{l} -r_{1j}\cos\left(\theta^H_{1H}\right) \\ +r_{1j}\sin\left(\theta^H_{1H}\right)\theta^A_{1Am} + r_{2j}\theta^A_{3Am} \end{array} & \begin{array}{l} -r_{1j}\sin\left(\theta^H_{1H}\right) \\ -r_{1j}\cos\left(\theta^H_{1H}\right)\theta^A_{1Am} - r_{2j}\theta^A_{2Am} \end{array}
\end{array}\right] \tag{E.2.78}$$

The $[{}_iBS1_j]$–matrix.

$$\begin{aligned}
{}_iBS1_j(1,1) = \\
&2\omega\left(r_{2j}\cos\left(\theta^H_{1H}\right) - r_{3j}\sin\left(\theta^H_{1H}\right)\right) \\
&-2\omega\left(r_{2j}\sin\left(\theta^H_{1H}\right) + r_{3j}\cos\left(\theta^H_{1H}\right)\right)\theta^A_{1Am} \\
&+2\omega r_{1j}\theta^A_{3Am} \\
&+\left(r_{2j}\cos\left(\theta^H_{1H}\right) - r_{3j}\sin\left(\theta^H_{1H}\right)\right)\dot{\theta}^A_{2Am} \\
&+\left(r_{2j}\sin\left(\theta^H_{1H}\right) + r_{3j}\cos\left(\theta^H_{1H}\right)\right)\dot{\theta}^A_{3Am}
\end{aligned} \tag{E.2.79}$$

$$\begin{aligned}
{}_iBS1_j(1,2) = \\
&-2\omega r_{1j} \\
&+2\omega\left(r_{2j}\cos\left(\theta^H_{1H}\right) - r_{3j}\sin\left(\theta^H_{1H}\right)\right)\theta^A_{3Am} \\
&-r_{1j}\dot{\theta}^A_{2Am} \\
&+2\left(r_{2j}\cos\left(\theta^H_{1H}\right) - r_{3j}\sin\left(\theta^H_{1H}\right)\right)\dot{\theta}^H_{1H}
\end{aligned} \tag{E.2.80}$$

$$\begin{aligned}
{}_iBS1_j(1,3) = \\
&-2\omega\left(r_{2j}\cos\left(\theta^H_{1H}\right) - r_{3j}\sin\left(\theta^H_{1H}\right)\right)\theta^A_{2Am} \\
&-r_{1j}\dot{\theta}^A_{3Am} \\
&+2\left(r_{2j}\sin\left(\theta^H_{1H}\right) + r_{3j}\cos\left(\theta^H_{1H}\right)\right)\dot{\theta}^H_{1H}
\end{aligned} \tag{E.2.81}$$

$$
\begin{aligned}
{}_{i}BS1_j(2,1) = \\
&+2\omega\Big(r_{2j}\cos\left(\theta_{1H}^{H}\right)\sin\left(\theta_{1H}^{H}\right) - r_{3j}\sin^2\left(\theta_{1H}^{H}\right)\Big)\theta_{2Am}^{A} \\
&-2\omega\Big(r_{2j}\cos^2\left(\theta_{1H}^{H}\right) - r_{3j}\cos\left(\theta_{1H}^{H}\right)\sin\left(\theta_{1H}^{H}\right)\Big)\theta_{3Am}^{A} \\
&-r_{2j}\dot{\theta}_{1Am}^{A} + r_{1j}\cos\left(\theta_{1H}^{H}\right)\dot{\theta}_{2Am}^{A} + r_{1j}\sin\left(\theta_{1H}^{H}\right)\dot{\theta}_{3Am}^{A} \\
&-2r_{2j}\dot{\theta}_{1H}^{H}
\end{aligned}
\tag{E.2.82}
$$

$$
\begin{aligned}
{}_{i}BS1_j(2,2) = \\
&-2\omega\Big(r_{2j}\sin^2\left(\theta_{1H}^{H}\right) + r_{3j}\cos\left(\theta_{1H}^{H}\right)\sin\left(\theta_{1H}^{H}\right)\Big) \\
&-2\omega\Big[2r_{2j}\cos\left(\theta_{1H}^{H}\right)\sin\left(\theta_{1H}^{H}\right) + r_{3j}\Big(\cos^2\left(\theta_{1H}^{H}\right) - \sin^2\left(\theta_{1H}^{H}\right)\Big)\Big]\theta_{1Am}^{A} \\
&+2\omega r_{1j}\cos\left(\theta_{1H}^{H}\right)\theta_{3Am}^{A} \\
&-\Big(r_{2j}\sin^2\left(\theta_{1H}^{H}\right) + r_{3j}\cos\left(\theta_{1H}^{H}\right)\sin\left(\theta_{1H}^{H}\right)\Big)\dot{\theta}_{2Am}^{A} \\
&+\Big[2r_{2j}\cos\left(\theta_{1H}^{H}\right)\sin\left(\theta_{1H}^{H}\right) + r_{3j}\Big(\cos^2\left(\theta_{1H}^{H}\right) - \sin^2\left(\theta_{1H}^{H}\right)\Big)\Big]\dot{\theta}_{3Am}^{A}
\end{aligned}
\tag{E.2.83}
$$

$$
\begin{aligned}
{}_{i}BS1_j(2,3) = \\
&+2\omega\Big(r_{2j}\cos\left(\theta_{1H}^{H}\right)\sin\left(\theta_{1H}^{H}\right) - r_{3j}\sin^2\left(\theta_{1H}^{H}\right)\Big) \\
&+2\omega\Big[r_{2j}\Big(\cos^2\left(\theta_{1H}^{H}\right) - \sin^2\left(\theta_{1H}^{H}\right)\Big) - 2r_{3j}\cos\left(\theta_{1H}^{H}\right)\sin\left(\theta_{1H}^{H}\right)\Big]\theta_{1Am}^{A} \\
&+2\omega r_{1j}\sin\left(\theta_{1H}^{H}\right)\theta_{3Am}^{A} \\
&-\Big(r_{2j}\cos^2\left(\theta_{1H}^{H}\right) - r_{3j}\cos\left(\theta_{1H}^{H}\right)\sin\left(\theta_{1H}^{H}\right)\Big)\dot{\theta}_{3Am}^{A}
\end{aligned}
\tag{E.2.84}
$$

$$
\begin{aligned}
{}_{i}BS1_j(3,1) = \\
&+2\omega\Big(r_{2j}\cos^2\left(\theta_{1H}^{H}\right) - r_{3j}\cos\left(\theta_{1H}^{H}\right)\sin\left(\theta_{1H}^{H}\right)\Big)\theta_{2Am}^{A} \\
&+2\omega\Big(r_{2j}\cos\left(\theta_{1H}^{H}\right)\sin\left(\theta_{1H}^{H}\right) - r_{3j}\sin^2\left(\theta_{1H}^{H}\right)\Big)\theta_{3Am}^{A} \\
&-r_{3j}\dot{\theta}_{1Am}^{A} - r_{1j}\sin\left(\theta_{1H}^{H}\right)\dot{\theta}_{2Am}^{A} + r_{1j}\cos\left(\theta_{1H}^{H}\right)\dot{\theta}_{3Am}^{A} \\
&-2r_{3j}\dot{\theta}_{1H}^{H}
\end{aligned}
\tag{E.2.85}
$$

$$
\begin{aligned}
{}_{i}BS1_j(3,2) = \\
&-2\omega\Big(r_{2j}\cos\left(\theta_{1H}^{H}\right)\sin\left(\theta_{1H}^{H}\right) + r_{3j}\cos^2\left(\theta_{1H}^{H}\right)\Big) \\
&-2\omega\Big[r_{2j}\Big(\cos^2\left(\theta_{1H}^{H}\right) - \sin^2\left(\theta_{1H}^{H}\right)\Big) - 2r_{3j}\cos\left(\theta_{1H}^{H}\right)\sin\left(\theta_{1H}^{H}\right)\Big]\theta_{1Am}^{A} \\
&-2\omega r_{1j}\sin\left(\theta_{1H}^{H}\right)\theta_{3Am}^{A} - \Big(r_{2j}\cos\left(\theta_{1H}^{H}\right)\sin\left(\theta_{1H}^{H}\right) + r_{3j}\cos^2\left(\theta_{1H}^{H}\right)\Big)\dot{\theta}_{2Am}^{A} \\
&+\Big[r_{2j}\Big(\cos^2\left(\theta_{1H}^{H}\right) - \sin^2\left(\theta_{1H}^{H}\right)\Big) - 2r_{3j}\cos\left(\theta_{1H}^{H}\right)\sin\left(\theta_{1H}^{H}\right)\Big]\dot{\theta}_{3Am}^{A}
\end{aligned}
\tag{E.2.86}
$$

$$
\begin{aligned}
{}_iBS1_j(3,3) = \\
&+2\omega\left(r_{2j}\cos^2\left(\theta_{1H}^H\right) - r_{3j}\cos\left(\theta_{1H}^H\right)\sin\left(\theta_{1H}^H\right)\right) \\
&-2\omega\left[2r_{2j}\cos\left(\theta_{1H}^H\right)\sin\left(\theta_{1H}^H\right) + r_{3j}\left(\cos^2\left(\theta_{1H}^H\right) - \sin^2\left(\theta_{1H}^H\right)\right)\right]\theta_{1Am}^A \\
&+2\omega r_{1j}\cos\left(\theta_{1H}^H\right)\theta_{3Am}^A \\
&+\left(r_{2j}\cos\left(\theta_{1H}^H\right)\sin\left(\theta_{1H}^H\right) - r_{3j}\sin^2\left(\theta_{1H}^H\right)\right)\dot{\theta}_{3Am}^A
\end{aligned}
\tag{E.2.87}
$$

The $[{}_iBS0_j]$–matrix.

$$[{}_iBS0_j] =$$

$$(\omega)^2 \left[\begin{array}{c|c|c} 0 & 0 & r_{2j}\cos\left(\theta_{1H}^H\right) - r_{3j}\sin\left(\theta_{1H}^H\right) \\ \hline -2r_{2j}\cos\left(\theta_{1H}^H\right)\sin\left(\theta_{1H}^H\right) & 0 & r_{1j}\cos\left(\theta_{1H}^H\right) \\ -r_{3j}\left[\cos^2\left(\theta_{1H}^H\right) - \sin^2\left(\theta_{1H}^H\right)\right] & & \\ \hline -r_{2j}\left[\cos^2\left(\theta_{1H}^H\right) - \sin^2\left(\theta_{1H}^H\right)\right] & 0 & -r_{1j}\sin\left(\theta_{1H}^H\right) \\ +2r_{3j}\cos\left(\theta_{1H}^H\right)\sin\left(\theta_{1H}^H\right) & & \end{array}\right] \tag{E.2.88}$$

The $\left\{{}_iBH2_j^B\right]$–vector.

$$\left\{{}_iBH2_j^B\right\} = \left\{\begin{array}{c} 0 \\ -r_{3j} \\ r_{2j} \end{array}\right\} \tag{E.2.89}$$

The $\left\{{}_iBH1_j^B\right]$–vector.

$$\left\{{}_iBH1_j^B\right\} = \left\{\begin{array}{c} 2\omega\left[r_{2j}\cos\left(\theta_{1H}^H\right) - r_{3j}\sin\left(\theta_{1H}^H\right)\right] \\ -2\omega\left[r_{2j}\sin\left(\theta_{1H}^H\right) + r_{3j}\cos\left(\theta_{1H}^H\right)\right]\theta_{1Am}^A \\ \hline -2\omega r_{2j}\theta_{3Am}^A - r_{2j}\dot{\theta}_{1H}^H \\ \hline -2\omega r_{3j}\theta_{3Am}^A - r_{3j}\dot{\theta}_{1H}^H \end{array}\right\} \tag{E.2.90}$$

The $\left\{{}_iBC0_j^B\right]$–vector.

$$\left\{{}_iBC0_j^B\right\} = (\omega)^2 \left\{\begin{array}{c} -r_{1j} \\ -r_{2j}\sin^2\left(\theta_{1H}^H\right) - r_{3j}\cos\left(\theta_{1H}^H\right)\sin\left(\theta_{1H}^H\right) \\ -r_{2j}\cos\left(\theta_{1H}^H\right)\sin\left(\theta_{1H}^H\right) - r_{3j}\cos^2\left(\theta_{1H}^H\right) \end{array}\right\} \tag{E.2.91}$$

E.3 Extraction of angular accelerations from inertia vector.

As can be seen from [Part 1, Eq. 4.11.34], the $[A_S]$-matrix, $S = A$ or $S = B$, is part of the vector components of the inertia force vector $\left\{F^S_{4S}\right\}$. Further, the way the matrix enters the components makes it difficult to extract the DOFs in a simple way solely by symbolic manipulations. It has to be done the hard way, by multiplication of the expression and afterwards sorting the result after DOFs and finally writing the vector, or part of it, as a matrix product.

It has been chosen here only to extract terms related to the second time derivative of the rotations. This corresponds to the terms in the skew-symmetric part of the $[A_S]$-matrix and will contribute to the mass matrix. These terms are important, when the eigensolutions are sought. The first time derivatives could equally well be dealt with in the same manner and would then contribute to the Coriolis-matrix. It has been chosen here to leave the first time derivatives in the vector, allthough the time integration might appear to be a little slower, because more iterations might be needed in order to reach equilibrium according to the wanted accuracy.

When extracting angular accelerations, the vector is written for elements on the shaft as

$$\left\{{}_iF^A_{4A}\right\} = \left[{}_iFT2_{4A}\right]\left\{\ddot{\theta}^T_{T\ell}\right\} + \left\{{}_iFT^A_{4A}\right\} \tag{E.3.1}$$

and correspondingly for elements on the blade

$$\left\{{}_iF^B_{4B}\right\} = \left[{}_iFT2_{4B}\right]\left\{\ddot{\theta}^T_{T\ell}\right\} + \left[{}_iFA2_{4B}\right]\left\{\ddot{\theta}^A_{Am}\right\} + \left\{FH2^B_{4B}\right\}\ddot{\theta}^H_{1H} + \left\{{}_iFT^B_{4B}\right\} \tag{E.3.2}$$

Here $\left\{{}_iFT^A_{4A}\right\}$ and $\left\{{}_iFT^B_{4B}\right\}$ is the remainder, when the other terms have been extracted from $\left\{{}_iF^A_{4A}\right\}$ and $\left\{{}_iF^B_{4B}\right\}$, respectively. The coefficient matrices and vector for the extracted terms are composed as shown below.

$$\left[{}_iFT2_{4A}\right] = \left[{}_iK_{0A}\right]\left[A_{AT}\right] \tag{E.3.3}$$

$$\left[{}_iFT2_{4B}\right] = \left[{}_iK_{0B}\right]\left[A_{BT}\right] \tag{E.3.4}$$

$$\left[{}_iFA2_{4B}\right] = \left[{}_iK_{0B}\right]\left[A_{BA}\right] \tag{E.3.5}$$

$$\left\{FH2^B_{4B}\right\} = -\left[{}_iK_{03B}\right] \tag{E.3.6}$$

In these equations the matrix $\left[{}_iK_{0S}\right]$, $S = A$ or $S = B$, expresses dependence on local geometry and material parameters

$[{}_iK_{0S}] =$

$$M_i\,[{}_4T_{EiS}]\left[\begin{array}{c|c|c}
\begin{array}{l}[K_{1x}T_1 - K_{2y}T_4]\\ [-K_{1y}T_1 - K_{2x}T_7]\\ [-K_{1y}T_4 - K_{1x}T_7]\end{array} & \begin{array}{l}[K_{1x}T_2 - K_{2y}T_5]\\ [-K_{1y}T_2 - K_{2x}T_8]\\ [-K_{1y}T_5 - K_{1x}T_8]\end{array} & \begin{array}{l}[K_{1x}T_3 - K_{2y}T_6]\\ [-K_{1y}T_3 - K_{2x}T_9]\\ [-K_{1y}T_6 - K_{1x}T_9]\end{array}\\ \hline
\begin{array}{l}[K_{3y}T_1 - K_{4x}T_7]\\ [K_{3x}T_1 + K_{4y}T_4]\\ [-(K_{5x}+K_{5y})T_1\\ \quad +K_{6y}T_4 - K_{6x}T_7]\end{array} & \begin{array}{l}[K_{3y}T_2 - K_{4x}T_8]\\ [K_{3x}T_2 + K_{4y}T_5]\\ [-(K_{5x}+K_{5y})T_2\\ \quad +K_{6y}T_5 - K_{6x}T_8]\end{array} & \begin{array}{l}[K_{3y}T_3 - K_{4x}T_9]\\ [K_{3x}T_3 + K_{4y}T_6]\\ [-(K_{5x}+K_{5y})T_3\\ \quad +K_{6y}T_6 - K_{6x}T_9]\end{array}\\ \hline
\begin{array}{l}[K_{1x}T_1 + K_{2y}T_4]\\ [-K_{1y}T_1 + K_{2x}T_7]\\ [-K_{1y}T_4 - K_{1x}T_7]\end{array} & \begin{array}{l}[K_{1x}T_2 + K_{2y}T_5]\\ [-K_{1y}T_2 + K_{2x}T_8]\\ [-K_{1y}T_5 - K_{1x}T_8]\end{array} & \begin{array}{l}[K_{1x}T_3 + K_{2y}T_6]\\ [-K_{1y}T_3 + K_{2x}T_9]\\ [-K_{1y}T_6 - K_{1x}T_9]\end{array}\\ \hline
\begin{array}{l}[-K_{3y}T_1 - K_{4x}T_7]\\ [-K_{3x}T_1 + K_{4y}T_4]\\ [-(K_{5x}+K_{5y})T_1\\ \quad -K_{6y}T_4 + K_{6x}T_7]\end{array} & \begin{array}{l}[-K_{3y}T_2 - K_{4x}T_8]\\ [-K_{3x}T_2 + K_{4y}T_5]\\ [-(K_{5x}+K_{5y})T_2\\ \quad -K_{6y}T_5 + K_{6x}T_8]\end{array} & \begin{array}{l}[-K_{3y}T_3 - K_{4x}T_9]\\ [-K_{3x}T_3 + K_{4y}T_6]\\ [-(K_{5x}+K_{5y})T_3\\ \quad -K_{6y}T_6 + K_{6x}T_9]\end{array}
\end{array}\right] \tag{E.3.7}$$

Here M_i is the total mass of the element, and $[{}_4T_{EiS}]$ is a (12×12) transformation matrix composed of 4 (3×3) usual transformation matrices $[T_{EiS}]$ located on the submatrix diagonal. All other elements are zero.

The matrix $[{}_iK_{03S}]$ is the column matrix corresponding to the 3^{rd} column of $[{}_iK_{0S}]$.

In $[{}_iK_{0S}]$ the T_r-terms, $r = 1,..,9$, are

$$\left.\begin{array}{l}
T_1 = T_{11}T_{22} - T_{12}T_{21}\\
T_2 = T_{11}T_{32} - T_{12}T_{31}\\
T_3 = T_{21}T_{32} - T_{22}T_{31}\\
T_4 = T_{11}T_{23} - T_{13}T_{21}\\
T_5 = T_{11}T_{33} - T_{13}T_{31}\\
T_6 = T_{21}T_{33} - T_{23}T_{31}\\
T_7 = T_{12}T_{23} - T_{13}T_{22}\\
T_8 = T_{12}T_{33} - T_{13}T_{32}\\
T_9 = T_{22}T_{33} - T_{23}T_{32}
\end{array}\right\} \tag{E.3.8}$$

where the T_{rs}-terms are components of the tranformation matrix $[T_{EiS}]$, located at row r and column s.

The K_{rc}-parameters, $r = 1,..,6$, and $c = x$ or $c = y$, in $[{}_iK_{0S}]$ are

$$\left.\begin{aligned}
K_{1x} &= \tfrac{1}{2} r_x \\
K_{1y} &= \tfrac{1}{2} r_y \\
K_{2x} &= \tfrac{1}{\ell} r_{Ix}^2 \varrho_x \\
K_{2y} &= \tfrac{1}{\ell} r_{Iy}^2 \varrho_y \\
K_{3x} &= \tfrac{1}{12} r_x \ell \\
K_{3y} &= \tfrac{1}{12} r_y \ell \\
K_{4x} &= 6 \varrho_x \eta_x r_{Ix}^2 \\
K_{4y} &= 6 \varrho_y \eta_y r_{Iy}^2 \\
K_{5x} &= \tfrac{1}{2} r_{Ix}^2 \\
K_{5y} &= \tfrac{1}{2} r_{Iy}^2 \\
K_{6x} &= \tfrac{1}{\ell} \varrho_x r_{Ix}^2 e_{s1} \\
K_{6y} &= \tfrac{1}{\ell} \varrho_y r_{Iy}^2 e_{s2}
\end{aligned}\right\} \qquad \text{(E.3.9)}$$

The matrices in Eqs. E.3.3, E.3.4, and E.3.5 are composed of transformation terms related to transformation between substructures, the origin of which is the skew-symmetric part of the $[A_S]$-matrix. The actual values are

$[A_{AT}] =$

$$\left[\begin{array}{c|c|c}
-[sin(\theta) + cos(\theta)\theta^T_{2T\ell}] & cos(\theta)[\theta^T_{1T\ell} - sin(\theta)\theta^T_{3T\ell}] & -[cos(\theta) - sin(\theta)\theta^T_{2T\ell}] \\
\hline
-\theta^T_{3T\ell} & 1 & \theta^T_{1T\ell} \\
\hline
-[cos(\theta) - sin(\theta)\theta^T_{2T\ell}] & -[sin(\theta)\theta^T_{1T\ell} + cos(\theta)\theta^T_{3T\ell}] & [sin(\theta) + cos(\theta)\theta^T_{2T\ell}]
\end{array}\right] \qquad \text{(E.3.10)}$$

$[A_{BT}] =$

$$\left[\begin{array}{c|c|c}
\begin{array}{l}[-sin(\theta)cos(\theta^H_{1H}) \\ -cos(\theta)cos(\theta^H_{1H})\theta^T_{2T\ell} \\ -sin(\theta^H_{1H})\theta^T_{3T\ell} \\ +sin(\theta)sin(\theta^H_{1H})\theta^A_{1Am} \\ -cos(\theta)cos(\theta^H_{1H})\theta^A_{2Am} \\ -cos(\theta)sin(\theta^H_{1H})\theta^A_{3Am}]\end{array} & \begin{array}{l}[sin(\theta^H_{1H}) \\ +cos(\theta)cos(\theta^H_{1H})\theta^T_{1T\ell} \\ -sin(\theta)cos(\theta^H_{1H})\theta^T_{3T\ell} \\ +cos(\theta^H_{1H})\theta^A_{1Am}]\end{array} & \begin{array}{l}[-cos(\theta)cos(\theta^H_{1H}) \\ +sin(\theta^H_{1H})\theta^T_{1T\ell} \\ +sin(\theta)cos(\theta^H_{1H})\theta^T_{2T\ell} \\ +cos(\theta)sin(\theta^H_{1H})\theta^A_{1Am} \\ +sin(\theta)cos(\theta^H_{1H})\theta^A_{2Am} \\ +sin(\theta)sin(\theta^H_{1H})\theta^A_{3Am}]\end{array} \\
\hline
\begin{array}{l}[sin(\theta)sin(\theta^H_{1H}) \\ +cos(\theta)sin(\theta^H_{1H})\theta^T_{2T\ell} \\ -cos(\theta^H_{1H})\theta^T_{3T\ell} \\ +sin(\theta)cos(\theta^H_{1H})\theta^A_{1Am} \\ +cos(\theta)sin(\theta^H_{1H})\theta^A_{2Am} \\ -cos(\theta)cos(\theta^H_{1H})\theta^A_{3Am}]\end{array} & \begin{array}{l}[cos(\theta^H_{1H}) \\ -cos(\theta)sin(\theta^H_{1H})\theta^T_{1T\ell} \\ +sin(\theta)sin(\theta^H_{1H})\theta^T_{3T\ell} \\ -sin(\theta^H_{1H})\theta^A_{1Am}]\end{array} & \begin{array}{l}[cos(\theta)sin(\theta^H_{1H}) \\ +cos(\theta^H_{1H})\theta^T_{1T\ell} \\ -sin(\theta)sin(\theta^H_{1H})\theta^T_{2T\ell} \\ +cos(\theta)cos(\theta^H_{1H})\theta^A_{1Am} \\ -sin(\theta)sin(\theta^H_{1H})\theta^A_{2Am} \\ +sin(\theta)cos(\theta^H_{1H})\theta^A_{3Am}]\end{array} \\
\hline
\begin{array}{l}[-cos(\theta) \\ +sin(\theta)\theta^T_{2T\ell} \\ +sin(\theta)\theta^A_{2Am}]\end{array} & \begin{array}{l}[-sin(\theta)\theta^T_{1T\ell} \\ -cos(\theta)\theta^T_{3T\ell} \\ -\theta^A_{3Am}]\end{array} & \begin{array}{l}[sin(\theta) \\ +cos(\theta)\theta^T_{2T\ell} \\ +cos(\theta)\theta^A_{2Am}]\end{array}
\end{array}\right] \qquad \text{(E.3.11)}$$

$[A_{BA}] =$

$$\left[\begin{array}{c|c|c} [-cos(\theta^H_{1H})\theta^A_{2Am} - sin(\theta^H_{1H})\theta^A_{3Am}] & [sin(\theta^H_{1H}) + cos(\theta^H_{1H})\theta^A_{1Am}] & [-cos(\theta^H_{1H}) + sin(\theta^H_{1H})\theta^A_{1Am}] \\ \hline [sin(\theta^H_{1H})\theta^A_{2Am} - cos(\theta^H_{1H})\theta^A_{3Am}] & [cos(\theta^H_{1H}) - sin(\theta^H_{1H})\theta^A_{1Am}] & [sin(\theta^H_{1H}) + cos(\theta^H_{1H})\theta^A_{1Am}] \\ \hline -1 & -\theta^A_{3Am} & \theta^A_{2Am} \end{array}\right]$$

(E.3.12)

The terms of the first row in these 3 matrices belong to the $A_S(1,2)$ element ($S = A$ or $S = B$), the terms of the second row to $A_S(1,3)$, and the terms of the third row to $A_S(2,3)$, the only elements of the skew-symmetic matrix different from zero. Column No. r is composed of coefficients to one of the angular acceleration DOFs $\ddot{\theta}^A_{rAm}$ or $\ddot{\theta}^T_{rT\ell}$.

F Wind field and aerodynamic model.

The main objective with the present theory is to carry out parametric studies related to influence of change in dynamic response parameters, rather than provide the basis for the final design of the wind turbine structure.

It is important that the results reflect what happens relatively, when essential dynamic parameters as e.g. stiffness and mass are varied. Therefore, the aerodynamic excitation of the blades must reflect essential characteristics of the real excitation in such a way that changes in response, when dynamic parameters are changed, are not caused by the different action of the aerodynamic model for the different structural configurations and load conditions.

As long as this requirement is fulfilled a certain freedom in the choice of model is present.

Because the phenomina to be investigated are of highly dynamic and non-steady nature it would be preferable to use an aerodynamic model, which was able to adequatley describe the non-steady interaction between flow field and blade element. This would require a non-steady vortex model in combination with a blade element theory, which was able to incorporate the effect of time variation of the resulting wind speed at the profile.

Turbulence is an important factor when the dynamics and the lifetime of a wind turbine are investigated. Due to rotational sampling, i.e. the effect of the blades moving through the turbulence in a vertical plane, the frequency content in the turbulence is redistributed, and this effect is important when a general model for the loads is established.

The influence of turbulence has been treated through the last years with increasing interest. The most convincing models are mainly attached to the frequency domain methods, where the treatment of turbulence is carried through with great advantage due to the ability of the models to deal with the stochastic nature of turbulence, [M3]. When nonlinear effects must be taken into account, the frequency domain models usually get very complicated.

Also skew wind caused by tilt, yaw misalignment, and slope inclination of surrounding terrain are important in characterizing the wind speed, because they give rise to time variation in size and direction of the resulting wind speed as felt by the blades.

Further, experiments have shown that other less obvious three-dimensional effects are of significant importance on a rotating blade. The most essential of these effects are [M1]

1. Centrifugal forces on the aerstream
2. Radial pressure gradients

These effects should also be incorporated in the model if the latest findings in the research field should be properly represented.

The non-steady vortex model is available as a sound theoretical basis, e.g. [H1], [S1], and [H3]. Still, the models suffer to some extent from the lack of verification through a comparison with experimental data. Further the model is very time consuming, when simulations are run on a computer and therefore not well suited for parametric studies.

The non-steady blade element theory is not yet developed to an operational model, where also three-dimensional effects are accounted for. Existing helicopter rotary wing models can not be adopted directly, mainly because the flow around a helicopter blade is characterized by Reynolds numbers of about one order of magnitude higher than for flows around a wind turbine blade. Extensive work is going on in the field, both theoretically and experimentally, e.g. [B2] and [M2].

Considering the freedom in choice of model for aerodynamic excitation, and the facts about the ideal models, as mentioned above, it has been decided to use the simple and well known blade element theory, with inductions derived by considering the momentum balance for a stream tube as basically outlined in [G3]. The method is slightly modified here to allow for axial inductions greater than $\frac{1}{2}$ by introduction of a reduction factor on the mass stream.

The limitations of the method are reflected in the development of new models. These limitations are well known to day, because extensive comparison with experimental results has taken place through the last decade, for wind turbines of the type and size, the investigation of which is the aim of the present work.

The three-dimensional effects mentioned above could to some extent be accounted for, because the investigations in [M1] have resulted in a set of profile coefficients, which reflect the influence of these effects. The coefficients are valid for one specific use of a specific blade, and that blade will be a part of one of the configurations, which will be the aim for simulations with the present model.

The experience with the simple blade element theory has shown that especially when the blades are stalled, the assumptions for the method are violated and the results might be erroneous, and perhaps even useless e.g. in a dynamic analysis. The hysteresis loop in [M2] shows that highly unsteady conditions might arise in the stalled region

Wind shear and tower shadow are included in the model and the tower shadow is the main source for dynamic excitation of the structure when turbulence is disregarded. Different turbulence models can be included with ease, because the wind vector is defined in space and time in the model by now.

The numerical turbulence time simulation models available generally require much processor memory because an adequate model must incorporate the true frequency content and correctly describe the spatial structure of the turbulence as function of time with a rather fine resolution in order to get something usable [V1]. Models better suited for computer simulation are under development. One method uses a backward difference equation in combination with generation of random numbers, but the method is not yet available for three dimensional flow [G5]. Another method is based on a series expansion of the turbulence [H4] and when the series is truncated a model usable in simulations is achieved. The estimation of the influence of the truncation on the results is then an important part of the use of the method.

In spite of its memory consumption the Sandia model [V1] has been chosen for the simulations in the present work. The method is rather well documented, allthough some aspects regarding the preservation and distribution of the variance do not seem to be completely explained. Still, this is of less importance in parametric studies where we primarily want to look for relative changes in response, rather than the absolute values.

The induction is calculated under the assumption that the 'frozen wake' approach is valid, which means that it is assumed that the wake is unaffected by the fluctuations in wind speed, only the mean values influence the generation of the wake [T2]. For simulations carried out at constant mean wind speed this assumption has as a consequence that the induction can be calculated initially and used throughout the simulation.

Because the usual way of setting up the induction equations is based on scalar expressions for axial and tangential directions, respectively, and the present theory is set up in vector notation, it has been found valuable to go through a summary derivation of the equations with the aim of providing the expressions needed in the present context.

Below, the wind field is first described. The free wind is assumed to follow the logarithmic

shear law as mentioned in Sec. F.1. The tower shadow is modelled by use of the potential flow model. This is mentioned in Sec. F.2. Below in Secs. F.3, F.4, and F.5 the derivation of the expressions for induced velocity and aerodynamic forces at a cross section is carried out. Next, in Sec. F.6 the actual radial distribution of cross sections, where aerodynamic calculation takes place (denoted calculation points) is described. Finally, in the same section, the consistent transformation of the aerodynamic loads to the element nodes is derived.

F.1 The free wind.

The local free wind speed, $\{v^M\}$, is defined as the wind speed that would be found at the location if the wind turbine to be analyzed was not present. The upper index M indicates that the vector components are with reference to a coordinate system, which is well suited for description of the free wind field and here denoted the meteorological coordinate system.

The free wind vector at a point, defined by the position vector $\{r^M\}$, is usually resolved in two vector components

$$\{v^M\} = \{v^M[\{r^M\}, t]\} = \{v_m^M[\{r^M\}]\} + \{v_t^M[\{r^M\}, t]\} \tag{F.1.1}$$

where

$\{v_m^M[\{r^M\}]\}$	is the mean wind speed. Usually the averaging period is 10 minutes
$\{v_t^M[\{r^M\}, t]\}$	is the wind speed fluctuation, the turbulence, reflecting the stochastic characteristics of the free wind (the lower index t refers to turbulence)
$\{r^M\}$	is the position vector to the point in question
t	used as independent variable is the time

In general all factors influencing the free wind should be taken into account, e.g. terrain roughness, atmospheric stability and local topography. Terrain roughness should here be understood in a wide sense also including e.g. other wind turbines.

F.1.1 Mean wind.

The air flow at a real wind turbine site is often influenced of important irregularities in the upwind direction. A design model should of course allow for incorporation of these effects also in relation to the mean wind speed, e.g. reversed flow near the edge of a slope. But considering the objective with the present work these effects will not be modelled here, because the primary need is just an appropriate reference case.

The free mean wind speed can often be adequately described by a simple shear law when the terrain is homogeneous in the upwind direction.

One possibility is to use the logarithmic shear law which will be adopted here:

$$v_m = \left|\{v_m^M[\{r^M\}]\}\right| = \frac{\ln\left(\frac{|z_M|}{z_0}\right)}{\ln\left(\frac{|z_{M,hub}|}{z_0}\right)} \left|\{v_m^M[z_{M,hub}]\}\right| \tag{F.1.2}$$

This equation gives the numerical value of the wind speed at a given height over the ground z_M, and assumes that the mean free wind vector is parallel to the surface of the ground, and that the z_M–axis is perpendicular to the surface.

The new symbols in Eq. F.1.2 has the meaning:

$z_{M,hub}$ z_M–coordinate for the hub ($|z_{M,hub}|$ =hubheight) in M–coordinates

z_0 roughness length for the surrounding terrain in upwind direction

The only reason for considering the hub height $|z_{M,hub}|$ in M–coordinates, indicating that $|z_{T,hub}|$ and $|z_{M,hub}|$ may be different, is that the simple shear law is believed to be an acceptable model also for the flow following a slope as long as the location is far enough from significant changes in slope inclination. The subject of describing the factors influencing the flow in general is without the scope of the present work and shall not be pursued any further.

F.1.2 Turbulence.

The turbulent part of the free wind speed is completely described in the M–coordinate system in terms of spectral densities of the velocity components at a fixed point and coherence and phase spectra to specify the statistical correlation between velocities at two separate points.

Allthough fluctuations in a plane perpendicular to the mean wind direction are part of a complete description they are disregarded in the present work because their influence on the blade loads usually can be neglected, at least when the blade profile is unstalled as shown in [M5].

The longitudinal wind fluctuation, $v_{ty}^M = u$, the fluctuation in direction of the mean wind speed, is modeled as a stationary and homogeneous random field with zero mean.The stationarity implies that the probability distributions only depend on separation in time and not on absolute time. Equivalently, the homogeneity implies that the probability distributions only depend on spatial separation in a plane perpendicular to the mean wind direction and not on absolute location in the plane.

The stationarity assumption is necessary in order to make use of the description of the process by correlation functions. For time periods of the order of magnitude 10 minutes, which will be the case in the present simulations, it is realistic to assume stationarity and the problem of how to deal with the instationarity can be preserved untill the longer periods must be analyzed e.g. in a fatigue analysis.

The homogeneity assumption implies that the probability distributions of the turbulence at given points must be invariant with respect to a parallel displacement of the given point configuration. Within an area of the size of the rotor disc this approximation is usually good, at least for small and medium size wind turbines. Comparison of models which assume homogeneity with extensive measurements on rotor diameters up to 40 m has shown good agreement, e.g. for the Nibe wind turbines [P5], at sites without important irregularties.

It is further assumed that Taylors "frozen turbulence" hypothesis is valid, i.e.

$$u(y_M, t) = u(y_M - v_m\tau, t - \tau) = u(y_{M0}, t_0) \tag{F.1.3}$$

y_M is the y_M–coordinate at time t

y_{M0} is the y_M–coordinate at time t_0

τ $= t - t_0$ is the time separation

The hypothesis expresses that an observer would experience the same turbulence whether he was at rest at a point with the turbulent wind field passing by or he was moving with the mean velocity $-v_m$ through a "frozen turbulence", i.e. a volume with all the air particles fixed at a given instant.

The power spectrum for the longitudinal fluctuation is here described by a one–sided power spectrum (i.e. a spectrum only defined for positive frequencies but with a value of twice the standard two–sided spectrum), which is due to [K1]

$$S_u(\omega) = \sigma^2 \frac{\frac{L}{v_m}}{\left(1 + 1.5\frac{\omega L}{v_m}\right)^{\frac{5}{3}}} \tag{F.1.4}$$

where the symbols have the following meaning and relation to other characteristic parameters

ω	frequency in $\frac{\text{rad}}{\text{sec}}$
σ^2	variance
$L = \frac{\lvert z_M \rvert}{2\pi f_m}$	spectrum length scale
$f_m = \frac{\hat{\omega}\lvert z_M \rvert}{2\pi v_m}$	peak frequency
$\hat{\omega}$	frequency at which $\omega S_u(\omega)$ has its maximum

According to extensive investigations [M3] it is general practice in wind turbine analysis to assume that the phase spectrum is identically zero and further that the coherence function has the simple exponential form [D1]

$$\chi(D,\omega)^2 = \exp(-A\mu) \tag{F.1.5}$$

where

A	is the decay factor
μ	$= \left[\left(\frac{\omega D}{v_m}\right)^2 + \left(\frac{D}{L}\right)^2\right]^{\frac{1}{2}}$ is the similarity factor
D	is the separation between the two points in a plane perpendicular to the mean wind direction

Also, it will be assumed that the cross–spectrum between the longitudinal wind components at points on a plane perpendicular to the mean wind direction can be factorized giving

$$S_u(\{r_1\},\{r_2\},\omega) = S_u(\omega)\chi(D,\omega) \tag{F.1.6}$$

where

$\{r_i\}$	$i = 1, 2$, is the position vector in the plane to point no. i

Without going into further detail about the actual definition of the meteorological coordinate system relative to the tower coordinate system, it is at present simply assumed that the transformation matrix $[T_{MT}]$, which transforms a vector from the meteorological coordinate system (index M) to the tower coordinate system (index T), is known for a specific wind turbine location and actual wind conditions. The wind–vector is transformed to tower coordinates through the transformation

$$\left\{v^T\right\} = [T_{MT}]\left\{v^M\right\} = \begin{Bmatrix} v_x^T \\ v_y^T \\ v_z^T \end{Bmatrix} \tag{F.1.7}$$

and the wind speed is now specified in space and time to a level where the interaction between wind field and wind turbine structure can be analyzed. The first step in this analysis is the incorporation of the influence of tower interaction on the flow field. This will be done in Sec. F.2. In the following section a short review of the method used for turbulence simulation will be given.

F.1.2.1 Simulation of turbulence.

In the following the numerical procedure adopted for simulation of the fluctuating part of the wind field, the turbulence $\left\{v_i^M\left[\{r^M\},t\right]\right\}$, is described. As explained in Sec. F.1.2 only the longitudinal component is taken into account in the present analysis, $v_{iy}^M = u$.

The turbulence is considered to be adequately described as a homogeneous and stationary three dimensional random field covering a cylinder with the same diameter as the rotor.

The simulation method is almost identical to the one outlined by Veers [V1] for wind turbine application and originally developed in [S2] for general simulation of random processes.

On the assumptions mentioned in Sec. F.1.2 the turbulence is completely described by the power spectral density $S(\omega)$ and the coherence function $\chi(D,\omega)^2$.

The objective is now to simulate the turbulence at discrete points adequately distributed in the cylindrical volume which during a given time T_0 passes through the rotor disc moving with the mean wind speed v_m.

The points are assumed to be positioned along lines parallel to the mean wind direction. The lines are mutually positioned according to some simple geometrical relations which facilitate the coding. In a plane perpendicular to the mean wind direction the position of the lines might e.g. be as shown in Fig. 1.

According to the coordinate definitions, the mean wind speed v_m is in direction of the y_M–axis. The simulation points are located at two cylindrical surfaces with radii r_1 and r_2, respectively, and further a row of points along the y_M–axis. The N_{azi} azimuthal positions are equally spaced ($\Delta\theta = 2\pi/N_{azi}$) and numbered from 1 to $N_{azi} = 6$, with the numbers enclosed in circles. The simulation points belonging to each time series, or equivalently to each line, are all given the same number, ranging from 1 to $N_{sim} = 13$. As the Taylor hypothesis is assumed valid, the generation of the turbulence at a given instant and covering the cylindrical disc volume can be used in the time simulation by propagating the cylinder with the mean wind speed v_m, and the cylinder having its axis coinciding with the y_M–axis.

If the y_M–axis is inclined relative to the turbine rotor axis (the y_A–axis) the cylindrical volume with turbulence will only cover an elliptic cross section of the rotor and a time delay is further introduced. As these effects are of the order of magnitude $[1-\cos(\text{inclination})]\times 100\%$ they have been ignored here.

As the point spectrum and the cross spectra contain the information about the process, the spectra are the basis in the simulation.

For the simulation we want discrete time series, which give values of the turbulence at moments where we intend to sample the turbulence. In order to make transformations from the frequency

The numbers enclosed in circles denote azimuthal positions.
The free numbers denote simulation points.
The y_M–axis and the mean wind speed are directed into the paper.

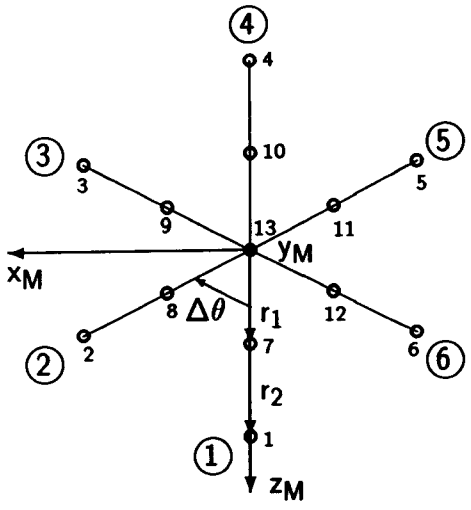

Figure 1: Example showing distribution of simulation points at the rotor disc.

domain to the time domain easier by use of the fast Fourier transform (FFT) algorithm for the discrete Fourier transformations (DFT's) involved, the discretization is carried out already in the frequency domain.

To proceed we thus have to discretize the spectra which here is equivalent to discretizing the point spectrum.

If the actual sampling interval is Δt, and we want the time series to cover N samples, then the total sampling time is

$$T_0 = \Delta t N \tag{F.1.8}$$

By choosing these two parameters we have also chosen the frequency resolution. In order to make the FFT effective N is chosen as a power of 2, $N = 2^n$ with n being an integer. The corresponding frequency increment is

$$\Delta\omega = \frac{2\pi}{T_0} = \frac{2\pi}{\Delta t N} \tag{F.1.9}$$

and the highest frequency represented in the resulting time series is the Nyquist frequency

$$\omega_{max} = \frac{\pi}{\Delta t} = \frac{N}{2}\Delta\omega \tag{F.1.10}$$

When using the DFT the spectra must have the two sided representation with also negative frequencies represented. The discrete auto–spectrum is now derived from Eq. F.1.4 at point No. r as

$$S_{u,rr}(\omega_k) = \frac{1}{2} S_u(\omega_k)\,\Delta\omega \tag{F.1.11}$$

where

ω_k $= k\Delta\omega$, and $k = 0, ..., \frac{N}{2}$

$\frac{1}{2}$ gives the two sided spectrum values for positive frequencies

The ordinates of the discrete power spectrum for negative frequencies are found from the ordinates for positive frequencies because the two sided spectrum is an even function in ω, so that

$$S_{u,rr}(-\omega_k) = S_{u,rr}(\omega_k) \tag{F.1.12}$$

where now

$k = 1, ..., \left(\frac{N}{2} - 1\right)$ corresponding to positive frequencies with index $\left(\frac{N}{2} + 1\right), ..., (N-1)$, when used in the DFT

giving a total of N discrete spectrum values, consistent with the definition of the discrete Fourier transform.

In the following the counters for discrete values of time (p) and frequency (k) are placed as upper right indices on the respective discrete values (except for ω_k), while counters for row and column positions are placed as lower right indices on the vector and matrix elements.

The discrete cross–spectrum for points no. r and s is found as (from Eq. F.1.6)

$$S_{u,rs}(\omega_k) = S_{u,rr}(\omega_k)\,\chi(D_{rs}, \omega_k) = S^k_{rs} \tag{F.1.13}$$

where

D_{rs} is the separation between points No. r and s

In [V1] it is proposed to use the auto– and cross–spectra corresponding to the actual location of the simulation points, so that the local mean wind speed enters the above expressions. But according to the homogeniety assumption the mean wind speed at the center point (in the example point No. 13), equivalent to the wind turbine hub, is used in the present implementation. There is then no need for distinguishing between auto–spectra at different points and the following notation can be introduced

$$S^k = S_{u,rr}(\omega_k) = S_{u,hub} \tag{F.1.14}$$

This simplification reduces the computational work and the need for storage considerably.

The spectra are now arranged in a $N_{sim} \times N_{sim}$ spectral matrix where the row and the column numbers correspond to the simulation point numbers. The diagonal spectra will then be identical to the auto–spectrum and the off–diagonal spectra are the cross spectra. The matrix is real and further symmetric due to the symmetry in the separation parameter, $D_{rs} = D_{sr}$

$$\left[S^k_0\right] = \begin{bmatrix} S^k & S^k_{12} & S^k_{13} & \cdots & \cdots & S^k_{1N_{sim}} \\ & S^k & S^k_{23} & \cdots & \cdots & S^k_{2N_{sim}} \\ & & S^k & S^k_{34} & \cdots & S^k_{3N_{sim}} \\ & Sym- & & \cdots & \cdots & \cdots \\ & & metric & & S^k & S^k_{(N_{sim}-1)N_{sim}} \\ & & & & & S^k \end{bmatrix} \tag{F.1.15}$$

When the distribution of simulation points in the rotor disc plane has equally angular spaced azimuthal locations ($\Delta\theta$ in Fig. 1), the number of different cross–spectra can be reduced with a factor N_{azi} relative to the trinagular off-diagonal matrix. Considerable computational work and storage can thus be saved by proper choice of simulation point geometry.

A lower triangular matrix $[H]$ is now defined by the matrix product

$$\left[S_0^k\right] = \left[H^k\right]\left[H^k\right]^{*T} \tag{F.1.16}$$

where '*' denotes complex conjugation and 'T' the transpose.

Because the spectra are real valued and $S^k \geq S^k_{rs}$, then a real solution is found for $\left[H^k\right]$ and the complex conjugation has no influence.

As $\left[S_0^k\right]$ is positive definite the $\left[H^k\right]$ matrix can be found by a simple recursive solution algorithm, solving for the H^k_{rs} elements column–wise.

Now, the Fourier coefficients $\left\{U^k\right\}$ for the N_{sim} correlated time series can be calculated from the following expression

$$\left\{U^k\right\} = \left[H^k\right]\left\{P^k\right\} \tag{F.1.17}$$

where the components of the vectors are defined as

V^k_r Fourier coefficient for frequency component k at simulation point No. r

P^k_s $= \exp i\theta^k_s$ is a complex number, with the random phase θ^k_s uniformly distributed between 0 and 2π. Here i is the imaginary unit.

The equation for the single Fourier coefficients corresponding to point No. r and frequency component No. k, written as a sum, is

$$U^k_r = \sum_{s=1}^{r} H^k_{rs} e^{i\theta^k_s} \tag{F.1.18}$$

where i in the exponent is the imaginary unit.

The effect of the multiplication with the complex number is at the level of Eq. F.1.17 to add a random phase to the Fourier coefficient in question and in the time domain to make the resulting time series approach a Gaussian process with zero mean when the number of frequency components increases according to the central limit theorem.

The time series at simulation point No. r is now found by an inverse discrete Fourier transform

$$u^p_r = \sum_{k=0}^{N-1} \left(\sum_{s=1}^{r} H^k_{rs} e^{i\theta^k_s} \right) e^{i(2\pi kp/N)} \tag{F.1.19}$$

A convincing exercise showing the validity of this expression can be carried out as follows.

By deriving the auto- and cross correlations for the resulting time series and taking the Fourier transform of the correlation it can be shown that the procedure generates the original target spectra in the limit [S2].

The above outlined procedure will generate a discrete time value in the disc plane at each time step. One would usually choose the discrete time values corresponding to the time of passage of a blade. For a horizontal axis wind turbine with the number of blades N_b and the angular velocity of the rotor ω_R the time step would be

$$\Delta t = \frac{2\pi}{\omega_R N_b} \tag{F.1.20}$$

When doing so, only discrete values of the time series are sampled at N_b azimuthal positions at each time step. The values at the $N_{azi} - N_b$ remaining positions are spilled.

A way of avoiding this, and at the same time making the calculation more effective, is to introduce an appropriate time delay to each time series corresponding to an azimuthal collection of simulation points, in order to generate discrete values only at the time of sampling.

In order to make the technique effective the number of azimuthal positions should be a multiple of the number of blades N_b. If now the number of azimuthal positions N_{azi} is divided into N_b groups, then each azimutal position within each group must have increasing time delay in direction of the rotation starting with zero delay at the first azimuthal position. If positions with number index j within each group are assigned local numbers from 0 to $(N_{azi}/N_b - 1)$, with the numbers increasing in direction of rotation, then azimuthal positions with the same number must have the same time delay. With reference to Fig. 1 the numbering is illustrated for the number of blades $N_b = 3$. Assume that the zero position is with blade 1 at azimuthal position 1, blade 2 at position 3, and blade 3 at position 5. Group 1 would then cover positions 1 and 2, group 2 positions 3 and 4, and group 3 positions 5 and 6. The local number 0 would be assigned to positions 1, 3, and 5, and the local number 1 to positions 2, 4, and 6. The time series at the center point (No. 13) is not delayed. The directly sampled values at the center will only cover sampling when the blades are in local position 1. The remaining values are achieved by interpolation. It is accepted because the accuracy is less important close to the hub.

The actual time delay for local position No. j within a group is calculated from

$$t_{delay,j} = \frac{j\Delta\theta}{\omega_R} = \frac{j2\pi}{N_{azi}\omega_R} \tag{F.1.21}$$

Because we actually are generating the time series in the frequency domain it is straight forward to introduce the time delay here, which is equivalent to introducing a phase delay, which then is frequency dependent. If one term in the Fourier series is considered

$$u^p = U^k e^{i(2\pi kp/N)} = U^k e^{i\left(\frac{2\pi kp\Delta t}{N\Delta t}\right)} \tag{F.1.22}$$

it is observed that the time delay $t_{delay,j}$, for the k'th harmonic, corresponds to a change in phase of

$$\theta^k_{delay,j} = \frac{2\pi k}{N\Delta t} t_{delay,j} = \frac{2\pi k}{N\Delta t}\frac{2\pi j}{N_{azi}\omega_R} \tag{F.1.23}$$

This relation is introduced in Eq. F.1.19 to give the final delayed time series as

$$u^p_r = \sum_{k=0}^{N-1}\left(\sum_{s=1}^{r} H^k_{rs} e^{i\left(\theta^k_s - \theta^k_{delay,r}\right)}\right) e^{i(2\pi kp/N)} \tag{F.1.24}$$

where discrete turbulence values now are generated on N_b helical sheets following the path of the blades.

In this equation a reference between the local number j and the global number r is implied.

For the actual dynamic simulations the time step, required in order to achieve stability and acceptable accuracy, will usually be much less than the time step which an angular resolution can offer, owing to the limits in computer storage. It will therefore often be necessary to interpolate in azimuthal direction equivalent to time. Interpolation will also be needed in the radial direction with the chosen radial resolution. These interpolations will to some extent influence the quality of the resulting wind input at the aerodynamic calculation points, but the problem is believed to be minor as long as the resolution of generated turbulence is good at the outer part of the blade. The error is due to limited frequency resolution and is detected in the power spectra as a loss of variance [V1]. This topic will not be investigated any further theoretically in the present work. The quality of the simulation will only be evaluated by comparison with measurements.

F.2 Tower interference.

In this section the influence from tower interference on the flow field is considered.

It is assumed that only the mean wind speed is affected by the tower and only its components in a horizontal plane. It is further assumed that the flow can be modeled as a potential flow field, and the tower is assumed to have a circular cross section.

In direction of the projection of the free mean wind speed $\{v_{mh}\}$ on the horizontal plane an y_H–axis is defined as shown in Fig. 2. The z–axis and the origo of this new coordiante system is coinciding with the z–axis and the origo of the tower coordinate system (index T) and the x_H–axis is the third axis in the triad. The potential flow field is initially described in a polar coordinate system (r_θ, θ) and then transformed to the rectangular coordinates (x_M, y_M, z_M).

In Fig. 2 the symbols not already mentioned has the meaning:

α_{yaw}	the yaw angle defined here as the angle from the x_H–axis to the x_T–axis, i.e. positive in the usual z–positive sense. As long as the rotor axis is aligned with the y_T–axis this yaw definition is in accordance with that commonly used
$\{v_R\}$	polar unit vector in radial direction
$\{v_\theta\}$	polar unit vector in tangential direction
θ	angle for polar coordinates
r_θ	radius for polar coordinates
r_T	radius of circular tower cross section

From potential flow theory it is well known that the flow around a circular cylinder is described in polar coordinates with the actual coordinate definitions in mind as

$$v_R = v_{mh}\left(1 - \frac{r_T^2}{r_\theta^2}\right)\sin\theta \tag{F.2.1}$$

$$v_\theta = v_{mh}\left(1 + \frac{r_T^2}{r_\theta^2}\right)\cos\theta \tag{F.2.2}$$

v_{mh} $= |\{v_{mh}\}|$, is the numerical value of the projection of the free mean wind speed on the horizontal plane

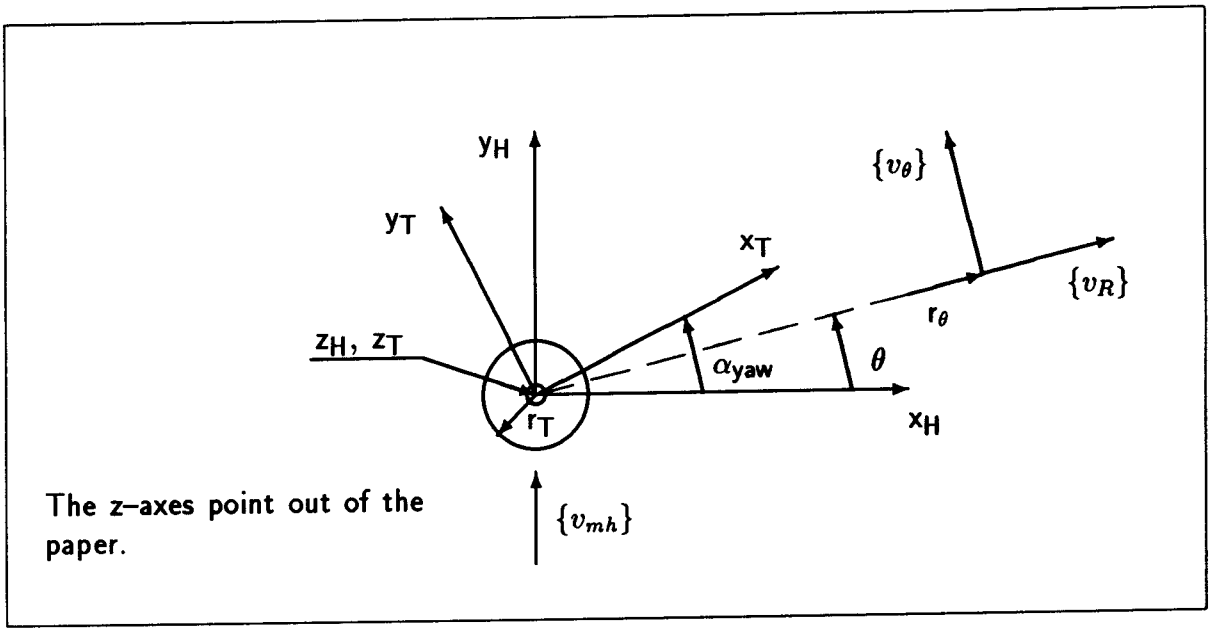

Figure 2: Horizontal plane coordinate system and polar coordinates for description of potential flow around the tower.

Transformation to rectangular coordinates is carried out by use of the geometric relations

$$\cos\theta = \frac{x_H}{r_\theta} \tag{F.2.3}$$

$$\sin\theta = \frac{y_H}{r_\theta} \tag{F.2.4}$$

$$r_\theta = \sqrt{x_H^2 + y_H^2} \tag{F.2.5}$$

which after substitution on the right hand side in Egs. F.2.1 and F.2.2 gives the wind vector components with reference to the unit vectors of the polar coordinate system.

Further these must be transformed to the H–coordinates by the transformation (only two dimensions are considered)

$$\begin{Bmatrix} v_{fmx}^H \\ v_{fmy}^H \end{Bmatrix} = \begin{bmatrix} \cos\theta & -\sin\theta \\ \sin\theta & \cos\theta \end{bmatrix} \begin{Bmatrix} v_R \\ v_\theta \end{Bmatrix} \tag{F.2.6}$$

Carrying out this multiplication and the substitutions from Eqs. F.2.3, F.2.4, and F.2.5 the result in rectangular coordinates is finally written after reduction

$$v_{fmx}^H = -2v_{mh}\frac{x_H y_H}{\left(x_H^2 + y_H^2\right)^2} r_T^2 \tag{F.2.7}$$

$$v_{fmy}^H = v_{mh}\left[1 + \frac{x_H^2 - y_H^2}{\left(x_H^2 + y_H^2\right)^2} r_T^2\right] \tag{F.2.8}$$

The resulting mean wind speed vector $\{v_{fm}^H\}$ in H–coordinates, including influence of tower, is now obtained as the new horizontal components from Eqs. F.2.7 and F.2.8 and the vertical component $v_{fmz}^H = v_{mz}^H$ which was not modified by the tower influence. Finally the vector is transformed to the tower coordinate system by use of the transformation

$$\begin{Bmatrix} v_{fmx}^T \\ v_{fmy}^T \\ v_{fmz}^T \end{Bmatrix} = \{v_{fm}^T\} = [T_{HT}]\{v_{fm}^H\} = \begin{bmatrix} \cos\alpha_{yaw} & \sin\alpha_{yaw} & 0 \\ -\sin\alpha_{yaw} & \cos\alpha_{yaw} & 0 \\ 0 & 0 & 1 \end{bmatrix} \begin{Bmatrix} v_{fmx}^H \\ v_{fmy}^H \\ v_{fmz}^H \end{Bmatrix} \quad \text{(F.2.9)}$$

which also defines the transformation matrix $[T_{HF}]$. The position in the horizontal plane where the wind speed is sought is usually known in the tower coordinates. The corresponding H–coordinates are found from

$$\begin{Bmatrix} x_H \\ y_H \end{Bmatrix} = \begin{bmatrix} \cos\alpha_{yaw} & -\sin\alpha_{yaw} \\ \sin\alpha_{yaw} & \cos\alpha_{yaw} \end{bmatrix} \begin{Bmatrix} x_T \\ y_T \end{Bmatrix} \quad \text{(F.2.10)}$$

The resulting wind speed in tower coordinates, equivalent to the flow field in the proximity of a wind turbine without rotor, is now written in tower coordinates as

$$\{v_f^T\} = \{v_{fm}^T\} + \{v_{ft}^T\} \quad \text{(F.2.11)}$$

where

$\{v_{ft}^T\}$ is the turbulent fluctuations directly transformed from meteorological coordinates

$$\{v_{ft}^T\} = [T_{MT}]\{v_t^M\} \quad \text{(F.2.12)}$$

The tower influence is only considered for points below the horizontal plane through the hub, defined by the z–coordinates $|z_T| <$ hubheight.

F.3 Momentum balance for a stream tube and induced velocity.

The aerodynamic forces on a blade element are assumed to be adequately described by the simple blade element theory. As shown in Fig. 3, the blade element is a radial section of the blade at radius z and of length Δz. The aerodynamic properties of the element are assumed to be completely defined by length and position of the chord, c, and profile coefficients, which relate the resulting wind speed to the force at a specific angle of attack, α (see Fig. 4).

The derivation of induced velocity is carried through by considering the momentum balance for a stream tube as shown in Fig. 3. The derivations found in the litterature e.g. [G3] consider the momentum balance for an annular stream tube and assumes that neighbouring tubes do not interact and further, that the induction is the same all over the annulus. The first of these assumptions is equivalent to assuming that the shear stress between adjacent annular tubes is negligible. The second assumption implies that the flow field must be axi-symmetric. These assumptions lead to rather simple equations for the induction. Only experiments can show

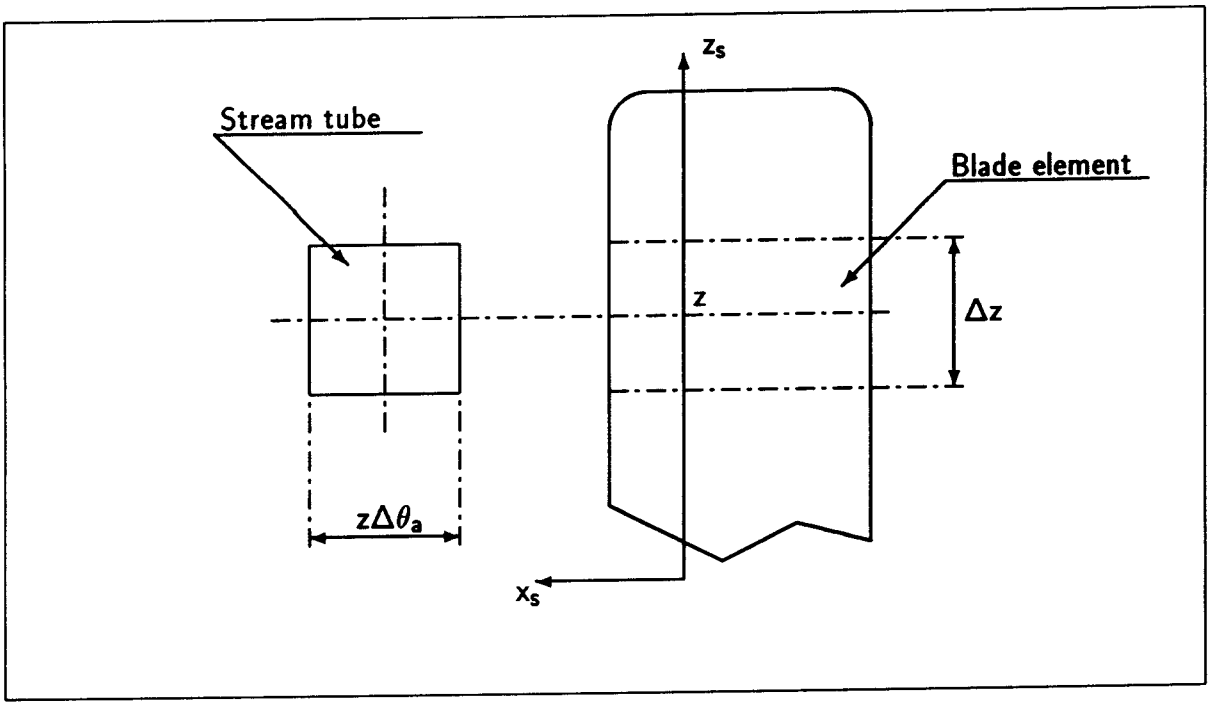

Figure 3: Stream tube and blade element.

whether the assumptions are reasonable. The flow through a wind turbine rotor is influenced, among other things, by wind-shear, tower shadow, and turbulence. The above assumptions are therefore always violated to a certain degree. Nevertheless, the equations are often used in their original form when incorporated in wind turbine models. It is equivalent to only considering a stream tube as shown in Fig. 3 and assuming that neighbouring tubes do not interact. This is done in the following, where the induced velocity is derived by considering the momentum balance for such a stream tube.

Below, the lower index s refers to the direction in which the momentum balance is considered.

The decrease in momentum for the flow through a stream tube, as shown in Fig. 3, is considered during the time for one rotor revolution

$$T = \frac{2\pi}{\omega} \tag{F.3.1}$$

where ω is the angular velocity of the rotor.

The mass-stream through the tube is

$$\dot{m} = \varrho u_s \left(z\Delta\theta_a \Delta z\right) \tag{F.3.2}$$

where

ϱ : density of the air
u_s : velocity of the air through the tube
z : actual radius
$\Delta\theta_a$: increment in azimuthal angle
Δz : radial length of the blade element

and the product in the brackets gives the area of the stream tube.

In the simple momentum theory the continuity condition for the flow implies that the decrease in wind-speed at the rotor plane is half the total decrease in speed for the air-stream passing the rotor disc. The half decrease is equal to the axial induction, w_s, and the total decrease is equal to $2w_s$. The same relation is assumed to be valid for the tube considered here.

By use of Eq. F.3.2 for the mass stream and the total decrease in velocity the total decrease in momentum for the flow through the stream tube, during one rotor revolution can be written

$$\dot{m}T(2w_s) = \varrho u_s \left(z\Delta\theta_a \Delta z\right) \frac{2\pi}{\omega} (2w_s) \tag{F.3.3}$$

This change in momentum is equal to the impulsive force from the rotor blades on the stream tube. The impulsive force from N blades (during one rotor revolution) is

$$NF_l\Delta t = N\left(l_s\Delta z\right)\left(\frac{\Delta\theta_a}{\omega}\right) \tag{F.3.4}$$

where

F_l = $l_s\Delta z$ expresses the lift force from one blade element on the stream tube
Δt = $\frac{\Delta\theta_a}{\omega}$ is the time this force acts on the tube during one revolution
l_s : projection of lift (per unit length) on the direction in which the momentum balance is considered

Equating the change in momentum and the impulsive force gives, after common factors have been cancelled

$$Nl_s = 4\pi\varrho u_s w_s z \tag{F.3.5}$$

The induced velocity on the right hand side w_s, is derived under the assumption that the rotor can be represented by a disc corresponding to an infinite number of blades. w_s is therefore also influenced by the actual number of blades. A correction for this is introduced in Eq. F.3.19 below.

The direction in which the momentum balance is considered, as referred to above with the index s, is defined by the vector $\{e_s\}$. In order to distinguish between $\{e_s\}$ and its projection on the profile cross section, the normalized projection is written with an extra lower index c, $\{e_{sc}\}$ as shown in Fig. 4. $\{e_s\}$ is parallel to the z–axis of the main shaft element closest to the hub and is directed downwind. The choice of this direction is based on the assumption that the total influence of the blades considered as a disc is in that direction.

It is convenient to define a coordinate system at the cross section, (x_s, y_s, z_s), where $\{e_{sc}\}$ is the unit vector in the y_s–direction. The z_s–axis coincides with the aerodynamic center and is parallel to the element z–axis. The x_s–axis is found as the last in the right hand triad.

This coordinate system is suitable for the calculations concerning the two–dimensional flow over the profile.

In Fig. 4 a cross section of the blade is shown. The two dimensional flow, from which the aerodynamic forces are derived, is considered. The vectors in the figure not already explained have the following meaning:

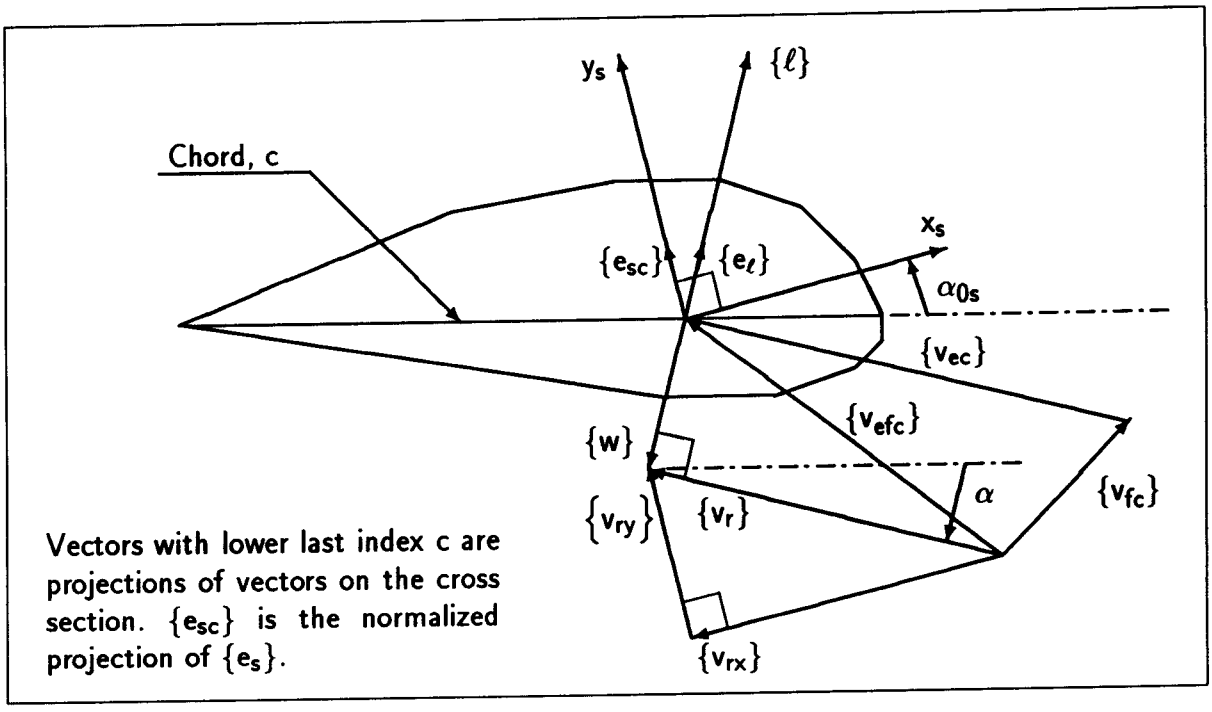

Figure 4: Projected wind speed and lift at a cross section.

$\{v_r\}$ resulting wind speed at the cross section

$$\{v_r\} = \{v_{fc}\} + \{v_{ec}\} + \{w\} \tag{F.3.6}$$

$\{v_{fc}\}$ projection on the cross sectional plane of the free wind speed $\{v_f\}$, including influence from tower shadow, shear, and turbulence, i.e. the wind speed that would be found at the same location if no blades were present

$\{v_{ec}\}$ projection on the cross sectional plane of the wind speed $\{v_e\}$, experienced by the blade due to its own velocity, including elastic deformation velocity

$\{v_{efc}\}$ projection on the cross sectional plane of the sum of $\{v_e\}$ and $\{v_f\}$

$\{w\}$ induced wind speed, directed opposite to the lift $\{l\}$ and perpendicular to $\{v_r\}$

$\{v_{rx}\}$ component of $\{v_r\}$ along x_s–axis, $|\{v_{rx}\}| = v_{rx}$

$\{v_{ry}\}$ component of $\{v_r\}$ along y_s–axis, $|\{v_{ry}\}| = v_{ry}$

$\{l\}$ resulting lift force, perpendicular to $\{v_r\}$

$\{e_l\}$ unit vector in direction of lift

The remaining symbols in Fig. 4 refer to

c chord length

α angle of attack. The angle from chord direction to resulting wind speed $\{v_r\}$. The angle is positive in negative z_s–sense (positive z_s–sense refers to the rotation direction, which a right hand screw should be turned in order to move in direction of z_s)

α_{0s} angle from chord direction to x_s. The angle is positive in positive z_s–sense

To proceed, it will be helpful to derive the scalar quantities in the momentum balance in Eq. F.3.5 from the vectors representing velocities and forces.

The following interpretation is given of the scalars above

u_s is the projection of the sum of the free wind speed, $\left\{v_f^S\right\}$ and the induced velocity, $\left\{w^S\right\}$, upon the shaft-parallel unit vector $\{e_s\}$. If the projections are expressed by the scalar product we get

$$\begin{aligned} u_s &= \left\{e_s^S\right\}^T \left\{v_f^S\right\} + \left\{e_s^S\right\}^T \left\{w^S\right\} \\ &= v_{fs} + w_s \end{aligned} \tag{F.3.7}$$

l_s is the projection of the lift vector upon $\{e_s\}$

$$l_s = \left\{l^S\right\}^T \left\{e_s^S\right\} \tag{F.3.8}$$

where

$$\begin{aligned} \left\{l^S\right\} &= \frac{1}{2}\varrho \left|\left\{v_r^S\right\}\right|^2 C_L(\alpha)\, c \left\{e_l^S\right\} \\ &= l \left\{e_l^S\right\} \end{aligned} \tag{F.3.9}$$

In this equation some symbols have been used for the first time and their meaning have to be explained:

$C_L(\alpha)$ the profile lift coefficient for 2–dimensional flow, which is a function of α.

l numerical value of the lift (Eq. F.3.9 defines the variable)

The vector introduced above, $\left\{e_l^S\right\}$, is found as the unit vector in the direction of $\left\{v_r^S\right\}$ rotated $\frac{\pi}{2}$ in negative z_s–sense. This relationship is explained by the law giving the size and direction of lift caused by the circulation around the profile $\left\{\gamma_v^S\right\}$ and the resulting velocity $\left\{v_r^S\right\}$

$$\left\{l^S\right\} = \varrho \left\{v_r^S\right\} \times \left\{\gamma_v^S\right\} \tag{F.3.10}$$

$\left\{\gamma_v^S\right\}$ is directed along the z–axis.

The unit vector in direction of $\left\{v_r^S\right\}$ is written

$$\left\{e_r^S\right\} = \frac{\left\{v_r^S\right\}}{|\{v_r^S\}|} = \left\{ \begin{array}{c} e_{rx} \\ e_{ry} \\ 0 \end{array} \right\} \tag{F.3.11}$$

Expressing $\left\{v_r^S\right\}$ in this equation by its components in the S–system

$$\left\{v_r^S\right\}^T = [v_{rx}, v_{ry}, 0] \tag{F.3.12}$$

we get

$$e_{rx} = \frac{v_{rx}}{\sqrt{v_{rx}^2 + v_{ry}^2}} \tag{F.3.13}$$

$$e_{ry} = \frac{v_{ry}}{\sqrt{v_{rx}^2 + v_{ry}^2}} \tag{F.3.14}$$

The unit vector in direction of the lift is the vector $\left\{e_r^S\right\}$ rotated $\frac{\pi}{2}$ in negative z_s–sense or equivalently defined by the cross product

$$\left\{e_l^S\right\} = \left\{e_r^S\right\} \times \left\{e_z^S\right\} = \left\{ \begin{array}{c} e_{ry} \\ -e_{rx} \\ 0 \end{array} \right\} \tag{F.3.15}$$

Now, the momentum balance can be written in vector notation

$$4\pi\varrho \left(\left\{e_s^S\right\}^T \left\{v_f^S\right\} + \left\{e_s^S\right\}^T \left\{w^S\right\}\right) \left(\left\{e_s^S\right\}^T \left\{w^S\right\}\right) z = \frac{1}{2} N \varrho \left|\left\{v_r^S\right\}\right|^2 C_L(\alpha)\, c \left(\left\{e_l^S\right\}^T \left\{e_s^S\right\}\right) \tag{F.3.16}$$

from which the induced velocity $\left\{w^S\right\}^T = \left[w_x^S, w_y^S, 0\right]$ has to be found. In fact Eq. F.3.16 is an equation with only one unknown scalar, when it is realized that

$$\{w^s\} = -w \left\{e_l^S\right\} \tag{F.3.17}$$

Introduction of this relationship in the momentum balance Eq. F.3.16 gives after reduction

$$w = \frac{N \left|\left\{v_r^S\right\}\right|^2 C_L(\alpha)\, c}{8\pi z \left[\{e_s^S\}^T \left\{v_f^S\right\} - w \{e_s^S\}^T \{e_l^S\}\right]} \tag{F.3.18}$$

giving a value for the induced wind speed. The solution is an iterative procedure because $\left\{v_r^S\right\}$, $\left\{e_l^S\right\}$, and α are functions of w.

In deriving the momentum equation it has been assumed that the rotor has an infinite number of blades. When only a finite number of blades are present the induction will not have its full strength close to the boundary of the wake due to a flow of air around the edges of the vortex sheets, which are shed from the trailing edges of the blades. An approximate description of this flow has been given originally by L. Prandtl and can be found in [G3]. According to this theory, the influence on the induced velocity is taken into account through the so called tipcorrection which is expressed by the reduction factor

$$F = \frac{2}{\pi} \arccos \left[\exp \left(-\frac{N}{2} \frac{R-z}{z \sin \phi} \right) \right] \tag{F.3.19}$$

where

R is the radius of the rotor

ϕ is the angle between the vortex sheet and the plane of rotation at the blade tip. The angle can be derived from

$$\sin \phi = \frac{\left\{v_r^S\right\}^T \left\{e_s^S\right\}}{\left|\left\{v_r^S\right\}\right|} \tag{F.3.20}$$

In the present application of the theory the tipcorrection is introduced in Eq. F.3.18 as a factor on w, only on the left hand side. This is in accordance with the use of the theory in [Ø1, 31 pp.] where a reference is given to [V2]. Here, it is shown that the tipcorrection should be used in this way, and w on the right hand side of the equation should not be corrected, as one would immediately expect.

Defining the axial induction factor as

$$a = \frac{w_s}{\left\{e_s^S\right\}^T \left\{v_f^S\right\}} \tag{F.3.21}$$

it is clear from the derivation of the momentum equation that the theory only is valid for the axial induction factor less or equal to $\frac{1}{2}$, in that $a = \frac{1}{2}$ corresponds to zero velocity in the wake.

In order to adapt the theory to situations of high induction an empirical correction factor f_m on the mass stream is introduced according to [Ø1, 31 pp.] and [F1, 18 pp.]

$$f_m = \begin{cases} 1 & \text{for} \quad a < \frac{1}{3} \\ 1.25 - 0.75a & \text{for} \quad a \geq \frac{1}{3} \end{cases} \tag{F.3.22}$$

The final equation for w is now

$$Fw = \frac{N \left|\left\{v_r^S\right\}\right|^2 C_L(\alpha)\, c}{8\pi z \left[\left\{e_s^S\right\}^T \left\{v_f^S\right\} - f_m w \left\{e_s^S\right\}^T \left\{e_l^S\right\}\right]} \tag{F.3.23}$$

which, as mentioned above, must be solved by an iterative procedure.

F.4 Simplification of the induction equation.

With the purpose of simplifying the solution of Eq. F.3.23 the equation is rewritten in the following by use of the geometric relations, which can be derived from Fig. 4.

By use of Eqs. F.3.13, F.3.14, F.3.15, and F.3.17 the induced wind speed can be written

$$\left\{w^S\right\} = w \left\{ \begin{array}{c} -\frac{v_{ry}}{v_{rx}} \\ 1 \\ 0 \end{array} \right\} \frac{\frac{v_{rx}}{|v_{rx}|}}{\sqrt{1+\left(\frac{v_{ry}}{v_{rx}}\right)^2}} = w \left\{ \begin{array}{c} -\lambda \\ 1 \\ 0 \end{array} \right\} \frac{\text{sign}\,(v_{rx})}{\sqrt{1+\lambda^2}} \tag{F.4.1}$$

where

$$\lambda = \frac{v_{ry}}{v_{rx}} \tag{F.4.2}$$

$$\text{sign} v_{rx} = \frac{v_{rx}}{|v_{rx}|} \tag{F.4.3}$$

Equating vector components for the resulting wind speed

$$\left\{v_r^S\right\} = \left\{ \begin{array}{c} v_{rx} \\ v_{ry} \\ 0 \end{array} \right\} = \left\{v_{efc}^S\right\} + \left\{w^S\right\} = \left\{ \begin{array}{c} v_{efcx} \\ v_{efcy} \\ 0 \end{array} \right\} + w \left\{ \begin{array}{c} -\lambda \\ 1 \\ 0 \end{array} \right\} \frac{\text{sign}\,(v_{rx})}{\sqrt{1+\lambda^2}} \tag{F.4.4}$$

we get

$$v_{rx} = v_{efcx} - w\frac{\lambda \text{sign}\,(v_{rx})}{\sqrt{1+\lambda^2}} \tag{F.4.5}$$

$$v_{ry} = v_{efcy} + w\frac{\text{sign}\,(v_{rx})}{\sqrt{1+\lambda^2}} \tag{F.4.6}$$

Dividing Eq. F.4.6 with Eq. F.4.5 gives

$$\lambda = \frac{v_{ry}}{v_{rx}} = \frac{v_{efcy} + w\frac{\text{sign}(v_{rx})}{\sqrt{1+\lambda^2}}}{v_{efcx} - w\frac{\lambda \text{sign}(v_{rx})}{\sqrt{1+\lambda^2}}} \tag{F.4.7}$$

By solving this quadratic equation in λ we get

$$\lambda = \frac{\gamma \pm \delta\sqrt{1+\gamma^2-\delta^2}}{\gamma^2-\delta^2} \tag{F.4.8}$$

where

$$\gamma = \frac{v_{efcx}}{v_{efcy}} \quad \left(\text{comparable to the speed ratio } \frac{\omega z}{\left|\left\{e_s^S\right\}^T \left\{v_f^S\right\}\right|}\right) \tag{F.4.9}$$

$$\delta = \frac{w}{v_{efcy}} \quad \text{(comparable to the axial induction factor } a\text{)} \tag{F.4.10}$$

During the solution both sides of the equation have been squared in order to remove the square roots. This implies that some limitations must be imposed on the result. When sign$(v_{rx}) = -1$ and further $v_{efcx} < 0$, which is usually the case because of the wind speed felt by the blade due to its rotation, λ must fulfil the condition

$$\lambda > \frac{v_{efcy}}{v_{efcx}} = \frac{1}{\gamma} \tag{F.4.11}$$

When this condition is met, it can be shown that the negative square root must be chosen in Eq. F.4.8. Similar conditions can be set for other sign intervals for the variables, and the correct solution can be chosen.

By introduction of the variables defined above in Eq. F.3.23 the equation can be written in a form more suitable for solution

$$F\delta = \frac{N\left(1+\gamma^2-\lambda^2\right)C_L\left(\lambda\right)}{8\pi z\left(\frac{1}{v_{efcy}}\left\{e_s^S\right\}^T\left\{v_f^S\right\} + f_m\delta\left\{e_s^S\right\}^T\left\{\begin{array}{c}-\lambda\\1\\0\end{array}\right\}\frac{\text{sign}(v_{rx})}{\sqrt{1+\lambda^2}}\right)} \tag{F.4.12}$$

The lift coefficient C_L is here given as a function of λ because the angle of attack can be written

$$\alpha = \arctan\left(-\lambda\right) - \alpha_{0s} \tag{F.4.13}$$

In this equation an extended definition for arctan has to be used in order to get values correct when $|\alpha| \geq \frac{\pi}{2}$. In Table 1 below the corresponding intervals for dependent and independent variables are given.

v_{rx}	v_{ry}	value of α
$=0$	>0	$\alpha = -\frac{\pi}{2}$
$=0$	<0	$\alpha = \frac{\pi}{2}$
>0	$=0$	$\alpha = 0$
<0	$=0$	$\alpha = \pi$
<0	>0	$0 < \alpha < \frac{\pi}{2}$
<0	<0	$-\frac{\pi}{2} < \alpha < 0$
>0	>0	$\frac{\pi}{2} < \alpha < \pi$
>0	<0	$-\frac{\pi}{2} < \alpha < -\pi$

Table 1: Values of modified *arctan*-function.

The solution of Eq. F.4.12 implies that the S coordinate– system must be determined as well as the transformation betweeen element coordinates (E) and the S–coordinates. The latter is used both when establishing the wind–speeds in the S–system and when the loads found in the S–system are transformed to the E–coordinates. Therefore the direction cosines and the transformation matrix is derived in the following with reference to Fig. 5.

The shaft parallel unit vector $\left\{e_s^A\right\}$ with coordinates in the shaft substructure coordinates (A) is transformed to the element coordinate system (E) by use of the transformation

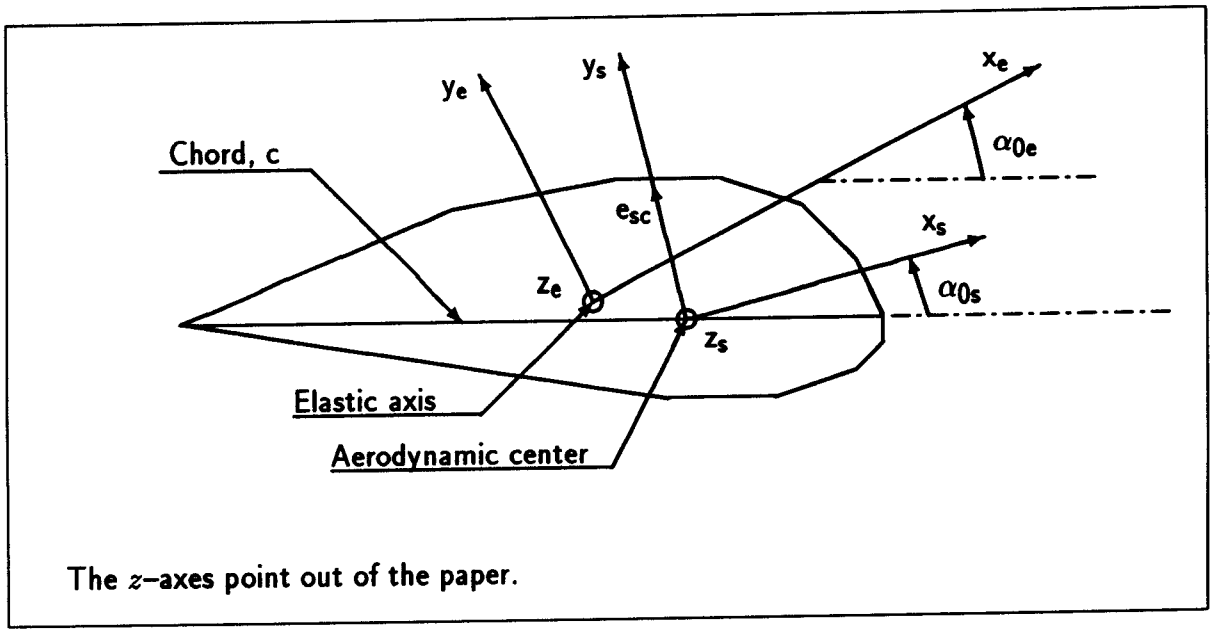

Figure 5: Coordinate systems at cross section.

$$\left\{e_s^E\right\} = [T_{BE}]\,[T_{AB}]\left\{e_s^A\right\} = \left\{\begin{array}{ccc} e_{sx}^E & e_{sy}^E & e_{sz}^E \end{array}\right\} \tag{F.4.14}$$

The projection of this vector on the cross sectional plane determines the $\left\{e_{sc}^E\right\}$ vector after normalizing. The projection is equivalent to setting the e_{sz}^E component equal to zero. The vector defines the unit vector in direction of y_s

$$\left\{e_{sc}^E\right\}^T = [e_{scx}, e_{scy}, 0] = \left\{e_{ys}^E\right\}^T \tag{F.4.15}$$

where

$$e_{scx} = \frac{e_{sx}^E}{\sqrt{\left(e_{sx}^E\right)^2 \left(e_{sy}^E\right)^2}} \tag{F.4.16}$$

$$e_{scy} = \frac{e_{sy}^E}{\sqrt{\left(e_{sx}^E\right)^2 \left(e_{sy}^E\right)^2}} \tag{F.4.17}$$

The unit vector in direction of z_e is normal to the cross sectional plane and we have

$$\left\{e_{zs}^E\right\}^T = [0, 0, 1] \tag{F.4.18}$$

The last unit vector in the triad is found as the cross product

$$\left\{e_{xs}^E\right\} = \left\{e_{ys}^E\right\} \times \left\{e_{zs}^E\right\} = \left\{\begin{array}{c} e_{scy} \\ -e_{scx} \\ 0 \end{array}\right\} \tag{F.4.19}$$

The components of the three unit vectors define the direction cosines and the vectors are identified as the columns in the transformation matrix

$$[T_{SE}] = \begin{bmatrix} e_{scy} & e_{scx} & 0 \\ -e_{scx} & e_{scy} & 0 \\ 0 & 0 & 1 \end{bmatrix} \tag{F.4.20}$$

The angle, which the S–system is rotated relative to the E–system in the cross sectional plane, is found from Fig. 5 as

$$\alpha_{es} = \alpha_{0s} - \alpha_{0e} \tag{F.4.21}$$

with the sign in accordance with the positive z–sense rotation. The value of the angle is found from one of the direction cosines, e.g. e_{scx} as

$$\alpha_{es} = \arcsin(-e_{scx}) \tag{F.4.22}$$

The angle α_{0e} is known from the blade geometry as the angle from the chord to the x_e–axis, which is the principal x–bending axis. The location of the chord is given through the pitch setting angle. The influence of the elastic deformation of the blade on the aerodynamic load due to change in geometry may be taken into account, either by updating the FEM geometry of the blade during solution or by updating only the pitch setting angle according to torsional deformation.

The angle of attack can finally be found from Eqs. F.4.13, F.4.20, and F.4.21 as

$$\alpha = \arctan(-\lambda) - \alpha_{es} - \alpha_{0e} \tag{F.4.23}$$

and all the variables are now determined.

F.5 Cross sectional loads in element coordinates.

When the induced velocity and the angle of attack has been found, the aerodynamic loads at a cross section can be derived.

Denoting the pressure

$$p_v = \frac{1}{2}\varrho \left|\{v_r^S\}\right|^2 \tag{F.5.1}$$

we get from Eq. F.3.9

$$\{l^S\} = p_v C_L(\alpha)\, c \{e_l^S\} \tag{F.5.2}$$

The profile drag is in direction of $\{v_r\}$ and is expressed by

$$\{d^S\} = p_v C_D(\alpha)\, c \{e_r^S\} \tag{F.5.3}$$

where

$C_D(\alpha)$ is the profile moment coefficient for two dimensional flow. The coefficient is a function of α.

$\left\{e_r^S\right\}$ is defined in Eq. F.3.11

Finally, the torque is derived from

$$\left\{m^S\right\}^T = \left[0, 0, p_v C_M(\alpha) c^2\right] \tag{F.5.4}$$

where

$C_M(\alpha)$ is the profile moment coefficient for two dimensional flow and with respect to the aerodynamic center. The coefficient is also a function of α.

The transformation of the aerodynamic loads from the S– to the E–coordinates is considered next.

The forces in the E–system yields

$$\left\{l^E\right\} = p_v C_L(\alpha) c [T_{SE}] \left\{e_l^S\right\} = \begin{Bmatrix} l_x^E \\ l_y^E \\ 0 \end{Bmatrix} \tag{F.5.5}$$

$$\left\{d^E\right\} = p_v C_D(\alpha) c [T_{SE}] \left\{e_r^S\right\} = \begin{Bmatrix} d_x^E \\ d_y^E \\ 0 \end{Bmatrix} \tag{F.5.6}$$

Because the aerodynamic center generally lies outside the elastic axis (refer to Fig. 5), the forces contribute to the moment when referred to the elastic axis coordinate system (E). If the coordinates for the aerodynamic center in E–coordinates is given by

$$\left\{r_{ac}^E\right\}^T = [x_{ac}, y_{ac}, 0] \tag{F.5.7}$$

the total moment with respect to the z_e–axis yields

$$\left\{m^E\right\} = [T_{SE}] \left\{m^S\right\} + \left\{r_{ac}^E\right\} \times \left(\left\{l^E\right\} + \left\{d^E\right\}\right) = \begin{Bmatrix} 0 \\ 0 \\ m_z^E \end{Bmatrix} \tag{F.5.8}$$

Adding the force components gives the resulting force vector

$$\left\{f^E\right\}^T = \left[\left(l_x^E + d_x^E\right), \left(l_y^E + d_y^E\right), 0\right] = \begin{Bmatrix} f_x^E \\ f_x^E \\ 0 \end{Bmatrix} \tag{F.5.9}$$

Now, both force and moment are given in the element coordinates, where the consistent transformation to the nodes is straight forward. This transformation will be shown in the following chapter.

F.6 Consistent transformation of distributed aerodynamic loads to the nodes.

For a good structural model a high resolution in beam elements is wanted at the root section of the blade, where the highest deformations can be expected, and for a good aerodynamic model a dense distribution of aerodynamic calculation points is wanted close to the tip, because the influence of the loads is most important here and because the resulting wind-speed has biggest variation here.

To ensure the most correct dynamic behaviour, the structural modelling is given the highest priority, which means that the element division close to the tip of the blade might be rather coarse. An aerodynamic calculation only at the nodes could therefore prove to be a bad aerodynamic model in that area. In spite of that, a distribution of aerodynamic calculation points following the element is accepted, because only a qualitatively correct aerodynamic excitation is needed.

The reason for not doing things more correctly, and just define the aerodynamic calculation points independently of the beam elements, is partly to speed up the simulations and partly to simplify the programming.

A compromise is accepted, where the derivation of the aerodynamic node loads is not only based on a calculation of the aerodynamic load at the nodes, but at three points along each blade element. Thus every added element gives rise to three added calculation points instead of only one, as would be the case if the calculation was restricted to the nodes.

The calculation points are distributed along the element so that the spacing is equal between consecutive points on an assembly of elements of the same length. The distribution of calculation points is shown in Figure 6, where ℓ is the element length. The meaning of the vectors and the indexing is explained below.

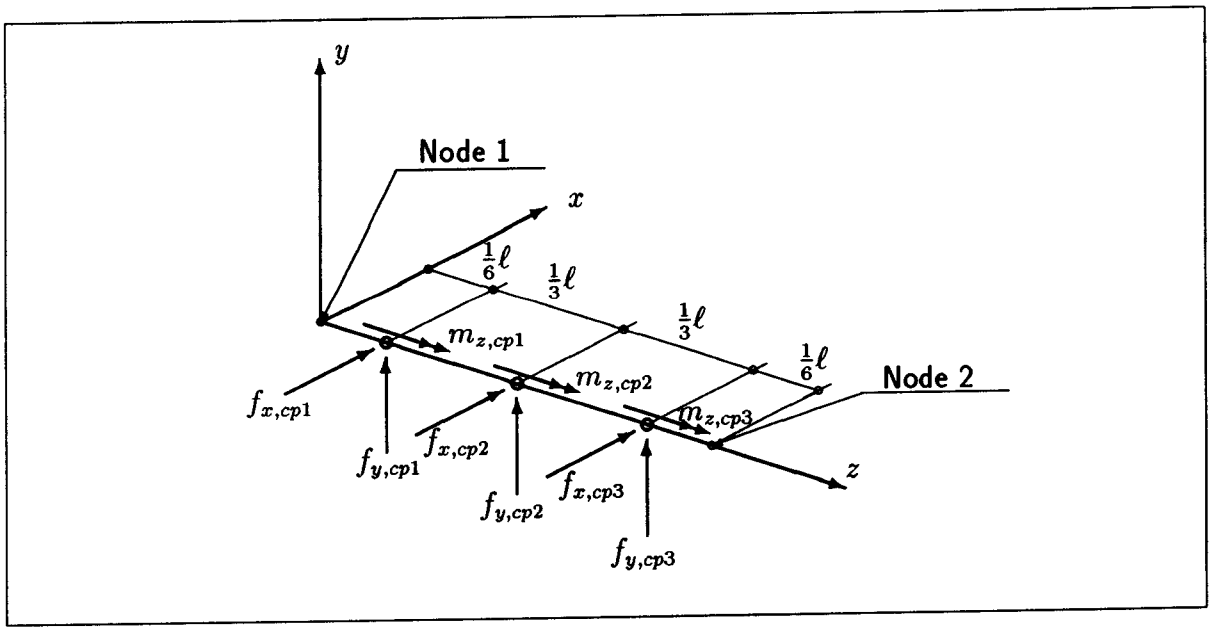

Figure 6: Aerodynamic calculation points.

From the calculated aerodynamic load at each point a parabolic interpolation is used as the actual distributed load along the element. This distribution is the basis for a transformation of the loads consistently to the nodes. The theory outlined in [Part 1, Sec. 4.10] with the result in [Part 1, Eq. 4.10.14] is used. The loads are all referred to the element principal axis

coordinate–system, and are only functions of the z–coordinate. Thus the transformation for element no. i is carried out according to

$$\left\{F^{Ei}_{aer,n}\right\} = \int_0^\ell [N_{SB}(z)]^T \{f_\ell(z)\}\, dz \tag{F.6.1}$$

where the factors in the product can be truncated according to the only aerodynamic load components, which are different from zero

$f^{Ei}_{x,cpi}$: aerodynamic force component in x–direction
$f^{Ei}_{y,cpi}$: aerodynamic force component in y–direction
$m^{Ei}_{z,cpi}$: aerodynamic moment component in z–direction

where the index cpi refers to calculation point no. i, $i = 1,2,3$. The index Ei implies, that the components are with reference to the element coordinates. As described in Sec F.5 the situation, where the aerodynamic center lies outside the elastic axis has been taken into account.

According to the parabolic interpolation the truncated load vector can be written

$$\begin{aligned}\left\{f_\ell(z)^{Ei}\right\}_{tr} &= \left\{f_{aer}(z)^{Ei}\right\} \\ &= \begin{Bmatrix} a_x z^2 + b_x z + c_x \\ a_y z^2 + b_y z + c_y \\ a_m z^2 + b_m z + c_m \end{Bmatrix} \\ &= \{f_a\}\, z^2 + \{f_b\}\, z + \{f_c\}\end{aligned} \tag{F.6.2}$$

where the index tr refers to truncation. The vector has only three components as explained above.

In Eq. F.6.2 the coefficient vectors are linear combinations of the loads derived at the calculation points. The coefficient components are found by solving Eq. F.6.2 for each load component at all three calculation points, giving rise to three equations with three unknowns for each load component.

For the coefficient–vector to z^2 we get

$$\begin{aligned}\{f_a\} &= \begin{Bmatrix} a_x \\ a_y \\ a_m \end{Bmatrix} \\ &= \begin{Bmatrix} \frac{9}{\ell^2}\left[\frac{1}{2}f_{x,cp1} - f_{x,cp2} + \frac{1}{2}f_{x,cp3}\right] \\ \frac{9}{\ell^2}\left[\frac{1}{2}f_{y,cp1} - f_{y,cp2} + \frac{1}{2}f_{y,cp3}\right] \\ \frac{9}{\ell^2}\left[\frac{1}{2}f_{m,cp1} - f_{m,cp2} + \frac{1}{2}f_{m,cp3}\right] \end{Bmatrix} \\ &= \frac{1}{\ell^2}\frac{9}{2}\left[\{f_{cp1}\} - 2\{f_{cp2}\} + \{f_{cp3}\}\right]\end{aligned} \tag{F.6.3}$$

With equivalent notation the coefficient–vector for z is found to be

$$\{f_b\} = \frac{1}{\ell} 3 \left[-2\{f_{cp1}\} + 3\{f_{cp2}\} - \{f_{cp3}\}\right] \tag{F.6.4}$$

and finally the constant term is

$$\{f_c\} = \frac{1}{8} \left[15\{f_{cp1}\} - 10\{f_{cp2}\} + 3\{f_{cp3}\}\right] \tag{F.6.5}$$

Now, inserting Eq. F.6.2 in Eq. F.6.1 results in the following integral

$$\left\{F^{Ei}_{aer,n}\right\} = \int_0^\ell \left[N_{SB}(z)\right]^T_{tr} \left[\{f_a\} z^2 + \{f_b\} + \{f_c\}\right] dz \tag{F.6.6}$$

As above, the index tr refers to truncation. The matrix has only three columns, corresponding to the load components different from zero. Substituting matrix symbols for the integrals, which are defined below, we get

$$\left\{F^{Ei}_{aer,n}\right\} = [I_{4L}]_{tr} \{f_a\} \ell^2 + [I_{3L}]_{tr} \{f_b\} \ell + [I_{2L}]_{tr} \{f_c\} \tag{F.6.7}$$

Here

$$[I_{2L}]_{tr} = \int_0^\ell \left[N_{SB}(z)\right]^T_{tr} dz \tag{F.6.8}$$

and

$$[I_{3L}]_{tr} = \int_0^\ell \left[N_{SB}(z)\right]^T_{tr} \frac{z}{\ell} dz \tag{F.6.9}$$

have been derived as full 12×6 matrices in [Part 1, Eqs. 4.11.33 and 4.11.36], respectively. The result of the integration along the element length of the remaining integral

$$[I_{4L}]_{tr} = \int_0^\ell \left[N_{SB}(z)\right]^T_{tr} \left(\frac{z}{\ell}\right)^2 dz \tag{F.6.10}$$

(listed without truncation) is the 12×6 matrix

$[I_{4L}] =$

$$\ell \begin{bmatrix}
\varrho_y\left(\eta_y+\frac{1}{15}\right) & 0 & 0 & 0 & -\frac{3\varrho_y}{10\ell} & 0 \\
0 & \varrho_x\left(\eta_x+\frac{1}{15}\right) & 0 & \frac{3\varrho_x}{10\ell} & 0 & 0 \\
0 & 0 & \frac{1}{12} & 0 & 0 & 0 \\
\hline
0 & -\ell\varrho_x\left(\frac{3}{10}\eta_x+\frac{1}{60}\right) & 0 & \varrho_x\left(\eta_x-\frac{1}{15}\right) & 0 & 0 \\
\ell\varrho_y\left(\frac{3}{10}\eta_y+\frac{1}{60}\right) & 0 & 0 & 0 & \varrho_y\left(\eta_y-\frac{1}{15}\right) & 0 \\
-e_{s2}\left[\varrho_y\left(\eta_y+\frac{1}{15}\right)-\frac{1}{12}\right] & e_{s1}\left[\varrho_x\left(\eta_x+\frac{1}{15}\right)-\frac{1}{12}\right] & 0 & \frac{3\varrho_x}{10\ell}e_{s1} & \frac{3\varrho_y}{10\ell}e_{s2} & \frac{1}{12} \\
\hline
\varrho_y\left(3\eta_y+\frac{4}{15}\right) & 0 & 0 & 0 & \frac{3\varrho_y}{10\ell} & 0 \\
0 & \varrho_x\left(3\eta_x+\frac{4}{15}\right) & 0 & -\frac{3\varrho_x}{10\ell} & 0 & 0 \\
0 & 0 & \frac{1}{4} & 0 & 0 & 0 \\
\hline
0 & \ell\varrho_x\left(\frac{3}{10}\eta_x+\frac{1}{30}\right) & 0 & \varrho_x\left(3\eta_x+\frac{1}{10}\right) & 0 & 0 \\
-\ell\varrho_y\left(\frac{3}{10}\eta_y+\frac{1}{30}\right) & 0 & 0 & 0 & \varrho_y\left(3\eta_y+\frac{1}{10}\right) & 0 \\
-e_{s2}\left[\varrho_y\left(3\eta_y+\frac{4}{15}\right)-\frac{1}{4}\right] & e_{s1}\left[\varrho_x\left(3\eta_x+\frac{4}{15}\right)-\frac{1}{4}\right] & 0 & -\frac{3\varrho_x}{10\ell}e_{s1} & -\frac{3\varrho_y}{10\ell}e_{s2} & \frac{1}{4}
\end{bmatrix}$$

(F.6.11)

The resulting node load from Eq. F.6.7 is with reference to the element coordinates (Ei). After transformation to blade coordinates (B)

$$\left\{F^B_{aer,n}\right\} = [T_{EiB}]\left\{F^{Ei}_{aer,n}\right\} \tag{F.6.12}$$

the load is ready for combination into the equation of motion for the total structure, where it is part of $\left\{F^B_{BBE}\right\}$ in [Part 1, Eq. 6.5.7].

G References.

[Part 1] Petersen, J.T. *Kinematically Nonlinear Finite Element Model of a Horizontal Axis Wind Turbine.*
This thesis, Part 1: Mathematical Model and Results.
Dept. of Meteorology and Wind Energy.
Risø National Laboratory. Roskilde, Denmark, 1990.

[B1] Bathe, K-J. *Finite Element Procedures in Engineering Analysis.* Prentice-Hall, Englewood Cliffs, New Jersey, 1982.

[B2] Butterfield, C.P. *Three-Dimensional Airfoil Performance Measurements on a Rotating Wing.* Proceedings of the European Wind Energy Conference. Glasgow, Scotland, July 1989.

[C1] Clough, R.W. and Penzien, J. *Dynamics of Structures.* McGraw-Hill, New York, 1975.

[C2] Cowper, C.R. *The Shear Coefficient in Timoshenko's Beam Theory.* Journal of Applied Mechanics. June, 1966, pp. 335-340.

[D1] Davenport, A.G. *The Spectrum of Horizontal Gustiness near the Ground in High Winds.* Quart. Jr. Met. Soc., Vol. 87, 1961, pp. 194-211.

[F1] Fabian, O. *A new method for aeroelastic analysis of wind turbines.* Department of Fluid Mechanics. Technical University of Denmark. Lyngby, Denmark, 1981.

[G1] Garrad, A.D. *The Use of Finite Element Methods for Wind Turbine Dynamics.* Proceedings of the Ninth BWEA Wind Energy Association Conference. Edinburgh, England, April 1987, pp. 79-83.

[G2] Garrad, A.D. and Quarton, D.C. *Symbolic Computing as a Tool in Wind Turbine Dynamics.* Journal of Sound and Vibration. Vol. 109, No. 1, 1986, pp. 65-78.

[G3] Glauert, H. *Airplane Propellers. In: Aerodynamic Theory.* Ed. by W.F. Durand. Springer, Berlin, 1935.

[G4] Goldstein, H. *Classical Mechanics.* Addison-Wesley, Reading, Massachusetts, 1981.

[G5] Goyder, H.G.D. *A Novel Method for the Numerical Simulation of Turbulence.* Proceedings of the Tenth BWEA Wind Energy Association Conference. London, England, March 1988, pp. 121-127.

[H1] Hansen, K.S. and Larsen, A.M. *Hvirvelmodel til simulering af horisontalakslede vindturbiner.* Department of Fluid Mechanics. Technical University of Denmark. Lyngby, Denmark, 1981.

[H2] Hearn, A.C. *Reduce User's Manual.* Version 3.3, RAND Publication CP78 (Rev. 7/87). The RAND Corporation. Santa Monica, California, 1987.

[H3] Hemon, A., Zervos, A., and Huberson S. *Numerical Computation of Unsteady Forces on a Hawt.* Proceedings of the European Wind Energy Conference. Glasgow, Scotland, July 1989.

[H4] Holley, W.E., Thresher, R.W., and Lin, S.R. *Atmospheric Turbulence inputs for Horizontal Axis Wind Turbines.* Proceedings of the European Wind Energy Conference. Hamburg, West Germany, October 1984.

[J1] Janetzke, D.C. and Kaza, K.R.V. *Whirl Flutter Analysis of a Horizontal-Axis Wind Turbine with a Two-Bladed Teetering Rotor.* Proceedings of the Second DOE/NASA Wind Turbine Workshop. Cleveland, Ohio, 1981, pp. 201-210.

[K1] Kaimal, J.C. et al. *Spectral Characteristics of Surface Layer Turbulence.* Quart. Jr. Met. Soc., Vol. 98, 1972, pp. 563-589.

[K2] Krenk, S. and Jeppesen, B. *Calculation of Cross Section Properties of Wind Turbine Blades.* Proceedings of the European Community Wind Energy Conference. Herning, Denmark, June 1988, pp. 332-336.

[L1] Larsen, G.C., Frandsen, S., Sørensen, P., and Courtney, M.S. *Design Basis for Horizontal Axis Wind Turbines – Theoretical Background.* Risø report. M-2836. Risø National Laboratory. Roskilde, Denmark, 1989.

[L2] Lobitz, D.W. *A NASTRAN-Based Computer Program for Structural Dynamic Analysis of Horizontal Axis Wind Turbines.* Sandia report. SAND-84-0924C. Sandia National Laboratories. Albuquerque, New Mexico, 1984.

[L3] Lundsager, P., Frandsen, S., and Christensen, C.J. *The Measurements on the Gedser Windmill. 1977-1979.* Risø report. M-2250. Risø National Laboratory. Roskilde, Denmark, 1980.

[M1] Madsen, H.A. and Rasmussen, F. *Derivation of Three-Dimensional Airfoil Data on the Basis of Experiment and theory.* Paper presented at: Wind Power 1988. Honolulu, Hawaii, September, 1988 .

[M2] Madsen, H.A. *Measured Airfoil Characteristics of Three Blade Segments on a 19 M HAWT Rotor.* Paper presented at: The Thirteenth Annual Energy-Sources Technology Conference and Exhibition, New Orleans, Louisiana, January, 1990.

[M3] Madsen, P.H., and Rasmussen, F. *Rotor Loading on a Three-Bladed Wind Turbine.* Proceedings of the European Wind Energy Conference, EWEC'89. Glasgow, Scotland, July 1989.

[M4] Madsen, P.H., Frandsen, S., Holley, W.E., and Hansen, J.C. *Dynamics and Fatigue Damage of Wind Turbine Rotors during Steady Operation.* Risø National Laboratory. Roskilde , Denmark, 1984.

[M5] Madsen, P.H., Hock, S.M., and Hausfeld, T.E. *Turbulence Loads on the Howden 26 m Diameter Wind Turbine* Proceedings of Seventh ASME Wind Energy Symposium. New Orleans, Lousiana, January 1988, pp. 139-147.

[M6] Meirovitch, L. *Computational Methods in Structural Dynamics.* Sijthoff & Noordhoff. Alphen aan den Rijn, The Nederlands, 1980.

[M7] Meirovitch, L. *Methods of Analytical Dynamics.* McGraw-Hill, New York, 1970.

[P1] Patel, M.H. and Garrad, A.D. *Wind turbine tower and blade dynamics.* Proceedings of the Tenth BWEA Wind Energy Association Conference. London, England, March 1988, pp. 401-405.

[P2] Pedersen, B.M. and Nielsen, P. *Description of the two Danish 630 kW Wind Turbines, Nibe-A and Nibe-B, and some preliminary test results.* Proceedings of the 3rd International Symposium on Wind Energy Systems. Copenhagen, Denmark, August 1980. pp. 223-238.

[P3] Pedersen, P. *Et Notat om Elementanalyse for FEM (Finite Element Metoden).* Afdelingen for Faststofmekanik, Danmarks Tekniske Højskole. Lyngby, 1984, pp. 51-54.

[P4] Pedersen, P.T. and Jensen, J.J. *Styrkeberegning af Maritime Konstruktioner.* Del 2. Numeriske Metoder. Afdelingen for Skibs- of Havteknik, Danmarks Tekniske Højskole. Lyngby, 1983.

[P5] Petersen, J.T., Frandsen, S., and Courtney M. *Stall Induced Vibrations of Wind Turbine Blades.* Proceedings of the European Community Wind Energy Conference. Herning, Denmark, June 1988, pp. 246-250.

[P6] Przemieniecki, J.S. *Theory of Matrix Structural Analysis.* McGraw-Hill, New York, 1975.

[R1] Rasmussen, F., Petersen, S.M., Larsen, G., Kretz, A. and Andersen, P.D. *Investigations of Aerodynamics, Structural Dynamics and Fatigue on Danwin 180 kW.* Risø report. M-2727. Risø National Laboratory. Roskilde, Denmark, 1988.

[R2] Rosen, A. and Friedmann, P. *The Nonlinear Behaviour of Elastic Slender Straight Beams Undergoing Small Strains and Moderate Rotations.* Journal of Applied Mechanics. Vol. 46, March 1979, pp. 161-168.

[R3] Rosen, A. and Rand, O. *A General Model of the Dynamics of Moving and Rotating Rods.* Computers and Structures. Vol. 21, No.3, 1985, pp. 543-561.

[S1] Schöttl, Ch. and Wagner, S. *Dynamic and Aeroelastic Response of Wind Energy Converter to Aerodynamic Loads.* Proceedings of the European Community Wind Energy Conference. Herning, Denmark, June 1988, pp. 191-196.

[S2] Shinozuka, M. and Jan, C.-M. *Digital Simulation of Random Processes and its Applications.* Journal of Sound and Vibration, Vol. 25, No. 1, pp. 111-128. 1972

[T1] Thresher, R.W. and Hersberg, E.L. *Development of an Analytical Model and Code for the flapping Response of a HAWT Rotor Blade.* SERI. Solar Energy Research Institute. Golden, Colorado, 1985.

[T2] Thresher, R.W., Holley, W.E., and Jafaray, N. *Wind Response Characteristics of Horizontal Axis Wind Turbines.* Proceedings of the Second DOE/NASA Wind Turbine Workshop. Cleveland, Ohio, 1981, pp. 87-100.

[V1] Veers, P. *Three-dimensional wind simulation.* Sandia report. SAND88-015. Sandia National Laboratories. Albuquerque, New Mexico, 1988.

[V2] de Vries, O. *Fluid Dynamic Aspects of Wind Energy Conversion.* AGARDograph No. 243, AGARD 1979. Chapter 4.4.

[Y1] Yang, T.Y. *Matrix Displacement Solutions to Elastica Problems of Beams and Frames.* Int. Journal of Solids and Structures, Vol. 9, 1973, pp. 829-842.

[Ø1] Øye, S. *FIX. Dynamisk, Aeroelastisk Beregning af Vindmøllevinge.* Department of Fluid Mechanics. Technical University of Denmark. Lyngby, Denmark, 1983.

[Ø2] Øye, S. *CBEAM4. Beregning af Egensvingninger m.v. for Centrifugalbelastede Bjælker.* Department of Fluid Mechanics. Technical University of Denmark. Lyngby, Denmark, 1983.

Tryk: Grafisk Service, RISØ